Identification and characterisation of novel mechanisms affecting prostate cancer cell growth

Karen Elizabeth Livermore

A thesis submitted for the degree of Doctor of Philosophy

Newcastle University

Faculty of Medical Science

Institute of Genetic Medicine

November 2020

Abstract

Prostate cancer development and progression to lethal metastatic castration-resistant prostate cancer (CRPCa) is driven by the androgen receptor. Androgen deprivation therapy (ADT) is the first line of treatment used to control cancer growth. Although ADT is usually effective, the recurrence of castration-resistant prostate cancer is common and ultimately lethal. Progression to CRPCa is thought to involve persistence of AR signalling and reprogramming of the AR transcriptional landscape, allowing tumour cells to continue to grow despite low levels of circulating androgens.

The overall aim of this study was to identify and characterise mechanisms affecting prostate cancer cell growth. To do this I used RNA-sequencing in the androgen-responsive LNCaP cell line, coupled with previously published RNA-sequencing of advanced prostate cancer treated with ADT and clinical prostate cancer expression data to identify androgen-regulated genes, alternative isoforms and pathways. A set of 660 genes showed reciprocal changes in expression in response to acute androgen stimulation in culture, and androgen deprivation in patients with prostate cancer. A multiple dataset meta-analysis strategy coupled with gene ontology analysis has identified glycosylation as a novel androgen regulated pathway. Although patterns of glycosylation are known to change in prostate cancer the mechanisms underlying these changes are not well understood. The data in this study suggest androgens may increase the aggressiveness and metastatic potential of PCa cells through mediating changes in glycosylation patterns.

Further investigation into the sialyltransferase enzyme ST6Gal1 has shown that high levels alter the expression of key epithelial to mesenchymal transition (EMT) makers and increase the invasion potential of prostate cancer cells, whilst reduction significantly decreased cell proliferation, cell to matrix adhesion, migration and invasion capability. Together with the androgen regulated transcriptional changes, the RNA sequencing data also identified a number of androgen regulated alternative mRNA isoforms, including promoter switches for the RLN1 and RLN2 genes.

In summary correlation of gene expression changes in prostate cancer cells in response to acute androgen stimulation with those repressed in patients by ADT has revealed a new panel of clinically relevant androgen regulated genes. Analysis of this panel has demonstrated important androgen control over glycosylation modifications has important implications for prostate cancer biology, and also suggests further targets for future analysis.

Acknowledgements

Firstly, I would like to thank my project supervisors Professor David Elliott and Dr Jennifer Munkley for their guidance, constant encouragement and continual support throughout this project. I would also like to thank all members of the Elliott laboratory group, in particular Dr Jennifer Munkley and Dr Ingrid Ehrmann for their invaluable technical advice and practical support. Thanks also to Dr Caroline Dalgliesh and fellow PhD students Gerald Hysenaj and Mohammed Alshehri, you have all made my time in the lab enjoyable and I feel privileged to have worked with such a great group of people. I wish you all great success and happiness in your future endeavours.

Special thanks to the following collaborators who have contributed their time and knowledge to this project: Professor Craig Robson (Northern Institute of Cancer Research, Newcastle University), Professor Hing Leung (Beatson Institute of Cancer Research, University of Glasgow), Dr Ian Mills (Centre for Cancer Research and Cell Biology, Queens University, Belfast), Dr Prabhakar Rajan (Centre for Molecular Oncology, Barts Cancer Institute), Dr Katherine James (School of Computing Science, Newcastle University) and Dr Lorna Harris (North Institute of Biomedical and Clinical Sciences, University of Exeter). Thanks also to Dr Urzula McClurg (Northern Institute of Cancer Research, Newcastle University) for her assistance with the tissue microarray work and Dr Jannetta Steyn and Kat Cheng for their assistance with the bioinformatics analysis (Bioinformatics Support Unit, Newcastle University).

I would like to thank my family in particular my husband Rob and my daughter Briony for their continuing love, laughter and support throughout this project. Thanks also to my assessors Professor Craig Robson and Dr Neil Rajan for their valuable advice and guidance on my PhD progress. I also gratefully acknowledge Prostate Cancer UK (PCUK) for funding this project and the Newcastle University Travel Grant for financial assistance which allowed me to present my work in a poster at the 23rd International Symposium on Glycoconjugates (Glyco 23) in Split, Croatia.

Declaration

I, Karen Elizabeth Livermore, declare that no portion of the work compiled in this thesis has been submitted in support of another degree or qualification at this or any other University or Institute of Learning. This thesis includes nothing which is the work of others, nor the outcomes of work done in collaboration, except where otherwise stated.

…….....

Karen Elizabeth Livermore

Table of Contents

List of Figures

Chapter 1

Chapter 3

Chapter 4

Chapter 5

List of Tables

Chapter 1

Chapter 2

Chapter 3

Chapter 4

Abbreviations

AAH	atypical adenomatous hyperplasia
ABBC4	ATP-binding cassette, sub-family C, member 4
ADT	androgen deprivation therapy
AKR1C3	aldo-keto reductase family 1 member C1
AKR1C3	aldo-keto reductase family 1, member C3
Akt	protein kinase B
ALG5	dolichyl-phosphate beta-glucosyltransferase
APS	ammonium persulphate
AR	androgen receptor
AREs	androgen response elements
ARF4	ADP ribosylation factor 4
Asn	asparagine
AUR	acute urinary retention
AURKA	aurora kinase A
BBN	bombesin
BICC1	BicC family RNA binding protein 1
BME	basement membrane extract
BPH	benign prostatic hyperplasia
BSA	bovine serum albumin
BST1	bone marrow stromal cell antigen 1
CALR	calreticulin
CAMK1D	calcium/calmodulin-dependent protein kinase 1D
CAMKK2	calcium/calmodulin-dependent protein kinase 2
cAMP	cyclic adenosine monophosphate
CDA	cytidine deaminase
CDH1	cadherin 1 (E-cadherin)

CDH2	cadherin 2 (N-cadherin)
cDNA	complementary DNA
CDS	coding sequence
cfDNA	cell free DNA
CgA	chromogranin A
CML	chronic myelogenous leukemia
CMP	cytidine monophosphate
CORO1B	coronin actin binding protein 1b
CREB3L4	cAMP responsive element binding protein 3 like 4
CRPC	castrate resistant prostate cancer
CTCs	circulating tumour cells
CTNNB1	beta-catenin
CYP17A1	cytochrome P450 17A1
CYS1	cystin1
C1orf116	chromosome 1 open reading frame 116
DAPI	4',6-diamidino-2-phenylindole
DBD	DNA binding domain
DDX5	DEAD-box helicase 5
DEPC	diethylpyrocarbonate
DHEA	dehydroepiandrosterone
DHT	dihydrotestosterone
DMEM	Dulbecco's modified eagle medium
DNA	deoxyribonucleic acid
dNTPs	deoxynucleotide triphosphates
DSP	desmoplakin
DTT	dithiothreitol
DU145	human prostate carcinoma cell line

ECL	enhanced chemiluminescence
EDEM3	ER degradation enhancing alpha-mannosidase like protein 3
EDTA	ethylenediaminetetraacetic acid
EdU	5-ethynyl-2'-deoxyuridine
EMT	epithelial to mesenchymal transition
ER	endoplasmic reticulum
ERAD	endoplasmic reticulum-associated degradation
ERα	estrogen receptor alpha
ERK1/2	extracellular signal-regulated kinase ½
ESRP2	epithelial spicing regulatory protein 2
EVC	empty vector control
EXT1	exostosin glycosyltransferase 1
FBS	fetal bovine serum
FN1	fibronectin
FSH	follicle stimulating hormone
Fuc-PSA	fucosylated PSA
FUT8	α1-6 fucosyltransferase 8
FZD	fizzled class receptor
Gal	galactose
GalNAc	N-acetyl-galactosamine
GALNT7	polypeptide N-acetylgalactosaminyltransferase
GAPDH	glyceraldehyde-3-phosphate dehydrogenase
GCNT1	glucosaminyl (N-acetyl) transferase 1
GFP	green fluorescent protein
GlcNAc	N-acetyl-glucosamine
GLIS2	GLIS family zinc finger protein
GNPNAT1	glucosamine-phosphate N-acetyltransferase 1

GnRH	gonadotropin releasing hormone
GO	Gene Ontology
GPCRs	G-protein-coupled-receptors
GST	glutathione s-transferase
GSTA4	glutathione s-transferase alpha 4
HBP	hexosamine biosynthetic pathway
HEK-293	human embryonic kidney 293 cell line
HeLa	human cervical carcinoma cell line
HGPIN	high-grade prostatic intraepithelial neoplasia
HIFU	high-intensity focused ultrasound
HLA-G	histocompatibility antigen, class I (beta 2-microglobulin)
HPG	hypothalamic-pituitary-gonadal
HSD17B6	hydroxysteroid (17-Beta) dehydrogenase 6
HSP	heat shock protein
H&E	hematoxylin and eosin
ICGC	International Cancer Genome Consortium
IFIT2	interferon induced protein with tetratricopeptide repeats 2
IgG	immunoglobulin G
IL6	interleukin-6
IPTG	isopropyl β-D-1-thiogalactopyranoside
JUP	junction plakoglobin
KEGG	Kyoto Encyclopaedia of Genes and Genomes
KHDRBS1	KH domain-containing, RNA-binding, signal transduction-associated protein 1
KLK3	kallikrein related peptidase 3 (PSA)
KLKP1	kallikrein pseudogene 1
JAK	janus kinase
LB	Luria Bertani

LBD	ligand binding domain
LGPIN	low-grade prostatic intraepithelial neoplasia
LH	luteinising hormone
LHRH	luteinising hormone-releasing hormone
lncRNA	long non-coding RNA
Man	mannose
MAPK	mitogen-activated protein kinase
mRNA	messenger RNA
miRNA	micro RNA
MTT	3-(4,5-dimethylthiazol-2-yl)-2,5-diphenyltetrazolium bromide
MYCN	v-myc avian myelocytomatosis viral oncogene neuroblastoma derived homolog
NANS	N-acetylneuraminate synthase
NCI	National Cancer Institute
NDUFV3	NADH:ubiquinone oxidoreductase subunit v3
NEAT1	nuclear paraspeckle assembly transcript 1
NED	neuroendocrine differentiation
NEPC	neuroendocrine prostate cancer
Neu5Ac	N-acetylneuraminic acid
NF-κB	nuclear factor kappa B
NHGRI	National Human Genome Research Institute
NSE	neuron-specific enolase
NTC	no template control
NTD	N-terminal domain
OAS3	2'-5'-oligoadenylate synthetase 3
ORF	open reading frame
PBS	phosphate buffered saline
PC-3	human prostate carcinoma cell line

PC-3M	human prostate carcinoma cell line – highly metastatic
PCa	prostate cancer
PCA3	prostate cancer antigen 3
PCR	Polymerase Chain Reaction
PCUK	Prostate Cancer United Kingdom
PIA	proliferative inflammatory atrophy
PI3K	phosphoinositol 3-kinase
PIN	prostatic intraepithelial neoplasia
piRNA	Piwi-interacting RNA
PKA	protein kinase A
PKP2	plakophilin 2
PKP3	plakophilin 3
PKP4	plakophilin 4
PMSF	phenylmethane sulfonyl fluoride
PNN	pinin (desmosome associated protein)
Pro	proline
PSA	prostate specific antigen
PTHrp	parathyroid hormone-related protein
PTM	post translational modification
PVDF	polyvinylidene difluoride
PYCR1	pyrroline-5-carboxylate reductase 1
RAP1GAP	RAP1 GTPase activating protein
qPCR	quantitative real-time PCR
RHOU	Ras Homolog Family Member U
RNA	ribonucleic acid
RNAi	RNA inteferance
RNA-seq	RNA sequencing

RPN2	ribophorin II
RT-PCR	Reverse Transcription Polymerase Chain Reaction
RXFP	relaxin family peptide receptors
SAM68	Src-associated in mitosis 68 KDa protein
SD	steroid deplete
SDS	sodium dodecyl sulfate
SDS-PADE	sodium dodecyl sulfate polyacrylamide gel electrophoresis
SE	standard error
Ser	serine
SERP1	stress associated endoplasmic reticulum protein 1
SIP-T	sipuleucel-T
siRNA	small interfering RNA
SLC18A2	solute carrier family 18 member A2
SLC9A9	solute carrier family 9 member A9
α-SMA	α-smooth muscle actin
SMARCD3	SWI/SNF related, matrix associated, actin dependent regulator of chromatin, subfamily D, member 3
SMRT	single molecule real time
SNAI1	snail family transcriptional repressor 1 (snail)
SNAI2	snail family transcriptional repressor 1(slug)
snoRNA	small nuclear RNA
SPDEF	SAM pointed domain containing ETS transcription factor
SRD5A1/2	steroid-5-alpha-reductase, alpha polypeptide 1/2
SRPK1	serine-arginine protein kinase 1
ST6GalNAc1	ST6 N-acetylgalactosaminide α-2,6-sialyltransferase 1
STAT	signal transducers and activators of transcription
STT3A	catalytic subunit of the oligosaccharyltransferase complex
STYK1	serine/threonine/tyrosine kinase 1

TBE	tris-borate-EDTA
TBS-T	tris-Buffered Saline and Tween 20
TCGA	The Cancer Genome Atlas
TE	tris/EDTA
TEMED	tetramethylethylenediamine
TGF- β	transforming growth factor-β
Thr	threonine
TMA	tissue microarray
TMEM8A	transmembrane protein 8a
TNFR1	tumour necrosis receptor 1
TNM	tumour, lymph node, metastasis
TSC2	tuberous sclerosis complex 2
TSPAN1	tetraspanin 1
TSS	transcriptional start site
TWIST1	twist family BHLH transcription factor 1
TUSC3	tumour suppressor candidate 3
UAP1	UDP-N-acetylglucosamine pyrophosphorylase 1
UBE2J1	ubiquitin conjugating enzyme E2 J1
UCSC	University of California, Santa Cruz
UGGT1	UDP-glucose glycoprotein glucosyltransferase 1
UTI	urinary tract infections
UTR	untranslated region
VEGF	vascular endothelial growth factor
VIM	vimentin
WNT1	Wnt family member 1
ZBTB16	zinc finger and BTB domain containing 16
ZNF121	zinc finger protein 121

Chapter 1

Introduction

Chapter 1 Introduction

1.1 Prostate cancer

1.1.1 The prostate gland

The prostate is a small glandular organ found within the male reproductive and urinary system. It is situated within the pelvic cavity, beneath the bladder and surrounding the urethra. The prostate consists of approximately 70% glandular tissue and 30% fibromuscular stroma. Arranged within the basement membrane of these glandular epithelium structures are several different cell types including luminal secretory cells (60%), basal cells (40%) and transient stem cells (~1%) with a small number of interspersed neuroendocrine cells. The surrounding stromal tissue contains smooth muscle cells, fibroblasts, nerve cells, blood vessels, extracellular matrix and lymphatics (Figure 1.1) (Mcneal, 1988). The main function of the prostate is to produce prostatic fluid, a component of semen containing sugars, enzymes and alkaline chemicals which protects and enhances the survival of spermatozoa. The glandular secretory cells are responsible for producing this seminal fluid whilst the fibromuscular stromal tissue provides a structural network and controls ejaculation. As the prostate gland surrounds the urethra it also assists in controlling the flow of urine from the bladder.

Structurally, the mature prostate is divided into four distinct zones, (1) the transition zone, (2) the central zone, (3) the peripheral zone and (4) a fibromuscular stroma (Figure 1.1). The transition zone is situated in the centre of the prostate surrounding the urethra and is between the central and peripheral zones (Figure 1.2). The transition, central and peripheral zones contain highly organised glandular epithelium structures which are separated by the fibromuscular stromal network (Figure 1.2) (McNeal, 1981).

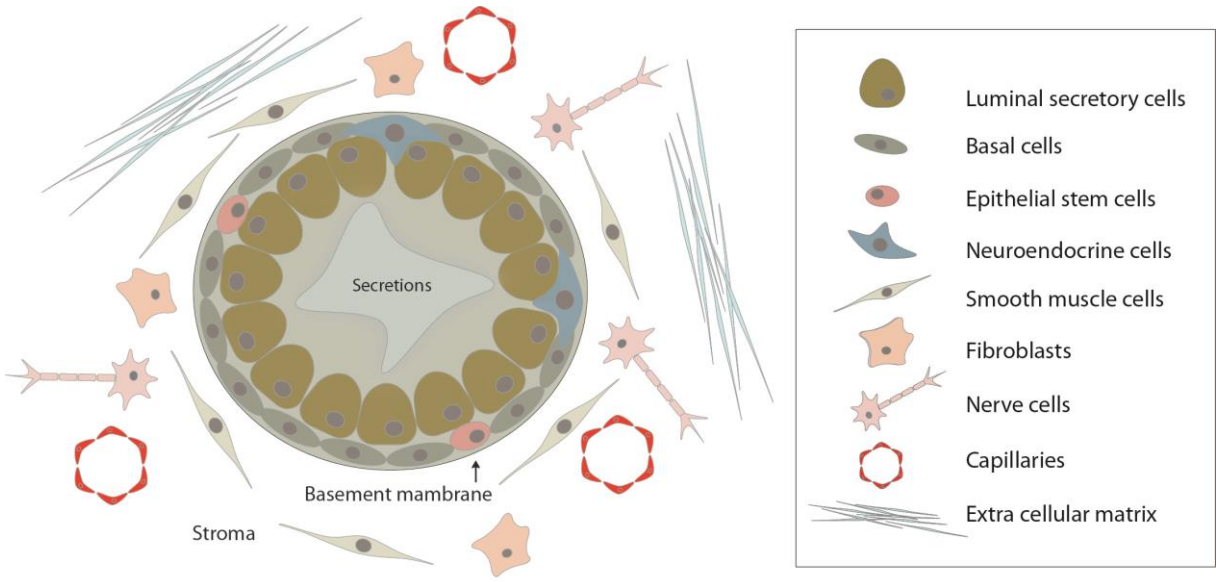

Figure 1.1 Cellular structure of the prostate gland.

Arranged within the basement membrane of prostate glands are basal cells, luminal secretory cells and a small number of neuroendocrine cells. The fibromuscular stroma contains smooth muscle cells, fibroblasts, nerve cells, blood vessels within an extracellular matrix.

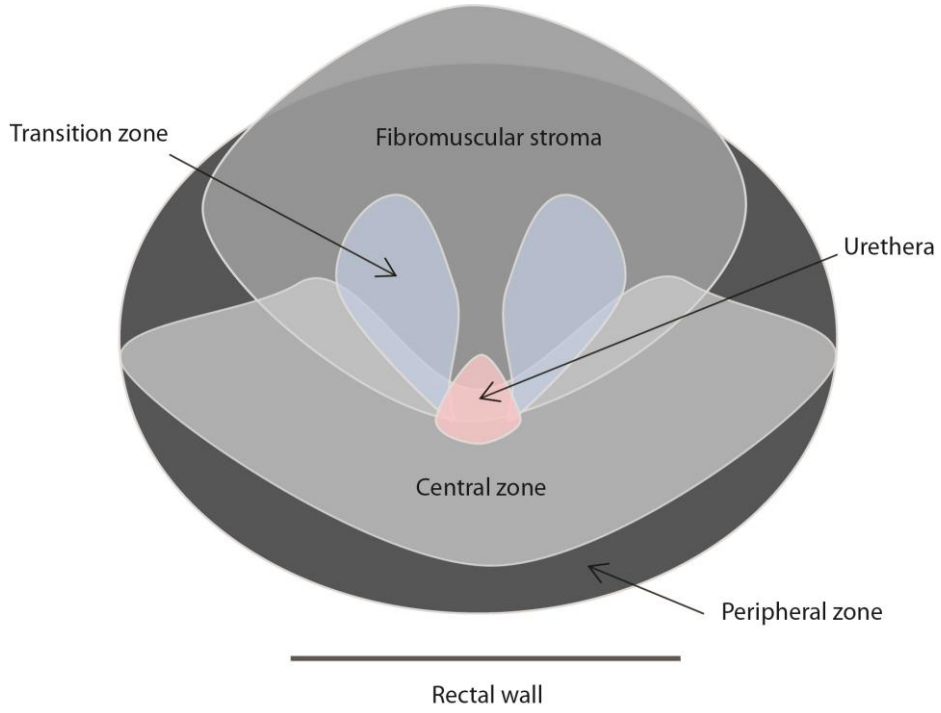

Figure 1.2 Zonal anatomy of the prostate.

The prostate is divided into four distinct zones; three glandular zones (peripheral zone, central zone and transition zone) and a fibromuscular stroma.

The size of the prostate can increase with age, resulting in a condition termed benign prostatic hyperplasia (BPH). This non-malignant condition is common in men > 60 years (Isaacs, 1994) and is characterised by progressive hyperplasia of glandular and stromal tissues within the transitional zone of the prostate (McNeal, 1978). As the transition zone increases in size it pushes the peripheral zone towards the rectum. BPH is not usually serious, however the increased growth can sometimes impact on the urethra causing discomfort and leading to complications such as acute urinary tract infections (UTI) and acute urinary retention (AUR) (Berry *et al.*, 1984; Briganti *et al.*, 2009). Although BPH and prostate cancer (PCa) can be linked at the molecular and cellular levels there remains no substantial evidence to suggest an increased cancer risk for men with BPH

(Fukushima *et al.*, 1998; Rudd *et al.*, 2001; Chang *et al.*, 2012; Orsted and Bojesen, 2013).

1.1.2 Prostate cancer

PCa is the most common type of cancer in men in the United Kingdom. Incidence rates have increased since the late 1970s and there were around 46,700 new cases of PCa in 2014 (corresponding to 130 cases diagnosed every day). With around 11,287 deaths a year prostate cancer accounts for 13% of all cancer deaths. It is predicted that approximately 1 in every 8 men will be diagnosed with PCa during his lifetime (Cancer Research UK, 2013; Ferlay *et al.*, 2015). Over half of all cases are diagnosed in men aged 70 and over and these figures are expected to rise with an increasingly aging population. Risk factors include family history, age, ethnicity, diet, hormones, sexual activity and environmental influences (Bonilla *et al.*, 2016; Lynch *et al.*, 2016; Rider *et al.*, 2016; Shui *et al.*, 2016; Travis *et al.*, 2016; Harrison *et al.*, 2017; Taylor *et al.*, 2017; Wu *et al.*, 2017).

Adenocarcinoma accounts for the majority of tumours, and originates from the glandular structures within the peripheral zone of the prostate. PCa is a heterogeneous disease and the process of initiation is not fully understood. As with many cancers, two main models of tumour initiation and progression have been proposed. The clonal evolution model involves multiple genetic and epigenetic changes within a single cell of origin which confer a selective growth and survival advantage to produce a dominant clone. Genetic instability within the expanding tumour population produces further mutant cells creating tumour cell heterogeneity (Nowell, 1976). The alternative cancer stem cell model suggests that the tumour originates from a small sub-population of tumour initiating cells that have retained the ability to self-renew, generating heterogeneity through differentiation (Collins et al., 2005; Visvader and Lindeman, 2012). Whatever the model, this complex tumour heterogeneity creates a major challenge for treatment.

In some cases, PCa is preceded by a premalignant condition called prostatic intraepithelial neoplasia (PIN). PIN involves neoplastic cellular proliferation which is confined to pre-existing ducts and acini with nuclear and nucleolar enlargement (Amano *et al.*, 2003). PIN can be sub-categorised based on histological characteristics into low-grade (LGPIN) and high-grade (HGPIN). Other possible premalignant prostate conditions include atypical adenomatous hyperplasia (AAH) and proliferative inflammatory atrophy (PIA). AAH is characterised by localised proliferation of acini within the transition zone of the prostate that are histologically similar to adenocarcinoma (Park *et al.*, 2012), whilst PIA is proliferation that occurs in association with chronic inflammation. HGPIN is the only premalignant condition that has a significant association with the development of PCa (Shaikh *et al.*, 2008; Liu *et al.*, 2014b; Meng *et al.*, 2015; Hsieh *et al.*, 2017).

1.1.3 Androgen receptor

Androgens play a key role in the growth and function of the prostate. In 1941, Huggins and Hodge were the first to demonstrate the androgen dependency of PCa growth and progression (Huggins and Hodges, 1972; Huggins and Hodges, 2002). Androgens and the androgen receptor (AR) have since been portrayed as the crucial players in both localised and advanced disease (Harris *et al.*, 2009; Livermore *et al.*, 2016) and have been the major target for therapeutic treatment of PCa for many years (Guo *et al.*, 2017).

Androgens are a group of steroid hormones of which testosterone is the most prevalent in males. Testosterone is primarily produced in the testes by the Leydig cells (90%), although small amounts are also produced by the adrenal glands (10%). Testosterone production is regulated through the hypothalamic-pituitary-gonadal (HPG) axis. Pulses of gonadotropin releasing hormone (GnRH) are secreted from the hypothalamus to stimulate the release of luteinising hormone (LH) and follicle stimulating hormone (FSH) from the anterior pituitary gland, and this in turn stimulates the synthesis of testosterone. Circulating testosterone levels regulate the further production of GnRH to create a feedback loop (Conn and Crowley, 1994).

In the prostate, testosterone is converted to dihydrotestosterone (DHT) by 5α-reductase enzymes (Radmayr *et al.*, 2008). The action of DHT is dependent upon binding to the AR. In the prostate DHT has a 10-fold higher binding affinity for the AR than testosterone (Saartok *et al.*, 1984). In its inactive form, the AR is located in the cytoplasm bound to heat shock proteins (HSP), specifically HSP90 and other chaperone molecules (Cano *et al.*, 2013). Binding of DHT to the ligand binding domain (LBD) of the AR induces a series of conformational changes that dissociate the AR from the HSPs and chaperone molecules. These changes promote AR phosphorylation and translocation to the nucleus, where the activated AR interacts with co-activators and binds as a dimer to androgen response elements (AREs) found in the promoter regions of target genes (He *et al.*, 1999). The AR controls transcription of many genes which are involved in cell growth and survival (Massie *et al.*, 2011) as well as prostate-specific antigen (PSA) (Cleutjens *et al.*, 1996) (Figure 1.3).

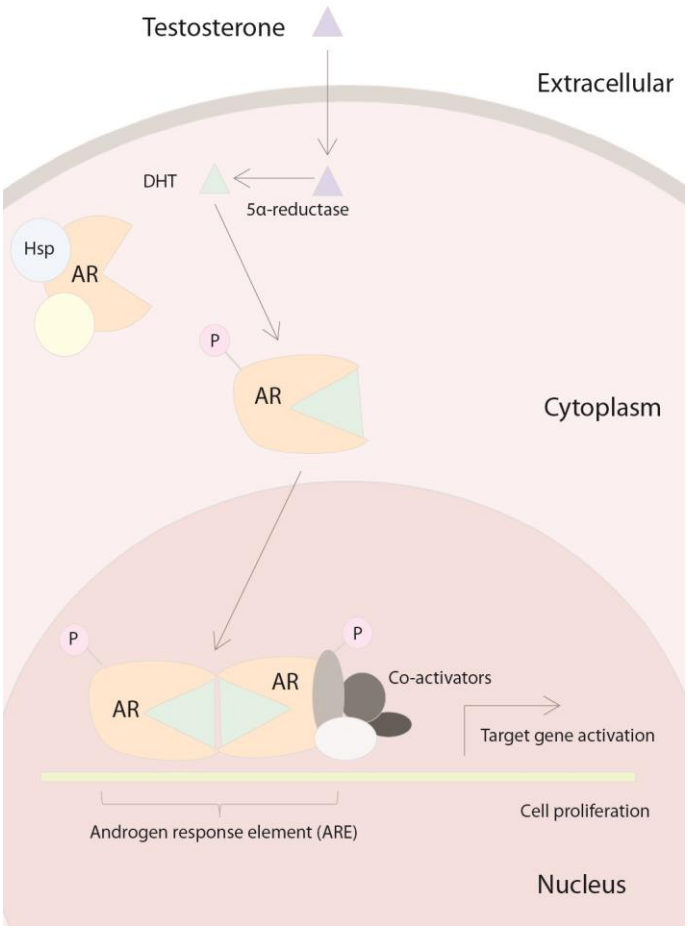

Figure 1.3 Androgen signalling in the prostate.

Testosterone enters the prostate cell where it is converted to DHT by the enzyme 5α-reductase. Inactive AR is located in the cytoplasm bound to heat shock proteins (HSP) and other chaperone molecules. Binding of DHT to the AR induces a series of conformational changes that dissociate the AR from the HSPs and promotes AR phosphorylation and translocation to the nucleus. Inside the nucleus, the activated AR interacts with co-activators and binds as a dimer to androgen response elements (AREs) of target genes.

The AR is a nuclear steroid hormone receptor which functions as a ligand dependant transcription factor. The human AR gene is located on the X chromosome (Xq11-12) and spans > 90-kb of DNA (Lubahn *et al.*, 1988). It has eight coding exons (Gelmann, 2002) which produce a 919 amino acid protein with four functionally distinct domains: an N-terminal domain (NTD), a DNA binding domain (DBD), a small hinge region and a ligand binding domain (LBD). The first large exon encodes the highly variable NTD, which contains several regions of repetitive DNA sequences (CAG tri-nucleotide repeat) (Edwards *et al.*, 1992). The highly conserved DBD contains two zinc finger domains and is encoded by exons 2 and 3 (Verrijdt *et al.*, 2003), whilst exons 4 to 8 code for the C-terminal LBD (Figure 1.4). The AR contains two trans-activation domains, the hormone independent activation function 1 (AF1) is located within the NTD and the hormone-dependent activation function 2 (AF2) within the LBD. The most common AR splice variants AR-V7 and Arv567es lack a functional LBD and are constitutively active as transcription factors in the absence even of androgens. Not all cell types within the normal prostate gland are AR-positive. Whilst the luminal secretory cells express high levels of AR (Maitland *et al.*, 2011), the majority of basal cells, neuroendocrine cells, and stem cells express little or no AR and function independently of androgens (Mirosevich *et al.*, 1999; Wen *et al.*, 2014).

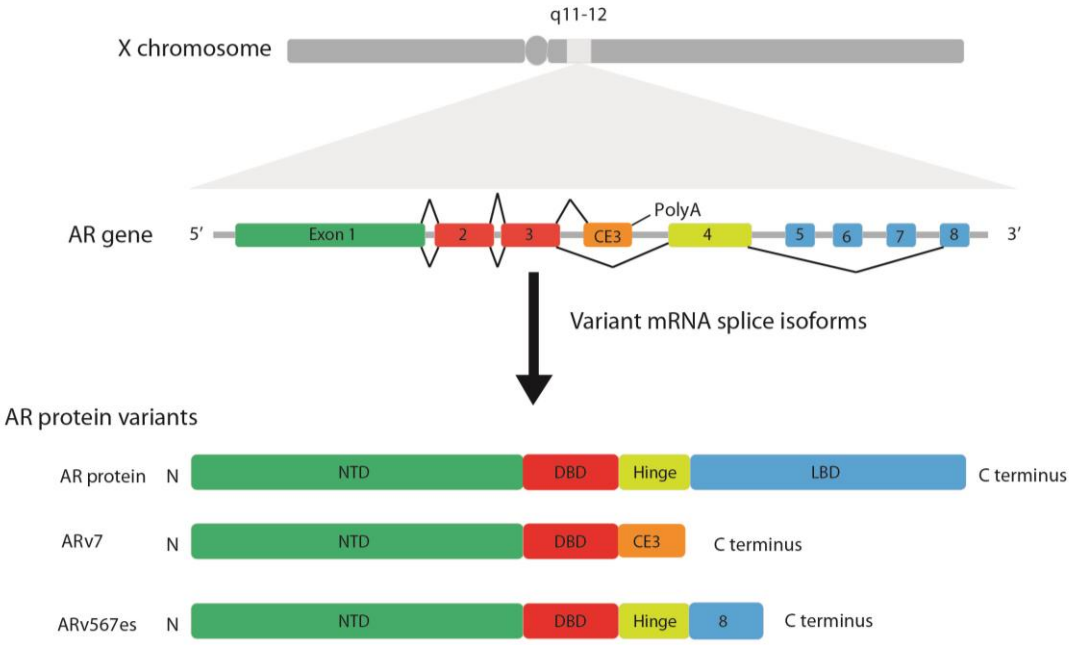

Figure 1.4 Androgen receptor gene and common cancer associated splice variants. The AR gene is located on the X chromosome (Xq11-12) and has eight coding exons. The full-length AR protein has four functionally distinct domains: an N-terminal domain (NTD), a DNA-binding domain (DBD), a small hinge region and a ligand-binding domain (LBD). The most common AR splice variants AR-V7 and Arv567es lack a functional LBD and are constitutively active.

1.1.4 Diagnosis and treatment

PCa diagnosis usually involves measurement of serum prostate-specific antigen (PSA) levels, a digital rectal examination, and a needle core biopsy sampling. PSA is a serine protease which is secreted almost exclusively by the epithelial cells of the prostate (Ablin et al., 1970). PSA is commonly used as a biomarker of PCa as disruption of the prostatic epithelium allows PSA to leak into the circulating blood stream (Papsidero et al., 1980). However, its use as a PCa biomarker is controversial as it does not distinguish between PCa and other non-malignant conditions such as BPH, viral infections or chronic

prostatitis (Nadler *et al.*, 1995; Shappell, 2008; Joshi *et al.*, 2010; Henning *et al.*, 2017). Several new PCa biomarkers are currently being investigated, including the use of tumour specific PSA isoforms (Romero Otero *et al.*, 2014; Heidegger *et al.*, 2015) and PSA glycan signatures (Gilgunn *et al.*, 2013; Ishikawa *et al.*, 2017), as well as non-invasive urine-based assays such as microRNA (miRNA) profiling (Fabris *et al.*, 2016; Luu *et al.*, 2017) and exosome/ microvesicle gene expression analysis (McKiernan *et al.*, 2016; Motamedinia *et al.*, 2016). These new approaches may prove to be more reliable at detecting PCa, thus helping to reduce the over diagnosis and over treatment issues associated PSA screening.

The Gleason grading system is used in combination with PSA screening to categorise haematoxylin and eosin (H&E) stained prostatic tissue sections from biopsy samples. The size, morphology and structural arrangement of carcinoma cells help separate prostate tumours into five basic grades, from grade 1 (well-differentiated, small uniform glands) to grade 5 (poorly-differentiated, occasional gland formation) (Figure 1.5) (Gleason and Mellinger, 1974). These grades are used to generate an average Gleason score indicating the clinical stage of the tumour, possibility of progression to metastatic disease, and the patient's treatment/survival prognosis (Mellinger *et al.*, 1967).

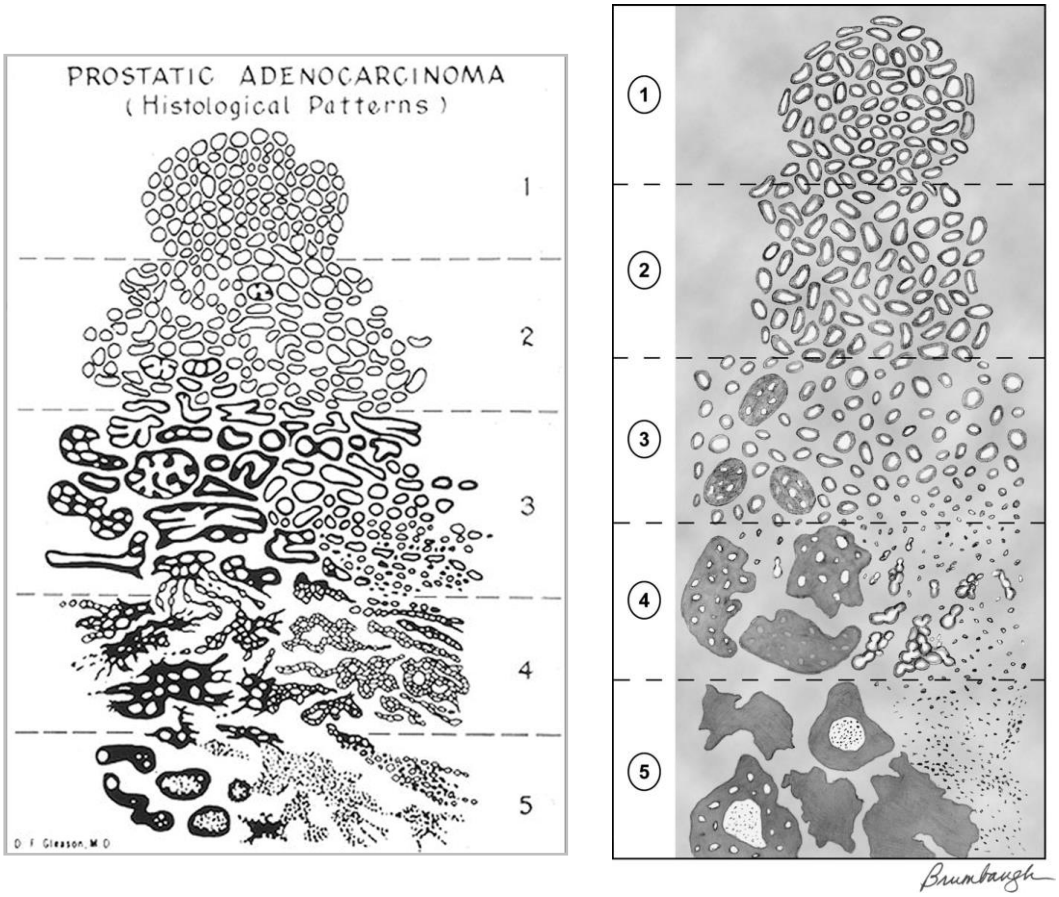

Figure 1.5 Schematic diagrams of the Gleason grading systems.

Schematic diagrams of the Gleason grading system (a) the original Gleason grading system and (b) the updated modified Gleason grading system (Mondal *et al.*, 2010).

The current treatment options for localised PCa and locally advanced PCa include active surveillance, radical prostatectomy and radiation type therapy such as external beam radiotherapy, permanent seed brachytherapy, high-intensity focused ultrasound (HIFU) or cryotherapy to remove or kill tumour cells. The main treatment options for more advanced PCa include taxane chemotherapy treatment with docetaxel (Taxotere®) or cabazitaxel (Jevtana®) and androgen deprivation therapy (ADT), or a combination of both (Rajan *et al.*, 2015; Tucci *et al.*, 2016). ADT targets the androgen axis by reducing serum testosterone levels. This can be achieved by surgically removing the testicles

(orchidectomy) (Klugo et al., 1981) or using a combination of luteinising hormone-releasing hormone (LHRH) agonists and antagonists to suppress the production of testosterone (Labrie et al., 1986) and AR antagonists such as bicalutamide (Casodex®) and flutamide (Eulexin®), which block AR function (Labrie *et al.*, 1993; George, 2013; Ritch and Cookson, 2016).

Despite an initial response to ADT, many patients go on to develop castration-resistant prostate cancer (CRPC) within a few years (Karantanos et al., 2013). CRPC occurs when tumour cells develop mechanisms which allow them to continue to grow despite depleted androgen levels. This has led to the development of second generation AR signalling inhibitors such as Abiraterone (Zytiga®) and Enzalutamide (Xtandi®). Abiraterone is an irreversible inhibitor of the enzyme CYP17A1, which is designed to inhibit extra-gonadal testosterone synthesis from the adrenal glands and the tumour microenvironment (de Bono et al., 2011). Enzalutamide is an AR antagonist which works by binding to the LBD of the AR, inhibiting its translocation to the nucleus, chromatin binding and interactions with co-regulators (Tran et al., 2009). Radium-233 (Xofigo®), a radiopharmaceutical agent has recently been approved for the treatment of CRPC patients with bone metastases (Kluetz *et al.*, 2014; Suominen *et al.*, 2017) and immunotherapy treatment with sipuleucel-T (SIP-T) in combination with the monoclonal antibody Ipilimumab is in clinical trials (Scholz *et al.*, 2017). Although these agents have been modestly successful at prolonging the overall survival of PCa patients, resistance mechanisms inevitably develop which will continue to drive disease progression. CRPC is highly aggressive and ultimately lethal, meaning there is an urgent need to understand the mechanisms that drive this form of the disease and to develop new therapeutic targets.

1.1.5 Mechanisms of castrate resistant prostate cancer

There are many mechanisms and alternative pathways that have been associated with the androgen-independent growth observed in CRPC, the majority of which involve androgens and are mediated by the AR.

1.1.5.1 Altered steroidogenesis

Despite the low serum testosterone levels obtained by ADT, intratumoral testosterone levels remain sufficient enough to induce cancer progression, suggesting that altered steroidogenesis pathways have been activated. Several studies have demonstrated that PCa cells are able to produce testosterone from different androgen precursors, such as cholesterol (Mostaghel et al., 2012) and the adrenal androgen dehydroepiandrosterone (DHEA) (Hamid et al., 2012). Several genes involved in testosterone biosynthesis become up-regulated in CRPCs compared with primary prostate tumours (Mohler *et al.*, 2004; Stanbrough *et al.*, 2006; Montgomery *et al.*, 2008). These include aldo-keto reductase family 1, member C3 (AKR1C3), which encodes an enzyme which catalyses the conversion of androstenedione to testosterone, steroid-5-alpha-reductase, alpha polypeptide 1/2 (SRD5A1/2) which converts testosterone to DHT, cytochrome P450 17A1 (CYP17A1) and hydroxysteroid (17-Beta) dehydrogenase 6 (HSD17B6) (Knuuttila et al., 2014). Osteoblasts have been shown to mediate intratumoral steroidogenesis and may be responsible for castration-resistant growth in bone by stimulating increased expression of steroidogenic enzymes and DHT-inactivating enzymes in osteogenic CRPC cells (Hagberg Thulin *et al.*, 2016).

1.1.5.2 AR amplification and hypersensitivity

Increased AR levels have been identified in CRPC cell lines (Liu et al., 2008) and CRPC patient samples (Taylor *et al.*, 2010; Grasso *et al.*, 2012). AR amplification allows the tumour cells to become hypersensitive to low levels of testosterone. An excess in AR production can result from AR gene amplification, increased mRNA transcription or stabilisation of the AR mRNA or protein (Edwards *et al.*, 2003). The mechanisms underlying AR hypersensitivity remain unclear but are thought to be a response mechanism to the selective pressure within an androgen-depleted environment (Holzbeierlein et al., 2004).

1.1.5.3 AR mutations and splice variants

AR mutations have been found in around 20% of CRPC patients and account for almost 60% of cases when combined with AR amplification (Wallen *et al.*, 1999; Taylor *et al.*, 2010; Robinson *et al.*, 2015). The McGilll Androgen Receptor Gene Mutation Database (available at: http://androgendb.mcgill.ca) contains extensive details of 1110 AR mutations, 168 of which have been associated with PCa. The majority of mutations identified in CRPC are found within the LBD (49%) followed by the NTD (40%), DBD (7%) and hinge region (2%) (Gottlieb et al., 2012). The most frequent AR mutation is the point mutation T877A which substitutes a threonine for alanine at position 877. The T877A mutation is found within the LBD of the AR (Gaddipati et al., 1994). Mutations in the LBD broaden binding specificity resulting in activation by multiple endogenous hormones including estrogens, progesterone and even the androgen antagonist flutamide (Steketee et al., 2002). Mutations that occur in the NTD and DBD could modulate the receptor's affinity for co-regulators and influence nuclear localisation (Steinkamp et al., 2009). AR mutations have been detected in plasma derived cell-free DNA (cfDNA) using next generation sequencing technology, although techniques still require further optimisation (Lallous *et al.*, 2016; Goldstein *et al.*, 2017).

A large number of constitutively active AR splice variants have been identified in CRPC patients. AR splice variants are usually truncated variants of the full-length AR that lack the LBD and therefore retain transcriptional activity (Kumar and McEwan, 2012). The clinically most prevalent AR isoforms are AR-V7 (Hu et al., 2009) and ARv567es (Sun et al., 2010), both of which lack a functional LBD and facilitate ligand-independent AR signalling (Figure 1.4). AR-V7 and ARv567es levels are significantly increased in CRPC and CRPC bone metastases (Hornberg *et al.*, 2011; Zhang *et al.*, 2011). Patients with high expression levels of AR-V7 and ARv567es have a particularly poor prognosis with significantly shorter survival rates (Hornberg et al., 2011). RNA binding protein such as the KH domain-containing, RNA-binding, signal transduction-associated protein 1 (*KHDRBS1,* also known as *Sam68)* can control the expression of AR-V7 and its transcriptional function (Stockley *et al.*, 2015).

New treatments which directly target AR and its mutated forms and splice variants are in development to help overcome the acquired resistance seen with these therapies. The FDA approved antihelminthic drug niclosamide, originally developed to treat tapeworm infections, binds both full length AR and ARv7, reducing their DNA binding capacity and enhancing protein degradation. Furthermore, when used in combination with enzalutamide, niclosamide significantly inhibited enzalutamide-resistant tumour growth (Liu *et al.*, 2014a; Liu *et al.*, 2016). Galeterone, a CYP17 inhibitor and potent AR antagonist (Vasaitis *et al.*, 2008), inhibits androgen synthesis and promotes degradation of full length AR and ARv7 (Kwegyir-Afful *et al.*, 2015). Other new therapies include, ASC-J9®, an AR degradation enhancer (Wang *et al.*, 2016c), EPI-001 (De Mol *et al.*, 2016) and AR silencing with siRNAs (Wang *et al.*, 2014a; Yamamoto *et al.*, 2015).

1.1.5.4 Ligand independent activation

Although ADT works to repress AR signalling, there are a number of cytokines and growth factors that continue to activate and stabilise the AR, enhancing transcriptional activity independently of ligand binding. Interleukin-6 (IL-6) is a multifunctional cytokine important for immune regulation and which regulates cell growth (Kishimoto, 1989). Androgens induce the expression of IL-6 in the androgen sensitive LNCaP PCa cell line (Okamoto et al., 1997). Reciprocally, IL-6 can regulate AR activity in a ligand-independent and synergistic manner even in low concentrations of androgens (Hobisch *et al.*, 2000; Culig *et al.*, 2002; Malinowska *et al.*, 2009). Serum IL-6 levels are a significant prognostic factor in PCa and elevated IL-6 serum levels have been reported in CRPC patients (Twillie et al., 1995). The JAK-STAT (janus kinase - signal transducers and activators of transcription), MAPK (mitogen-activated protein kinase) and PI3K-AKT (phosphoinositol 3-kinase) signalling pathways have been shown to be important in AR activation by IL-6 (Chen *et al.*, 2000; Heinrich *et al.*, 2003). Reciprocal regulation between AR signalling and the PI3K signalling pathway has been observed in PCa cells (Carver *et al.*, 2011). AR mediated repression of the PI3K regulatory subunit PI3KR1 (p85α) results in PI3K pathway inhibition and reduced PCa cell growth (Munkley *et al.*, 2015a).

The epidermal growth factor receptor (Her2/neu) is a receptor tyrosine kinase onco-protein that plays a major role in cell growth and differentiation (Olayioye et al., 2000). Gene amplification and over expression of the Her2/neu protein drive the progression of many types of cancers, including breast and ovarian cancers (Her2/neu gene amplification is found in ~25% of breast cancers) (Slamon et al., 1989). In PCa, Her2/neu expression has been shown to increase with progression to CRPC (Signoretti et al., 2000), promoting cell growth and survival in the absence of androgens through the activation of protein kinase B (Akt) (Wen et al., 2000).

The transcription factor nuclear factor kappa B (NF-κB) plays a critical role in cancer development and progression (Karin, 2006). The AR is thought to activate NF-κB signalling in the absence of androgens and repress NF-κB in the presence of androgens (Suh et al., 2002). Constitutive activation of NF-κB signalling in the absence of androgens significantly increases AR mRNA and protein levels, AR trans-activation activity and cell proliferation in vitro (Zhang et al., 2009). NF-κB2 (p52) interacts directly with the NTD of the AR, enhancing nuclear translocation, activation and enhancing the recruitment of co-activators such as p300 to the promoter region of AR-dependent genes (Nadiminty et al., 2010).

1.1.5.5 Neuroendocrine differentiation

Neuroendocrine cells in the prostate are rare and are found interspersed between the luminal secretory and basal cells within the prostate gland. Unlike the luminal secretory and basal cells, neuroendocrine cells do not express the AR or PSA and are independent from androgen regulation (Krijnen *et al.*, 1993; Bonkhoff *et al.*, 1995). Instead, they act in an autocrine/paracrine fashion, secreting a range of growth factors and hormones which can stimulate proliferation and inhibit apoptosis in surrounding tumour cells; these include chromogranin A (CgA), neuron-specific enolase (NSE), parathyroid hormone-related protein (PTHrp), bombesin (BBN), vascular endothelial growth factor (VEGF) and many more (Li *et al.*, 2016b).

Neuroendocrine differentiation (NED) is a unique feature of PCa which refers to the trans-differentiation of PCa cells toward a neuroendocrine phenotype. NED is significantly increased in CRPC (Hirano *et al.*, 2004), and relates to a more aggressive cancer behaviour and less favourable prognosis due to late recognition and limited effective therapies (Sagnak *et al.*, 2011; Terry and Beltran, 2014). The process of NED is thought to be induced either in response to treatments such as ADT (Hirano *et al.*, 2004; Ma *et al.*, 2014; Chen *et al.*, 2016) and radiotherapy (Zhang *et al.*, 2016) or by molecular signalling molecules which activate distinct signalling pathways. A number of agents and pathways have been shown to promote NED in PCa cells including, cAMP activating the PKA/CREB signalling pathway (Chen and Colley, 2000; Clamp *et al.*, 2007; Antony *et al.*, 2014) and IL-6 activation of the PI3K/Etk/Bmx and STAT3 pathways (Qiu *et al.*, 1998; Spiotto and Chung, 2000; Jensen, 2004; Wu and Huang, 2007).

Neuroendocrine prostate cancer (NEPC) is difficult to diagnose and treat and there is currently no standard treatment for patients. This is mainly due to a lack of predictive biomarkers and understanding of the genetic and epigenetic mechanisms involved. The vast majority of NEPC over-express the cell cycle aurora kinase A (AURKA) and the proto-oncogene V-myc avian myelocytomatosis viral oncogene neuroblastoma derived homolog (MYCN) compared to adenocarcinoma (Beltran et al., 2011). Epigenetic modifiers have been shown to play a role in the induction and maintenance of a neuroendocrine phenotype in CRPC patients (Lander, 2011). Genome wide DNA methylation analysis of metastatic tumour samples showed significant differences between prostate adenocarcinomas and CRPC-NE subtypes. These include hypermethylation of the tumour suppressor gene SAM pointed domain containing ETS transcription factor (*SPDEF*) and increased expression of the histone methyltransferase enhancer of zeste homolog 2 (*EZH2*) in CRPC-NE samples (Beltran *et al.*, 2016). In contrast to prostate adenocarcinomas, no AR mutations have been observed in CRPC-NE and the ratio of ARv7 to wild type AR is significantly decreased (Beltran *et al.*, 2016). Circulating tumour cells (CTCs) from patients with CRPC-NE have unique morphologic characteristics which could be used to identify patients transitioning toward a neuroendocrine phenotype (Beltran *et al.*, 2014).

1.1.5.6 Tumour micro-environment

The tumour micro-environment also plays an important role in regulating PCa progression. In the normal prostate, signalling cross-talk between the stromal and epithelial compartments maintains cellular homeostasis. Stromal AR activity can regulate the composition of the prostate micro-environment. The AR activity of cancer-associated fibroblasts (CAFs) has been shown to promote PCa cell growth and invasion through the regulation of growth factors (Yu *et al.*, 2013). An important regulator which inhibits epithelial proliferation called transforming growth factor-β (TGF-β) is under control of the AR (Roberts *et al.*, 1985). Over expression of TGF-β has been observed in prostate tumours isolated from patients following ADT (Fuzio *et al.*, 2012). Elevated levels of TGF-β in prostate stroma have been shown to promote prostate tumour growth and angiogenesis (Yang *et al.*, 2005), and indirectly activate the AR (Yang *et al.*, 2014).

1.2 Glycosylation

1.2.1 N-linked and O-linked glycosylation

Glycosylation is a common post transcriptional modification (PTM) which involves the addition of carbohydrate chains (glycans) to proteins, lipids and other macromolecules. There are two major types of glycosylation that occur on proteins, named according to their linkage; nitrogen (N) or oxygen (O). N-linked protein glycosylation occurs at Asparagine (Asn) residues in the consensus peptide sequences Asn-X-Ser/Thr (X denotes any amino acid except proline (Pro)). Pre-assembled glycan chains, which share the same initial core region of 2 N-acetyl-glucosamine (GlcNAc) molecules followed 3 mannose (Man) molecules are transferred to the asparagine residue on the target protein. These structures are modified further by the addition of terminal structures such as GlcNAc, galactose (Gal) and sialic acid. O-linked protein glycosylation is initiated by the addition of a single N-acetyl-galactosamine (GalNAc) residue to the hydroxyl group of serine (Ser) or threonine (Thr) which can be extended into various structures (Figure 1.6). Other types of O-linked glycosylation including those attached via mannose (O-Man) and N-acetyl-glucosamine (O-GlcNAc) (reviewed in (Keren *et al.*, 2010; Pinho and Reis, 2015; Munkley *et al.*, 2016a).

Glycosylation can produce an abundant and diverse range of glycan structures on the cell surface as well as secreted and intracellular proteins. Glycan biosynthesis takes place in the lumen of the endoplasmic reticulum (ER) and in the Golgi apparatus and requires a complex series of tightly regulated steps involving multiple glycoenzymes. In humans, there are around 500 glycoenzymes including glycosyltransferases and glycosidases (Rajan *et al.*, 2009). The expression and activity of these glycoenzymes is controlled at the transcription, translation and post-translation levels (Neelamegham and Mahal, 2016).

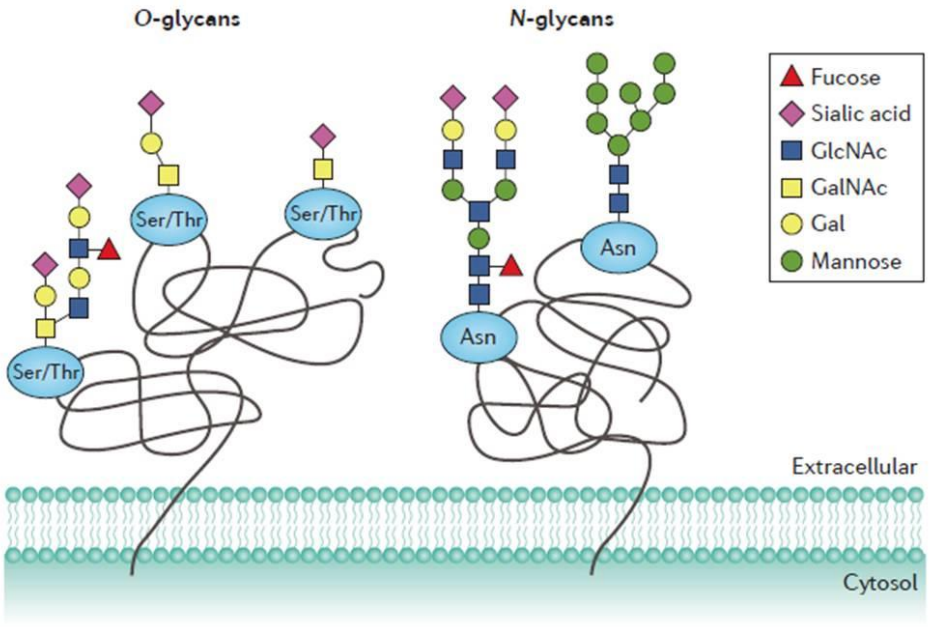

Figure 1.6 N-linked and O-linked protein glycosylation.

Protein glycosylation: N-linkage to asparagine (Asn) residues via a nitrogen atom or O-linkage to serine and/or threonine (Ser/Thr) residues via an oxygen atom. Image taken form a recent review by (Munkley *et al.*, 2016a).

1.2.2 Cancer associated glycans

The combination of glycans on a cells surface acts as an important interface between cells and their surrounding environment. The development and progression of cancer

can lead to fundamental changes in the glycan composition of cells (glycome). Changes in the glycome can alter important regulatory processes and can affect protein structure (Shental-Bechor and Levy, 2009), cell interactions, signalling (Haltiwanger, 2002), immune surveillance (Rudd *et al.*, 2001) and metabolism (Munkley and Elliott, 2016). Aberrant glycosylation, primarily caused by altered expression or the mislocalisation of glycoenzymes is a common feature of cancer cells (Pinho and Reis, 2015; Stowell *et al.*, 2015). The most frequently observed cancer-associated glycosylation changes include altered sialylation, fucosylation, O-glycan truncation, and glycan branching (Hakomori, 2002; Christiansen *et al.*, 2014).

The incomplete synthesis of O-glycans usually occurs in the early stages of cancer on and can lead to expression of truncated structures such as the T (Galβ1–3GalNAc-α1-O-Ser/Thr), Tn (GalNAcα-O-Ser/Thr) and the sialyl-Tn (sTn) (NeuAcα2-6GalNAcα-O-Ser/Thr) antigens (Miles *et al.*, 1994; Radhakrishnan *et al.*, 2014). Glycan neo-synthesis is observed in more advanced cancers and involves the induction of genes linked to the expression of the sialyl Lewis a (SLe^a) and sialyl Lewis x (SLe^x) epitopes (Narita *et al.*, 1993; Amado *et al.*, 1998; Baldus *et al.*, 1998). Increased sialylation and fucosylation due to altered glycosyltransferase and fucosyltransferase expression has also been associated with cancer (Dall'Olio and Chiricolo, 2001; Saldova *et al.*, 2011; Osuga *et al.*, 2016). Sialic acid is often found at the terminal position on cell membrane glycoproteins and plays an important role in cell communication, signalling and adhesion. Abnormal sialylation observed in cancer has been associated with malignant properties including adhesion, invasiveness and metastatic potential in part due to their negative electric charge (Dall'Olio *et al.*, 2000; Lu *et al.*, 2014; Suzuki *et al.*, 2015; Wei *et al.*, 2016).

1.2.3 Glycosylation in prostate cancer development and progression

The differential expression of glycoenzymes has been linked to PCa (Chen *et al.*, 2014; Itkonen *et al.*, 2014; Munkley *et al.*, 2015b; Munkley *et al.*, 2016b). A recently published meta-analysis study of clinical PCa gene expression data identified a novel prostate cancer gene signature which included 4 glycoenzymes: ST6 N-acetylgalactosaminide α-

2,6-sialyltransferase 1 (*ST6GalNAc1)*, glucosaminyl (N-acetyl) transferase 1 (*GCNT1)*, UDP-N-acetylglucosamine pyrophosphorylase 1 (*UAP1)*, and β-1,3-Glucuronyltransferase 1 (*B3GAT1)* (Barfeld et al., 2014). Previous work in our laboratory has found that expression of *ST6GalNAc1*, a sialytransferase that catalyses the transfer of sialic acid onto the Tn antigen, is regulated by andorgens and can affect cell adhesion. Increased *ST6GalNAc1* expression is found in primary prostate tumours, although this expression is down-regulated in metastatic tissue compared to non-malignant prostate tissue, suggesting a more transient role in tumour progression (Munkley *et al.*, 2015b). Increased expression of *GCNT1*, which is involved in the formation of branched O-linked glycans, has been shown to positively correlate with the aggressive potential of PCa (Hagisawa et al., 2005; Chen et al., 2014). UAP1 is the last enzyme in the hexosamine biosynthetic pathway (HBP) and is highly over-expressed in patients with PCa and negatively correlates with Gleason score (Itkonen et al., 2015). Polypeptide N-acetylgalactosaminyltransferase 7 (GALNT7), an enzyme involved in O-glycosylation initiation, is also up-regulated in several cancers including malignant PCa (Barfeld *et al.*, 2014; Lu *et al.*, 2016; Nie *et al.*, 2016) and GALNT7 knockdown has been found to inhibit tumour cell migration and invasion (Brockhausen, 2006; Nie *et al.*, 2016). Increased glycan fucosylation has been detected in the serum of PCa patients compared to patients with BPH (Saldova *et al.*, 2011). Expression of α1-6 fucosyltransferase 8 (FUT8), which is involved in the attachment of fucose to the innermost *N*-acetylglucosamine in *N*-glycans is increased in metastatic PCa and is associated with aggressive disease (Wang *et al.*, 2014b).

1.2.4 Glycans and glycoproteins as biomarkers for prostate cancer

“Biomarkers (or biological markers) are any substance, structure, or process that can be measured in the body, or its products, that influence or predict the incidence of outcome or disease” (*WHO International Programme on Chemical Safety Biomarkers in Risk Assessment: Validity and Validation.*, 2001). The main methods to monitor cancer biomarkers include gene expression measurements using DNA, RNA, and microRNA gene arrays and protein microarray technologies. However, increasing interest in the role of glycosylation in cancer has uncovered several new promising glycomics-based

biomarkers, including cancer associated global glycan signatures (Kang *et al.*, 2012; Ozcan *et al.*, 2014; Krishn *et al.*, 2016; Ruhaak *et al.*, 2016) and protein-specific glycosylation changes (Haab *et al.*, 2010; Kim *et al.*, 2016; Drabik *et al.*, 2017).

As a secretory gland, the prostate secretes glycoproteins of all types. The prostate cancer biomarker, PSA has a single N-glycosylation site at asparagine (Asn) 69. A tumour specific PSA glycan signature has recently been identified in which decreased core fucosylation and increased α2,3-linked sialylation of PSA is found in PCa patients compared to healthy controls or BPH patients (Dwek *et al.*, 2010; Sarrats *et al.*, 2010; Gilgunn *et al.*, 2013; Hsiao *et al.*, 2016; Llop *et al.*, 2016). Serum levels of fucosylated PSA (Fuc-PSA) are significantly increased in PCa and can differentiate between aggressive and nonaggressive forms of PCa (Li *et al.*, 2015), whereas decreased urinary Fuc-PSA is associated with high Gleason score (Fujita *et al.*, 2016). This has lead to the development of lectin based immunoassays which can detect changes in the glycosylation patterns of PSA in serum of PCa patients and could potentially improve the accuracy of PCa diagnosis (Bhanushali *et al.*, 2016; Ishikawa *et al.*, 2017).

1.3 ST6 β-galactoside α-2,6-sialytransferase 1 (ST6Gal1)

1.3.1 The structure and function of ST6Gal1

Sialic acids represent a family of nine-carbon sugar neuraminic acids of which N-acetylneuraminic acid (Neu5Ac) is the most common form in humans. Variability comes from their location on cells and molecules. Sialic acids can be linked to sugar molecules through an α2-6-bond to GalNAc or GlcNAc; an α2,3 or α2,6 bond to galactose or through a α2-8-bond to another sialic acid. Sialic acids are hydrophilic molecules with a strong electronegative charge and often found at the terminal end of glycoconjugates. Given their location, sialic acids play a crucial role in regulating molecular and cellular interactions including transmembrane signalling, cell-cell interactions and recognition, differentiation and membrane stabilisation (Traving and Schauer, 1998).

Sialyltransferases are a class of glycosyltransferase enzymes which catalyse the transfer of sialic acid from a common donor substrate, cytidine monophosphate (CMP-sialic acid) to the carbohydrate chain of glycans. At least 20 distinct sialyltransferases have been identified in humans (Table 1.1), which can be divided into 4 subgroups according to their carbohydrate linkage: ST3Gal, ST6Gal, ST6GalNAc and ST8sia (Lu and Gu, 2015).

Abbreviation	Sialyltransferase	Substrate	Glycan specificity
ST3GAL1	ST3 beta-galactoside alpha-2,3-sialyltransferase 1	Galβ1,3GalNAc	O-glycan
ST3GAL2	ST3 beta-galactoside alpha-2,3-sialyltransferase 2	Galβ1,3GalNAc	O-glycan
ST3GAL3	ST3 beta-galactoside alpha-2,3-sialyltransferase 3	Galβ1,3(4)GlcNAc	O-glycan, N-glycan
ST3GAL4	ST3 beta-galactoside alpha-2,3-sialyltransferase 4	Galβ1,4(3)GlcNAc	N-glycan, O-glycan
ST3GAL5	ST3 beta-galactoside alpha-2,3-sialyltransferase 5	Galβ1,4Glc-ceramide	Glycolipid
ST3GAL6	ST3 beta-galactoside alpha-2,3-sialyltransferase 6	Galβ1,4GlcNAc	N-glycan, glycolipid
ST6GALNAC1	ST6 N-acetylgalactosaminide alpha-2,6-sialyltransferase 1	GalβNAcα1, O-Ser/Thr	O-glycan
ST6GALNAC2	ST6 N-acetylgalactosaminide alpha-2,6-sialyltransferase 2	Galβ1,3GalNAcα1, O-Ser/Thr	O-glycans
ST6GALNAC3	ST6 N-acetylgalactosaminide alpha-2,6-sialyltransferase 3	Siaα2,3Galβ1,3GalNAc	O-glycan
ST6GALNAC4	ST6 N-acetylgalactosaminide alpha-2,6-sialyltransferase 4	Siaα2,3Galβ1,3GalNAc	O-glycan
ST6GALNAC5	ST6 N-acetylgalactosaminide alpha-2,6-sialyltransferase 5	GM1b	Glycolipid
ST6GALNAC6	ST6 N-acetylgalactosaminide alpha-2,6-sialyltransferase 6	All α-series gangliosides	Glycolipid
ST6GAL1	ST6 beta-galactoside alpha-2,6-sialyltransferase 1	Galβ1,4GlcNAc	N-glycan
ST6GAL2	ST6 beta-galactoside alpha-2,6-sialyltransferase 2	Galβ1,4GlcNAc	N-glycan
ST8SIA1	ST8 alpha-N-acetyl-neuraminide alpha-2,8-sialyltransferase 1	Siaα2,3Galβ1,4Glc-ceramide	Glycolipid
ST8SIA2	ST8 alpha-N-acetyl-neuraminide alpha-2,8-sialyltransferase 2	Siaα2,3Galβ1,4GlcNAc	N-glycan on NCAMa
ST8SIA3	ST8 alpha-N-acetyl-neuraminide alpha-2,8-sialyltransferase 3	Siaα2,3Galβ1,4GlcNAc	N-glycan on NCAM
ST8SIA4	ST8 alpha-N-acetyl-neuraminide alpha-2,8-sialyltransferase 4	(Siaα2,8)nSiaα2,3Galβ1-R	N-glycan on NCAM
ST8SIA5	ST8 alpha-N-acetyl-neuraminide alpha-2,8-sialyltransferase 5	GM1b, GT1b, GD1a, GD3	Glycolipid
ST8SIA6	ST8 alpha-N-acetyl-neuraminide alpha-2,8-sialyltransferase 6	Siaα2,3(6)Gal	Sialic acid on O-glycan

Table 1.1 Human sialyltransferases.

Table of the 20 different human sialyltransferases discovered to date with their substrate and glycan specificity. Modified from Wang *et al,* 2016.

ST6 β-galactoside α-2,6-sialytransferase 1 (ST6Gal1) is a member of the ST6 sialytransferase family which catalyses the transfer of sialic acid from CMP-sialic acid to galactose containing acceptor substrates on N-glycans in the α-2,6 formation (Weijers *et al.*, 2008). The human ST6Gal1 gene is located on chromosome 3: 186930485 - 187078553 (q27.3). Three mRNA transcript variants have been identified which encode two protein isoforms. All the variants share a common protein coding region (Dall'Olio, 2000). Variants 1 and 2 have different 5′ un-translated regions but both encode the same protein isoform, whereas variant 3 lacks the exon containing the translation start site of variants 1 and 2 and produces a protein isoform with a shorter N-terminus (Figure 1.7).

ST6Gal1 is a trans-membrane protein which is localised to the Golgi apparatus (Fenteany and Colley, 2005). The full length ST6Gal1 protein sequence comprises 406 amino acids; the first nine N-terminal residues are cytoplasimic, followed by a hydrophobic trans-membrane region and a C-terminal catalytic luminal domain (Kuhn *et al.*, 2013). The cytoplasmic domain contains two asparagine-X-serine/threonine (NXS/T) motifs required for N-glycosylation and protein stabilisation (Chen and Colley, 2000). The shorter protein sequence comprises of just 175 amino acids and is missing the N-terminal cytoplasmic and trans-membrane domains and is more likely to be soluble rather than membrane-bound.

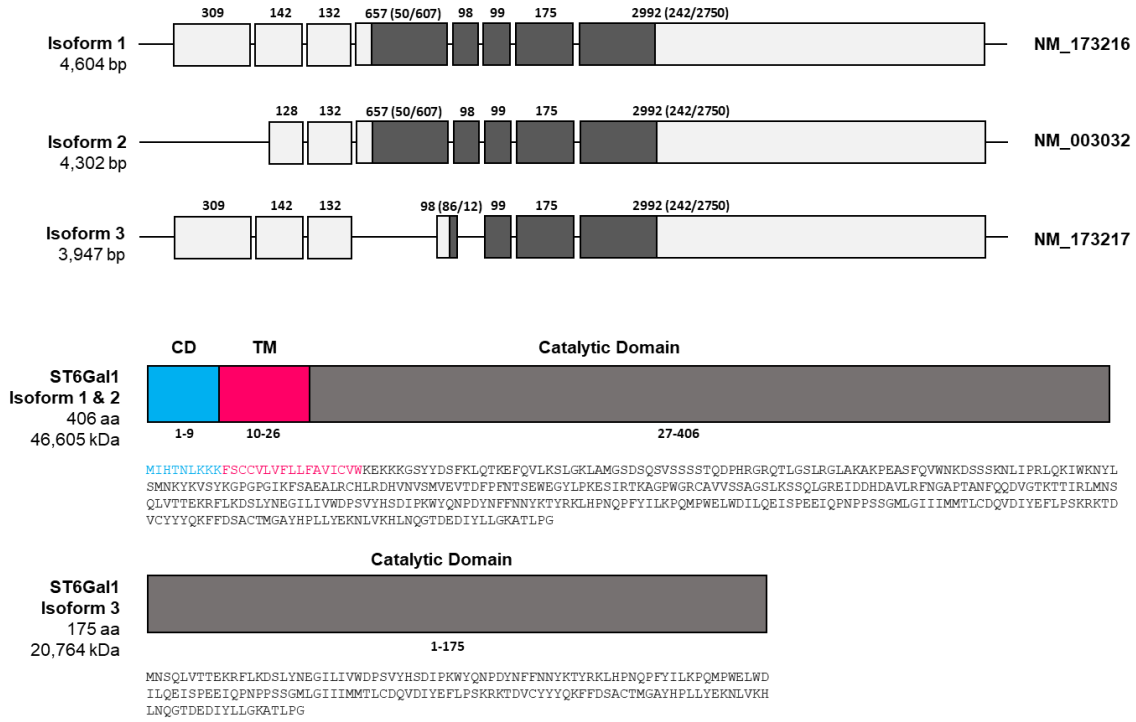

Figure 1.7 ST6Gal1 protein isoforms

There are three ST6Gal1 mRNA transcript variants (NM_173216, NM_003032 and NM_173217), which encode two protein isoforms. Variants 1 and 2 have different 5′ un-translated regions but both encode the same protein, which contains a cytoplasmic N-terminal domain (CD), transmembrane domain (TM) and a catalytic luminal domain.

Variant 3 lacks the exon containing the translation start site of variants 1 and 2 and produces a protein with a shorter N-terminus, lacking the CD and TM.

1.3.2 The role of ST6Gal1 in cancer

Increased sialyation is already known to be associated with cancer cell progression and metastasis affecting cell adhesion, migration and invasion (Seales *et al.*, 2005; Bull *et al.*, 2013; Pinho and Reis, 2015). Up-regulation of ST6Gal1 has been described in several cancers including colon cancer (Dall'Olio *et al.*, 1989), breast cancer (Lin *et al.*, 2002), choriocarcinoma (Fukushima *et al.*, 1998), hepatocarcinoma (Dall'Olio *et al.*, 2004; Poon *et al.*, 2005), cervical cancer (Wang *et al.*, 2001), and myeloid leukaemias (Skacel *et al.*, 1991). Previous studies have shown that ST6Gal1 functions as a regulator of cell survival; α2,6 sialylation of the Fas death receptor reduces apoptotic signalling by obstructing internalisation of Fas after ligand induced activation (Swindall and Bellis, 2011). ST6Gal1 sialylation of tumour necrosis receptor 1 (TNFR1) and the CD45 receptor inhibits apoptosis (Amano *et al.*, 2003; Liu *et al.*, 2011). ST6Gal1 up-regulation promotes cell migration and invasion through its interaction with the β1 integrin and EGFR receptors (Seales *et al.*, 2005; Shaikh *et al.*, 2008; Park *et al.*, 2012), whilst knockdown of ST6Gal1 inhibits metastasis in breast cancer (Lin *et al.*, 2002), osteosarcoma (Meng *et al.*, 2015) and colon cancer (Zhu *et al.*, 2001). Expression of ST6Gal1 promotes TGF- β induced epithelial to mesenchymal transition (EMT), through the down-regulation of E-cadherin mediated cell adhesion and up-regulation of integrin mediated cell migration (Lu *et al.*, 2014). ST6Gal1 expression is an adverse predictor of survival and recurrence in localised clear-cell renal carcinoma (Liu *et al.*, 2014b), whilst in pancreatic cancer, high ST6Gal1 expression was a predictor of poorer patient prognosis (Hsieh *et al.*, 2017). High ST6Gal1 expression also positively correlates with high risk of paediatric acute leukemia (Mondal *et al.*, 2010). Although the role for ST6Gal1 in PCa is yet to be established, a recent study has found that ST6Gal1 expression up-regulated in PCa tumour tissue and is related to poor overall survival and poor progression-free survival (Wei *et al.*, 2016). Knockdown of ST6Gal1 in prostate cancer cell lines significantly inhibits the proliferation, growth, migration and invasion capabilities (Wei *et al.*, 2016). Targeting ST6Gal1 therapeutically has shown potential,

the fluorinated sialic acid analogue P-3F_{ax}-Neu5Ac is a potent inhibitor of α2,3 and α2,6 sialylation (Bull *et al.*, 2013). P-3F_{ax}-Neu5Ac treatment blocks tumour cell adhesion to extra cellular matrix and migration in *vitro* and tumour engraftment in *vivo* (Bull *et al.*, 2013).

Furthermore, increased ST6Gal1 expression can regulate the effects of chemotherapy and radiotherapy treatments. ST6Gal1 over-expression facilitates resistance to the chemotherapy drug cisplatin in ovarian tumour cells (Schultz *et al.*, 2013) and ST6Gal1 knockdown increased cisplatin sensitivity in cervical cancer cells (Zhang *et al.*, 2016). Over-expression of ST6Gal1 enhanced the resistance of chronic myelogenous leukemia (CML) cells to the chemotherapy drugs adriamycin, paclitaxel and vincristine and suppression of ST6Gal1 enhanced sensitivity (Ma *et al.*, 2014). Reciprocally, ST6Gal1 knockdown increased the sensitivity of hepatocarcinoma cells to docetaxel treatment by instigating the process of apoptosis (Chen *et al.*, 2016).

Whilst there are many studies that support the oncogenic role of ST6Gal1 in cancer, there is also contradictory evidence to suggest that ST6Gal1 may also have tumour suppressor potential. Down-regulation of ST6Gal1 in colorectal cancer cell lines increased cell proliferation and tumour growth (Park *et al.*, 2012). ST6Gal1 is down-regulated in invasive bladder cancer compared to normal urothelium and ST6Gal1 expression loss correlates with high grade, invasive clinical tumours (Wild *et al.*, 2005). This expression loss is caused by aberrant ST6Gal1 promoter methylation, suggesting a possible suppressive role for ST6Gal1 in advanced bladder cancer (Antony *et al.*, 2014).

1.4 Alternative splicing in cancer

1.4.1 One gene, multiple mRNAs

The human genome contains around 21,000 protein-coding genes (Clamp *et al.*, 2007), yet it is estimated to produce over one million different protein species (Harrison *et al.*, 2002; Jensen, 2004). This is because almost every human gene can produce more than one mRNA isoform through the use of post-translational modifications including alternative splicing, alternative polyadenylation, RNA editing and epigenetic modulation (Lander, 2011). These transcriptional modifications increase transcriptome complexity and expand the number of proteins encoded by the genome enormously.

1.4.2 Alternative splicing

Alternative splicing (AS) is a common post-transcriptional process that generates multiple distinctive mRNA transcripts from a single gene. In pre-mRNA transcripts, coding exons are interrupted by non-coding introns. Removal of these intronic sequences and the subsequent ligation of exons is achieved by the spliceosome, a large ribonucleoprotein (RNP) complex composed of five different small nuclear RNP (snRNP) subunits (U1, U2, U3, U4, U5 and U6), together with many hundreds of additional proteins (Chow *et al.*, 1977). AS allows different combinations of exons in a gene to be joined to each other generating alternative mRNA transcripts, all of which increase mRNA diversity (Reviewed in (Matlin *et al.*, 2005; Keren *et al.*, 2010). There are several different types of AS events, including competing alternative 5' and 3' splice sites whereby two or more splice sites are differentially recognised at one end of an exon (Figure 1.7 a & b). Mutually exclusive exons are alternatively selected from two or more exons within the pre-mRNA (Figure 1.7 c). Exons within a gene can be included or skipped (Figure 1.7 d). Intronic sequences can remain within the mature mRNA transcript (Figure 1.7 e) and the use of alternative promoters and polyadenylation sites can increase mRNA diversity (Figure 1.7 f & g).

The majority (~95%) of multi-exon genes undergo alternative splicing (Pan *et al.*, 2008). AS has been observed in all tissues, can be can be cell and tissue specific and can occur at different developmental stages. The different translated protein isoforms often have distinct functions and localisations (Stamm *et al.*, 2005). AS is a tightly regulated and complex process, involving hundreds of regulatory factors and proteins, such as RNA-binding proteins, regulatory RNAs, and cis-acting RNA sequences. These cis-acting regulatory sequences are characterised by their location and activity and can be divided into four categories: exon splicing enhancers (ESEs) and silencers (ESSs) and intron splicing enhancers (ISEs) and silencers (ISSs). Splicing enhancers assemble to promote the use of a weak or regulated splice site and silencers repress the use of splice sites. Successful AS can depend upon the expression levels of these splicing regulators (Matlin *et al.*, 2005).

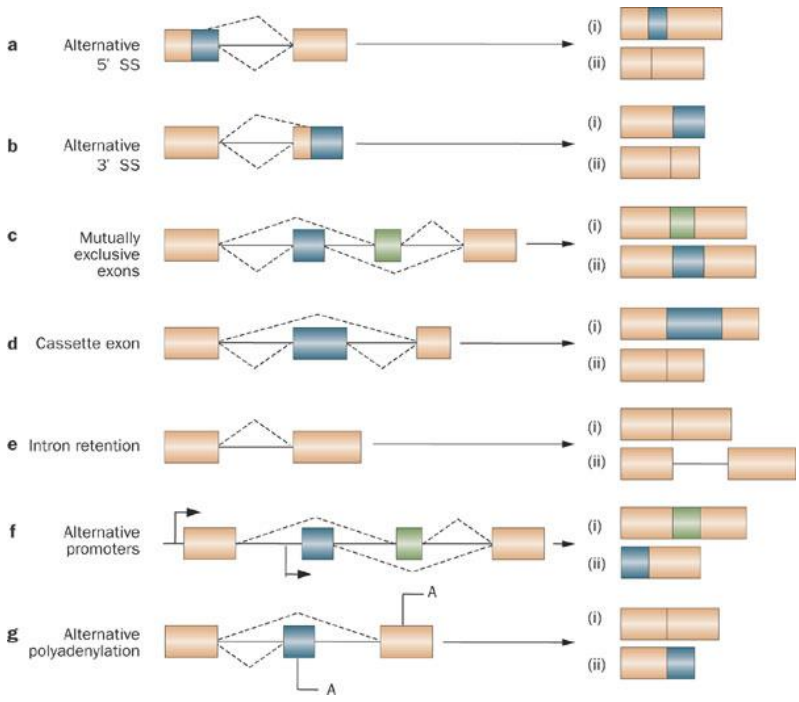

Figure 1.8 Alternative splicing events.

Alternative splicing events and their alternative outcomes: (a) competing 5' splice sites, (b) competing 3' splice sites, (c) mutually exclusive exons, (d) cassette exons, (e) intron

retention, (f) alternative promoters and (g) alternative polyadenylation. Image taken form a review by (Rajan *et al.*, 2009).

1.4.3 Alternative splicing in prostate cancer

Aberrant splicing is a common feature or 'hallmark' in cancer (Venables, 2004; Hanahan and Weinberg, 2011; Ladomery, 2013; Oltean and Bates, 2014). These aberrant splicing events can produce novel mRNA transcripts and altered transcript ratios which have oncogenic properties (Figure 1.9) (reviewed in (Rajan *et al.*, 2009; Sette *et al.*, 2013; Munkley *et al.*, 2017a). As previously mentioned, AR splice variants play a major role in enabling prostate cancer cells to develop hormone resistance (Lu and Luo, 2013). Around 22 AR splice variants have been described, many of which encode protein isoforms, which unlike the full-length AR protein, lack the LBD and can operate in the absence of androgens. The most prevalent AR splice variant, ARv7 is produced by the inclusion of a cryptic exon (3b). Exon 3b is located within intron 3 and introduces a new poly (A) site, creating a truncated protein, which lacks the LBD, the target of enzalutamide and abiraterone treatment. Unlike full length AR, the ARv7 splice variant is located within the nucleus and functions independently of androgen stimulation, regulating the expression of genes involved in cell division (Hu *et al.*, 2012).

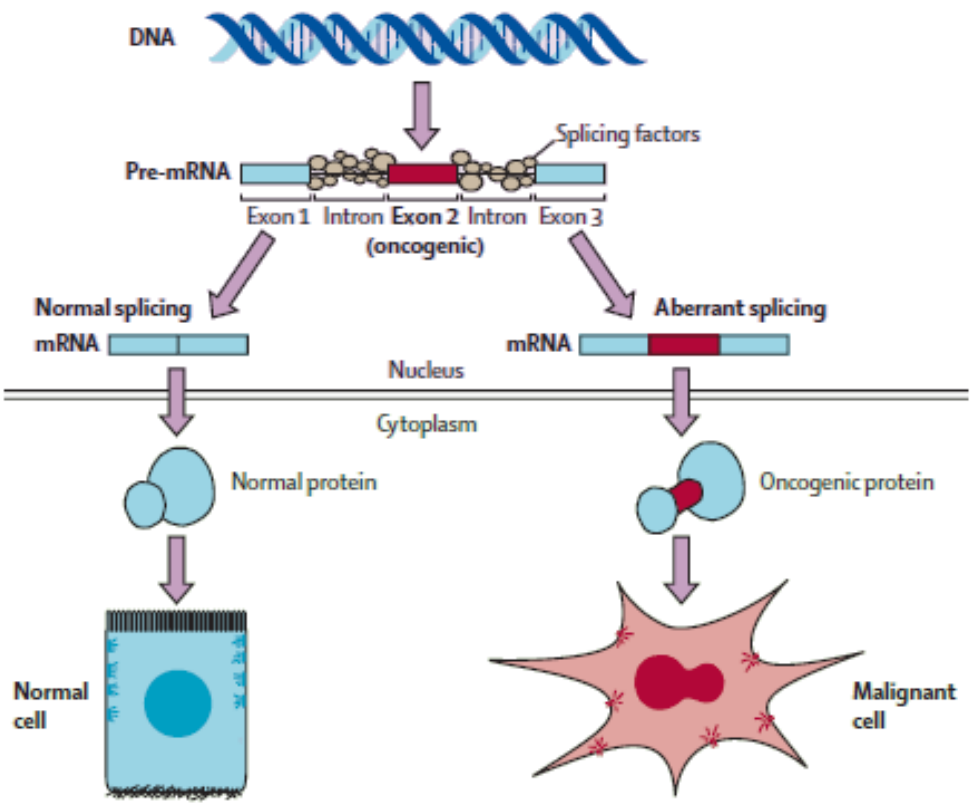

Figure 1.9 Alternative splicing in cancer.

Changes in AS can contribute to tumour progression through the production of oncogenic protein isoforms. Novel protein isoforms or changes in the ratio of pre-existing isoforms can contribute to changes in cell phenotype. Image taken from (Pajares *et al.*, 2007).

There is increasing evidence which suggests ARv7 expression could be used as a potential predictive biomarker and a therapeutic target in advanced prostate cancer. Expression levels of ARv7 RNA transcripts are higher in CRPC tumours compared to hormone-naïve tumours (Hu *et al.*, 2009; Hornberg *et al.*, 2011; Welti *et al.*, 2016). Patients expressing high levels of ARv7 transcripts also have significantly shorter survival than those with low expression (Hornberg *et al.*, 2011; Welti *et al.*, 2016; Qu *et al.*, 2017). The expression and localisation of ARv7 in CTCs from patients with CRPC is

associated with resistance to enzalutamide and abiraterone (Antonarakis *et al.*, 2014) but is not associated with resistance to taxane based chemotherapy (docetaxel or cabazitaxel) (Antonarakis *et al.*, 2015; Onstenk *et al.*, 2015; van Soest *et al.*, 2015). ARv7 detection shows promise as a biomarker of CRPC poor prognosis, and as a predictive marker of enzalutamide or abiraterone resistance (Antonarakis, 2015).

Cancer cells can also exploit the tightly regulated process of alternative splicing to their advantage by disrupting core spliceosome components and regulators. Mis-regulation of several splicing regulators has been observed in clinical PCa tumours including over-expression of the RNA binding proteins *SAM68*, heterogeneous nuclear ribonucleoprotein A2/B1 (*HNRNPA2B1*), DEAD-box helicase 5 (*DDX5,* also known as *p68)* and transformer 2 Beta Homolog (*Tra2-β*) (Busa *et al.*, 2007; Clark *et al.*, 2008; Rajan *et al.*, 2008; Diao *et al.*, 2015; Stockley *et al.*, 2015). Serine-arginine protein kinase 1 (*SRPK1*), a splicing regulator of VEGF is u p-regulated in PCa and correlates with disease stage and invasion (Bullock *et al.*, 2016). Increased expression of the RNA splicing factor serine/arginine repetitive matrix 4 (SRRM4) drives the trans-differentiation to neuroendocrine PCa (Zhang *et al.*, 2015b; Li *et al.*, 2017).

Recent advances in genome annotation and high-throughput technologies such as splicing-specific microarrays and RNA sequencing, have highlighted a number of genes that change their splice isoform expression in PCa compared to normal tissue (Rajan *et al.*, 2011; Erho *et al.*, 2012; Srinivasan *et al.*, 2012). Steroid hormones have been shown to regulate the production of novel isoforms in hormone responsive cancer. Estrogen stimulated novel mRNA isoforms have been shown to affect cell mobility, migration and division in breast cancer which correlates with disease prognosis (Dutertre *et al.*, 2010). Androgen regulated alternative mRNA isoforms have also previously been described (Rajan *et al.*, 2011). The tumour suppressor gene tuberous sclerosis complex 2 (*TSC2*) produces an alternative mRNA isoform derived from an androgen-regulated alternative promoter (Rajan *et al.*, 2011). TSC2 isoform A has been shown to increase cell proliferation in PCa cells (Munkley *et al.*, 2014). Androgens induce the expression of

a novel splice variant of the ST6GalNAc1 protein in PCa cells. This androgen regulated splice variant encodes a shorter protein isoform which is missing 132 amino acids from the N-terminal, but is still fully functional as a sialyltransferase. Expression of this ST6GalNAc1 isoform in PCa cells reduces adhesion, increases motility and promotes a transition towards a mesenchymal like phenotype (Munkley *et al.*, 2015b). Androgen regulated phosphodiesterase 4D7 (PDE4D) alternative promoter isoform switches have also been described; PDE4D7 isoform expression positively correlates with primary tumour development but is significantly decreased in CRPC (Bottcher *et al.*, 2015). The PDE4D5 and PDE4D9 isoforms are significantly down-regulated in primary PCa and CRPC compared to benign samples (Bottcher et al., 2016). This evidence suggests that the AR can switch the pattern of isoforms produced in prostate cancer cells towards those with pro-oncogenic functions.

1.5 Relaxin peptide hormones

1.5.1 The relaxin gene family

Relaxins are peptide hormones that belong to the insulin-like super family. In humans, the family consists of seven cystine-rich peptides; relaxin 1, 2 and 3 (RLN1, RLN2 and RLN3) and the insulin-like peptides INSL3, INSL4, INSL5 and INSL6. The evolutionary history of this family originates from a common ancestor - insulin. Early in the chordate lineage, the peptide relaxin 3 (RLN3) evolved and became the ancestral gene from which successive duplication events give rise to other members of the relaxin family. RLN3 and INSL5 are closely related to each other and cluster within a sub-tree that is distinct from the group comprising RLN1, RLN2, INSL3, INSL4, and INSL6 (Figure 1.10) (Wilkinson et al., 2005).

1.5.2 The structure and function of relaxin peptide hormones

1.5.2.1 RLN1 and RLN2

In higher primates, the *RLN1* gene is thought to be the result of an ancestral duplication of the human *RLN2* gene on chromosome 9 (location 9p24) (Crawford *et al.*, 1984; Arroyo *et al.*, 2014), as other mammals have only have *RLN2*. The *RLN1* and *RLN2* genes share 90% DNA sequence similarity and have 82% predicted sequence identity at amino acid level. All relaxin family peptides are synthesised as pro-hormones with four distinct regions: a signal peptide, a B-chain a C-chain and a COOH-terminal A-chain (Hudson *et al.*, 1981; Haley *et al.*, 1982). The signal peptide is required for secretion of the immature pre-prohormone, whilst the C-chain facilitates protein folding. Following secretion, enzymatic removal of the C-peptide produces an asymmetrical mature peptide heterodimer (Marriott *et al.*, 1992). The relaxin peptides bind to G-protein-coupled-receptors (GPCRs). Both RLN1 and RLN2 peptides signal through the leucine-rich-repeat relaxin family GCPR peptide receptor RXFP1 (previously known as LGR7) (Hsu *et al.*, 2002). Relaxin stimulation of RXFP1 can activate several signalling pathways including the cyclic adenosine monophosphate/protein kinase A (cAMP/PKA) pathway, the mitogen-activated protein kinase/extracellular signal-regulated kinase 1/2 (MAPK/ERK1/2) pathway, the PI3K/Akt pathway and the notch pathway (Zhang *et al.*, 2002; Nguyen *et al.*, 2003; Sun *et al.*, 2003; Halls *et al.*, 2006; Halls *et al.*, 2007; Halls *et al.*, 2009; Boccalini *et al.*, 2015).

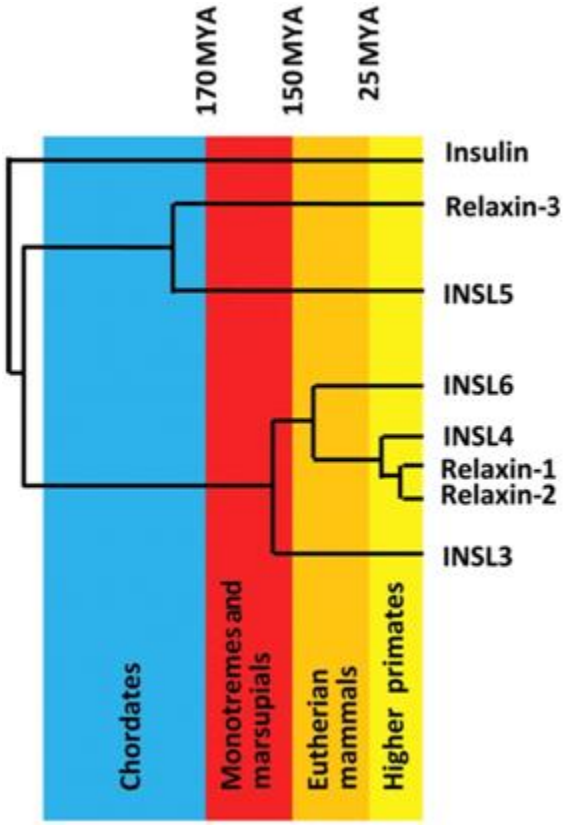

Figure 1.10 Phylogenetic relationships of the relaxin-family peptides. A simplified phylogenetic relationship between relaxin family peptides, insulin, and insulin-like peptides. RLN3 divergence and successive duplication events give rise to the relaxin family. Image taken from (Ivell *et al.*, 2011).

In humans, RLN2 is predominantly known for its roles in reproduction and pregnancy, however it is now clear that it performs vital roles in many other physiological functions. In females, RLN2 is expressed intermittently by the corpus luteum during the luteal phase of the menstrual cycle and by the corpus luteum and placenta during pregnancy (Ivell *et al.*, 1989). During pregnancy, RLN2 acts by promoting cervical development, remodelling and growth of the uterus and in the development of mammary nipples. In addition, RLN2 has also been shown to play an important role in pregnancy related cardiovascular adaptations, such as increased plasma volume, cardiac output and heart rate, as well as decreased blood pressure and vascular resistance (reviewed in (Bathgate *et al.*, 2013).

In males, RLN2 is produced by the secretory epithelial cell of the prostate gland and secreted into the seminal fluid (Yki-Jarvinen *et al.*, 1983; Ivell *et al.*, 1989). Although the function of RLN2 in males is not entirely understood, it is thought to play a role in prostate growth, development of the reproductive tract and sperm motility as the prostate, testis and sperm express the RXFP1 receptor (Hsu *et al.*, 2002; Samuel *et al.*, 2003; Ferlin *et al.*, 2012). Unlike RLN2, the function of the RLN1 remains unclear. Synthetic RLN1 peptides have been shown to activate the RXFP1 receptor and expression of RLN1 mRNA has been detected in prostate cancer cells (Garibay-Tupas *et al.*, 2000).

1.5.2.2 RLN3

The human *RLN3* gene was first discovered in 2002 (Bathgate *et al.*, 2002) and is located on chromosome 19 (19p13.2). RLN3 has a low overall sequence identity to RLN1 (26%) and RLN2 (22%) and is more structurally like INSL5, with a shorter C-chain. RLN3 signals through the RXFP3 receptor but can also activate RXFP1 and RXFP4 receptors (Hsu *et al.*, 2002; Liu *et al.*, 2003a; Liu *et al.*, 2003b). Unlike the other relaxin family members, RLN3 is known to be a neuropeptide. Highest RLN3 expression levels are found in the central nervous system (Smith *et al.*, 2011; Bathgate *et al.*, 2013), but low levels of RLN3 and the receptors RXFP3 and RXFP4 have also been detected in the testes and stromal cells of the prostate (Silvertown *et al.*, 2010). Although the exact physiological mechanisms of RLN3 action in humans remain unclear, recent studies in mice have suggested that RLN3 plays a role in arousal, feeding, anxiety and stress and drug addiction (Ryan *et al.*, 2013; Smith *et al.*, 2014; Hosken *et al.*, 2015; Zhang *et al.*, 2015a; Shirahase *et al.*, 2016).

1.5.3 The role of relaxins in prostate cancer

Relaxin 2 has been shown to promote cancer progression in multiple cancers including breast cancer (Binder *et al.*, 2004), thyroid cancer (Bialek *et al.*, 2011), endometrial cancer (Kamat *et al.*, 2006), osteosarcoma (Ma *et al.*, 2013; Ren *et al.*, 2015) and prostate cancer (Feng *et al.*, 2007; Feng *et al.*, 2009). In PCa, RLN2 expression is

elevated relative to BPH samples (Vinall *et al.*, 2011). RLN2 expression is negatively regulated by androgens and increases during the progression of PCa to androgen independence by promoting tumour growth and vascularisation (Silvertown *et al.*, 2006; Thompson *et al.*, 2006). RLN2 expression is also increased in PCa cells undergoing neuroendocrine differentiation (Figueiredo *et al.*, 2005). RNAi mediated RXFP1 knockdown and inhibition RLN2/ RXFP1 signalling impairs PCa tumour growth and invasion capabilities (Feng *et al.*, 2007; Silvertown *et al.*, 2007). A synthetic RLN2 antagonist (AT-001) has been shown to reduce the growth of human CRPC xenografts by up to 60% (Neschadim *et al.*, 2014). Combined inhibition of the PKA and NF-κB signalling pathways, which are activated by RLN2, reduced PCa tumour growth and induced apoptosis (Vinall *et al.*, 2011).

Although there is a clear role for RLN2 in the progression of prostate cancer, the role of RLN1 is yet to be investigated. Expression levels of RLN1 are up-regulated in LNCaP cells in response to androgens (Tevz *et al.*, 2016) and RLN1 is abundantly expressed in PCa LNCaP cell lines, normal prostate tissue and PCa tissue (Hansell *et al.*, 1991; Gunnersen *et al.*, 1996; Tevz *et al.*, 2016). Recently, a novel fusion transcript has been identified by next generation sequencing which contains incomplete sequences of both RLN1 and RLN2. This fusion transcript is expressed in PCa LNCaP cells and normal prostate tissue and is down-regulated by androgens. The fusion is predicted to encode a protein which contains intact RLN2 functional domains but has lost the signalling peptide sequence essential for secretion (Tevz *et al.*, 2016).

1.6 Research aims and objectives

1.6.1 Preliminary data

Prior to the start of my project RNA sequencing had been used to analyse a single pooled library of PCa LNCaP cells grown in two different media condition: steroid deplete (SD) media and synthetic androgen (10nM R1881) stimulated (A+) media for 24 hours. Our collaborator Dr Ian Mills correlated the up-regulated genes with associated AR binding sites in the genome (Massie *et al.*, 2011). This highlighted three genes, two of which have well known roles in PCa; ATP-binding cassette, sub-family C, member 4 (ABBC4) (Ho *et al.*, 2008) and calcium/calmodulin-dependent protein kinase 2, beta (CAMKK2) (Massie *et al.*, 2011); and a less characterised gene called ST6GALNac1. Work from Dr Jennifer Munkley has shown that ST6GalNAc1 is rapidly induced within the first three hours of androgen stimulation and increased expression is also observed in primary prostate tumours compared to non-malignant prostate tissue. Androgens also induced the expression of a shorter isoform of ST6GalNAc1, which when over-expressed in DU145 cells reduced adhesion and increased the rate of cell migration. Changes in the expression of key epithelial to mesenchymal transition (EMT) markers were also observed suggesting that the shorter isoform may induce a mesenchymal switch in prostate cancer, promoting cell invasion and metastasis (Munkley *et al.*, 2015b).

The original RNA sequencing analysis was carried out on a single pooled library and there were quite a high level of false positives. To remedy this, the RNA sequencing was repeated in separate triplicate samples of LNCaP cells again grown in steroid deplete (SD) and androgen stimulated (A+) conditions for 24 hours. The data produced showed changes in gene expression and mRNA isoform switches that were regulated by androgens. To identify changes that were clinically relevant, a collaborator in Oslo, Dr Daniel Vodak correlated the RNA sequencing data with clinical RNA sequencing data from seven PCa patients before and after ADT (Rajan *et al.*, 2014).

1.6.2 Research aims and objective

The hypothesis of my PhD project was that exposure to androgens will change gene transcription and drive the production of different mRNA isoforms in prostate cancer cells which will be clinically relevant. The main objective was to use the correlated the RNA sequencing datasets to identify and characterise clinically relevant gene expression changes and alternative events.

The combined RNA sequencing identified almost 700 androgen reciprocally regulated gene expression changes and 73 alternative events (56 alternative promoters, 4 alternative 3' ends and 13 alternative splicing events). To focus the project, gene ontology (GO) analysis and a meta-analysis was carried out using publically available datasets. This identified the PCa glycoproteome and specifically a core of seven glycosylation enzymes that significantly changed expression in clinical PCa for further investigation. Of the alternative events, androgen regulated alternative promoter usage were identified for two relaxin genes RLN1 and RLN2. Main aims of my project were to establish the downstream effects and functional properties of one of the glycosylation enzymes, the sialytransferase enzyme ST6Gal1, and the alternative isoforms of RLN1 and RLN2.

Chapter 2

Materials and Methods

Chapter 2 Materials and Methods

2.1 General laboratory practice

All experimental procedures were conducted in accordance with Newcastle University standards for safe working with chemical substances in laboratories, which comply with the Control of Substances Hazardous to Health (COSHH) regulations. Tissue culture experiments were carried out in compliance with regulations for containment of class II pathogens.

2.2 Media and solutions

All media and solutions were prepared in Type 1 (18.2 Mega Ohms) Ultrapure H_20 (dH_2O) produced by Barnstead Nanopure (Thermo Scientific) filtration systems and were sterilised by autoclaving (Astell).

Luria Bertani (LB) medium (500 ml):

5 g sodium chloride (Sigma S3014)

5 g tryptone (Fisher Scientific BPE1421)

2.5 g yeast extract (Fisher Scientific BP1422)

to 500 ml with sterile dH_20

Luria Bertani (LB) agar (500 ml):

5 g chloride (Sigma S3014)

5 g tryptone (Fisher Scientific BPE1421)

2.5 g yeast extract (Fisher Scientific BP1422)

7.5 g agar (Fisher Scientific BP1423)

to 500 ml with sterile dH_20

Media was supplemented with 50 µg/ml ampicillin (Sigma A5354) as appropriate.

1X phosphate-buffered saline (PBS):

1 x 0.1M PBS tablet (Sigma P4417)

to 200 ml with dH_20

50X tris-acetate-EDTA (TAE):

8 g paraformaldehyde (Sigma P6148)

to 200 ml 1X PBS

Tris buffered saline with Tween 20 (TBS-T):

8.75 g sodium chloride (Sigma S3014)

6.5 g Tris base (Sigma T1503)

0.2 % Tween 20 (Sigma P9416)

to 1000 ml with dH_20 - pH to 7.5

Block for protein Western immunoblotting analyses:

1 g skimmed dried milk powder (Asda)

to 20 ml with TBS-T

20% sodium dodecyl sulphate (SDS):

20 g sodium dodecyl sulphate (Sigma 71725)

to 100 ml with dH_20

1X Western blot transfer buffer

2.9 g glycine (Sigma G8898)

5.8 g Tris-base (Sigma T1503)

1.85 ml 20% SDS

200 ml methanol (VWR Chemicals K977)

to 1000 ml with dH_20

2X sodium dodecyl sulphate (SDS) sample loading buffer:

100 mM Tris-HCl (Sigma T5941) - pH 6.8

20 % glycerol (Sigma G9012)

4 % SDS

0.2 % bromophenol blue (Sigma B0126)

200 mM DL-Dithiothreitol (DTT) (Sigma D0632)

10X SDS-polyacrylamide gel electrophoresis (PAGE) running buffer:

30.2 g Tris base (Sigma T1503)

50 ml 20 % SDS

188 g glycine (Sigma G8898)

to 1000 ml with dH_20

4% (w/v) paraformaldehyde (PFA)

8g paraformaldehyde (Sigma P6148)

to 200 ml with 1X PBS

3% (w/v) bovine serum albumin (BSA)

1.5 g bovine serum albumin (Thermo Scientific 10270106)

to 50 ml with 1X PBS

1X Laemmli running buffer

3.02 g Tris-base (Sigma T1530)

18.8 g glycine (Sigma G8898) – pH 8.3

to 1000 ml with dH_20

1M sodium hydrogen phosphate

53.61 g sodium hydrogen phosphate Sigma D5670)

to 200 ml with dH_20

1M monobasic sodium phosphate

119.98 g monobasic sodium phosphate (Fluka 71505)

to 500 ml with dH_20

0.1M sodium phosphate buffer pH 8

93.2 ml 1M sodium hydrogen phosphate

6.8 ml 1M monobasic sodium phosphate

to 1000 ml with dH_20

2.3 Standard molecular biology techniques

2.3.1 Polymerase chain reactions (PCR)

2.3.1.1 Colony PCR

PCR screening of transformed bacterial colonies was performed using GoTaq G2 DNA polymerase (Promega M7845). The template was a single bacterial colony (picked using a sterile 20 µl filter tip). Primers used are listed in appendix B.

Reaction mixes were set up as follows:

Reagent	**Volume (µl)**
5X green GoTaq buffer	5
dNTPs (10 mM)	0.5
Forward primer (10µM)	0.5
Reverse primer (10µM)	0.5
GoTaq G2 DNA polymerase	0.125
RNAse-free H_20	to 25

Table 2.1 Standard PCR reaction mix for colony PCR.

PCR was carried out using the SensoQuest Thermal Cycler (Geneflow) as follows:

Stage	Temperature	Time
1. Initial denaturation	95 °C	5 minutes
2. Denaturation	95 °C	30 seconds
3. Annealing	58 °C	30 seconds
4. Extension	72 °C	variable depending on product size (cycle to step 2 x 29)
5. Final Extension	72 °C	5 minutes
6. Cooling	4 °C	∞

Table 2.2 Thermocycler programme for colony PCR.

The size of the PCR products was verified by agarose-TAE gel electrophoresis.

2.3.1.2 Reverse transcription PCR (RT-PCR)

cDNA was transcribed from RNA using SuperScript VILO cDNA Synthesis Kit (Thermo Scientific 11754-250), following the standard manufacturer's instruction (see section 2.3.3 RNA extraction and cDNA synthesis). The cDNA was used as a template for PCR amplification using GoTaq G2 DNA polymerase (Promega M7845). Primers used are listed in appendix B.

Reaction mixes were set up as follows:

Reagent	Volume (µl)
5X colourless GoTaq buffer	5
dNTPs (10 mM)	0.5
Forward primer (10µM)	0.5
Reverse primer (10µM)	0.5
Alternative primer (10µM)	0.5
cDNA template (50ng/µl)	2
GoTaq G2 DNA polymerase	0.125
RNAse-free H_20	to 25

Table 2.3 Standard PCR reaction mix for RT-PCR.

PCR was carried out using the SensoQuest Thermal Cycler (Geneflow) as follows:

Stage	Temperature	Time
1. Initial denaturation	95 °C	2 minutes
2. Denaturation	95 °C	30 seconds
3. Annealing	58 °C	30 seconds
4. Extension	72 °C	variable depending on product size (cycle to step 2 x 29)
5. Final Extension	72 °C	5 minutes
6. Cooling	4 °C	∞

Table 2.4 Thermocycler programme for RT-PCR.

PCR products were quantified using the QIAxcel Advanced System (Qiagen) multi-capillary electrophoresis.

2.3.1.3 Cloning PCR (nested PCR)

Initial PCR reactions were performed using Phusion High-Fidelity DNA polymerase (Thermo Scientific F-530S). Primers used are listed in Appendix B.

Reaction mixes were set up as follows:

Reagent	**Volume (µl)**
5X HF reaction buffer	10
dNTPs (10 mM)	1
Forward primer (10µM)	2.5
Reverse primer (10µM)	2.5
DMSO	1.5
cDNA template (50ng/µl)	4
RNAse-free H_20	to 50
Phusion DNA polymerase	0.5

Table 2.5 Standard PCR reaction mix for initial nested PCR.

PCR was carried out using the SensoQuest Thermal Cycler (Geneflow) as follows:

Stage	Temperature	Time
1. Initial denaturation	98 °C	30 seconds
2. Denaturation	98 °C	20 seconds
3. Annealing/Extension	72 °C	45 seconds (cycle to step 2 x 34)
4. Final Extension	72 °C	10 minutes
5. Cooling	4 °C	∞

Table 2.6 2-step thermocycler programme for initial nested PCR.

PCR products were column purified using QIAquick PCR Purification Kit (Qiagen 28106), following the standard manufacturer's instruction and eluted into 30 µl dH_2O. The PCR products were quantified and used in a subsequent PCR reaction with primers deigned with specific restriction sites. The PCR reaction was performed using Phusion High-Fidelity DNA polymerase (Thermo Scientific). Primers used are listed in Appendix B.

Reaction mixes were set up as follows:

Reagent	Volume (µl)
5X HF reaction buffer	10
dNTPs (10 mM)	1
Forward primer (10µM)	2.5
Reverse primer (10µM)	2.5
DNA template (50ng/µl)	-
RNAse-free H_20	to 50
Phusion DNA polymerase	0.5

Table 2.7 Standard PCR reaction mix for cloning PCR.

PCR was carried out using the SensoQuest Thermal Cycler (Geneflow) as follows:

Stage	Temperature	Time
1. Initial denaturation	98 °C	30 seconds
2. Denaturation	98 °C	10 seconds
3. Annealing	64 °C	20 seconds
4. Extension	72 °C	30 seconds (cycle to step 2 x 31)
5. Final Extension	72 °C	5 minutes
6. Cooling	4 °C	∞

Table 2.8 Thermocycler programme for cloning PCR.

The size of the PCR products was verified by agarose-TAE gel electrophoresis. DNA fragments were purified from the agarose gel using the QIAquick Gel Extraction Kit (Qiagen 28706) according to manufacturer's instructions and eluted into 30 µl dH_2O.

2.3.1.4 Quantitative real-time PCR (qPCR)

Relative gene expression was determined by quantitative real-time PCR (qPCR) using a SYBR Green PCR Master Mix Kit (Applied Biosystems 4309155) and the QuantStudio 7 Flex Real-Time PCR System (Applied Biosystems). cDNA was synthesised as described in section 2.3.3 and diluted 1:20 with RNase-free water prior to qPCR.

1X SYBR Green reaction mixes were set up as follows:

Reagent	Volume (µl)
2X SYBR Green PCR master mix	5
Forward primer (10µM)	1
Reverse primer (10µM)	1
RNAse-free H_20	2
TOTAL	9

Table 2.9 Standard 1X SYBR Green PCR reaction mix for quantitative PCR (qPCR).

For each reaction, 9µl of PCR master mix was added per well to a 384-well qPCR plate, 1µl of the diluted cDNA was added per well and the plate was sealed with MicroAmp Optical Adhesive Film (Thermo Scientific 4311971). All qPCR experiments were performed using 3 biological replicates and a 'no template control' (NTC) reaction was used for each master mix.

The thermo-cycling conditions used were as follows:

Stage	Temperature	Time
1. Hold	95 °C	20 seconds
2. PCR	95 °C	1 second
	60 °C	60 seconds (cycle to step 2 x 39)
3. Melt curve	95 °C	15 seconds
	60 °C	1 minute
4. Dissociation	95 °C	15 seconds

Table 2.10 Thermocycler programme for SYBR Green quantitative PCR (qPCR).

Gene expression was calculated relative to three housekeeping genes β-*Actin (A CTB)*, *glyceraldehyde-3-phosphate dehydrogenase* (*GAPDH)* and β-*Tubulin (TUBB)*. Ct values for each sample were calculated using QuantStuio 7 System Software v1.0 (Applied Biosystems). Melt curves were checked to ensure a single product and NTC's checked for contamination. Relative mRNA expression was calculated using the $2^{-\Delta\Delta Ct}$ method. Primers used are listed in Appendix B.

2.3.2 Gel electrophoresis

2.3.2.1 Agarose TAE gel electrophoresis

DNA samples containing 5X green GoTaq reaction buffer were fractionated by submerged horizontal 1.3% w/v agarose gel electrophoresis in 1X TAE buffer at a constant voltage of 80-100 volts (Owl EC-105 power supply).

1.2% w/v agarose gels were cast as follows:

1.2 g molecular grade agarose (Bio-line 41025)

1X TAE buffer

70 µl 1000X Gel-red nucleic acid gel stain (Biotium 41003)

Sizes of DNA fragments were determined by comparison with a 1Kb Plus DNA ladder (Thermo Scientific 10787018; sizes are 12-2 Kb in evenly spaced 1 Kb intervals and 1650bp, 850bp, 650bp, 400bp, 300bp, 200bp, 100bp). Bands were visualised under ultraviolet light using the GelDoc-IT Imaging System (UVP). Images were printed using a Digital Graphic Printer (Sony UP-D897).

2.3.2.2 Capillary gel electrophoresis (QIAxcel)

RT-PCR samples were diluted with 1:1 with QIAxcel DNA dilution buffer (Qiagen 929601) and electrophoresed using the QIAxcel multi-capillary electrophoresis system for analysis. Samples were analysed using the QIAxcel Biocalculator Software to determine the size of each PCR product and the relative concentration of each band (ng/µl).

2.3.2.3 SDS polyacrylamide gel electrophoresis (SDS-PAGE)

Protein samples for analysis by SDS-PAGE were pulse sonicated to disrupt any intact DNA and denatured at 100°C for 5 minutes and centrifuged briefly before loading onto an SDS-PAGE gel. Gels were made with a 4% stacking gel (0.125 mM Tris pH 6.8, 0.1%

SDS, 0.1% ammonium persulphate (APS), 0.2% tetramethylethylenediamine (TEMED) and 4% acrylamide) with either a 8%, 10% or 12% acrylamide resolving gel (375 mM Tris pH 8.8, 0.1% SDS, 0.1% APS, 0.2% TEMED and either 8%, 10% or 12% acrylamide) depending on the sizes of proteins to be resolved. SDS-PAGE gels were run in 1X SDS-PAGE running buffer at 100 volts (Bio-Rad Pac 200) until the dye front reached the bottom of the gel. Protein sizes were estimated using Page Ruler Plus Pre-Stained Protein Ladder (Thermo Scientific 26619) 10 to 250 kDa.

2.3.3 RNA extraction and cDNA synthesis

Total RNA was extracted from cultured cells using TRIzol reagent (Thermo Scientific 15596026), following the manufacturer's instructions. Briefly, cell pellets were re-suspended in 1 ml TRIzol reagent and incubated at room temperature for 5 minutes. 200 µl of chloroform (Sigma C2432) was added and the samples vortexed for 15 seconds to mix. After further incubation at room temperature for 3 minutes, the samples were centrifuged at 9,000 rpm for 15 minutes in a cooled centrifuge (4°C) (Eppendorf 5417R). The top aqueous layer was transferred to a new tube and 500 µl of 100% isopropanol (VWR Chemicals 20880.320) and 1 µl of GlycoBlue Coprecipitant (Thermo Scientific AM9516) were added to precipitate the RNA. The samples were incubated at room temperature for 10 minutes and then centrifuged again at 9,000 rpm for 15 minutes in a cooled centrifuge (4°C). The supernatant was removed and the RNA pellet washed in 75% ethanol (VWR Chemicals 20821.330). The RNA pellet was centrifuged at 5,500 rpm for 5 minutes in a cooled centrifuge (4°C). The supernatant was removed and the RNA pellet was left to air dry at room temperature (5-10 minutes). The RNA pellet was re-suspended in 30 µl nuclease free dH_2O and incubated at 55ºC for 10 minutes. RNA was quantified using a NanoDrop Spectrophotometer (NanoDrop Technologies). RNA not used was stored at -80°C.

RNA was treated with DNase I (Sigma 10104159001) and cDNA was transcribed from RNA using SuperScript VILO cDNA Synthesis Kit (Thermo Scientific 11754-250), following the standard manufacturer's instruction. Reaction mixes were set up as follows:

Reagent	Volume (µl)
5X VILO reaction mix	1
10X SuperScript enzyme mix	0.5
1 µg RNA	-
RNAse-free H_20	to 5

Table 2.11 Standard SuperScript VILO cDNA synthesis reaction mix.

PCR was carried out using the SensoQuest Thermal Cycler (Geneflow) as follows:

Stage	Temperature	Time
Initial incubation	25 °C	10 minutes
RT Incubation	42 °C	2 hours
Termination	85 °C	5 minutes
Cooling	4 °C	∞

Table 2.12 Thermocycler programme for SuperScript VILO cDNA synthesis.

2.4 Molecular cloning

2.4.1 Restriction digests

Restriction digests were performed on purified PCR products and selected vectors. For each reaction, approximately 1 µg of vector or PCR product was digested using 10 units of the appropriate restriction enzymes with the appropriate buffer (Promega or New England Biolabs) in a total volume of 50 µl. Samples were incubated at 37°C for 2-3 hours (or the optimum temperature for the enzyme suggested by the manufacturer), followed by an incubation at 65°C for 10 minutes to inactivate enzyme activity. For removal of any unincorporated dNTPs, enzymes and buffers the samples were purified using a QIAquick PCR Purification Kit (Qiagen 28106) according to the manufacturer's instructions and eluted into 30 µl dH_2O. The DNA concentration of each sample after the restriction digest was determined using a Nanodrop Spectrophotometer. Genes, vectors, restriction enzymes and recleave enzymes are listed in Table 2.13

Gene	Vector	Restriction sites	Recleave
ST6Gal1	p3xFLAG CMV-10 (Sigma E7658)	*NotI* / *BamHI*	*XbaI*
ST6Gal1	pcDNA4/TO (Thermo Scientific V102020)	*HindIII* / *XbaI*	*BamHI*
ST6Gal1	pcDNA5/FRT/TO (Thermo Scientific V652020)	*BamHI* / *XhoI*	*NotI*
RLN1 promoter 2	pET-32a (+) (Merk Millipore 69016)	*BamHI* / *XhoI*	*HindIII*
RLN1 promoter 2	pGEX-5X-1 (GE Life Sciences 28-9545-53)	*EcoRI* / *XhoI*	*SalI*

RLN1 promoter 1	p3XFLAG-CMV-10 (Sigma E7659)	*HindIII/BamHI*	*XbaI*
RLN1 promoter 2	p3XFLAG-CMV-10 (Sigma E7659)	*HindIII/BamHI*	*XbaI*
RLN2 promoter 1	p3XFLAG-CMV-10 (Sigma E7659)	*HindIII/XbaI*	*EcoRI*
RLN2 promoter 2	p3XFLAG-CMV-10 (Sigma E7659)	*HindIII/XbaI*	*EcoRI*

Table 2.13 Vectors and restriction sites used for cloning.

2.4.2 Antarctic phosphatase treatment

All plasmids were further treated with Antarctic Phosphatase (New England Biolabs M0289S) to prevent re-circularisation during ligation. For this the cut plasmids were combined with 5 units of Antarctic phosphatase and Antarctic phosphatase reaction buffer in a total volume of 100 µl. Samples were incubated at 37°C for 1 hour and the enzyme inactivated at 65°C for 10 minutes. For removal of any enzymes and buffers the samples were purified using a QIAquick PCR Purification Kit (Qiagen 28106) according to the manufacturer's instructions and eluted into 30 µl dH_2O. The concentration of each plasmid after Antarctic Phosphatase treatment was determined using a Nanodrop Spectrophotometer.

2.4.3 Ligation

Following purification and quantification of the digested PCR products and plasmids, the two fragments were ligated using T4 DNA Ligase (Promega M1801). The following equation was used to determine the concentration of DNA insert when using a 1:10 molar ratio of plasmid to insert DNA:

$$\frac{\text{ng of vector} \times \text{kb size of insert}}{\text{kb size of plasmid}} \times \text{molar ratio of } \frac{\text{insert}}{\text{plasmid}} = \text{ng of DNA insert}$$

The appropriate volume of plasmid and insert DNA were ligated in a 20 µl reaction volume including 1 unit of T4 DNA Ligase and T4 DNA Ligase Buffer. Ligations were incubated at 22°C for 3 hours in the SensoQuest Thermal Cycler (Geneflow). To remove any non-digested or re-circularized plasmid background the ligation mixes were re-cleaved with restriction enzymes. Re-cleavage mixes were incubated at 37°C for 2 hours, followed by heat inactivation at 65°C for 15 minutes.

2.4.4 Heat shock transformation

Ligated plasmids were transformed in *E. coli* DH5α competent cells using the heat shock protocol. 10 µl of ligated plasmids and 100 µl *E. coli* DH5α cells were incubated on ice for 30 minutes. The samples were placed in a heat block at 42°C for 2 minutes then transferred back to ice for 5 minutes. Cells were allowed to recover in 300 µl of LB broth at 37°C in a MaxQ 8000 shaker (Thermo Fisher Scientific) at 225 rpm for 30 minutes. LB agar plates containing 50µg/ml ampicillin were used to grow and select competent cells which had been transformed. The LB agar plates were incubated at 37°C overnight. Single colonies from the plates were picked and grown in 5 ml LB broth plus 50 µg/ml ampicillin and the tubes were incubated at 37°C in the shaker overnight. The cultures were centrifuged at 5,000 rpm for 5 minutes to pellet the cells (Rotanta 460R Benchtop Centrifuge). Plasmid DNA was extracted from the cells using a QIAprep Miniprep Kit (Qiagen 27106) following manufacturer's instructions.

2.4.5 DNA sequencing

Plasmids were sent for DNA sequencing at Source Bioscience Lifescience Services to confirm the correct sequences had been cloned.

2.5 Protein methods

2.5.1 Isolation of protein extracts from cultured cells

To isolate protein extracts from cultured cells the culture media was removed and cells were washed in PBS to remove any remaining serum. Following addition of 1 ml of 1X Trypsin-EDTA (Thermo Scientific 25300054), cells were incubated at 37°C for 5 minutes. Cell suspensions were harvested in fresh media, and samples pelleted at 3,000 rpm for 10 minutes. Cell pellets were re-suspended in 2X SDS sample loading buffer.

2.5.2 Bacterial expression of fusion proteins

For expression of glutathione s-transferase (GST) and histidine-tagged fusion proteins, *E. coli* BL21 competent cells were transformed with the appropriate plasmid encoding the fusion protein. 1 µl of plasmid DNA and 100 µ of competent *E. coli* BL21 competent cells were incubated on ice for 20 minutes. Samples were placed in a heat block at 42°C for 1 minute then transferred back to ice for 5 minutes. Cells were allowed to recover in 1 ml of LB broth at 37°C in a MaxQ 8000 shaker (Thermo Scientific) at 225 rpm for 1 hour. LB agar plates containing 50µg/ml ampicillin were used to grow and select competent cells which had been transformed. The LB agar plates were incubated at 37°C overnight. For protein expression, single colonies from the plates were picked and grown in 5 ml LB broth plus 50 µg/ml ampicillin and the tubes were incubated at 37°C in the shaker overnight. 100ml of LB broth was inoculated with 1ml of the overnight culture. These cultures were incubated with shaking at 37°C for 3 hours or until an optical density of 0.5 at A600nm was reached. At this point 500 µl samples of the cultures were taken to compare with the protein expression profile after induction. To induce protein expression from the plasmids, isopropyl β-D-1-thiogalactopyranoside (IPTG) (Sigma

I6758) was added to the 100 ml cultures to a final concentration of 1 mM and incubated at 37°C for a further 3 hours. After induction, further 500 µl samples were taken and the remaining cultures were centrifuged in a cooled centrifuge (4°C) at 3,000 rpm for 10 minutes and the supernatants removed. To test for the induction of protein expression, the 500 µl samples taken before and after induction were analysed by SDS-PAGE, checking for the presence of fusion protein in the post induction sample.

2.5.3 Purification of fusion proteins

2.5.3.1 Glutathione agarose purification of GST-tagged fusion peptide

The bacterial cell pellets containing the GST-fusion proteins were re-suspended in 10 ml 1X PBS. 2 mg of Lysozyme (Sigma L1667) was added and the samples were incubated at room temperature for 20 minutes to lyse the cells. The samples were then pulse sonicated on ice to disrupt intact DNA. 1mM dithiothreitol (DTT) (Thermo Scientific R0861), 2% Triton-X 100 (Plusone 17-1315-01), 1X phenylmethanesulfonyl fluoride (PMSF) (Sigma P7626) and 200 units of DNase I (Sigma 10104159001) were added to the samples which were incubated with shaking at room temperature for 30 minutes. 5 ml 1M potassium chloride was added and the sample volume was made up to 20 ml with 1X PBS. The samples were pulse sonicated on ice and then freeze thawed in an ethanol dry ice bath. At this point, 500 µl samples were taken to assess the solubility of the fusion protein for purification under non-denaturing conditions. The remaining sample was centrifuged in a cooled centrifuge (4°C) at 3,000 rpm for 10 minutes, retaining the supernatant and discarding the pellet containing any insoluble material. The samples from before and after centrifugation were analysed by SDS-PAGE, examining for the presence of the fusion protein in the supernatant after centrifugation. For purification of the peptide, 50 mg of glutathione agarose (Sigma G4510) was re-suspended in 1 ml dH_2O and incubated at room temperature for 2 hours with rotation. The glutathione agarose was washed four times in 1X PBS and after the last wash re-suspended in an equal volume of PBS to create 50 % slurry. 300 µl of the slurry was added to 10 ml of the cell lysates containing the GST-fusion proteins and incubated at 4°C with rotation for 30 minutes. Samples were centrifuged at 3,000 rpm for 5 minutes and the supernatants

removed. Samples were washed six times in 1ml of wash buffer. The glutathione agarose with the GST-fusion protein attached were re-suspended in an equal volume of PBS and stored at 4°C.

2.3.5.2 NiCAM resin purification of histidine-tagged fusion peptide

The bacterial pellets containing the histidine tagged fusion proteins were re-suspended in 10 ml Equilibration Buffer (50 mM sodium phosphate pH 8.0, 0.3 M sodium chloride and 10 mM imidazole). 2 mg of Lysozyme (Sigma L1667) was added to each sample and incubated for 20 minutes at room temperature. Samples were then pulse sonicated on ice and 200 units of DNase I (Sigma 10104159001) was added and incubated with shaking at room temperature for 30 minutes. The samples were sonicated again and freeze-thawed between -80°C and room temperature. The samples were again pulse sonicated on ice and then freeze thawed in an ethanol dry ice bath. At this point, a 500 µl sample was taken to assess the solubility of the fusion proteins for purification under non-denaturing conditions as before. The samples were centrifuged at 14,000 rpm in a cooled centrifuge (4°C) for 10 minutes, retaining the supernatant and discarding the pellet containing any insoluble material. For attachment to nickel resin, Ni-CAM HC Resin (Sigma N3158) was re-suspended in dH_2O to form a 50% slurry and washed three times in dH_2O, followed by three washes in Equilibration buffer. 1 ml of 50% slurry was added to 10 ml of each of the cell lysates containing the fusion proteins and incubated with rotation for 1 hour at room temperature. The samples were centrifuged at 3,000 rpm in a cooled centrifuge (4°C) and the supernatants discarded. The samples were then washed six times in Wash buffer (50 mM sodium phosphate pH 8.0, 0.3 M sodium chloride and 20 mM imidazole). 1 ml of Elution Buffer (50 mM sodium phosphate pH 8.0, 0.3 M sodium chloride and 250 mM imidazole) was added to the samples and incubated with rotation for 10 minutes at room temperature. The samples were then centrifuged at 3000 rpm for 30 seconds and the supernatants retained. The elution process was repeated three times and the supernatants retained. The NiCAM resin with the histidine-fusion protein attached were stored at 4°C.

2.6 Immunological methods

2.6.1 Generation of antibody

GST-fusion peptides were purified and resolved by SDS-PAGE using preparative gels, made with a non-toothed comb. The gels were then washed in dH_2O and stained with Aqueous Coomassie Brilliant Blue (0.1% Coomassie Brilliant Blue Dye (Thermo Scientific 20279) dissolved in 1X Laemmli running buffer) and de-stained with 1X SDS-PAGE running buffer without SDS. The protein bands were excised from the gels using a clean scalpel and frozen at -80°C. The excised gel slices containing the protein were then ground to a fine powder using liquid nitrogen and a pestle and mortar on dry ice. The powdered antigens were used to inoculate a rabbit (immunization was carried out by Scottish Diagnostics, Pentlands Science Park, Midlothian, Scotland). Two further injections of the antigens were given after one and two months. After three months of the immunization program, sera from the animals were collected for antibody purification.

Total IgG was separated from the rabbit sera using caprylic acid (Sigma C2875). 20 ml of the sera was diluted 80 ml of 60 mM sodium acetate pH 4.0. For each ml of sera, 25 µl of caprylic acid was added dropwise whilst stirring to precipitate non-IgG proteins. The mixtures were incubated with stirring at room temperature for 30 minutes and then centrifuged at 10,000 rpm in a cooled centrifuge (4°C) for 30 minutes. The supernatant was filtered to remove the protein precipitate. The resulting IgG was neutralised with 10 ml of 10X PBS and cooled to 4°C. To precipitate the IgG, 0.277 g/ml ammonium sulphate was added slowly and incubated with stirring for 30 minutes at 4°C. IgG was collected by centrifuging at 10,000 rpm in a cooled centrifuge (4°C) for 15 minutes and the supernatants discarded. IgG was re-suspended in 1 X PBS and dialysed overnight against 1X PBS. The IgG solution was removed from the dialysis tubing, sodium azide (Sigma 71289) was added to 0.05% and stored at 4°C.

The histidine-tagged fusion peptide was reduced by adding 1M DTT to a final concentration of 0.1M and incubated at 37°C for 1 hour then desalted over a PD-10

column contain Sephadex G-25 resin (GE Life Sciences 17085101), following manufacturer's instructions. The desalted histidine-tagged fusion peptide was coupled to SulfoLink Resin (Thermo Scientific 20401) in Poly-Prep Chromatography Columns (Bio-Rad 731-1550) following manufacturer's instructions. Non-specific sites were blocked with 50 mM cysteine (Sigma C7755). The column was washed with 10 mM Tris pH 7.5, followed by washes with 100 mM glycine pH 2.5, 10 mM Tris pH 8.8, 100 mM triethylamine pH 11.5 and 10 mM Tris pH 7.5. Isolated IgG was run through the column to attach the antibody and the column was washed with 10 mM Tris pH 7.5 and then with 10 mM Tris pH 7.5 containing 0.5 M sodium chloride. For elution of the antibody under acidic conditions, 100 mM glycine pH 2.5 was added to the column in 850 µl fractions and the collected 850 µl elutions neutralised by adding to 150 µl 1M Tris pH 8.0. The column was then washed with 10 mM Tris pH 8.8. The fractions were assayed for protein content using the Bradford Protein Assay Dye (Bio-Rad 5000006) and the protein positive fractions were dialysed overnight against 1X PBS and analysed by SDS- PAGE. 10% glycerol and 0.05% sodium azide were added to the antibody for long term storage at -80°C.

2.6.2 Western immunoblotting

Electrophoresed samples on SDS PAGE gels were electro-blotted onto Immobilon-P PVDF transfer membrane 0.45 µm (Merk Millipore IPVH00010) using a Trans- Blot SD Semi-Dry Transfer Cell (Bio-Rad) and 1X Western blot transfer buffer at a constant voltage of 15 V for 30 minutes. Membranes were stained with Ponceau S Solution (Sigma P7170) to determine protein blotting efficiency and washed in TBS-T. Membranes were blocked in blocking solution (TBS-T with 5% non-fat dry milk) for one hour with rotation. The blocking buffer was removed and membranes incubated with primary antibody for 1 hour at room temperature or overnight at 4°C with rotation. Membranes were washed three times in TBS-T (5-10 mins/wash) and incubated with a secondary antibody conjugated to horseradish peroxidise for 1 hour at room temperature with rotation. Membranes were further washed three times in TBS-T (5-10 mins/wash). Membranes were incubated for 1 min with Amersham enhanced chemiluminescent (ECL) Western Blotting Detection Reagent (GE Life Science RPN2106), mixed at a ratio of 1:1.

Excess ECL was removed and the membranes were exposed to medical X-ray film (Konica Minolta A9LS). Bands were developed using a SRX-101A X-ray film processor (Konica Minolta). Primary and secondary antibodies used for Western immunoblotting are listed in Table 2.14. All Western blot images are representative of at least 3 repeats.

Antibody	Species	Supplier	Dilution
ST6GAL1	Rabbit polyclonal	Abgent (AP19891c)	1:1000
E-cadherin	Rabbit polyclonal	Proteintech (20874-1-AP)	1:100
N-cadherin	Rabbit monoclonal	Cell Signaling (D4R1H)	1:1000
Vimentin	Mouse monoclonal	GeneTex (GTX629743)	1:1000
Desmoplakin	Rabbit polyclonal	Bethyl (A303-356A-T)	1:1000
SNAI1	Rabbit polyclonal	GeneTex (GTX125918	1:1000
Slug	Rabbit polyclonal	GeneTex (GTX128796)	1:1000
Twist 1/2	Rabbit polyclonal	GeneTex (GTX127310)	1:1000
Fibronectin	Rabbit polyclonal	Sigma-Aldrich (HPA027066)	1:1000
Relaxin 2	Mouse monoclonal	Abcam (ab183505)	1:1000
FLAG M2	Mouse monoclonal	Sigma-Aldrich (F3165)	1:2000
GAPDH	Rabbit polyclonal	Abgent (AP7873b)	1:1000
Actin	Rabbit polyclonal	Sigma-Aldrich (A2066)	1:1000
α-Tubulin	Mouse monoclonal	Sigma-Aldrich (T5168)	1:2000
Rabbit IgG - HRP	Goat	Jackson (111-035-003)	1:2000
Mouse IgG - HRP	Sheep	GE Lifesciences (NA931vs)	1:2000

Table 2.14 Primary and secondary antibodies used for Western immunoblotting.

2.6.3 Immunohistochemistry (IHC)

Prior to IHC on prostate cancer tissue microarrays (TMA), antibodies were optimised on test TMA slides. Antigen retrieval was performed by pressure cooking the TMA in 10 mM citrate pH 6.0 followed by staining the tissues with serial antibody dilutions. Antibodies were validated using blocking peptides to determine specificity and rule out non-specific binding. Bound antibodies were visualised using biotinylated secondary antibodies and streptavidin horseradish peroxidase complex kit with DAB chromogen (Vectorlabs SK-4100). Slides were counter-stained with haematoxylin (Sigma H9627) and dehydrated through graded alcohols and xylene (Sigma 296325) before mounting. Staining of a TMA containing 0.6 mm cores of benign prostatic hyperplasia (BPH) (n = 26), PCa (n = 72), and control tissues including breast, kidney, placenta, ovary, and liver was carried out by Dr Urszula McClurg at the Northern Institute of Cancer Research (NICR) and was scored using the 0-300 Histoscore score method 83. Briefly, percentage and intensity of positively stained cells was estimated on a 0-3 scale and used for calculating the H-score = (% of cells with 1 level positivity) + 2*(% of cells with 2 level positivity) + 3*(% of cells with 3 level positivity).

Gleeson grade	4 n=1	5 n=1	6 n=5	7 n=11	8 n=17	9 n =24	10 n=7	UK n=11
Age at diagnosis (years)	40-49 n=1	50-59 n=5	60-60 n=12	70-79 n=28	8-89 n=4			UK n=27
Stage	T1 n=16	T1B n=7	T2 n=11	T3 n=24	T3C n=3	T4 n=11	T4B n=1	UK n=4
PSA	<10 n=8	10-19 n=11	20-29 n=4	30-49 n=10	50-99 n=6	100-200 4	>200 n=4	UK n=30

Table 2.15: Basic clinical data for patient tissue samples used in TMA.

Samples used in this study were collected between January 1989 and June 2003 from the Freeman Hospital patients. All samples were first analysed by a trained pathologist before selection of cores for TMA construction was performed. UK = unknown.

2.6.4 Indirect immunofluorescence

Confluent cells on cover-slips were washed with 1X PBS, followed by fixation of the cells with 4% paraformaldehyde (PFA) (Sigma P6148) for 20 minutes at room temperature or 100% methanol (VWR Chemicals K977) for 10 minutes at -20°C. Cells were permeabilised by incubation in 0.1% Triton X-100 (Plusone 17-1315-01) detergent for 10 minutes, and blocked in 10% horse serum (Sigma H0146) in 1X PBS for 1 hour. Cells were incubated in primary antibody diluted in 10% horse serum in 1X PBS for 1 hour at room temperature or overnight at 4°C. After three washes in 1X PBS for 5 minutes, the cells were incubated in fluorescent-conjugated secondary antibody diluted in 10% horse serum in 1X PBS for 1 hour at room temperature and protected from any light source with aluminium foil. After incubation, the cells were washed three times with 1X PBS for 5 minutes. The coverslips were mounted onto glass slides using VectaShield Antifade Mounting Medium with 4',6-diamidino-2-phenylindole (DAPI) (Vector Laboratories H-1200). Fluorescent images were obtained on an Axiovision microscope (Zeiss) and associated software. Primary and secondary antibodies used for indirect immunofluorescence are listed in Table 2.16.

Antibody	Species	Supplier	Dilution
ST6GAL1	Rabbit polyclonal	Abgent (AP19891c)	1:100
Desmoplakin I & II	Mouse monoclonal	Abcam (ab16434)	1:100
Relaxin 2	Mouse monoclonal	Abcam (ab183505)	1:100
FLAG M2	Mouse monoclonal	Sigma-Aldrich (F3165)	1:100
Rabbit 488 Alexa Fluor	Donkey	Abcam (ab150073)	1:100
Mouse 488 Alexa Fluor	Donkey	Life Technologies (A21202)	1:100

Table 2.16 Primary and secondary antibodies used for indirect immunofluorescence.

2.7 Cell culture

2.7.1 Cell lines and culture conditions

All cell lines were routinely cultured in the appropriate medium: Dulbecco's Modified Eagle's Medium (DMEM) (Sigma D6429) or Gibco RPMI-1640 with L-Glutamine (Thermo Scientific 21875-034), supplemented with 10% Heat Inactivated Fetal Bovine Serum (FBS) (Thermo Scientific 10270106), 1% Penicillin Streptomycin (Thermo Scientific 15070063) and maintained at 37°C in a humidified atmosphere containing 5% carbon dioxide (CO_2). For androgen treatment of LNCaP cells, culture medium was supplemented with 10% dextran charcoal stripped fetal bovine serum (Sigma F6765) to produce a medium stripped of steroids. Following culture for 72 hours, 10 nM synthetic androgen analogue methyltrienolone (R1881) (Sigma R0908) was added (Androgen +) or absent (Steroid deplete) for the times indicated. A list of cell lines and culture media used are listed in Table 2.17.

Cell line	Characteristics	Culture media
LNCaP ATCC: CRL-1740	Prostate cancer cell line derived from a needle aspiration biopsy of the left supraclavicular lymph node of a patient with metastatic prostate cancer (50 year old Caucasian male) (Horoszewicz *et al.*, 1983). Androgen sensitive.	RPMI-1640 with L-Glutamine
VCaP ATCC: CRL-2876	Prostate cancer cells derived from vertebral bone metastasis from a patient with hormone refractory prostate cancer (59 year old Caucasian male) (Korenchuk *et al.*, 2001). Androgen sensitive.	RPMI-1640 with L-Glutamine

DU145 ATCC: HTB-81	Prostate cancer cells derived from brain metastasis from a patient with prostate adenocarcinoma (69 year old Caucasian male) (Stone *et al.*, 1978). Androgen insensitive.	RPMI-1640 with L-Glutamine
PC-3 ATCC: CRL-1435	Prostate cancer cells derived from bone metastasis from a patient with grade IV prostatic adenocarcinoma (62 year old Caucasian male) (Kaighn *et al.*, 1979). Androgen insensitive.	RPMI-1640 with L-Glutamine
PC-3M	A variant of the PC-3 cell line grown in nude mice with greater metastatic behaviour (Kozlowski *et al.*, 1984). Androgen insensitive.	RPMI-1640 with L-Glutamine
CW-22Rv1 ATCC: CRL-250	Prostate cancer cells derived from a xenograft that was serially propagated in mice after castration-induced regression and relapse of the parental, androgen dependent CWR22 xenograft. Androgen sensitive. Androgen receptor mutation (Tepper *et al.*, 2002).	RPMI-1640 with L-Glutamine
LNCaP AI	An androgen insensitive variant of LNCaP cells generated through continuous culturing in an environment deprived of	RPMI-1640 with L-Glutamine

	androgens for a period of 8 months (Halkidou *et al.*, 2003). Androgen insensitive.	
LNCaP cdxR	A Casodex resistant variant of LNCaP cells generated by exposing LNCaP cells to increasing concentrations of Casodex in normal growth medium over a 4-month period (Rigas *et al.*, 2007). Androgen sensitive.	RPMI-1640 with L-Glutamine
HEK-293 ATCC: CRL-1573	A human embroyonic kidney cell line with high transfection efficiency (Graham *et al.*, 1977).	D-MEM
Flp-In 293 T-Rex (Thermo Scientific R750-07)	Cells contain a single stably integrated FRT site at a transcriptionally active genomic locus. Use to generate stable cell lines with high level protein of interest expression from Flp-In expression vectors.	D-MEM

Table 2.17 Cell lines, characteristic and culture media.

2.7.2 Routine cell passage

Cells were passaged every 3 to 5 days or at approximately 75% confluency. The culture medium was removed from the cells and the cells were washed in 1X PBS. 2nM Trypsin-EDTA (Thermo Scientific 25300054) was added to the cells and incubated at 37°C for 2 minutes or until the cells had detached from the surface. An equal volume of culture medium was added to the cells to inactivate the Trypsin and the cells were diluted for further culture.

2.7.3 Cryopreservation

Cell lines were routinely frozen to generate a stock of cells from early passage. Cryopreservation was performed in 500 µl aliquots of cryoprotective media containing 10% dimethyl sulphoxide (DMSO) (Sigma D4540) and stored in cryovials at -80°C. When required, frozen stocks were rapidly thawed and re-suspended in complete culture medium and plated in sterile tissue culture flasks.

2.7.4 Transfection

2.7.4.1 Lipofectamine 2000 transfection

Cells were seeded in sterile 6 well culture plates 24 hours before transfection to be ~80% confluent upon transfection. Control cells were transfected with an empty vector at the same concentration. For each transfection, 12 µl Lipofectamine 2000 Reagent (Thermo Scientific 11668027) was diluted in 150 µl Opti-MEM Reduced Serum Media (Thermo Scientific 31985062) and 14 µg of plasmid or empty vector DNA was diluted in 700 µl Opti-MEM Media. The diluted Lipofectamine 2000 Reagent was added to the diluted DNA (1:1 ratio) and incubated for 5 minutes at room temperature. The resulting transfection complexes were added to the cells in a drop wise manner and incubated at 37°C, 5% CO_2 for 24 hours. Positive colonies were selected with appropriate antibiotics – Zeocin (Thermo Scientific R25001), Puromycin (Thermo Scientific A11138-03) or

Blasticidin (Thermo Scientific A11139-03). Tetracycline hydrochloride (Sigma T7660) was used to induce expression from Flp-In 293 T-Rex cells.

2.7.4.2 Lipofectamine 3000 transfection

Cells were seeded in sterile 6 well culture plates 24 hours before transfection to be ~80% confluent upon transfection. Control cells were transfected with an empty vector at the same concentration. For each transfection, 5 µl Lipofectamine 3000 Reagent (Thermo Scientific L3000001) was diluted in 125 µl Opti-MEM Reduced Serum Media (Thermo Scientific 31985062) and 5 µg of plasmid or empty vector DNA was diluted in 250 µl Opti-MEM Media with 50 µl P3000 Reagent. The diluted Lipofectamine 3000 Reagent was added to the diluted DNA with P3000 reagent (1:1 ratio) and incubated for 15 minutes at room temperature. The resulting transfection complexes were added to the cells in a drop wise manner and incubated at 37°C, 5% CO_2 for 24 hours. Positive colonies were selected with appropriate antibiotics – Zeocin (Thermo Scientific R25001), Puromycin (Thermo Scientific A11138-03) or Blasticidin (Thermo Scientific A11139-03). Tetracycline hydrochloride (Sigma T7660) was used to induce expression from Flp-In 293 T-Rex cells.

2.7.4.3 GeneJammer transfection

Cells were seeded in sterile 6 well culture plates 24 hours before transfection to be ~60% confluent upon transfection. Control cells were transfected with an empty vector at the same concentration. For each transfection, 3 µl GeneJammer Transfection Reagent (Agilent Technology 204132) was diluted in 100 µl Opti-MEM Reduced Serum Media (Thermo Scientific 31985062) and incubated at room temperature for 5 minutes. Plasmid or empty vector DNA was added and incubated for a further 15 minutes at room temperature. The resulting transfection complexes were added to the cells in a drop wise manner and incubated at 37°C, 5% CO_2 for 24 hours. Positive colonies were selected with appropriate antibiotics – Zeocin (Thermo Scientific R25001), Puromycin (Thermo

Scientific A11138-03) or Blasticidin (Thermo Scientific A11139-03). Tetracycline hydrochloride (Sigma T7660) was used to induce expression from Flp-In 293 T-Rex cells.

2.7.4.4 RNAiMAX transfection

Depletion of the endogenous proteins was achieved by transfecting cells with pre-designed siRNAs (Integrated DNA Technologies). siRNAs were transfected using RNAiMAX Transfection Agent (Thermo Scientific 13778030). Control cells were transfected with the same concentration of negative control siRNA (Integrated DNA Technologies 51-01-14-03). Cells were seeded in sterile 6 well culture plates 24 hours before transfection to be ~60% confluent upon transfection. For each transfection, 9 µl RNAiMAX Reagent was diluted in 150 µl Opti-MEM Reduced Serum Media (Thermo Scientific 31985062) and 3 µl of the appropriate siRNA (10 µM) was diluted in 150 µl Opti-MEM. The diluted RNAiMAX Reagent was added to the diluted siRNA and incubated for 5 minutes at room temperature. The resulting transfection complexes were added to the cells in a drop wise manner and the cells were incubated at 37°C, 5% CO_2 for 72 hours and then harvested for both RNA extraction and Western Immunoblotting.

2.8 Functional assays

2.8.1 WST-1 cell proliferation assay

Proliferation assays were carried out using a WST-1 Cell Proliferation Assay Kit (Cyman Chemical Company 10008883). Cells were seeded in sterile 96 well plates at 10,000 cells per well and incubated at 37°C, 5% CO_2 for 24 hours. After initial incubation, 10 µl reconstituted WST-1 mixture was added to each well and mixed gently on an orbital shaker for 1 minute. Plates were incubated for a further 2 hours at 37°C, 5% CO_2 and mixed again for 1 minute to ensure homogeneous distribution of colour. The absorbance of each sample was measured against a background control using a Varioskan LUX (Thermo Fisher Scientific) microplate reader at a wavelength of 450 nm. This process was repeated over a 7day period.

2.8.2 Click-IT EdU proliferation assay

Proliferation assay were carried out using a Click-iT EdU Alexa Fluor 594 Imaging Kit (Thermo Scientific C10339). Confluent cells on cover-slips were incubated in 10 μM EdU labelling solution and incubated for 2 hours at 37°C, 5% CO_2. Cells were fixed with 4% PFA (Sigma P6148) for 20 minutes at room temperature and washed twice in 1 ml 3% bovine serum albumin (BSA) (Sigma A9418) in 1X PBS. Cells were permeabilised by incubation in 0.5% Triton X-100 detergent (Plusone 17-1315-01) for 20 minutes and washed twice in 1 ml 3% BSA in 1X PBS. Cells were incubated with 500 μl Click-IT EdU reaction cocktail (Table 12.18) for 30 minutes at room temperature and protected from any light source with aluminium foil. Cells were washed in 1 ml 3% BSA in 1X PBS and the coverslips were mounted onto glass slides using VectaShield Mounting Medium with 4',6-diamidino-2-phenylindole (DAPI) (Vector Laboratories H-1200). Fluorescent images were obtained on an Axiovision microscope (Zeiss) and associated software and analysed using Image J software (National Institutes of Health, Bethesda, Maryland, USA).

Reaction component	Volume
1X Click-IT EdU reaction buffer	4.3 ml
$CuSO_4$	200 μl
Alexa Fluor azide	12.5 μl
1X Click-IT EdU buffer additive	500 μl

Table 12.18 Components of Click-IT EdU reaction cocktail.

2.8.3 Calcein cell adhesion assay

Cells suspended in serum free media were labelled with 5 µM Calcein AM (Sigma 17783) and incubated for 30 minutes at 37°C, 5% CO_2. Labelled cells were washed twice in 1X PBS and seeded in sterile 96 wells plates; uncoated plates, human fibronectin coated plates (R&D Systems CWP001) and collagen I coated plates (Thermo Scientific A1142803) at 50,000 cells per well. After incubation for 2 hours at 37°C, 5% CO_2 non-adherent cells were removed by washing four times in 1X PBS. The fluorescence of each sample was measured against a background control using a Varioskan LUX (Thermo Fisher Scientific) microplate reader at an excitation of 400 nm, emission of 530 nm. The percentage adhesion was calculated by comparing with an identical unwashed plate.

2.8.4 Crystal violet staining

Cells were cultured under appropriate conditions as required then fixed and visualised using crystal violet staining. Cells were washed twice in cold PBS and fixed with 100% ice cold methanol (VWR Chemicals K977) for 10 minutes on ice. Cells were brought to room temperature and incubated for 10 minutes in 0.5% crystal violet solution (Sigma HT90132) in 25% methanol. Cells were washed in H_2O until free of crystal violet stain and allowed to air dry at room temperature overnight.

2.8.5 Scratch wound healing assay

Scratch wound healing assays were carried out using a Cell Comb Scratch Assay (Merk Millipore 17-10191). Cells were grown to a confluent monolayer on 86mm x 12mm scratch assay cell culture plates. Scratches were made across the plate using the cell comb, applying sufficient force to create even scratches on the monolayer. The cells were washed three times in 1× PBS to remove floating cells, and wound closure was observed at indicated time points and photographed with a bright-field microscope. Ten images were taken for each plate at each time point and the mean average was calculated. Images were analysed using the Image J software (National Institutes of Health, Bethesda, Maryland, USA). Wound repair percentage was calculated as

following: (diameter of wound before migration - diameter of wound after migration) / diameter of wound before migration x 100. The mean value of wound repair in three duplicate wells was calculated for each group.

2.8.6 Cell migration assay

Cell migration assays were carried out using an Oris 96 well migration assay (Platypus Technologies PROCMACC1). Cells were seeded in 96 well collagen I coated plates at 30,000 cells per well and incubated at 37°C, 5% CO_2 for 2 hours. Seeding stoppers were removed and pre-migration images were taken. Migration of cells into the centre of the wells was observed at indicated time points and photographed with a bright-field microscope. Images were analysed using the Image J software (National Institutes of Health, Bethesda, Maryland, USA). Migration was calculated by comparing the open area of pre-migration cells to the open area of post migration cells at a set time point.

2.8.7 Invasion assay

Invasion assays were carried out using a Cultrex 96 well basement membrane extract (BME) cell invasion assay (R&D Systems 3455-096-K). Cells were cultured in serum free media for 24 hours and then added to the top chamber at 10,000 cells per well. Full culture meida was added to the bottom wells and plates were incubated at 37°C, 5% CO_2 for 24 hours. Both chambers were washed in 1X wash buffer and incubated with Calcein AM / cell dissociation solution (final concentration: 0.8 µM) at 37°C, 5% CO_2 for 30 minutes. The fluorescence of each sample in the bottom chamber (invasive cells) was measured against a background control using a Varioskan LUX (Thermo Fisher Scientific) microplate reader at an excitation of 485 nm, emission of 520 nm.

Chapter 3

Results

Identifying clinically relevant androgen regulated gene expression changes in prostate cancer

Chapter 3 Results

Identifying clinically relevant androgen regulated gene expression changes in prostate cancer

3.1 Introduction

Androgen receptor (AR) signalling remains the key driver in advanced and CRPC (Livermore *et al.*, 2016). Over the past decade numerous genomic and transcriptomic studies have been carried out identifying AR binding sites and target genes. Until recently, the majority of these studies had focused on the use of a single cell line *in vitro* (Massie *et al.*, 2007; Wang *et al.*, 2007; Rajan *et al.*, 2011), on genes with nearby AR genomic binding sites (Massie *et al.*, 2011; Sharma *et al.*, 2013), or had limited coverage on microarrays (Massie *et al.*, 2007; Wang *et al.*, 2009a; Massie *et al.*, 2011; Rajan *et al.*, 2011). Hybridization-based microarrays were the technology of choice for large scale gene expression studies. They allowed interrogation of tens of thousands of transcripts simultaneously, but they were restricted by probe design. Microarrays only detect transcripts for which probes have been pre-designed, which requires existing genomic sequencing information. The probes can also differ considerably in their hybridisation properties and background hybridisation limits their accuracy.

The development of RNA sequencing technology has allowed for transcriptome interrogation on a much larger scale. RNA sequencing, often termed RNA-Seq, generally involves total RNA samples which have been fragmented and converted into a library of cDNA fragments with adaptors. The fragments are then sequenced in a high-throughput manner, from either one end (single-end sequencing) or both ends (paired-end sequencing). RNA sequencing can detect known, novel and low level transcripts, as well as allele-specific expression, splice junctions, point mutations and gene fusion transcripts (Wang et al., 2009b; Ozsolak and Milos, 2011). This method can also be used to quantify small RNA molecules such as microRNAs (miRNAs), short interfering RNAs (siRNAs), small nucleolar RNA (snoRNAs) and Piwi-interacting RNA (piRNA).

Within the last decade, the emergence of RNA sequencing technologies has resulted in a number of published clinical PCa transcriptome datasets, providing an comprehensive profile of advanced, metastatic, castrate resistant and neuroendocrine prostate cancer (Fenner, 2011; Rajan *et al.*, 2014; Robinson *et al.*, 2015; Beltran *et al.*, 2016; Kumar *et al.*, 2016; Mo *et al.*, 2017). More recently, technological advances have permitted single cell transcriptome sequencing (Guzvic *et al.*, 2014; Lohr *et al.*, 2014). Miyamoto *et al* confirmed the complex heterogeneity of individual tumours by profiling the transcriptome of circulating tumour cells (CTCs) (Miyamoto *et al.*, 2016). CTCs are shed into blood from primary tumours and may provide a non-invasive means of identifying pathways contributing to cancer progression and metastasis.

This advance in next generation sequencing technology has led to a greater understanding and characterisation of many cancers. The number of whole exome and transcriptome sequencing studies is ever increasing and has led to several large-scale cancer genome projects. The Cancer Genome Atlas project (TCGA; http://cancergenome.nih.gov), a collaboration between the National Cancer Institute (NCI) and the National Human Genome Research Institute (NHGRI) and the International Cancer Genome Consortium (ICGC; http://icgc.org) hold publically available genomic, transcriptomic and epigenomic data for a large number of different cancers and subtypes (Hudson *et al.*, 2010; Weinstein *et al.*, 2013). The cBioPortal for Cancer Genomics (http://cbioportal.org) provides a web-based portal which can be used to visualise and analyse these large cancer datasets (Cerami *et al.*, 2012). Another web-based platform, Oncomine (https://www.oncomine.org) contains gene expression data from 715 published cancer transcriptome datasets, including 60 PCa datasets (Rhodes *et al.*, 2004).

3.2 Aims of chapter

The majority of CRPC tumours remain dependent of AR signalling for growth (Crona and Whang, 2017). Detailed knowledge of their genetic and biological background is therefore essential for understanding drivers of disease progression, and will assist in the development of effective biomarkers and patient treatments.

The aims of this chapter were to:

- Use RNA sequencing technology to identify AR regulated transcriptome changes in prostate cancer cells.
- Identify clinically relevant gene expression changes by correlating this dataset with a clinical PCa RNA sequencing dataset.
- Carry out a meta-analysis of multiple PCa gene expression datasets using the Oncomine web-based platform to increase the statistical power of any identified changes.
- Use Gene Ontology analysis to identify key AR regulated biological processes in clinical PCa.

A comprehensive map of AR regulated genes, associated pathways and biological processes in clinical prostate cancer will help in our understanding of the development of PCa and the treatment response to ADT.

3.3 Results

3.3.1 Identification of clinically relevant androgen responsive target genes in prostate cancer

To analyse how the PCa transcriptome responds to androgens, paired-end RNA sequencing was carried out on six samples; three biological replicates of LNCaP cells grown in charcoal stripped steroid deplete media (SD), and three biological replicates from LNCaP cells grown in the presence of 10 nM synthetic androgen R1881 (A+) for 24 hours using an Illumina HiSeq 2000. These RNA samples were prepared by Dr Jennifer Munkley and sequenced prior to the start of my PhD project.

All bioinformatics analysis of the data was performed by Dr Daniel Vodak (Institute of Cancer Genetic and Informatics, Oslo, Norway). Initial analysis of the RNA sequencing data identified 3,339 genes which were significantly up-regulated by androgens, and 2,760 genes which were significantly down-regulated ($p < 0.05$). As previous studies have demonstrated differences between *in vivo* and *in vitro* AR-regulated genes (Sharma *et al.*, 2013), we correlated our cell line data with a previously published clinical RNA sequencing dataset (Rajan *et al.*, 2014). In this dataset, RNA was sequenced from seven patients with locally advanced metastatic prostate cancer before and around 22 weeks post ADT (patient information detailed in Table 3.1). Differential gene and transcript expression analysis was performed as follows: all reads were first mapped to human transcriptome/genome (build hg19) with TopHat / Bowtie, followed by per-sample transcript assembly with Cufflinks. Transcript assemblies derived from the clinical samples were merged together with Cuffmerge, and differential expression between the two conditions (prior and post ADT) was assessed with Cuffdiff. Genes and isoforms labelled by the software as significantly ($p < 0.05$) differentially expressed were extracted from the results. The mapped LNCaP data was processed with the same pipeline.

Patient	Age (years)	Gleason sum score	TNM stage		
			T	N	M
1	64.7	8	3b	0	0
2	65.4	9	3b	0	0
3	69.6	8	3b	1	0
4	64.6	8	3a	0	1
5	51.8	7	3a	0	0
6	58.6	7	3b	1	0
7	62.9	7	3b	1	0

Table 3.1 Patient data for RNA sequencing clinical samples. Data and table taken from (Rajan *et al.*, 2014). Clinical samples from 7 patients with locally advanced or metastatic PCa (Gleason sum score >7) were used for RNA sequencing. The patients were aged between 51.8 years and 69.6 years with an average age of 62.5 years. TNM stage: T (tumour), N (lymph node) and M (metastasis). The T stage shows how far the cancer has spread in and around the prostate: T3a - the cancer has broken through the outer layer of the prostate, but has not spread to the seminal vesicles (which produce and store some of the fluid in semen), T3b - the cancer has spread to the seminal vesicles. The N stage shows whether the cancer has spread to the lymph nodes near the prostate and the M stage shows whether the cancer has metastasised to other parts of the body.

This process identified 660 potentially clinically relevant AR target genes with reciprocal expression signatures; androgen regulated in culture with reverse expression switches in patients in response to clinical ADT. A full gene list can be found in Appendix A.

Two subsets of differentially expressed genes were identified:

1) Genes up-regulated by androgens in LNCaP cells and down-regulated in all 7 patients following androgen-deprivation therapy, of which 548 genes were identified.
2) Genes down-regulated by androgens in LNCaP cells and up-regulated in 7 patients following androgen-deprivation therapy, of which 112 genes were identified.

Figure 3.1 Venn diagram of androgen regulated genes with reciprocal regulation patterns. Venn diagram showing the number of genes with significant differential expression ($p < 0.05$). Comparison of the two RNA sequencing datasets identified 660 androgen-regulated genes with reciprocal regulation. (A) 548 genes were up-regulated in response to androgen treatment in LNCaP cells, but down-regulated in 7 PCa patient samples post ADT. (B) 112 genes were down-regulated in response to androgens in LNCaP cells, but up-regulated in 7 PCa patient samples post ADT.

Within the dataset were many established classes of AR target genes, including cell cycle regulators: zinc finger and BTB domain containing 16 (ZBTB16) (Jiang and Wang, 2004); signalling molecules implicated in PCa including serine/threonine/tyrosine kinase 1 (STYK1) (Chung *et al.*, 2009); genes with roles in central metabolism, including cAMP responsive element binding protein 3 like 4 (CREB3L4) (Qi *et al.*, 2002) and pyrroline-5-carboxylate reductase 1 (PYCR1) (Jariwala *et al.*, 2007); and biosynthetic pathway genes, including calcium/calmodulin dependent protein kinase kinase 2 (CAMKK2) (Racioppi, 2013); as well as many additional novel androgen-regulated genes. Although kallikrein related peptidase 3 (KLK3) was present in both the up-regulated by androgens in LNCaP cells and the down-regulated following androgen-deprivation therapy gene lists, it was surprisingly not listed in the merged differentially expressed gene list. This highlights to effect of setting optimal thresholds during the bioinformatic analysis. Although helpful when focusing large gene lists, setting such stringent thresholds can sometimes limit analysis.

In order to validate the LNCaP RNA sequencing results, expression changes for several androgen-regulated genes were confirmed in an independent LNCaP sample set by real-time quantitative reverse transcription PCR (qRT-PCR) (Figure 3.2).

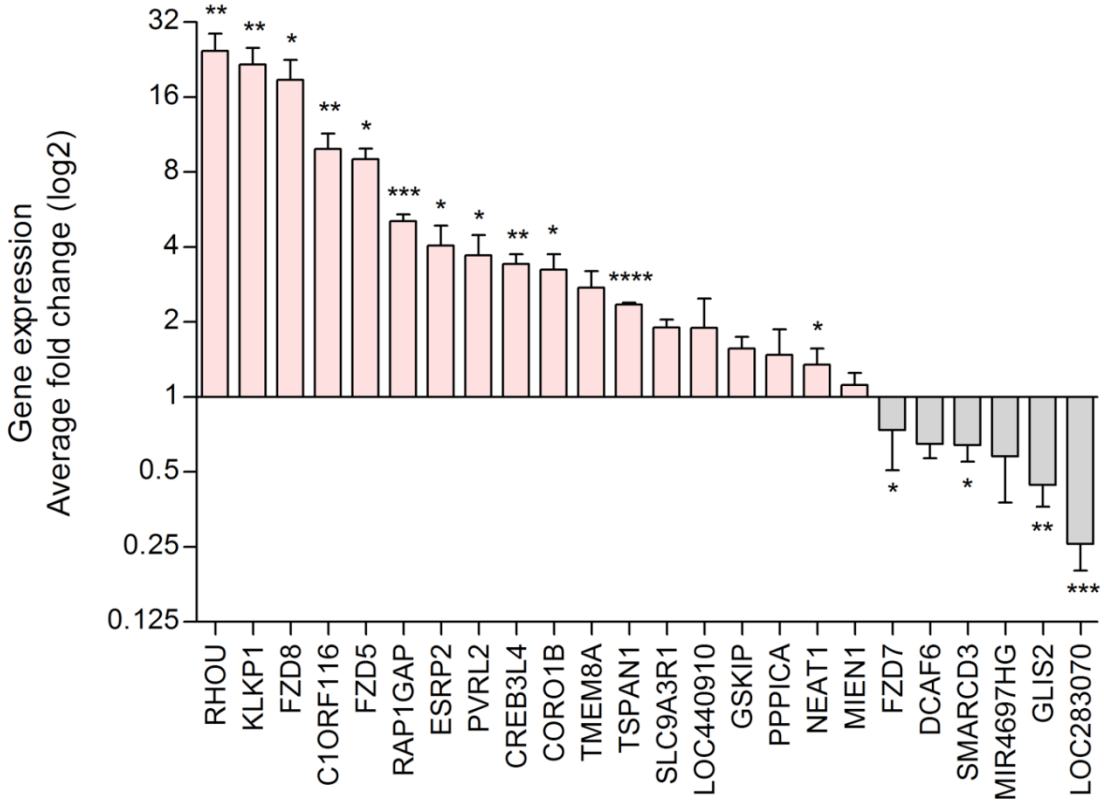

Figure 3.2 Differentially expressed genes in LNCaP cell line in response to androgens. Real-time quantitative reverse transcription PCR (qRT-PCR) analysis of 24 differentially expressed genes in LNCaP cells in response to 10 nM synthetic androgen (R1881) stimulation (24 hours). Gene expression was calculated as the average (from 3 biological replicates) fold change (log2) relative quantification of androgen treated LNCaP cells compared to steroid deplete cells (value set as 1). Samples were normalised using the average of three reference genes, GAPDH, β -tubulin and actin. Statistical significance was calculated using an independent two-sample t-test, where * $p < 0.05$, ** $p < 0.01$, *** $p < 0.0001$, **** $p < 0.00001$. All primer sequences are listed in Appendix B.

Several Wnt signalling pathway genes were analysed. Frizzled class receptor 8 and 5 (FZD8 and FZD5) were significantly up-regulated ($p < 0.05$) by androgens, whilst frizzled class receptor 7 (FZD7) was down-regulated. Ras homolog family member U (RHOU), a member of the Rho family of GTPases regulated by Wnt1 (Tao *et al.*, 2001) showed the highest increase in expression. Other genes significantly up-regulated by androgens include, chromosome 1 open reading frame 116 (C1ORF116), also known as SARG, the RAP1 GTPase activating protein RAP1GAP, the epithelial splicing regulatory protein ESRP2, the nectin cell adhesion molecule PVRL2, the cAMP responsive element binding protein CREB3L4, the coronin actin binding protein CORO1B, the transmembrane protein TMEM8A, tetraspanin 1 (TSPAN1) and the long non-coding RNA (lncRNA) nuclear paraspeckle assembly transcript 1 (NEAT1).

RHOU has recently shown potential as a biomarker to distinguish between metastatic PCa and localised PCa (Alinezhad *et al.*, 2016). Knockdown of RHOU in both 2D and 3D organotypic cell culture models resulted in reduced growth, tumour cell invasion, proliferation and cell-motility (Alinezhad *et al.*, 2016). The lncRNA NEAT1 is regulated by the estrogen receptor alpha (ERα). NEAT1 is up-regulated PCa and can promote tumour progression and therapeutic resistance (Chakravarty *et al.*, 2014). KLKP1 (Kaushal *et al.*, 2008), C1ORF116 (Steketee *et al.*, 2004), CREB3L4 (Labrie *et al.*, 2008) are known AR target genes.

Genes confirmed as significantly down-regulated by androgens include SWI/SNF related, matrix associated, actin dependent regulator of chromatin, subfamily D, member 3 (SMARCD3), the GLIS family zinc finger protein (GLIS2) and the lncRNA LOC283070. LOC283070 is frequently up-regulated in androgen insensitive PCa cell lines and is thought to mediate the transition of LNCaP cells into androgen independent cells via calcium/calmodulin dependent protein kinase 1D (CAMK1D) (Wang *et al.*, 2016a).

Androgen regulated expression of these genes was also analysed in another androgen responsive PCa cell line (VCaP) by real-time quantitative reverse transcription PCR (qRT-PCR) (Figure 3.3). Again, VCaP cells were treated with 10nM R1881 for 24 hours (A+) or without (steroid deplete, SD).

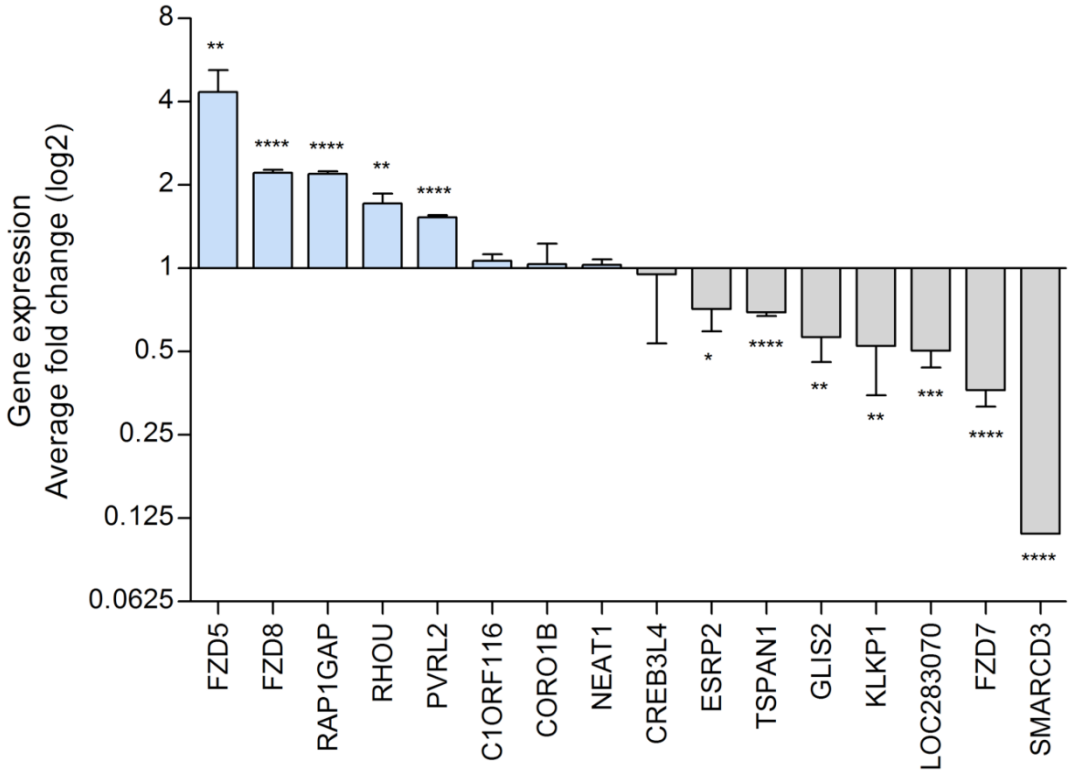

Figure 3.3 Differentially expressed genes in VCaP cell line in response to androgens. Real-time quantitative reverse transcription PCR (qRT-PCR) analysis of 16 differentially expressed genes in VCaP cells in response to 10 nM synthetic androgen (R1881) stimulation (24 hours). Gene expression was calculated as the average (from 3 biological replicates) fold change (log2) relative quantification of androgen treated VCaP cells compared to steroid deplete cells (value set as 1). Samples were normalised using the average of three reference genes, GAPDH, β -tubulin and actin. Statistical significance was calculated using an independent two-sample t-test, where * $p < 0.05$, ** $p < 0.01$, *** $p < 0.0001$, **** $p < 0.00001$. All primer sequences are listed in Appendix B.

Five genes (*FZD5, FZD8, RAP1GAP, RHOU* and *PVRL2*) were significantly up-regulated by androgens in both the LNCaP and VCaP cell lines and four genes were down-regulated (*SMARCD3, FZD7, LOC283070* and *GLIS2*). Interestingly, *ESRP2, TSPAN1* and kallikrein pseudogene 1 (*KLKP1*) had opposing expression patterns in the VCaP cells compared to the LNCaP cells. Although both cell lines are androgen sensitive, they have different backgrounds, characteristics and each represents a distinct molecular subtype of prostate cancer. LNCaP cells were derived from a needle biopsy taken from the left supraclavicular lymph node of a 50-year old Caucasian male (Horoszewicz *et al.*, 1983), and harbour an AR ligand binding domain mutation. Whilst VCaP cells (vertebral cancer of the prostate) were derived from a vertebral metastatic lesion from a 59-year old Caucasian male (Korenchuk *et al.*, 2001) and one harbour a AR gene amplification. Although proven invaluable for public health research, tumour derived cell lines can exhibit considerable genomic and transcriptomic diversity (Klijn *et al.*, 2015) and do not fully represent individual clinical tumour samples.

3.3.2 Meta-analysis of publically available datasets

The growth of publicly available gene expression data is staggering. The availability of this data can be a powerful tool and has led to the discovery of disease biomarker and therapeutic targets. Meta-analysis across multiple datasets has greater statistical power and can overcome the biases of individual studies (Ramasamy *et al.*, 2008). A meta-analysis approach was used to analyse expression of each of the genes within the two subsets in clinical prostate cancer samples. Oncomine (www. oncomine.org) is a cancer-profiling database containing published micro-array data that has been collected, standardised, annotated and analysed. This approach has been

Five micro-array datasets were interrogated using the Oncomine database:

1. **Grasso *et al***: A 122 sample dataset containing 35 castrate resistant metastatic PCa, 59 localised PCa, and 28 benign prostate tissue specimens. Data was

generated on the Agilent Whole Human Genome 44k array (19,189 genes, 41,000 reporters) (Grasso *et al.*, 2012).

2. **Taylor *et al***: A 367 sample dataset containing 218 tumour samples (181 primary prostate tumours and 37 metastatic prostate) and 149 matched normal samples. Data was generated on the Affymetrix Human Exon 1.0 ST array (18,823 genes, 19,084 reporters) (Taylor et al 2010).

3. **Varambally *et al***: A 19 samples dataset containing 6 castrate resistant metastatic PCa, 7 primary PCa and 6 normal prostate gland specimens. Data was generated using the Affymetrix Human Genome U133 plus 2.0 array (19,574 genes, 54,675 reporters) (Varambally *et al.*, 2005).

4. **Tomlins *et al***: A 101 sample dataset containing laser dissected cell populations from a progression of PCa cell types (benign, PIN, low-grade PCa, high-grade PCa, metastatic PCa) and normal adjacent tissue. Data was generated using a custom micro-array (10,656 genes, 19,928 reporters) (Tomlins *et al.*, 2007).

5. **Lapointe *et al***: A 112 sample dataset containing 62 prostate carcinomas, 41 matched normal prostate and 9 metastatic PCa (lymph node) specimens. Data was generated on a custom micro-array (10,166 genes, 19,116 reporters) (Lapointe *et al.*, 2004).

Gene expression in prostate cancer tissue was compared with that of normal or benign tissue (control) for each of the 660 genes in the gene set. The threshold criteria was set as: fold change >1, p value <0.05 in at least two of the studies analysed. Of the 548 genes up-regulated by androgens in LNCaP cells and down-regulated in patients post ADT, 140 genes (26%) met the threshold criteria (Table 3.2). Of these, 51 genes met the threshold criteria in at least four of the five studies (genes highlighted blue in Table 3.2), and 43 genes meet the threshold criteria in all five studies (genes highlighted green in

Table 3.2). None of the 112 genes down-regulated by androgens in LNCaP cells and up-regulated in patients post ADT meet the threshold criteria.

Gene	Grasso *et al*		Taylor *et al*		Varambally *et al*		Tomlins *et al*		Lapointe *et al*	
	fc	p value	fc	p value	fc	p value	fc	p value	fc	p value
ABAT	1.685	2.30E-04	1.225	0.008	1.453	0.011	-	-	1.151	0.031
ABHD2	1.613	2.68E-05	1.335	2.26E-05	1.834	5.48E-04	1.551	0.046	1.298	0.007
ACACA	1.181	3.41E-05	1.399	2.77E-05	1.239	0.043	2.083	6.24E-04	1.72	2.31E-13
ACLY	1.499	1.75E-05	1.356	2.10E-04	1.384	0.008	2.206	1.20E-02	1.292	5.12E-04
ACSM1	4.399	3.41E-09	2.736	1.90E-19	3.862	0.002	3.906	1.37E-04	-	-
ADIPOR1	1.379	2.76E-09	1.144	0.002	1.157	0.16	1.902	9.47E-05	1.23	6.00E-06
ADRB1	1.768	2.45E-04	1.31	3.79E-07	3.015	1.71E-07	3.379	3.99E-04	1.843	2.32E-05
ADRBK1	1.325	1.24E-04	1.071	0.073	1.574	1.99E-05	1.997	0.091	1.291	3.96E-04
AGR2	2.711	7.12E-04	1.601	0.003	-1.429	0.873	9.533	1.85E-04	2.391	8.06E-06
AKR1A1	1.512	2.91E-07	1.123	0.007	1.233	0.027	-	-	-	-
ALDH1A3	1.846	5.76E-05	1.517	1.77E-07	1.684	1.97E-04	2.136	0.026	1.354	0.006
ALG5	1.255	2.08E-04	1.043	0.141	-1.138	0.596	2.51	4.37E-05	-1.001	0.505
AMACR	13.502	4.57E-24	3.948	2.77E-21	10.451	6.75E-07	10.07	2.6E-13	7.228	4.11E-23
ARF4	1.23	4.62E-04	1.194	0.003	1.041	0.413	2.124	2.18E-04	-	-
ARFIP2	1.455	2.44E-05	1.216	9.94E-05	1.118	0.182	-1.289	0.943	1.265	8.68E-04
ATP11B	1.662	3.03E-07	1.41	4.92E-05	1.708	2.00E-03	1.725	0.038	1.687	1.67E-10
B3GAT1	2.714	2.15E-04	1.309	1.33E-09	5.739	0.002	1.213	0.189	2.222	4.05E-09
BDH1	1.363	8.76E-06	1.14	5.05E-06	1.34	2.00E-03	1.51	0.033	1.344	1.79E-05
BEND4	1.923	1.30E-05	1.456	2.97E-09	2.455	2.00E-03	-	-	2.228	7.76E-09
C19orf48	2.25	4.97E-07	1.292	4.10E-09	2.187	6.71E-05	2.249	0.006	-	-
C1orf116	1.773	5.57E-04	1.253	0.002	1.612	7.74E-04	-	-	1.437	1.10E-04
C9orf152	-	-	1.427	9.43E-05	1.594	0.007	-	-	-	-
C9orf91	1.154	1.50E-02	1.135	8.06E-05	1.44	6.00E-03	1.996	9.46E-05	1.456	2.82E-10
CALR	1.304	0.006	1.14	0.002	1.552	0.033	1.008	0.487	1.167	0.051
CCDC167	1.305	0.043	1.476	4.76E-04	2.652	3.97E-05	6.476	0.031	1.281	0.055
CENPN	1.526	0.002	1.31	3.77E-04	-1.274	0.701	-3.137	1	1.743	2.12E-06
CLDN8	3.098	5.55E-11	1.743	2.22E-10	2.441	2.90E-02	-	-	2.73	3.18E-10
CORO1B	1.555	5.20E-05	1.086	0.029	1.228	0.059	-	-	-	-
CREB3L4	1.941	5.88E-04	1.373	1.97E-04	1.548	0.014	-	-	1.47	3.02E-04
DCAF6	1.289	1.84E-04	1.191	0.003	1.477	0.23	2.14	2.45E-05	1.315	3.80E-07
DDAH1	1.474	3.42E-05	1.325	5.68E-05	1.751	6.31E-04	2.691	4.60E-05	1.372	1.54E-04
DEGS1	-1.063	0.707	1.113	0.011	-1.606	0.976	1.916	0.009	1.196	0.023
DHCR24	1.249	0.07	1.102	0.128	-1.137	0.744	1.614	0.046	1.197	0.04
DLX1	22.424	7.15E-27	1.406	3.84E-09	39.202	1.24E-05	-	-	-	-
DNAJC10	1.706	3.59E-10	1.723	2.44E-08	1.674	5.36E-04	2.788	7.26E-05	1.823	4.48E-18
DUS1L	1.733	1.03E-09	1.262	1.13E-06	1.744	7.12E-05	-	-	1.538	4.09E-08
EDEM3	1.637	2.18E-10	1.506	6.77E-07	1.641	0.003	-	-	1.405	1.86E-07
ERGIC1	1.745	8.37E-07	1.426	3.74E-06	1.929	8.00E-03	-	-	1.442	0.00017
ESRP2	1.891	1.50E-04	1.267	4.76E-07	1.453	0.01	1.123	0.191	1.939	4.91E-17
F5	2.666	2.99E-07	1.403	9.62E-05	2.166	0.008	4.911	2.55E-06	3.986	3.21E-12
FAAH	1.599	0.003	1.162	0.007	1.151	0.228	-1.404	0.852	1.439	0.018
FASN	1.638	0.002	1.564	2.87E-06	1.852	0.007	-1.339	0.759	-2.001	1
FGFRL1	2.051	1.15E-08	1.238	3.83E-08	1.394	3.10E-02	1.756	0.0007	1.772	1.82E-11
FUT1	1.26	2.70E-02	1.062	3.00E-03	1.243	1.10E-01	-	-	-	-
FZD8	1.717	1.47E-05	1.132	5.84E-05	2.803	0.002	5.057	3.67E-06	-	-
GABRB3	1.692	0.002	1.405	1.83E-06	1.369	0.06	3.803	0.014	2.118	1.51E-08
GALNT7	2.31	3.48E-07	1.764	1.12E-07	1.73	0.02	-	-	-	-
GCNT1	3.455	5.53E-13	1.941	1.53E-14	4.771	0.006	-	-	2.555	1.72E-14
GLUD1	1.154	0.031	1.158	0.017	1.19	0.101	2.156	4.72E-07	1.121	0.04
GMDS	2.349	2.09E-13	1.535	5.86E-11	1.447	0.059	-	-	1.286	0.012
GNPNAT1	1.541	3.24E-08	1.251	1.52E-07	1.478	1.16E-04	1.931	0.002	1.409	2.54E-07
GOLM1	3.137	9.13E-09	2.062	1.86E-08	2.89	2.00E-03	3.799	0.000355	2.905	1.86E-13
GOLPH3	1.386	2.87E-06	1.182	9.37E-06	1.176	0.074	1.69	0.007	1.329	7.14E-07
GSKIP	1.331	1.42E-05	1.172	0.026	-1.133	0.708	1.053	0.393	-	-
HGD	1.568	1.06E-07	1.531	2.65E-07	2.117	2.00E-03	2.518	0.000529	1.484	3.4E-07
HIPK2	1.378	1.00E-03	1.302	3.40E-05	1.499	8.54E-04	2.576	0.004	1.509	1.02E-06
HIST1H2BK	1.607	3.04E-04	1.131	2.75E-04	1.356	0.022	1.878	0.005	-	-
HMG20B	1.539	8.67E-07	1.189	3.25E-04	1.358	0.031	1.562	0.034	1.372	2.42E-05
HPN	4.346	3.77E-09	1.683	2.19E-20	5.836	7.81E-05	3.323	0.004	-	-
HSD17B4	1.792	1.19E-10	1.294	0.002	1.071	0.366	3.981	1.65E-05	1.474	1.37E-06
HSP90B1	1.235	0.002	1.334	5.97E-05	1.154	0.146	2.469	4.66E-04	1.28	3.45E-05
ICA1	3.072	2.56E-06	1.399	2.13E-05	1.295	1.30E-02	1.905	0.000327	1.659	1.72E-08
IQGAP2	2.052	2.40E-05	1.764	8.08E-08	2.901	2.84E-06	2.23	0.005	1.289	0.003
KDELR2	1.442	7.68E-05	1.394	8.16E-06	1.209	0.154	1.578	1.40E-04	1.284	2.43E-06
KIAA1244	1.475	7.89E-04	1.355	1.26E-04	1.376	0.059	2.837	3.66E-05	2.138	1.39E-09

Gene	Grasso *et al*		Taylor *et al*		Varambally *et al*		Tomlins *et al*		Lapointe *et al*	
	fc	p value	fc	p value	fc	p value	fc	p value	fc	p value
KLK15	2.188	4.16E-07	1.282	2.01E-07	3.073	0.002	-	-	-	-
KRT18	1.492	7.35E-04	1.261	1.16E-06	1.252	0.119	1.176	0.221	1.531	3.43E-06
LYPLA2	1.275	0.026	1.071	0.006	-	-	-	-	1.202	0.009
MAP7	1.806	2.13E-05	1.243	2.88E-04	1.215	0.201	1.7	0.016	1.669	6.31E-10
MBOAT2	1.681	8.51E-05	1.529	1.26E-07	1.504	4.00E-02	4.072	1.55E-05	1.837	4.80E-12
MCCC2	2.841	1.76E-11	1.357	5.92E-08	2.616	1.87E-04	1.789	0.061	2.607	6.97E-12
MICAL2	1.645	4.87E-06	1.233	2.07E-04	2.486	6.78E-04	1.84	0.006	1.161	0.035
MYBPC1	2.098	0.008	2.26	3.23E-06	5.041	0.016	-	-	-	-
NAA35	1.29	9.49E-07	1.142	0.046	1.216	0.057	2.716	1.78E-05	1.372	1.64E-08
NANS	1.698	4.52E-05	1.228	1.70E-02	1.289	8.70E-02	-	-	1.15	6.10E-02
NDUFV2	1.451	6.28E-09	1.182	0.007	1.08	0.292	2.18	3.73E-05	-	-
NEAT1	1.775	7.60E-09	1.011	0.386	1.173	0.161	2.756	8.77E-04	1.971	3.13E-10
P4HB	1.384	8.45E-04	1.222	4.68E-04	1.312	0.012	1.118	0.324	1.663	1.07E-06
PAOX	1.523	1.16E-05	1.15	1.09E-06	1.361	8.88E-04	-	-	-	-
PCTP	1.788	2.49E-11	1.275	5.27E-07	1.906	0.001	1.825	7.55E-04	1.23	1.01E-05
PDIA5	1.753	1.26E-05	1.513	2.32E-06	1.656	1.60E-02	2.691	2.30E-02	1.604	1.60E-08
PDLIM5	3.035	1.71E-12	1.221	2.05E-04	2.529	2.00E-03	4.562	4.48E-05	2.883	4.64E-13
PEX10	1.51	4.58E-05	1.196	7.19E-07	1.117	0.291	-	-	-	-
PLA1A	2.52	5.63E-10	1.768	3.59E-17	10.61	5.20E-07	2.857	4.00E-03	2.638	5.83E-10
PPP1CA	1.239	0.003	1.006	0.457	-1.108	0.077	2.624	0.012	1.245	5.92E-04
PRDX4	1.625	2.32E-06	1.31	3.25E-07	1.854	4.00E-04	2.938	8.21E-05	1.5	3.43E-05
PTPRN2	1.864	1.99E-04	1.552	3.01E-07	1.635	6.19E-04	1.693	0.052	1.637	2.01E-06
PVRL2	1.308	8.66E-04	1.205	5.79E-05	1.509	0.013	1.672	0.004	1.535	1.35E-05
PVRL3	1.326	7.00E-03	1.395	9.86E-07	2.17	2.01E-05	2.922	6.00E-03	1.603	2.21E-07
PXDN	1.626	1.50E-02	1.272	7.55E-06	1.602	5.64E-04	2.541	5.27E-05	1.531	2.23E-10
PYCR1	2.328	8.00E-08	1.366	1.67E-11	1.95	0.000347	-	-	-	-
RAB11A	1.656	2.41E-07	1.177	0.009	1.136	0.241	3.839	4.28E-06	1.361	2.85E-08
RAB3B	2.297	0.002	1.659	1.45E-04	2.181	0.006	1.489	0.089	1.995	1.50E-07
RAB3IP	1.547	1.46E-04	1.289	2.92E-04	1.717	0.144	1.213	0.139	1.546	3.89E-10
RABEP2	1.62	1.90E-07	1.197	5.41E-08	1.323	0.014	1.828	0.001	-	-
RAC3	1.31	1.22E-04	1.173	2.66E-06	2.577	0.039	1.728	0.036	-	-
RAP1GAP	1.815	1.83E-10	1.471	5.65E-12	1.723	0.001	1.844	0.002	1.22	0.023
REPS2	2.815	3.63E-13	1.363	5.82E-14	3.099	4.77E-05	2.75	0.001	1.664	0.000248
RER1	1.234	0.00027	-1.058	0.848	1.627	0.136	1.733	0.01	1.704	5.71E-10
RPN2	1.435	1.67E-04	1.201	3.00E-03	1.213	1.12E-01	-	-	1.083	1.21E-01
SDK1	2.959	1.98E-13	1.596	7.77E-23	2.679	6.18E-05	2.445	3.85E-04	-	-
SERINC2	1.246	0.04	1.094	0.015	1.093	0.301	-1.055	0.612	1.273	8.08E-04
SERP1	1.323	4.33E-04	1.221	4.51E-04	1.15	1.70E-01	3.597	1.06E-07	1.312	9.58E-07
SH3BP4	1.473	3.29E-04	1.159	4.00E-03	1.943	3.19E-04	-	-	1.18	0.015
SIM2	4.414	3.68E-07	1.788	1.54E-13	9.229	1.08E-05	-	-	2.8	2.92E-11
SLC25A16	1.275	0.004	1.049	0.059	-1.196	0.739	3.02	1.18E-05	-	-
SLC25A33	1.475	8.55E-06	1.299	3.54E-06	1.233	0.124	2.241	0.001	1.303	0.0001
SLC43A1	2.423	6.32E-13	1.627	1.00E-15	2.049	1.27E-05	1.965	0.005	2.597	7.36E-15
SOAT1	1.516	4.98E-04	1.375	5.80E-04	1.12	1.314	-1.512	0.953	1.203	0.004
SPOCK1	1.671	1.00E-03	1.518	1.40E-04	1.739	2.10E-02	5.598	4.87E-05	2.144	5.92E-13
SPTBN2	1.512	2.53E-06	1.248	4.30E-06	2.27	0.014	1.611	0.187	-	-
SRM	1.275	9.02E-05	1.153	6.24E-09	1.437	0.002	1.588	0.002	1.68	3.60E-09
SRPRB	1.372	1.87E-07	1.302	1.11E-04	1.311	2.70E-02	2.351	4.19E-05	1.324	3.28E-06
ST14	1.647	7.20E-05	1.264	2.99E-05	1.529	0.005	2.43	3.25E-06	1.513	1.13E-07
ST6GAL1	1.41	0.05	1.23	0.012	2.63	0.001	-3.906	1	1.32	0.003
ST6GALNAC1	2.951	5.18E-07	1.378	1.07E-09	4.049	1.99E-06	-	-	1.258	0.026
STRA13	1.419	5.53E-05	1.101	1.31E-05	1.156	0.138	1.255	0.205	1.589	1.72E-07
STT3A	1.263	4.02E-04	1.132	0.025	-	-	2.687	2.70E-05	1.278	1.68E-05
SYNGR2	1.629	0.001	1.138	8.29E-04	1.486	0.002	-	-	-	-
TARP	3.456	9.20E-08	2.466	8.17E-07	2.047	1.90E-02	2.73	0.007	2.623	8.55E-09
TMED3	1.359	2.17E-04	1.144	0.003	1.644	1.78E-04	-	-	1.426	3.24E-06
TMEFF2	2.846	7.51E-04	2.178	1.20E-05	3.308	1.70E-02	-	-	1.676	0.004
TMEM125	1.5	0.024	1.112	0.009	1.023	0.455	-	-	1.371	2.74E-04
TMSB15A	3.215	2.11E-05	1.42	5.18E-13	3.389	4.31E-05	-	-	-	-
TRIM36	2.37	7.28E-05	1.853	1.80E-07	3.454	2.21E-04	1.354	0.075	1.515	7.14E-04
TRPM4	3.059	7.08E-11	1.18	5.59E-04	3.622	3.94E-06	-	-	-1.275	1.00E+00
TSPAN1	2.214	1.13E-06	1.844	1.72E-07	2.303	7.00E-03	-	-	1.59	4.19E-04
TSPAN13	2.486	4.48E-08	1.564	2.45E-09	-1.119	0.704	3.324	8.72E-08	2.462	2.30E-18
TTC39A	1.533	0.012	1.141	0.025	1.133	0.31	-1.588	0.998	1.114	0.106
TUSC3	1.312	1.00E-03	1.257	1.00E-03	1.507	4.70E-02	1.759	0.013	1.066	0.163
TWIST1	1.901	7.38E-06	1.157	4.97E-05	4.697	9.62E-05	-	-	1.639	2.18E-06
UAP1	2.439	1.50E-13	1.761	1.37E-12	2.606	1.34E-07	3.521	1.31E-07	2.387	1.07E-16
UBE2J1	1.476	2.93E-04	1.323	2.84E-04	1.518	1.22E-05	3.781	0.011	1.186	0.000809
UGGT1	1.44	8.02E-05	1.099	7.60E-02	1.11	3.11E-01	1.044	0.394	1.224	1.00E-03
VPS26B	1.197	7.13E-04	1.058	0.049	1.147	0.048	-1.099	0.683	1.338	1.31E-05
YIPF1	1.516	1.15E-04	1.334	4.34E-04	-	-	-	-	1.106	0.088
ZCCHC6	1.836	9.83E-07	1.452	5.41E-05	1.291	1.30E-02	3.155	3.13E-07	1.716	2.52E-09
ZDHHC9	1.474	2.23E-04	1.45	1.53E-07	1.45	7.91E-06	2.018	4.44E-05	1.661	4.73E-11
ZNF350	1.541	2.68E-04	1.232	0.007	1.073	0.385	2.117	0.002	1.771	3.84E-08
ZNF697	1.517	0.000309	1.086	4.00E-03	1.831	0.002	2.107	0.000226	1.445	9.19E-06

Table 3.2 Meta-analysis using Oncomine online database of genes up-regulated by androgens in LNCaP cells and down-regulated in patients post ADT. Five micro-array datasets were interrogated using the Oncomine database. For each study, gene expression in prostate cancer tissue was compared with that of normal tissue (control). The table shows genes which passed the threshold criteria (fold change >1, p value <0.05 in at least two of the five studies) with their associated fold change (fc) and p value for each of the five datasets (Lapointe *et al.*, 2004; Varambally *et al.*, 2005; Tomlins *et al.*, 2007; Taylor *et al.*, 2010; Grasso *et al.*, 2012). Genes which meet the threshold criteria in at least four of the five studies are highlighted blue, and genes which meet the threshold criteria in all five studies are highlighted green.

3.3.3 Gene ontology analysis identifies glycosylation as a key androgen regulated processed in prostate cancer

To focus analysis of the dataset, Gene Ontology (GO) enrichment analysis was carried out by Dr Katherine James (Newcastle University). Briefly, GO analysis was used to investigate the pathways associated with biological processes as previously described (Young *et al.*, 2010). Genes were considered significant at a p-value threshold of 0.05 after adjustment using the Benjamini-Hochberg false discovery rate.

GO analysis of the reciprocally regulated gene sets identified 72 terms with significant gene enrichment ($p < 0.05$). The top 30 significantly enriched terms from the up-regulated gene set are shown in Figure 3.4. Only one GO term was identified with significant gene enrichment within the down-regulated gene set. This was cell morphogenesis involved in differentiation with a $-\log_{10}$ (p value) of 1.854739888.

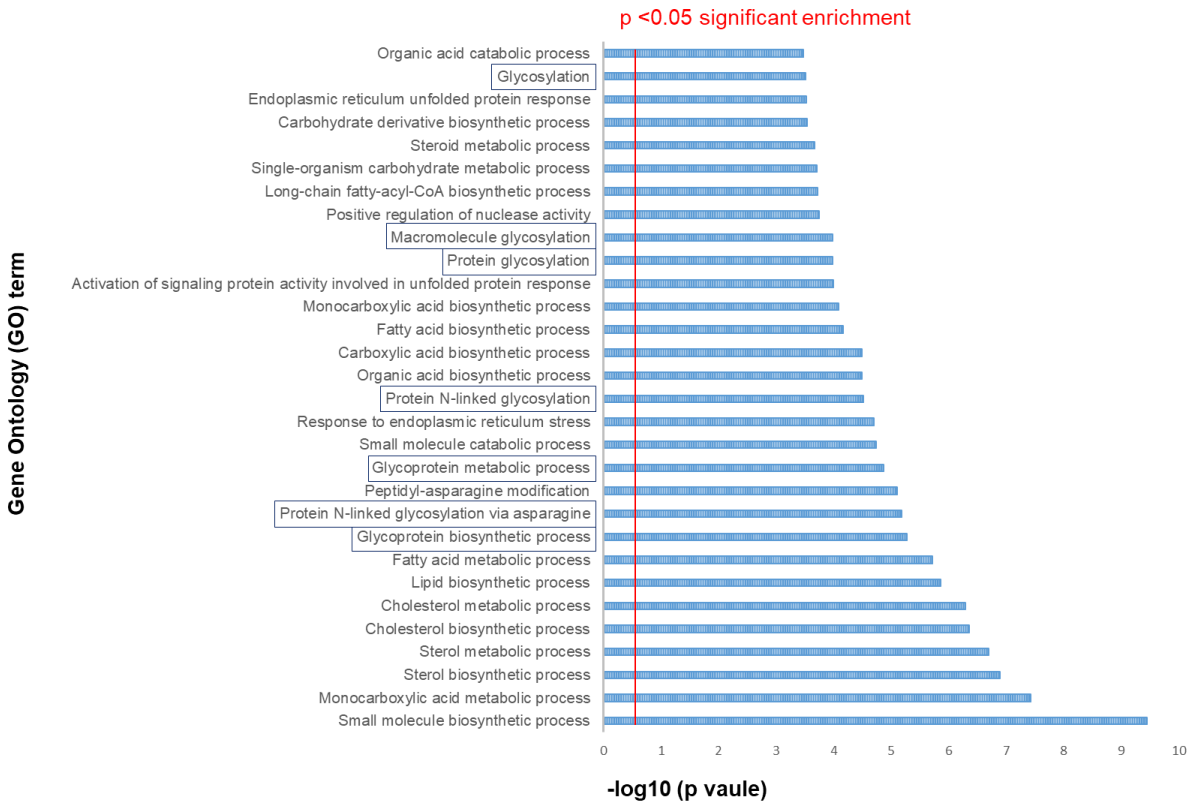

Figure 3.4 Gene Ontology (GO) analysis of the reciprocally regulated genes. GO analysis of the 660 reciprocally regulated gene set identified 72 terms with significant gene enrichment ($p < 0.05$). GO analysis was performed by Dr Katherine James (Newcastle University). The bar graph shows the $-\log_{10}$ (p values) for the top 30 significantly enriched terms. Glycosylation related terms; glycoprotein biosynthetic process, protein N-linked glycosylation via asparagine, glycoprotein metabolic process, protein N-linked glycosylation, protein glycosylation, macromolecule glycosylation and glycosylation are highlighted within the blue boxes.

GO investigation identified a number of known androgen regulated processes including lipid and cholesterol biosynthesis (Suburu and Chen, 2012; Wu *et al.*, 2014), fatty acid metabolism (Swinnen *et al.*, 2000; Li *et al.*, 2016a), and response to ER stress (Sheng *et al.*, 2015; Storm *et al.*, 2016). Glycosylation was identified as a previously unidentified system-wide androgen-regulated process, involving 7 of the top 30 significantly enriched GO terms; glycoprotein biosynthetic process (GO:0009101), protein N-linked

glycosylation via asparagine (GO:0018279), glycoprotein metabolic process (GO:0009100), protein N-linked glycosylation (GO:0006487), protein glycosylation (GO:0006486), macromolecule glycosylation (GO:0043413) and glycosylation (GO:0070085) (highlighted within the blue boxes in Figure 3.4).

There was an enrichment of genes encoding glycosylation enzymes within the dataset; a total of 31 genes involved in glycosylation were identified. Androgen regulation of these genes was confirmed in an independent LNCaP sample set by real-time quantitative reverse transcription PCR (qRT-PCR) (Figure 3.5). Further online GO software packages was used to confirm our findings, these included GOrilla (**G**ene **O**ntology en**RI**chment ana**L**ysis and visua**L**iz**A**tion tool), available at http://cbl-gorilla.cs.technion.ac.il/ and The Gene Ontology Resource, available at http://geneontology.org/.

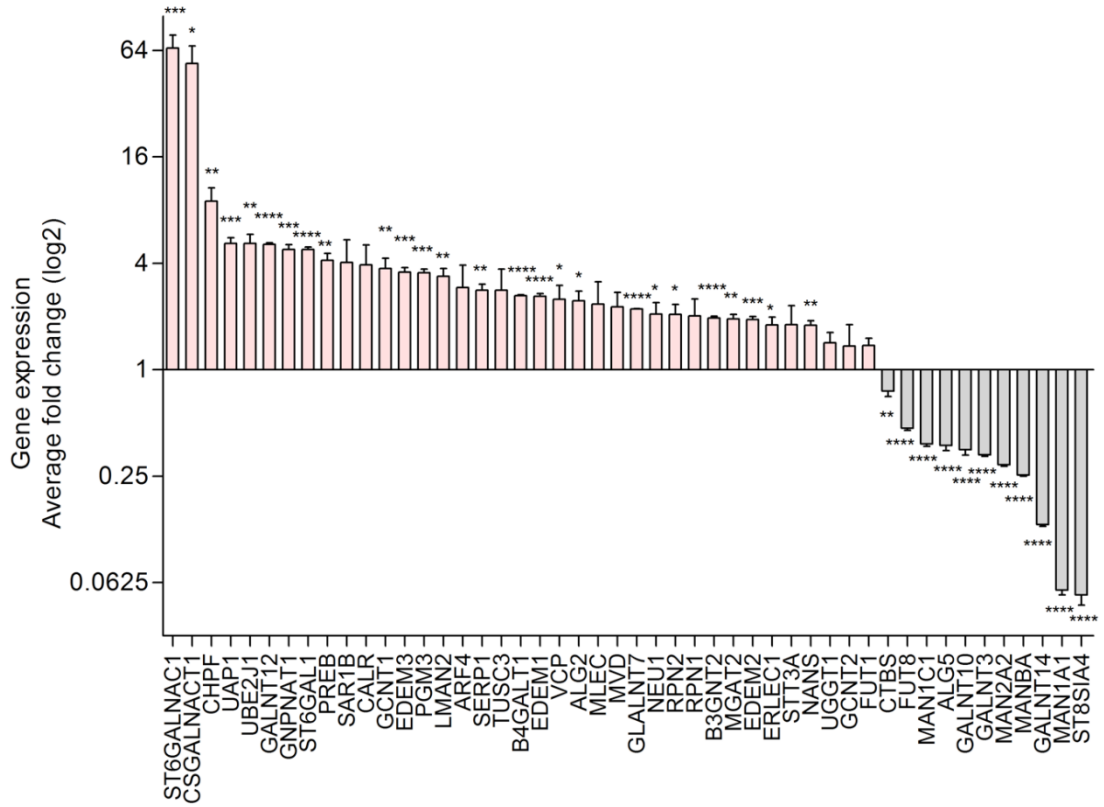

Figure 3.5 Expression of glycosylation related genes in LNCaP cell line in response to androgens. Real-time quantitative reverse transcription PCR (qRT-PCR) analysis of 31 glycosylation related genes in LNCaP cells in response to 10 nM synthetic androgen (R1881) stimulation (24 hours). Gene expression was calculated as the average (3 biological replicates) fold change (log2) relative quantification of androgen treated LNCaP cells compared to steroid deplete cells (value set as 1). Samples were normalised using the average of three reference genes, GAPDH, β -tubulin and actin. Statistical significance was calculated using an independent two-sample t-test. All primer sequences are listed in Appendix B.

Aberrant protein glycosylation is known to be associated with the development of many cancers. Changes in the glycan composition of PCa cells has been linked to disease progression: ST6 N-acetylgalactosaminide α-2,6-sialyltransferase 1 (*ST6GALNAC1*), UDP-N-acetylglucosamine pyrophosphorylase 1 (*UAP1*), glucosamine-phosphate N-acetyltransferase 1 (*GNPNAT1*) and glucosaminyl (N-acetyl) transferase 1 (*GCNT1*), are all known AR target genes that have previously been linked with PCa progression. *ST6GALNAC1* is a direct target of the AR and can affect cell adhesion (Munkley *et al.*, 2015b). *UAP1* is over-expressed in PCa patients and its expression negatively correlates with Gleason score (Itkonen *et al.*, 2015). *GNPNAT1* is significantly decreased in CRPC and is linked to increased proliferation and aggressiveness (Kaushik *et al.*, 2016), whilst *GCNT1* expression correlates with the aggressive potential of PCa (Hagisawa *et al.*, 2005; Chen *et al.*, 2014).

Although not previously directly identified as androgen responsive genes, tumour suppressor candidate 3 (*TUSC3*) and α (1,6) fucosyltransferase (*FUT8*) have been linked to PCa. *TUSC3* knockdown in PC3 and DU145 cell lines alters the ER stress response and accelerates proliferation and invasion (Horak *et al.*, 2014). Although the function of *TUSC3* has not yet been characterised, it shares homology with the *S. cerevisiae* oligosaccharyltransferase (OST) complex subunit Ost3p, implying a role in protein glycosylation. Over-expression of α (1,6) fucosyltransferase (FUT8) in LNCaP cells increases cell migration, while loss of FUT8 in PC3 cells decreased cell motility (Wang *et al.*, 2014b).

Androgen regulated expression of these glycosylation genes was also analysed in the VCaP cell line by real-time quantitative reverse transcription PCR (qRT-PCR) (Figure 3.6). Again, VCaP cells were treated with 10nM R1881 for 24 hours (A+) or without (steroid deplete, SD).

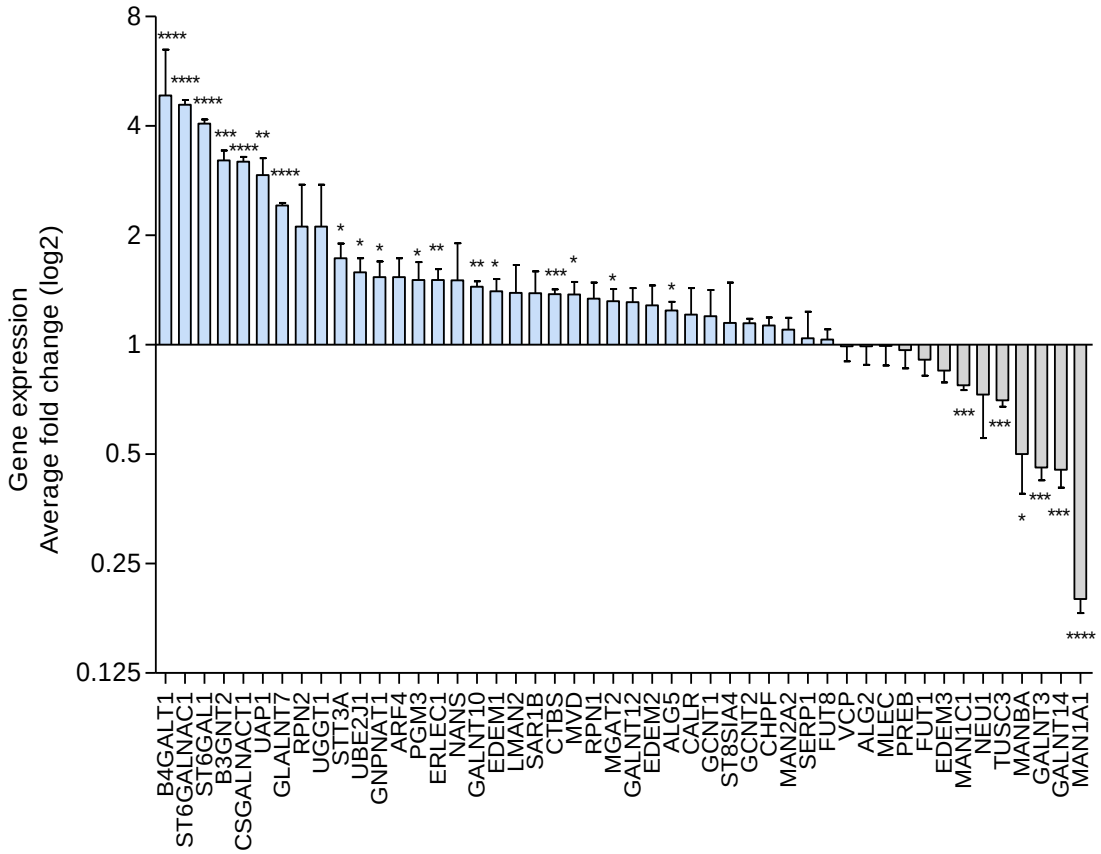

Figure 3.6 Expression of glycosylation related genes in VCaP cell line in response to androgens. Real-time quantitative reverse transcription PCR (qRT-PCR) analysis of 31 glycosylation related genes in VCaP cells in response to 10 nM synthetic androgen (R1881) stimulation (24 hours). Gene expression was calculated as the average (3 biological replicates) fold change (log2) relative quantification of androgen treated LNCaP cells compared to steroid deplete cells (value set as 1). Samples were normalised using the average of three reference genes, GAPDH, β -tubulin and actin. Statistical significance was calculated using an independent two-sample t-test. All primer sequences are listed in Appendix B.

Of the 31 identified glycosylation genes, 17 meet the threshold criteria for our earlier meta-analysis (fold change >1, p value <0.05 in at least two of the studies analysed): dolichyl-phosphate beta-glucosyltransferase (*ALG5*), ADP ribosylation factor 4 (*ARF4*), calreticulin (*CALR*), ER degradation enhancing alpha-mannosidase like protein 3 (*EDEM3*), fucosyltransferase 1 (*FUT1*), glucosaminyl (N-acetyl) transferase 1 (*GCNT1*), polypeptide N-acetylgalactosaminyltransferase 7 (*GALNT7*), glucosamine-phosphate N-acetyltransferase 1 (*GNPNAT1*), Nacetylneuraminate synthase (*NANS*), ribophorin II (*RPN2*), stress associated endoplasmic reticulum protein 1 (*SERP1*), catalytic subunit of the oligosaccharyltransferase complex (*STT3A*), ST6 N-acetylgalactosaminide α-2,6-sialyltransferase 1 (*ST6GALNAC1*), ST6 beta-galactoside alpha-2,6-sialyltransferase 1 (*ST6GAL1*), tumour suppressor candidate 3 (*TUSC3*), UDP-N-acetylglucosamine pyrophosphorylase 1 (*UAP1*), ubiquitin conjugating enzyme E2 J1 (*UBE2J1*) and UDP-glucose glycoprotein glucosyltransferase 1 (*UGGT1*). Of these, 7 meet the threshold criteria in at least four of the five studies: *EDEM3, GCNT1, SERP1, STT3A, ST6GALNAC1, ST6GAL1,* and *TUSC3* and 3 meet the criteria in all five of the studies: *GNPNAT1, UBE2J1* and *UAP1*. *ST6GALNAC1, UAP1, ST6GAL1* and *UBE2J1* have the highest expression fold change in response to androgens in both the LNCaP and VCaP cell lines.

To confirm androgen regulation of these genes, AR binding profiles created using chromatin immunoprecipitation with direct Solexa sequencing (ChIP-seq) were interrogated. Massie *et al* 2011 mapped AR binding profiles in LNCaP and VCaP cell lines, identifying 11,053 AR binding sites in LNCaP cells and 51,811 AR binding sites in VCaP cells (Massie *et al.*, 2011). Annotations from the UCSC genome browser were used to calculate the distance to the transcription start sites for each of the identified glycosylation genes (Table 3.3).

From the 10 genes which meet the threshold criteria in at least four of the five meta-analysis studies, 9 had AR binding site within 50kb of the transcription start site: *EDEM3* (9.3kb)*, GCNT1* (29.6kb)*, SERP1* (48.5kb)*, STT3A* (14.5kb)*, ST6GALNAC1* (2.6kb)*,*

ST6GAL1 (7.2kb), *TUSC3* (1.3kb), *UBE2J1* (6.1kb) and *UAP1* (9.3kb) suggesting that expression is under the control of the AR.

Gene	Distance from AR binding site (kb)
ST6GALNAC1	2.6
CSGALNACT1	1.4
CHPF	12.3
UAP1	9.3
UBE2J1	6.1
ST6GAL1	7.2
SAR1B	85.4
GNPNAT1	85.9
EDEM3	9.3
CALR	54.0
GCNT1	29.6
PGM3	24.6
PREB	4.1
ARF4	10.5
SERP1	48.5
TUSC3	1.3
B4GALT1	13.6
RPN2	0.5
VCP	83.1
ALG2	1.2
NANS	4.0
MLEC	134.0
MVD	131.7
GALNT7	10.4
NEU1	28.6
ERLEC1	5.3
STT3A	14.5
UGGT1	4.0
GCNT2	7.1
LMAN2	16.4
FUT1	12.9

Table 3.3 Distance in kilobases (kb) of androgen receptor binding sites from the transcriptional start site of the identified glycosylation genes. Published data from mapped AR binding profiles (Massie *et al.*, 2011) were used to calculate the distance in kilobases (kb) of AR binding sites from the transcriptional start sites of the

glycosylation genes. AR binding site annotations were created by uploading the published data to the UCSC genome browser and calculations were made for each gene. Numbers in red indicate the presence of an AR binding site within 50kb of the transcription start site of the gene. Genes highlighted in blue represent genes which meet the threshold criteria in at least four of the five meta-analysis studies.

3.4 Discussion

In this chapter, RNA sequencing has been used to identify reciprocal gene expression changes in response to acute androgen stimulation in cultured prostate cancer cells, and androgen deprivation in 7 patients with prostate cancer. This method highlighted a core set of 660 clinically relevant androgen-regulated genes: 548 genes whose expression was up-regulated by androgens in LNCaP cells and down-regulated in all 7 patients following ADT and 112 genes whose expression was down-regulated by androgens in LNCaP cells and up-regulated in 7 patients following ADT. This data provides a comprehensive map of AR-regulated genes in clinical prostate cancer. It offers a new window through which to understand the signalling pathways downstream of the AR and the role these pathways play in both the development of PCa and the response to ADT.

Previous studies have looked at androgen regulation *in vitro* (Massie *et al.*, 2007; Wang *et al.*, 2007; Rajan *et al.*, 2011) and somewhat fewer *in vivo* (Lohr *et al.*, 2014; Rajan *et al.*, 2014; Radtke *et al.*, 2017). The correlation of androgen regulation in cell lines with PCa patient samples, coupled with a multiple dataset meta-analysis strategy presented here has identified a number of AR-regulated genes that have not previously been considered, such as the epithelial splicing regulatory protein *ESRP2*, the nectin cell adhesion molecule *PVRL2* and cell migration protein *TSPAN1*. Further investigation has found that increased expression of *TSPAN1* in prostate cancer cells controls the expression of key proteins involved in cell migration, and is important for cancer cell survival (Munkley *et al.*, 2017b).]

Although we have identified a number of individual genes as androgen regulated, further analysis of the dataset indicates a system wide regulation, with a significant enrichment in the cellular process glycosylation. A total of 31 genes were identified in the GO analysis, of these 10 also showed significant gene expression changes (fold change >1, p value <0.05) in at least four of the five meta-analysis studies: *EDEM3, GCNT1, SERP1, STT3A, ST6GALNAC1, ST6GAL1, GNPNAT1, UBE2J1*, *TUSC3 and UAP1.* Of these, 9

genes had an AR binding site within 50kb of the transcription start site, suggesting changes in expression were directly under AR control.

Aberrant glycosylation, primarily caused by altered expression or the mislocalisation of glycoenzymes is a common feature of cancer cells (Pinho and Reis, 2015; Stowell *et al.*, 2015). Alterations in the expression of these glycoenzymes can lead to modifications which can alter many important biological processes such as cell-cell adhesion, migration, interactions with the cell matrix, immune surveillance, signalling and cellular metabolism (Munkley and Elliott, 2016). The enrichment of genes encoding glycosylation enzymes within our dataset suggests that these genes may play a role in modifying some of these processes in PCa and could therefore contribute to disease progression.

From the genes identified, *GCNT1, ST6GALNAC1, TUSC3* and *UAP1* have previously been linked to PCa. Increased expression of *GCNT1*, which is involved in the formation of branched O-linked glycans, has been shown to positively correlate with the aggressive potential of PCa (Hagisawa *et al.*, 2005; Chen *et al.*, 2014). Increased expression of *ST6GalNAc1* by androgens in prostate cancer cells can reduce prostate cancer cell adhesion (Munkley *et al.*, 2015b; Munkley *et al.*, 2016b). Knockdown of the novel tumour suppressor gene *TUSC3* in PCa cell lines alters the ER stress response and accelerates proliferation and invasion (Horak *et al.*, 2014). UAP1 is highly overexpressed in PCa and can protect cancer cells from ER stress by protecting against inhibitors (Itkonen *et al.*, 2014). Both SERP1 and UBE2J1 have been identified as androgen regulated in previous microarray profiling studies (Lin *et al*., 2013), however there has been no linked made to the prostate cancer progression. In fact, UBE2J1 expression has no impact on LNCaP androgen independent cell growth (Sun et al., 2014). As far as I am aware, this is the first time androgen regulation of *EDEM3, STT3A*, and *ST6GAL1* has been described.

The identification of glycosylation as an androgen regulated process in PCa could have important clinical implications both in patient diagnosis and therapeutic strategies. An

increased understanding of how these individual glycoenzmyes and glycosylation as a whole influences prostate cancer cell behaviour is required. This could assist in the development of new glyco-based specific biomarkers for use in the early detection and management of PCa. Glycans have been shown to play a role in all aspects of cancer progression and are therefore attractive targets for therapeutic intervention (Munkley and Elliott, 2016). Inhibiting glycosylation, even in conditions where the AR is active, can decrease PCa cell viability and invasion potential (Itkonen and Mills, 2013; Itkonen *et al.*, 2016)

Chapter 4

Results

Characterisation of ST6Gal1 in prostate cancer

Chapter 4 Results

Characterisation of ST6Gal1 in prostate cancer

4.1 Introduction

4.1.1 Glycosylation is an androgen regulated process

In the previous chapter I presented data that identified glycosylation as a global target for androgen control in prostate cancer cells. Understanding the role androgen-regulated pathways play in prostate cancer is important as it can have clinical implications in patient diagnosis and treatment. Analysis of our RNA sequencing data identified 31 individual glycosylation related genes with reciprocal expression patterns following androgen stimulation in vitro and ADT in patient samples. Meta-analysis of five individual PCa gene expression datasets (Lapointe et al., 2004; Varambally et al., 2005; Tomlins et al., 2007; Taylor et al., 2010; Grasso et al., 2012) identified a subset of 10 glycosylation genes with significant expression changes (p value <0.05) in PCa relative to normal prostate gland in at least four of the five datasets. These genes were: *EDEM3, GCNT1, SERP1, STT3A, ST6GALNAC1, ST6GAL1, TUSC3, GNPNAT1, UBE2J1* and *UAP1*.

EDEM3 stimulates mannose trimming of N-glycans and belongs to a group of proteins that are involved in the endoplasmic reticulum-associated degradation (ERAD) of misfolded glycoproteins (Hirao et al., 2006; Olivari and Molinari, 2007). ERAD is a highly controlled mechanism within the ER that degrades unwanted and misfolded glycoproteins. ERAD is especially important in cancer, where increased metabolic activity can lead to the accumulation of faulty proteins (Olzmann et al., 2013). The ERAD pathway is known to be androgen regulated; androgen treatment causes an up-regulation of ERAD associated genes and increases the degradation rate of ERAD substrates (Erzurumlu and Ballar, 2017). Work within our laboratory has found that expression of EDEM3 is androgen regulated in PCa cells and is important for PCa cell viability and growth (Munkley *et al.*, 2016b).

SERP1, a stress response protein which helps stabilises membrane proteins and facilitates N-linked glycosylation (Yamaguchi et al., 1999; Xiao et al., 2017) has recently been identified as a marker of poor prognosis in pancreatic ductal adenocarcinoma patients (Ma et al., 2017). UBE2J1 is another glyco-enzyme which functions within the ERAD pathway, catalysing the covalent attachment of ubiquitin to proteins for degradation. Androgen regulation of SERP1 and UBE2J1 has been described previously (Jin et al., 2013) but there are no currently reported links to prostate cancer.

GCNT1 is a glycosyltransferase that is involved in the formation of core 2 branched O-glycans. O-glycans are often altered in the early stages of cellular transformation and are important for initiation, invasion and metastasis (Pinho and Reis, 2015). GCNT1 expression is regulated by androgens in PCa cells and has been associated with aggressive potential (Munkley *et al.*, 2016b; Sato *et al.*, 2016). Detection of GCNT1 in PCa patients urine has been used differentiate between extracapsular extension and localised disease (Kojima et al., 2015). Increased expression of GCNT1 has also been implicated in the synthesis of the cancer associated SLex antigen (Chen et al., 2014).

STT3A encodes the catalytic subunit of the oligosaccharyltransferase (OST) complex (Yan and Lennarz, 2002; Nilsson et al., 2003). The OST complex functions in the endoplasmic reticulum to transfer complex glycan chains to asparagine residues of target proteins. The STT3A protein is present in the majority of OST complexes and is involved in the co-translational N-glycosylation of most sites on target proteins. Androgen regulation of STT3A expression has not previously been described and there no clear links to cancer have been reported. TUSC3 is another component of the OST complex. Localised to the ER, TUSC3 functions in final stages of N-glycosylation through its interaction with the STT3B subunit (Horak et al., 2014; Mohorko et al., 2014). TUSC3 knockdown in PCa cells alters the ER stress response and accelerates proliferation and invasion, suggesting a potential tumour suppressor role (Horak et al., 2014).

Previous work in our laboratory has found that expression of ST6GalNAc1, a sialytransferase that catalyses the transfer of sialic acid onto the Tn antigen, is regulated by androgens and can affect cell adhesion (Munkley *et al.*, 2015b). Increased ST6GalNAc1 expression is found in primary prostate tumours, although this expression is down-regulated in metastatic tissue compared to non-malignant prostate tissue, suggesting a more transient role in tumour progression. An androgen regulated novel splice variant of the ST6GalNAc1 protein in PCa cells reduces adhesion, increases motility and promotes a transition towards a mesenchymal like phenotype (Munkley *et al.*, 2015b).

ST6Gal1 is another sialytransferase that catalyses the transfer of sialic acid from CMP-sialic acid to N-terminus of galactose-containing substrates. Increased sialylation is already known to be associated with cancer cell progression and metastasis, affecting cell adhesion, migration and invasion (Seales et al., 2005; Bull et al., 2013; Pinho and Reis, 2015). Up-regulation of ST6Gal1 has been described in several cancers including colon cancer (Dall'Olio et al., 1989), breast cancer (Lin et al., 2002), choriocarcinoma (Fukushima et al., 1998), hepatocarcinoma (Dall'Olio et al., 2004; Poon et al., 2005), cervical cancer (Wang et al., 2001), and myeloid leukaemias (Skacel et al., 1991). Whilst there are many studies that support the oncogenic role of ST6Gal1 in cancer (Britain CM 2017) (Swindall and Bellis, 2011) (Amano et al., 2003; Seales et al., 2005; Shaikh et al., 2008; Liu et al., 2011; Park et al., 2012) (Lin et al., 2002) (Meng et al., 2015) (Zhu et al., 2001) (Lu et al., 2014) (Liu *et al.*, 2014b) (Hsieh et al., 2017) (Mondal et al., 2010), there is also contradictory evidence to suggest that ST6Gal1 may also have tumour suppressor potential (Park et al., 2012) (Wild et al., 2005) (Antony et al., 2014), and its role in PCa is yet to be established.

The hexosamine biosynthetic pathway (HBP) pathway works to metabolise glucose to produce UDP- N-acetylglucosamine (GlcNAc). UDP-GlcNAc functions as the main sugar donor for N-linked and O-linked glycosylation. GNPNAT1 is an acyltransferases which is involved in the HBP. GNPNAT1 expression is regulated by androgens and elevated in

androgen dependant PCa cells. GNPNAT1 expression is significantly decreased in CRPC compared to localised PCa and it has been linked to increased proliferation and aggressiveness (Kaushik et al., 2016). UAP1 is the last enzyme in the HBP and is highly over-expressed in PCa patients (Itkonen et al., 2015). We have also shown that depletion of UAP1 in PCa cells reduces cell viability (Munkley *et al.*, 2016b).

4.1.2 The role of ST6Gal1 in prostate cancer

Taken together, the above data suggests that glycosylation is an androgen regulated process and that the controlled expression of many glycosylation associated enzymes may help contribute towards PCa development and progression (Munkley *et al.*, 2016b; Munkley, 2017). Of the identified genes, I decided to investigate the role of ST6Gal1 in PCa further. ST6Gal1 is a member of the ST6 sialytransferase family which catalyses the transfer of sialic acid from CMP-sialic acid to galactose containing acceptor substrates on N-glycans in the α-2,6 formation (Weijers et al., 2008). Sialic acids are often expressed as the terminal glycan of glycoconjugates and due to their terminal locality have associated with functions such as adhesion, recognition, immune defence and stability (Hedlund et al., 2008; Swindall and Bellis, 2011; Schultz et al., 2012). Elevated sialyltransferase activity can result in hypersialylation and an upregulation of sialylated glycans, which has been linked to cancer (Pearce and Laubli, 2016; Wang *et al.*, 2016b). Hypersialylation is an established hallmark of cancer and has been associated with more malignant tumour phenotypes (Hauselmann and Borsig, 2014; Munkley and Elliott, 2016).

ST6Gal1 has been shown to function as a regulator of cell survival; α-2,6 sialylation of the Fas death receptor (CD95), tumour necrosis receptor 1 (TNFR1) and the CD45 receptor, protects against apoptosis (Amano et al., 2003; Liu et al., 2011; Swindall and Bellis, 2011). ST6Gal1 up-regulation promotes cell migration and invasion through its interaction with the β1 integrin and EGFR receptors (Seales et al., 2005; Shaikh et al., 2008; Park et al., 2012), whilst knockdown of ST6Gal1 inhibits metastasis in breast cancer (Lin et al., 2002), osteosarcoma (Meng et al., 2015) and colon cancer (Zhu et al.,

2001). In localised clear-cell renal carcinomas, ST6Gal1 expression is an adverse predictor of survival and recurrence (Liu *et al.*, 2014b), whilst in pancreatic cancer, high ST6Gal1 expression predicted poorer patient prognosis (Hsieh et al., 2017). High ST6Gal1 expression also positively correlates with high risk of paediatric acute leukemia (Mondal et al., 2010).

Whilst there are many studies that support the oncogenic role of ST6Gal1 in cancer, there is also contradictory evidence to suggest that ST6Gal1 may also have tumour suppressor potential. Down-regulation of ST6Gal1 in colorectal cancer (CRC) cell lines increased cell proliferation and tumour growth (Park et al., 2012). In CRC patient pair-matched tumour/normal tissue ST6Gal1 expression was significantly higher in non-metastatic tumours than that in metastatic tumours (Zhang et al., 2017). ST6Gal1 is also down-regulated in invasive bladder cancer when compared to normal urothelium, and expression loss correlates with high grade, invasive clinical tumours (Wild et al., 2005). This expression loss is caused by aberrant ST6Gal1 promoter methylation, suggesting repression of a possible tumour suppressive role for ST6Gal1 in advanced bladder cancer (Antony et al., 2014).

4.1.3 The role of ST6GAL1 in epithelial to mesenchymal transition (EMT)

Epithelial to mesenchymal transition (EMT) is a highly conserved trans-differentiation process in which epithelial cells lose their polarity and take on more migratory mesenchymal properties (Thiery and Sleeman, 2006). EMT involves the loss of tight junctions, adherens junctions and desmosomes, together with cytoskeleton changes, a transcriptional shift and increased cell migration and motility potential. EMT is characterised by decreased expression of cell adhesion molecules and epithelial markers such as actin, E-cadherin, β-catenin, claudins and desmosomal proteins, and increased expression of intermediate filament proteins and mesenchymal cell markers, including N-cadherin, α-smooth muscle actin (α-SMA), and vimentin. EMT can be induced by a number of different growth and transcription factors including transforming growth factor-β (TGF-β) (Xu et al., 2009). Increased expression of ST6Gal1 has been

shown to promote TGF- β induced EMT in the mouse epithelial cell line GE11, through the down-regulation of E-cadherin mediated cell adhesion and up-regulation of integrin mediated cell migration (Lu et al., 2014).

EMT plays an important role in the invasiveness of cancer cells and understanding the process of EMT may help unravel the mechanisms that control cancer progression. In particular, cancer cells undergoing EMT often present aberrant glycan structures, fuelled by metabolic reprogramming (Carvalho-Cruz et al., 2017).

4.2 Aims of the chapter

Current evidence suggests a complex role for ST6Gal1 in cancer development and progression. The work in this thesis has so far shown that ST6Gal1 expression is up-regulated in PCa cells in response to androgen stimulation, but the role ST6Gal1 plays in PCa requires further investigation.

The aims of this chapter were to:

- Use prostate cancer cells lines and clinical patient samples to identify ST6Gal1 expression patterns.
- Use molecular cloning techniques to create stable prostate cancer cell lines with either ST6Gal1 over-expression or knock-down.
- Investigate the effect of these expression changes on the cellular functions of prostate cancer cells (proliferation, migration, invasion potential).
- Use RNA sequencing techniques to identify ST6Gal1 regulated transcriptional changes in prostate cancer.

Achieving these aims will help us to understand the role that ST6Gal1 plays in prostate cancer and whether it has potential as a target for early PCa diagnosis and treatment.

4.3 Results

4.3.1 Expression of ST6Gal1 is up-regulated by androgens

Our RNA sequencing data of LNCaP cells showed that ST6Gal1 expression is up-regulated by androgen stimulation. A UCSC Genome Browser snapshot of this result is shown in Figure 4.1.

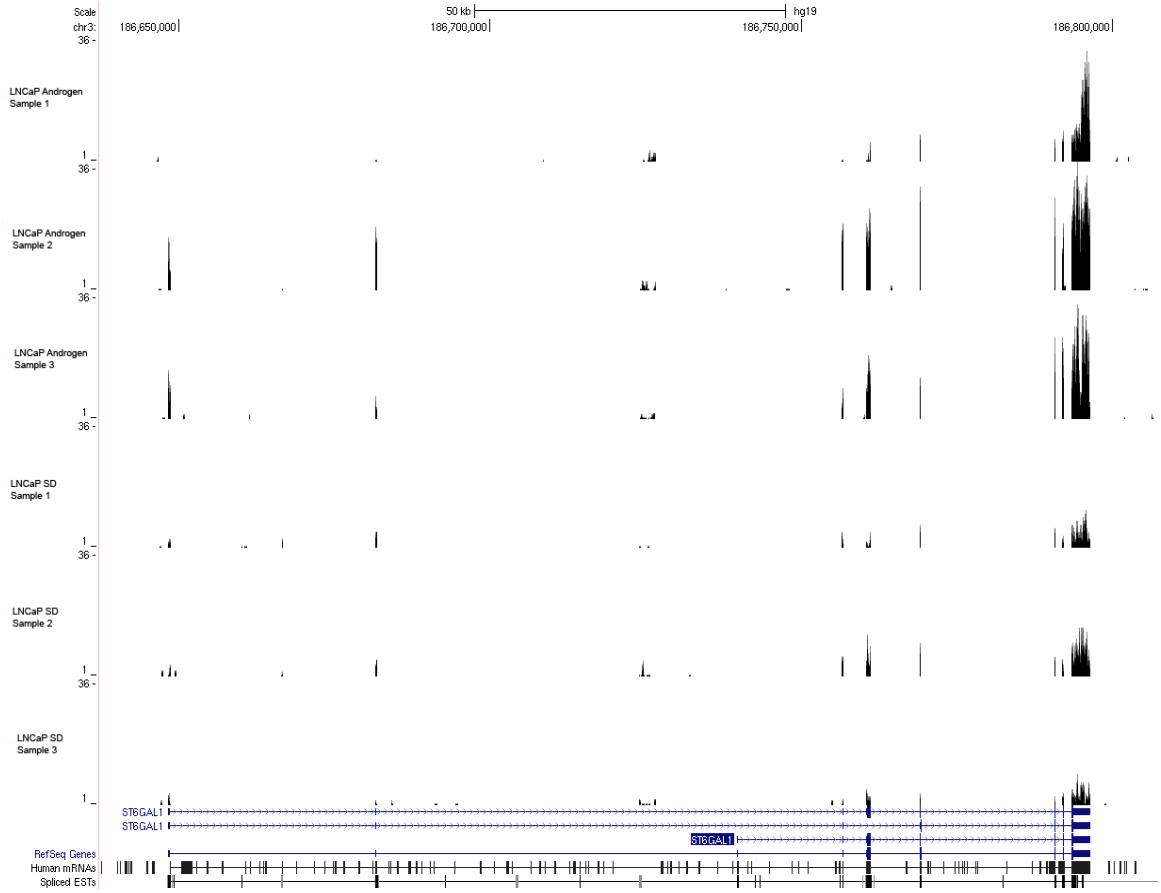

Figure 4.1 UCSC Genome Browser snapshot showing RNA sequencing reads aligned to ST6Gal1. RNAseq profiles are shown from three biological replicates of LNCaP cells grown in the presence of 10 nM synthetic androgen R1881 for 24 hours (LNCaP Androgen) and LNCaP cells grown in charcoal stripped steroid deplete media (LNCaP SD).

To confirm androgen regulated of ST6Gal1, a new triplicate sample set of LNCaP cells were grown in charcoal stripped steroid deplete media (SD) for 24 hours, then treated with 10 nM synthetic androgen R1881 (A+) for three different time periods prior to harvest: 24 hours, 48 hours and 72 hours. Figure 4.2 confirms that androgen treatment increased both mRNA and protein levels of ST6Gal1 in LNCaP cells.

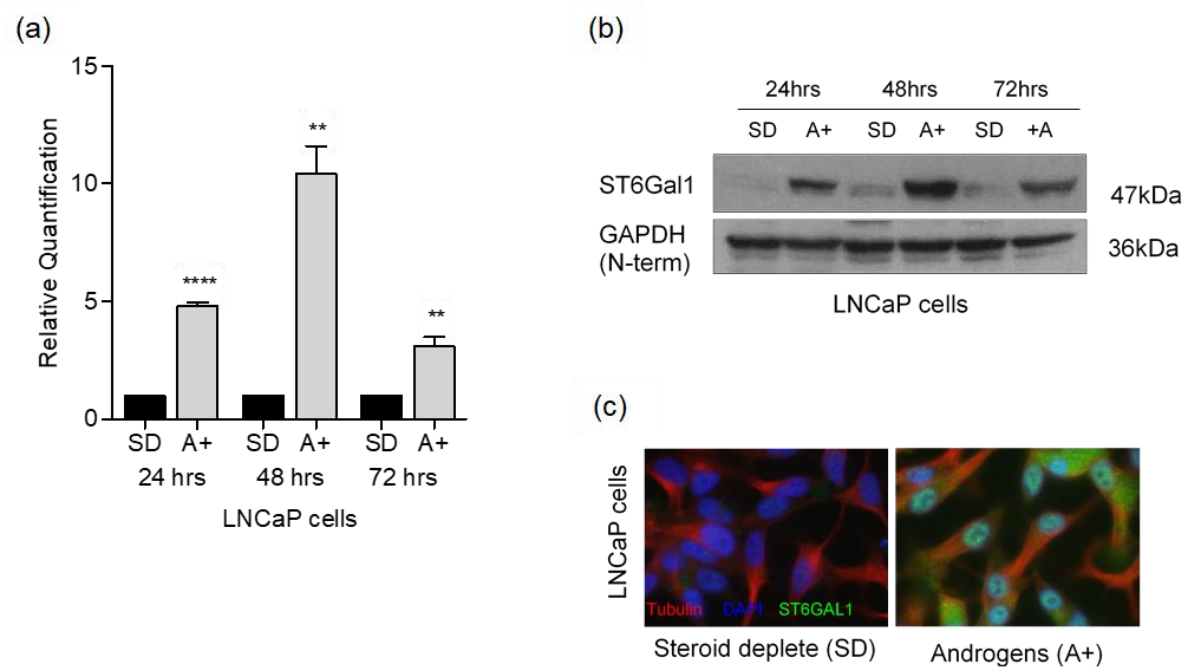

Figure 4.2 Expression of ST6Gal1 in the PCa LNCaP cell line.

(a) Real-time quantitative reverse transcription PCR (qRT-PCR) analysis of ST6Gal1 mRNA in LNCaP cells treated with androgens over a 72 hour time period. Samples were taken at 24 hours, 48 hours and 72 hours. Gene expression was calculated as the average (from 3 biological replicates) fold change relative quantification of androgen treated LNCaP (A+) cells compared to steroid deplete cells (SD) (SD value set as 1). Samples were normalised using the average of three reference genes, GAPDH, β-tubulin and actin. Statistical significance was calculated using an independent two-sample t-test, where * $p < 0.05$, ** $p < 0.01$, *** $p < 0.0001$, **** $p < 0.00001$. All primer sequences are listed in Appendix B.

(b) Representative Western blot - expression of ST6Gal1 protein was induced in LNCaP cells treated with androgens at 24 hours, 48 hours and 72 hours. GAPDH (N-terminal) was used as a loading control.
(c) Expression of ST6Gal1 protein detected in LNCaP cell treated with androgen for 24 hours by immunofluorescence.

Using a 24 hour time course in which cells were harvested at three hour intervals and qRT-PCR we found that androgen mediated induction of the ST6Gal1 gene could be detected in LNCaP cells after 6 hours androgen exposure (Figure 4.3a). This is a similar pattern of expression to PSA (Kim and Coetzee, 2004). ST6Gal1 expression was also blocked by treatment with the AR antagonist Casodex (bicalutamide) (Figure 4.3b), suggesting that ST6Gal1 is directly regulated by the AR.

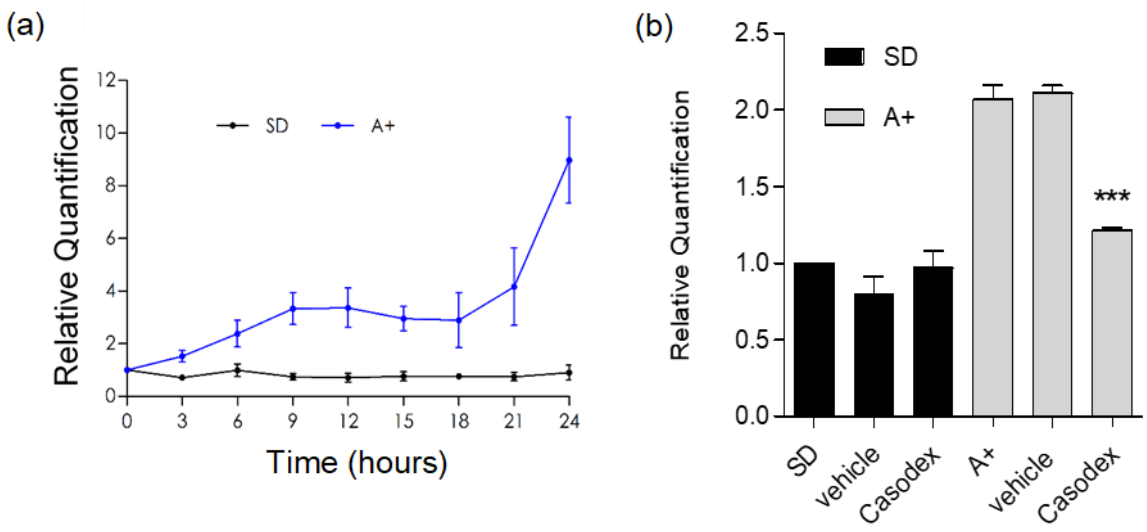

Figure 4.3 ST6Gal1 expression is directly regulated by the androgen receptor.

(a) Real-time quantitative reverse transcription PCR (qRT-PCR) analysis of ST6Gal1 mRNA in LNCaP cells treated with androgens (A+) over a 24 hour time period (samples were taken every 3 hours). Gene expression was calculated as the average (from 3 biological replicates) fold change of androgen treated LNCaP (A+) cells relative to steroid deplete cells (SD) (value set as 1). Samples were normalised using the average of three reference genes (GAPDH, β -tubulin and actin).

(b) Induction of ST6Gal1 mRNA by the AR is inhibited in the presence of 10 μM of the anti-androgen Casodex (bicalutamide). Statistical significance was calculated using an independent two-sample t-test, where * p <0.05, ** p <0.01, *** p <0.0001, **** p <0.00001.

Depletion of ST6Gal1 in LNCaP cells by two different siRNAs reduces cell viability. ST6Gal1 knockdown was confirmed at transcript level by qRT-PCR (Figure 4.4a) and at the protein level by Western blot (Figure 4.4b). Crystal violet staining of LNCaP cells 92 hours after siRNA transfection shows a significant reduction in cell numbers compared to cells transfected with non-targeted control siRNA, indicating an important biological role for ST6GAL1 in these cells.

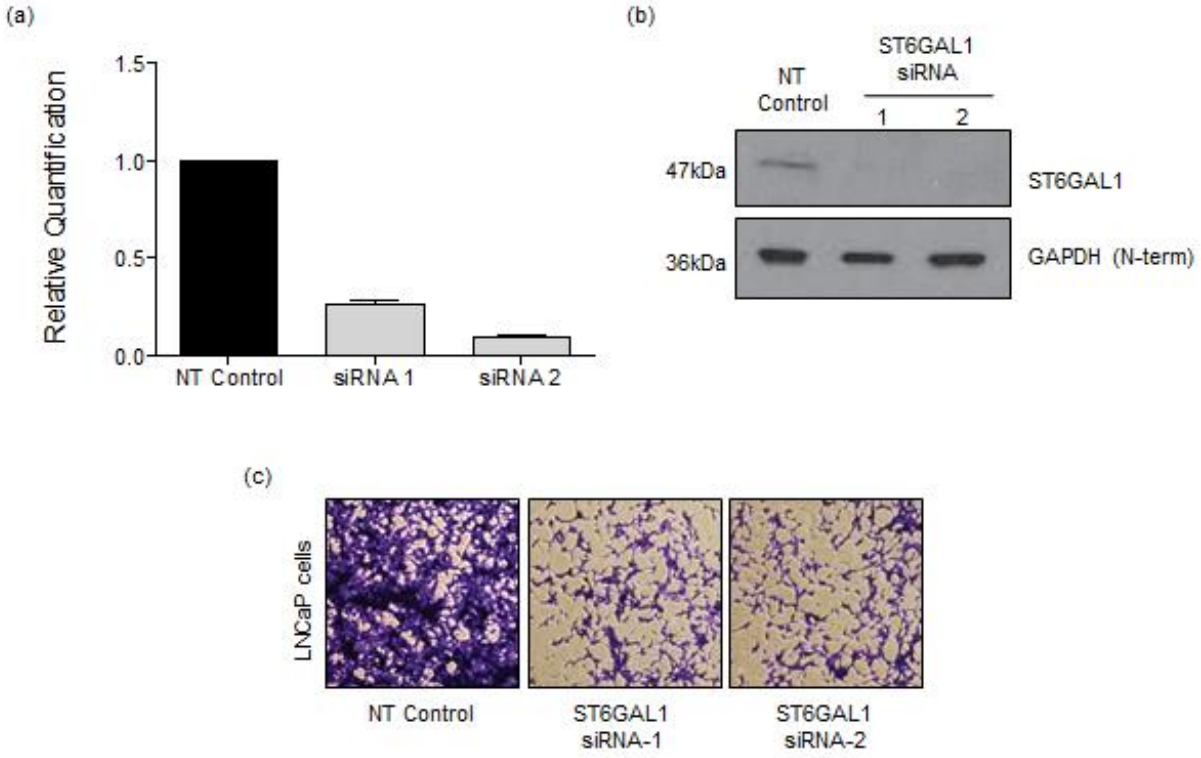

Figure 4.4 ST6Gal1 knockdown reduces LNCaP cell viability. ST6Gal1 expression is needed for prostate cancer cell viability.

(a) Real-time quantitative reverse transcription PCR (qRT-PCR) analysis of ST6Gal1 mRNA expression in LNCaP cells following siRNA transfection with 2 different siRNAs. Gene expression was calculated as the average (from 3 biological replicates) fold change of siRNA transfected cells relative to non-targeting siRNA

control cells (value set as 1). Samples were normalised using the average of three reference genes (GAPDH, β -tubulin and actin).

(b) Representative Western blot confirmation of ST6Gal1 depletion after 72 hours. GAPDH (N-terminal) was used as a loading control.

(c) Representative crystal violet stained images. Crystal violet dye binds to proteins and DNA of attached viable cells. There was a significant reduction in cell numbers in the ST6Gal1 siRNA depleted cells compared to cells transfected with non-targeted control siRNA.

4.3.2 ST6Gal1 expression in clinical prostate cancer patients

To investigate ST6Gal1 mRNA expression levels in prostate cancer patients, two independent clinical RNA validation cohorts were analysed using qRT-PCR. The first cohort compared RNA samples of benign prostatic hyperplasia (BPH) versus prostate carcinoma obtained from 49 patients, and the second cohort compared carcinoma versus adjacent normal tissue within 9 patients. Clinical samples were provided with ethical approval through the Exeter NIHR Clinical Research Facility tissue bank (Ref: STB20). Written informed consent for the use of surgically obtained tissue was provided by all patients. All carcinoma samples provided contained a tumour cellularity of at least 80% to ensure the presence of sufficient tumour tissue for the experiments.

In the BPH versus PCa tumour sample set, ST6Gal1 mRNA expression was increased in the tumour samples compared to the BPH samples (p=0.050) (Figure 4.5a). In the matched patient cohort, 6 of the 9 analysed patients showed a clear significant down-regulation (p = <0.05) of ST6Gal1 mRNA expression in prostate carcinoma tissue compared to adjacent normal tissue (patients 1, 3, 5, 7, 8 and 9). Only one patient showed a significant increase (p = <0.05) in ST6Gal1 expression in prostate carcinoma tissue compared to adjacent normal tissue (patient 4) and for 2 of the patients there was an insignificant change (patients 2 and 6) (Figure 4.5b).

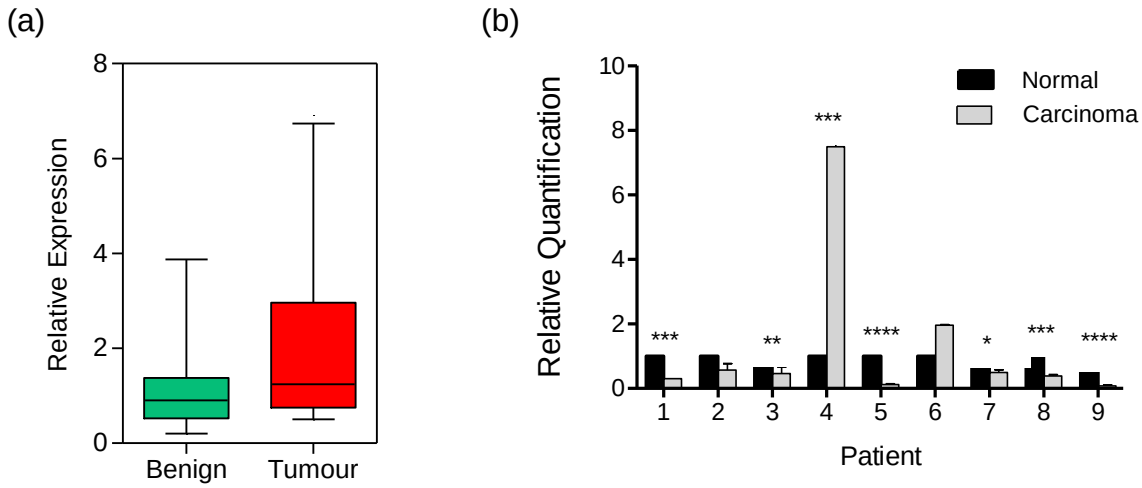

Figure 4.5 ST6GAL1 mRNA expression levels in prostate cancer patient samples. Real-time quantitative reverse transcription PCR (qRT-PCR) analysis of ST6Gal1 mRNA expression in two independent clinical RNA datasets.

(a) RNA from patients with benign prostatic hyperplasia (BPH) (n=32) and malignant samples from transurethral resection of the prostate (TURP) samples (n=17). ST6Gal1 expression was increased in the malignant patient samples compared to the BPH samples ($p = 0.050$).

(b) RNA from matched tumour tissue and adjacent normal tissue samples from 9 patients (* $p < 0.05$, ** $p < 0.01$, *** $p < 0.0001$, **** $p < 0.00001$). Six patients showed a clear significant down-regulation ($p = <0.05$) of ST6Gal1 mRNA expression in prostate carcinoma tissue compared to adjacent normal tissue (patients 1, 3, 5, 7, 8 and 9).

ST6Gal1 protein expression in PCa tissue was further examined using a tissue microarray (TMA) and an extensively validated ST6Gal1 antibody (Appendix C). Staining by this antibody was blocked by pre-incubation with a blocking peptide (Figure 4.6).

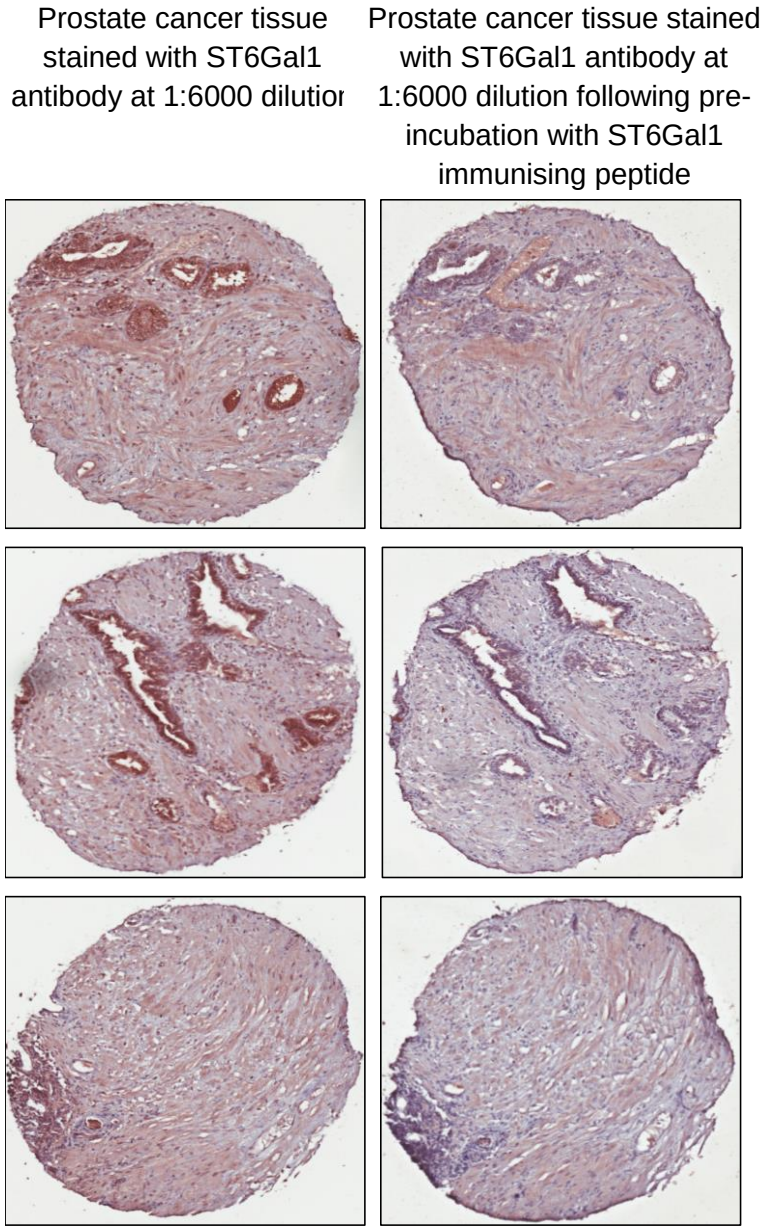

Figure 4.6 ST6Gal1 antibody validation. Representative 0.6mm cores of prostate cancer tissue samples stained with the ST6Gal1 antibody (1:6000 dilution) and following incubation with the immunising peptide. Staining with the ST6Gal1 antibody was blocked by the immunising peptide, confirming specificity of the antibody.

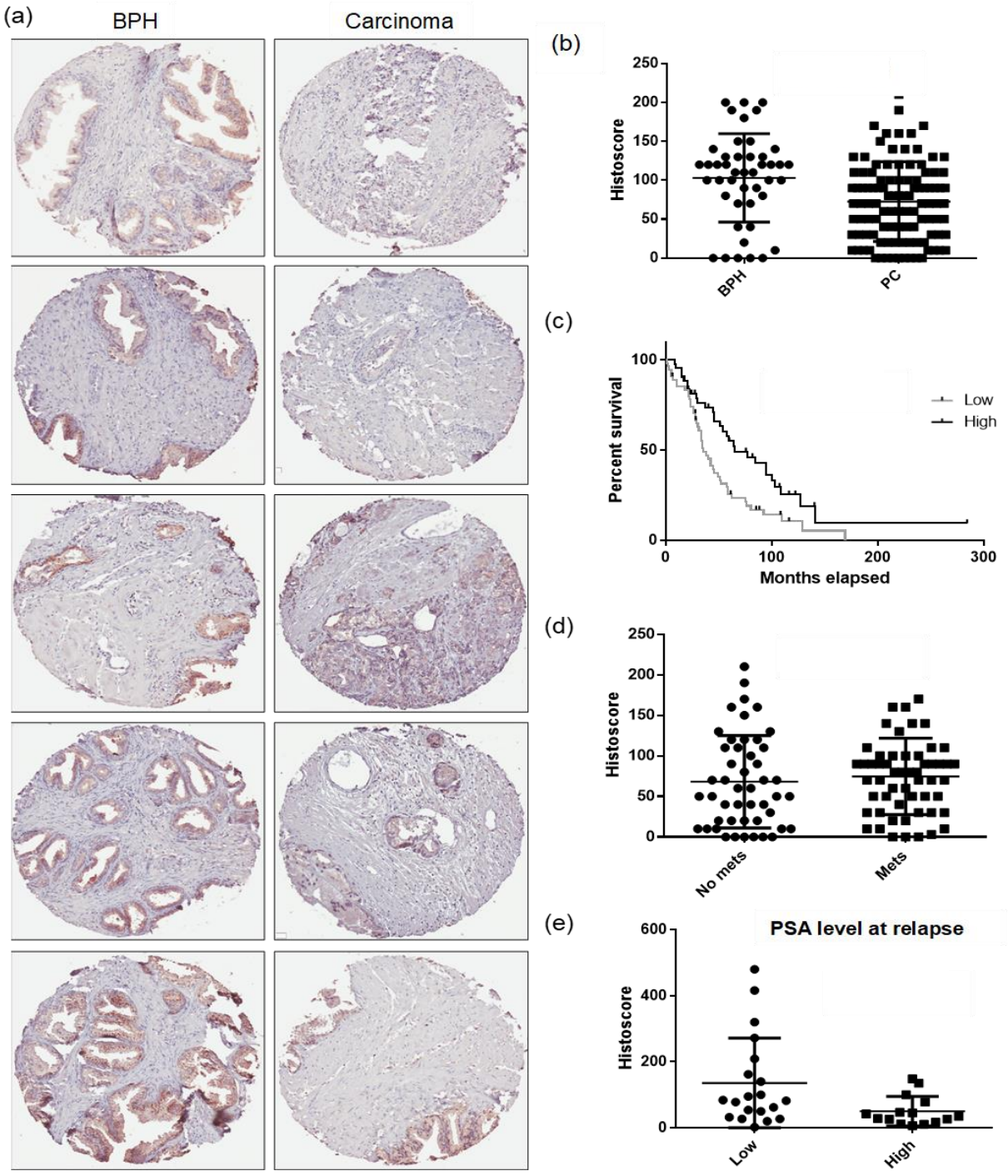

Figure 4.7 ST6Gal1 protein expression is down-regulated in prostate cancer tissue compared to benign prostate hyperplasia (BPH) tissue. Analysis of ST6Gal1 protein levels in patients with BPH or prostate cancer by tissue microarray (TMA). The

TMA was kindly provided by Professor Craig Robson (NICR, Newcastle) and the tissue staining and analysis was performed by Dr Urszula McClurg (NICR, Newcastle). Images, and graphs in this figure were also generated by Dr Urszula McClurg (NICR, Newcastle).

(a) Representative 0.6mm cores of BPH and prostate cancer tissue samples stained with the ST6Gal1 antibody (1:6000 dilution).
(b) Beeswarm plot shows significantly higher ST6Gal1 expression in the BPH samples compared to the prostate cancer samples ($p = 0.0015$). The TMA was scored using the 0-300 Histoscore score method (detailed in the methods section).
(c) Kaplan-Meier survival curve show that patients with lower ST6Gal1 expression had a significantly reduced probability of overall survival ($p = 0.0054$) than patients with higher ST6Gal1 expression.
(d) Beeswarm plot shows there is no significant difference in ST6Gal1 expression levels between the TMA prostate cancer patients with known metastasis and those without ($p = 0.5206$).
(e) Beeswarm plot shows that lower ST6Gal1 expression levels are linked to higher PSA levels at relapse in prostate cancer samples.

The TMA contained 0.6mm tissue cores from patients with BPH (n=26), prostate cancer (n=72) together with control tissues including breast, kidney, placenta, ovary, and liver. The TMA was stained and scored by Dr Urszula McClurg (NICR, Newcastle). Representative cores of BPH and prostate cancer tissues from the TMA are shown in Figure 4.7a. ST6Gal1 protein is expressed at significantly higher levels in the non-malignant BPH tissue compared to prostate cancer patient tissue ($p = 0.0015$) (Figure 4.7b). Lower levels of ST6Gal1 protein expression predict poor overall survival in months compared with higher levels of expression ($p = 0.0054$) (Figure 4.7c). Whilst there was no link between ST6Gal1 expression and metastasis ($p = 0.5206$) (Figure 4.7d), low ST6Gal1 levels were linked to higher PSA levels at relapse ($p = 0.0265$) (Figure 4.7e). The TMA shows that ST6Gal1 protein expression is significantly higher in the non-malignant BPH tissue compared to PCa patient tissue. Published data comparing PCa to BPH is limited. Tomlins et al compared 11 BPH tissue samples and 49 prostate

carcinoma tissue samples and found that ST6Gal1 expression is higher in the BPH tissue compared to PCa patient tissue (Tomlins *et al.*, 2007), which supports our data. Whilst Grasso et al compared 35 castrate resistant metastatic PCa, 59 localised PCa, and 28 BPH tissue samples and found that ST6Gal1 expression was increased in PCa samples compared to BPH (Grasso *et al.*, 2012).

4.3.3 Creation of prostate cancer cell lines with ST6Gal1 over-expression and knock-down properties

To investigate the biologically significance of increased ST6Gal1 expression on prostate cancer cell aggressiveness, molecular cloning and transfection techniques were used to establish cell lines with ST6Gal1 over-expression and knock-down properties. An initial screen of endogenous ST6Gal1 mRNA expression levels in various prostate cancer cells lines was performed using qRT-PCR (Figure 4.8).

To create a cell line with increased stable expression, the ST6Gal1 coding sequence from LNCaP cells was PCR amplified and digested with appropriate restriction enzymes. The resulting purified DNA fragment was inserted into the p3xFLAG CMV-10 expression vector (Figure 4.9a) and transformed into DU145 cells. DU145 cells were chosen for transformation as they exhibited the lowest levels of endogenous ST6Gal1 expression (and so over-expressing ST6Gal1 might have the strongest effect). Empty p3xFLAG CMV-10 vectors were also transformed as controls. Stable transformants were selected using 300µg/ml Geneticin antibiotic (G418) selection. ST6Gal1 expression levels were assessed for each clone using RT-PCR and Western blot. Clones with the highest ST6Gal1 expression were selected and grown up for further analysis.

A prostate cancer cell line with silenced ST6Gal1 expression was also created. The pLKO.1 HIV based lentiviral vector (Figure 4.9b) containing an shRNA targeting the ST6Gal1 coding sequence (NM_003032.2-1363s1c1) was transformed into CW-22Rv1 cells. PCM3 and CW-22Rv1 cells were chosen as they exhibited higher endogenous ST6Gal1 expression, however transfection was only successful in the CW-22RV1 cells.

pLKO.1 vectors containing a scrambled sequence (shNC) with no homology to any known human genes were also transformed as controls. Stable transformants were selected with 1µg/ml Puromycin antibiotic. ST6Gal1 expression levels were assessed for each clone using RT-PCR and Western blot. Clones with the lowest ST6Gal1 expression were selected and grown up for further analysis.

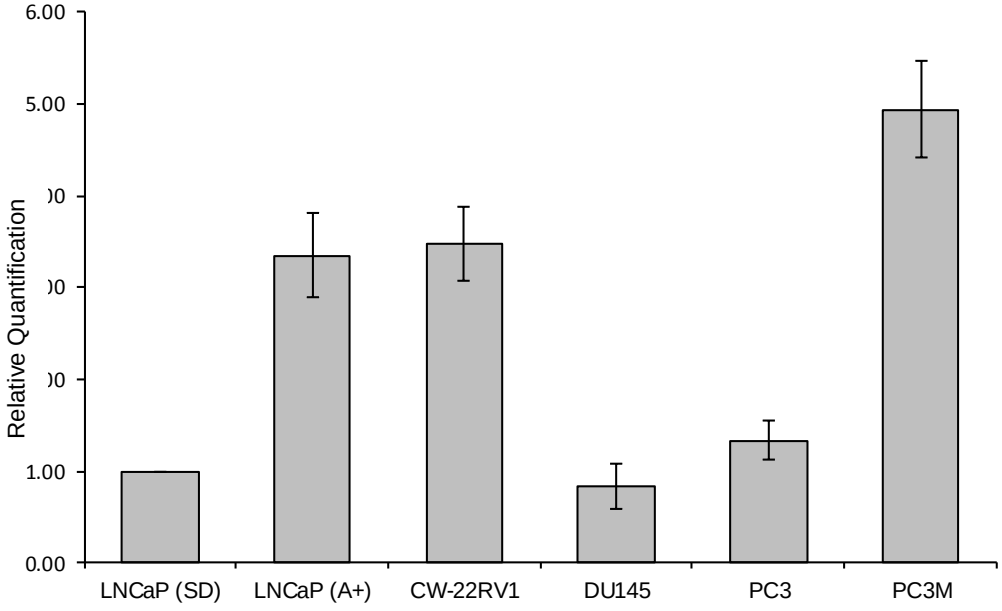

Figure 4.8 ST6Gal 1 mRNA expression in various prostate cancer cell lines. Real-time quantitative reverse transcription PCR (qRT-PCR) analysis of ST6Gal1 mRNA expression in human prostate cancer cell lines (LNCaP steroid deplete (SD) and androgen (R1881) treated (A+), CW-22RV1, DU145, PC3 and PC3M). ST6Gal1 expression was calculated as the average (from 3 biological replicates) fold change relative quantification compared to LNCaP steroid deplete cells (SD) (value set as 1). Samples were normalised using the average of three reference genes, GAPDH, β - tubulin and actin.

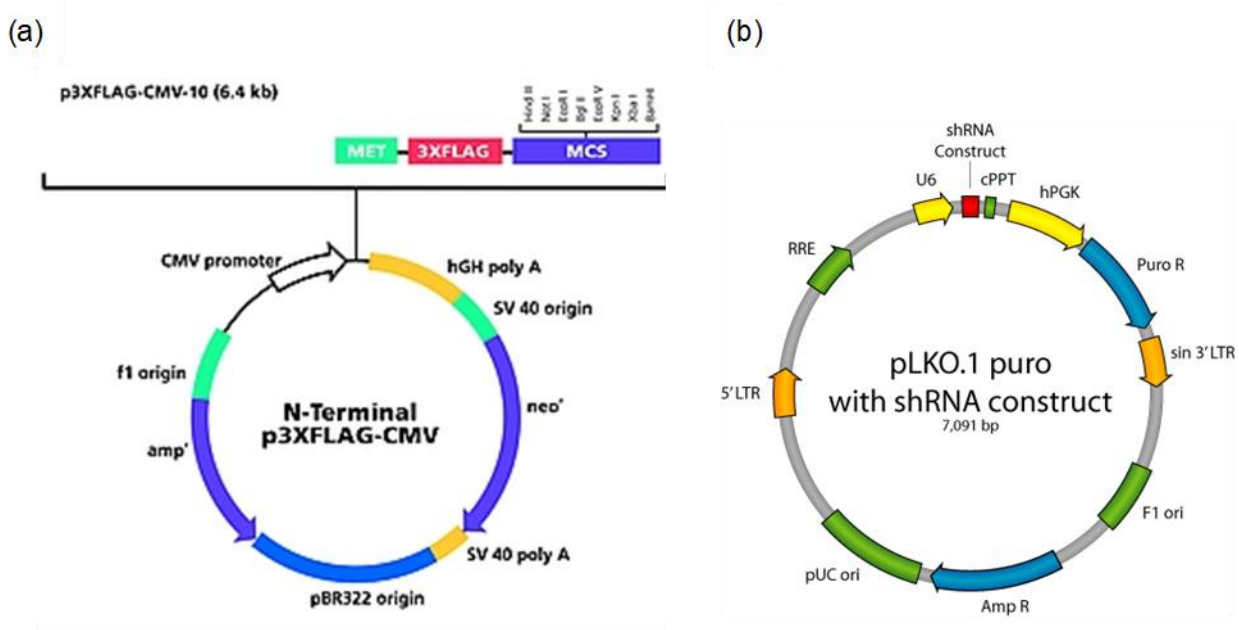

Figugre 4.9 Expression vector maps. Maps of the expression vectors used to create prostate cancer cell lines with ST6Gal1 over-expression and knock-down properties.

a) The full length ST6Gal1 construct was cloned into the p3xFLAG CMV-10 expression vector (Sigma E7658) using *NotI* and *BamHI* restriction enzymes.
b) The pLKO.1 HIV based lentiviral vector containing shRNA targeting the ST6Gal1 coding sequence (NM_003032.2-1363s1c1) was purchased from Sigma.

As predicted, the DU145 stable cell line exhibited significantly higher levels of ST6Gal1 mRNA and protein compared to the empty vector control cells, confirmed by RT-PCR (Figure 4.10a) and western blot (Figure 4.10c). For the knockdown cell line, ST6Gal1-shRNA transfection significantly inhibited ST6Gal1 mRNA expression in CW-22Rv1 cells compared to cells transfected with negative control shRNA, confirmed by RT-PCR (Figure 4.10b). ST6Gal1 protein levels were also significantly suppressed in ST6Gal-I-shRNA CW-22Rv1 cells compared with negative control cells, confirmed by western blot (Figure 4.10d).

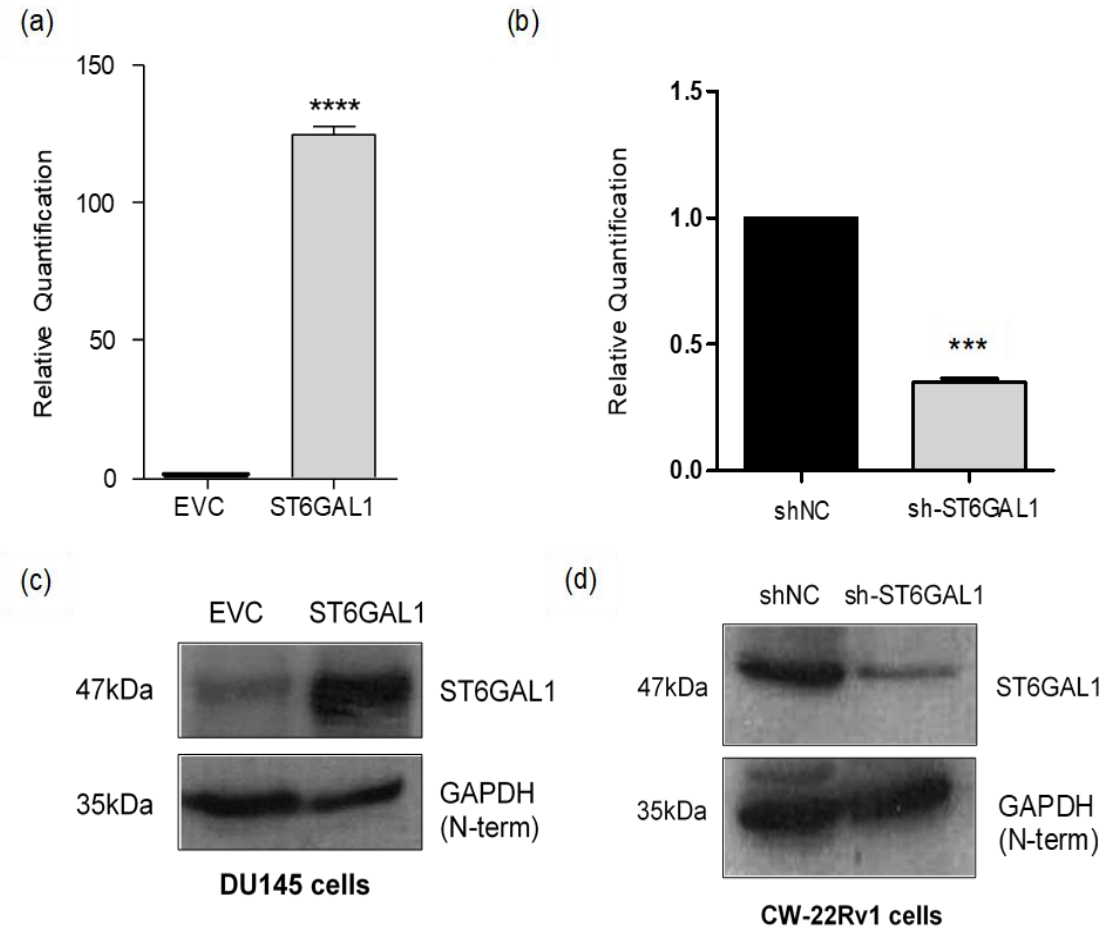

Figure 4.10 Validation of ST6Gal1 overexpression and knock-down by real-time PCR and western blot. Real-time quantitative reverse transcription PCR (qRT-PCR) validation of (a) ST6Gal1 overexpression in DU145 cells and (b) ST6Gal1 knock-down in CW-22Rv1 cells. ST6Gal1 expression was calculated as the average (from 3 biological replicates) fold change relative quantification compared to the empty vector control cells (EVC) (value set as 1). Samples were normalised using the average of three reference genes, GAPDH, β -tubulin and actin (* $p < 0.05$, ** $p < 0.01$, *** $p < 0.0001$, **** $p < 0.00001$). Representative Western blot protein level validation of (c) ST6Gal1 overexpression in DU145 cells, (d) ST6Gal1 knock-down in CW-22Rv1 cells. GAPDH (using an antibody directed against the N-terminal end of the protein) was monitored as a loading control

4.3.4 Effect of ST6Gal1 over-expression on cellular properties

The effect of increased ST6Gal1 expression on DU145 cell proliferation was investigated using two separate assays: the WST-1 proliferation assay kit and the Click-iT EdU Alexa Fluor 594 imaging kit. The WST-1 assay is a colorimetric assay based on the reduction of tetrazolium salt WST-1 to soluble form by electron transport across the plasma membrane of dividing cells. The Click-iT EdU assay uses a modified thymidine analogue (EdU) which is fluorescently labelled. Incorporation of EdU into DNA during active DNA synthesis produces a fluorescent signal which can be detected by fluorescent microscopy. Based on either assay, up-pregulated ST6Gal1 expression had no significant effect on cell proliferation (Figure 4.11).

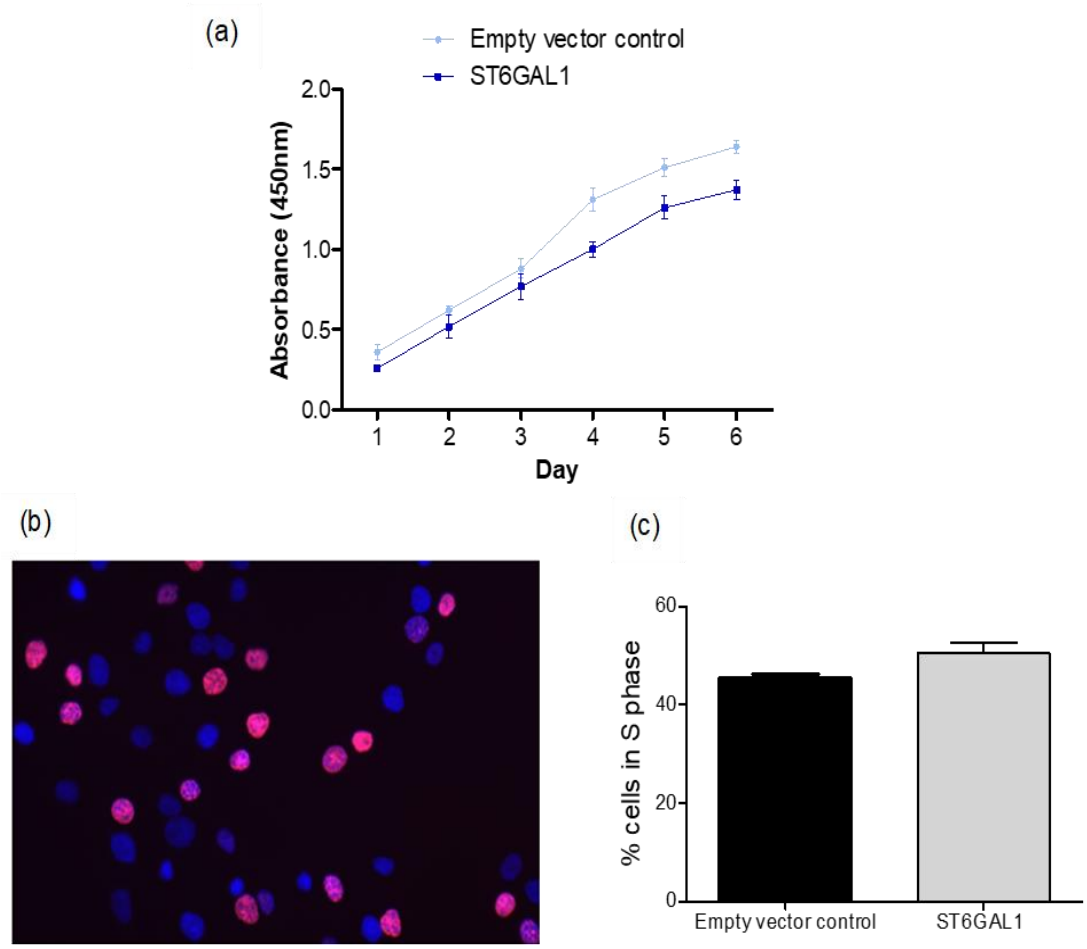

Figure 4.11 Increased ST6Gal1 expression has no effect on cell proliferation. Cell proliferation assays showed that increased ST6Gal1 had no significant effect on cell proliferation in DU145 cells.

a) WST-1 assay: DU145 cells expressing increased ST6Gal1 and empty vector control cells were grown in the presence of WST-1 reagent. Viable, actively dividing cells cleave the tetrazolium salt WST-1 to produce a formazan dye allowing spectrophotometric quantification. Cell proliferation was measured over a 6 day period.
b) Click-iT EdU assay: cells were grown on coverslips and labelled with EdU which is incorporated into newly synthesized DNA. Detection is based on click chemistry, a

covalent reaction between an alkyne (ethynyl moiety of EdU) and an azide coupled to a fluorescent dye (Alexa Fluor 594). Nuclei are counterstained with blue DAPI. Fluorescent microscopy was used to detect actively dividing cells (red) on non-diving cells (blue).

c) The number of actively dividing cells was calculated as a percentage of the total number of cells in DU145 cells expressing increased ST6Gal1 and empty vector control cells (25 images from each condition).

The effect of increased ST6Gal1 expression on cell adhesion was investigated using a calcein-AM based cell adhesion assay. Over-expression of ST6Gal1 significantly increased DU145 cell adhesion to uncoated plates, and also plates coated with fibronectin (Figure 4.12).

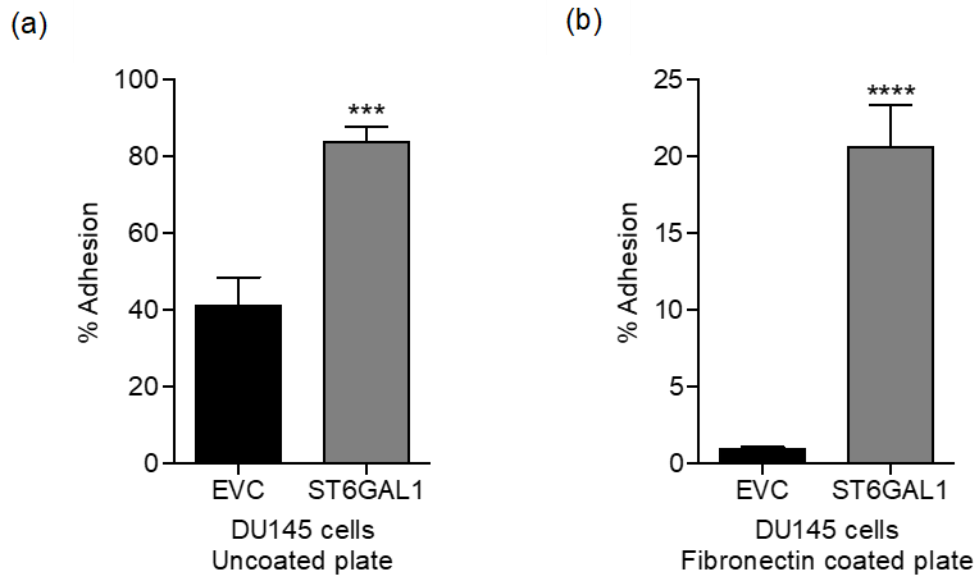

Figure 4.12 ST6Gal1 increases cell adhesion in DU154 cells. DU145 cells expressing increased ST6Gal1 and empty vector control cells were labelled with calcein-AM and allowed to adhere to (a) un-coated and (b) fibronectin coated plates. The percentage cell adhesion was calculated by comparing a washed plate (representative of adherent cells) to an identical unwashed plate (representative of the total number of cells seeded). DU145 cells with increased ST6Gal1 expression had a significantly greater adhesion to both the un-coated and fibronectin coated plates.

Metastasis is associated with the poor prognosis and survival in PCa patients. The effect of increased ST6Gal1 expression on cell migration was investigated using a standard scratch assay using a non-coated culture plates and the Oris Pro cell migration assay using a collagen I coated plate. Increased ST6Gal1 expression significantly reduced the migration properties of DU145 cells grown on un-coated and collagen I coated plates compared to the empty vector control cells (Figure 4.13).

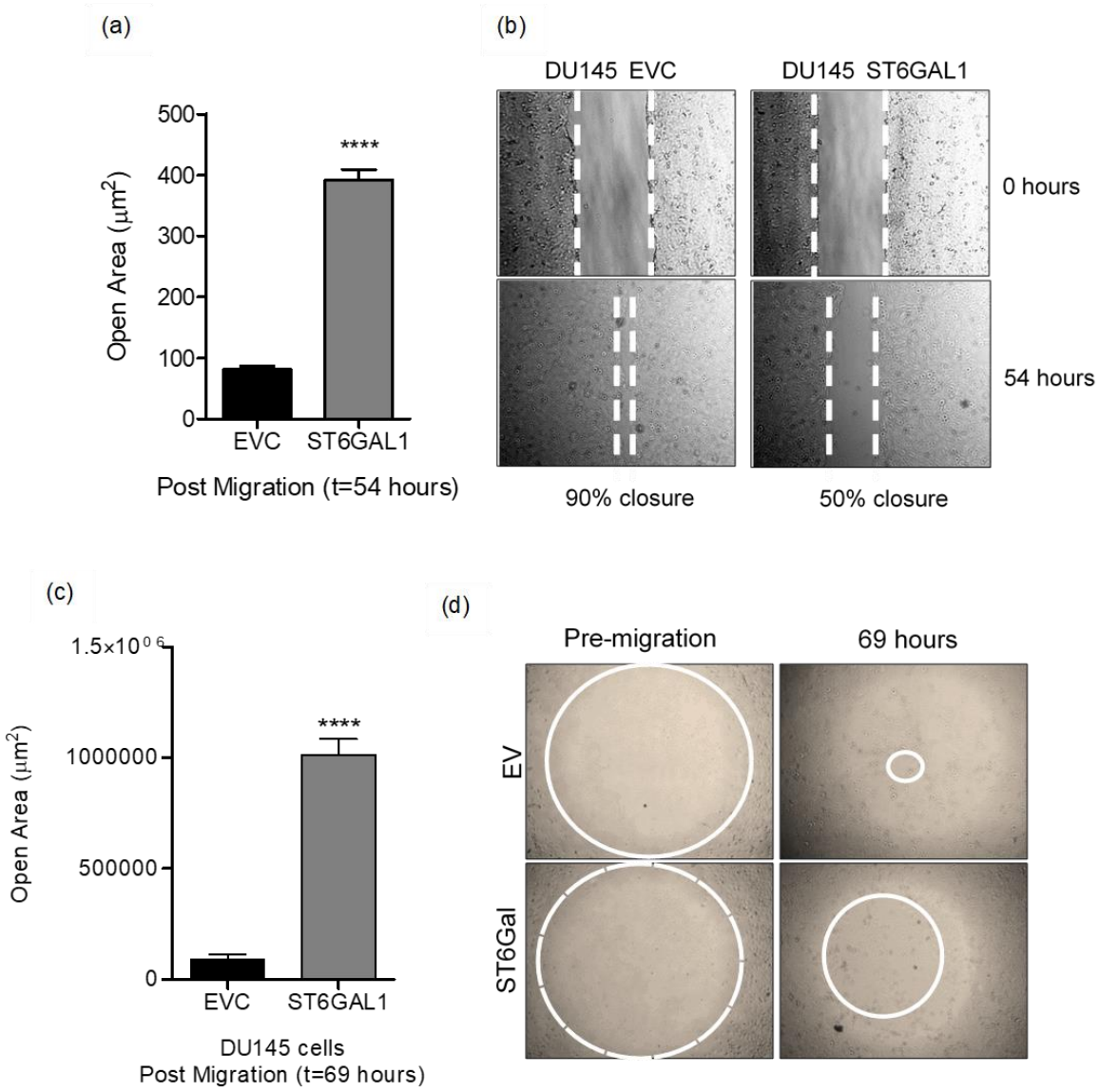

Figure 4.13 ST6Gal1 decreases cell migration in DU154 cells. ST6Gal1 significantly decreased cell migration in DU145 cells, as shown by standard scratch assay on un-coated plates (a-b), and Oris Pro cell migration assay on collagen I coated plates (c-d).

The invasion properties of DU145 cells with increased ST6Gal1 expression was investigated using a Cultrex 96 well basement membrane extract (BME) cell invasion assay. The assay was used to quantify the degree to which DU145 cells penetrate a barrier consisting of basement membrane components in response to chemo-attractants (Figure 4.14a-b).

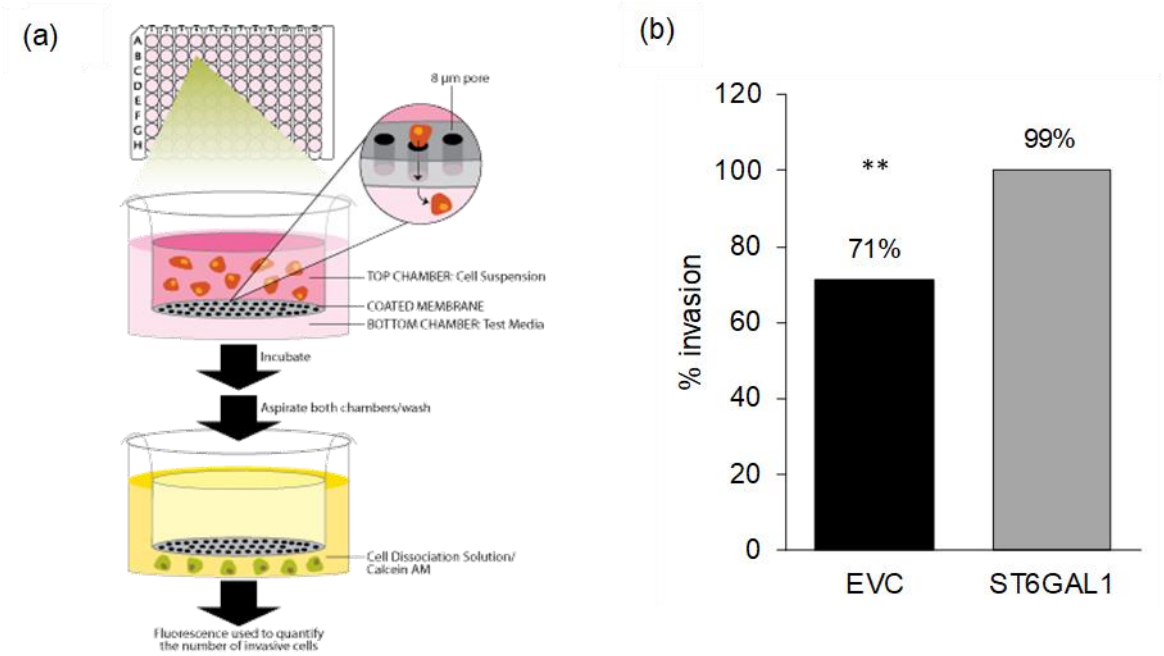

Figure 4.14 ST6Gal1 increases the invasion potential of DU145 cells. The cell invasion assay involves a 96 well tissue culture plate with two chambers which are separated by a filter coated with basement membrane components (a). Schematic of the Cultrex 96 well basement membrane extract (BME) cell invasion assay (*Cultrex BME Cell Invasion Assay, 96 well*, R&D Systems). Cells were cultured in serum free media for 24 hours and then added to the top chamber. The bottom chamber contained full culture media. Cells migrate through the pores in the filter to the bottom chamber in response to the chemoattractant gradient.

The migrated cells are stained and fluorescently quantified. (b) Percentage invasion was calculated by comparing the fluorescence of the cells that had migrated through the BME to the bottom chamber with the fluorescence of the total input cells. High ST6Gal1 expression significantly increased the cell invasion potential of DU145 cells ($p = 0.00202$).

To investigate the regulatory mechanism involved in ST6Gal1-dependent prostate cancer cell motility, the expression of genes with established roles in epithelial to mesenchymal transition (EMT) was analysed. In DU145 cells, 9 out of 12 EMT related genes showed significant changes in gene expression when ST6Gal1 was overexpressed (Figure 4.15). Seven of the genes that were up-regulated were VIM (vimentin), CTNNB1 (β-catenin), FN1 (fibronectin), CDH1 (E-cadherin), SNAI2 (slug), SNAI1 (snail) HLA-G (β2-microglobulin). Two of the genes that were down-regulated were TWIST1 (twist) and DSP (desmoplakin).

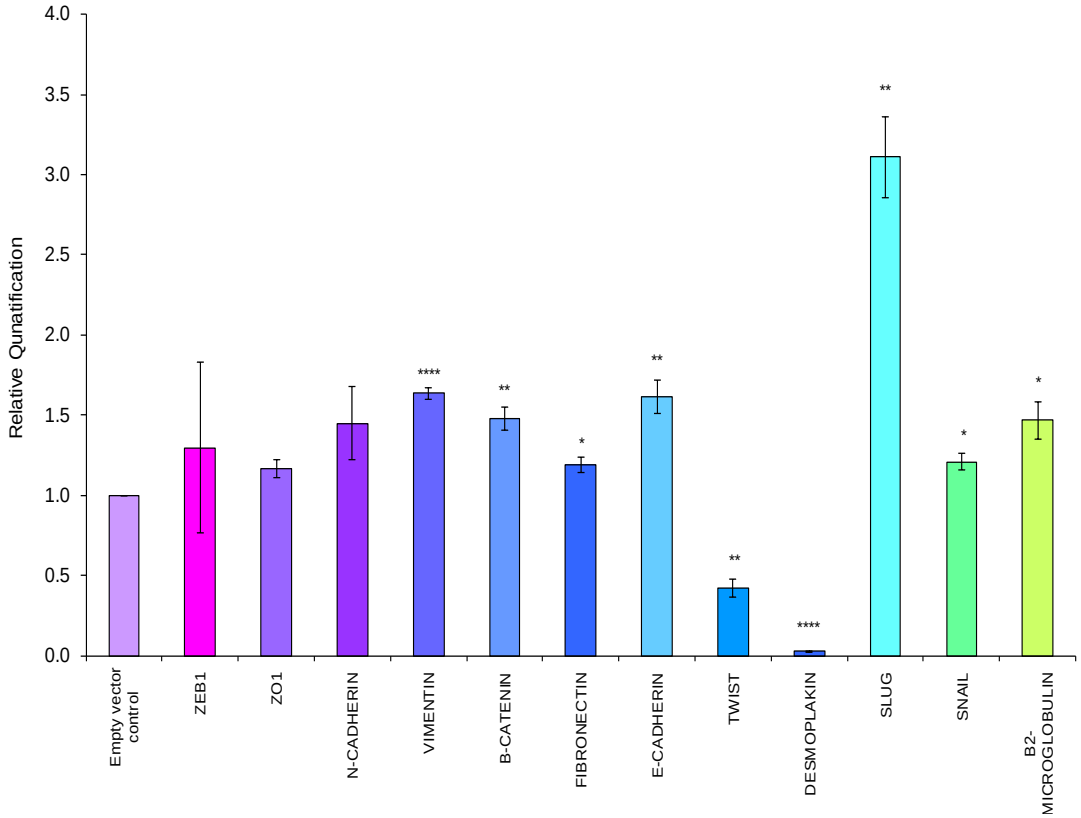

Figure 4.15 ST6Gal1 effects the expression of genes involved in epithelial to mesenchymal transition (EMT). Real-time quantitative reverse transcription PCR (qRT-PCR) analysis of a panel of genes involved in epithelial to mesenchymal transition (EMT) using mRNA from DU145 cells over expressing ST6Gal1. Gene expression was calculated as the average (from 3 biological replicates) fold change relative quantification of DU145 cells with increased ST6Gal1 expression compared to DU145 empty vector control cells (value set as 1). Samples were normalised using the average of three reference genes, GAPDH, β -tubulin and actin. Statistical significance was calculated using an independent two-sample t-test, where * p <0.05, ** p <0.01, *** p <0.0001, **** p <0.00001. All primer sequences are listed in Appendix B.

The most significant and dramatic change in expression was down-regulation and almost complete loss of desmoplakin in response to ST6Gal1 expression. Desmoplakin is an essential component of desmosomal plaques, structures involved in cell to cell adhesion. Expression analysis of other important desmosomal component genes was also carried out (Figure 4.16). In contrast to the down-regulation of desmoplakin, 5 of the 12 genes analysed were significantly up-regulated. These were JUP (junction plakoglobin), PKP2 (plakophilin 2), PKP3 (plakophilin 3), PKP4 (plakophilin 4) and PNN (desmosome-associated protein).

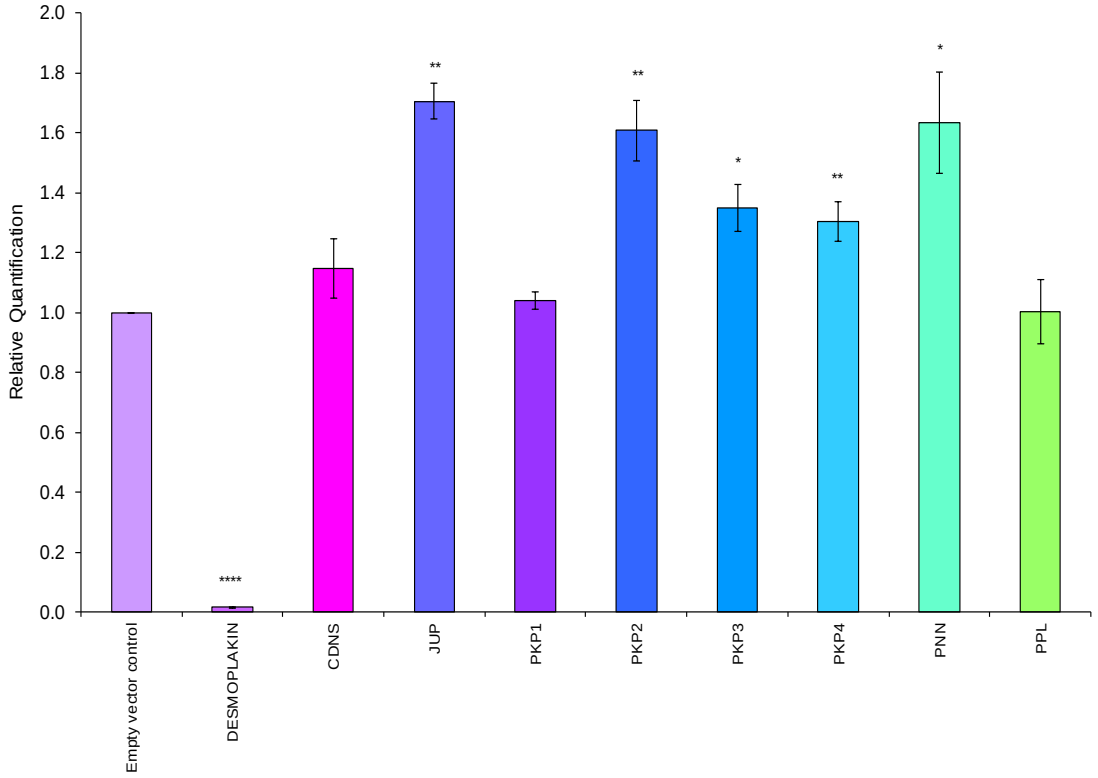

Figure 4.16 ST6Gal1 effects the expression of a number of desmosomal genes. Real-time quantitative reverse transcription PCR (qRT-PCR) analysis of a panel of desmosomal genes found within the desmosome junctional complex using mRNA from DU145 cells over expressing ST6Gal1. Gene expression was calculated as the average (from 3 biological replicates) fold change relative quantification of DU145 cells with

increased ST6Gal1 expression compared to DU145 empty vector control cells (value set as 1). Samples were normalised using the average of three reference genes, GAPDH, β -tubulin and actin. Statistical significance was calculated using an independent two-sample t-test, where * $p < 0.05$, ** $p < 0.01$, *** $p < 0.0001$, **** $p < 0.00001$. All primer sequences are listed in Appendix B.

Western blot and immunofluorescence analysis confirmed that desmoplakin protein expression was significantly depleted when ST6Gal1 was overexpressed (western blot Figure 4.17a and immunofluorescence Figure 17b).

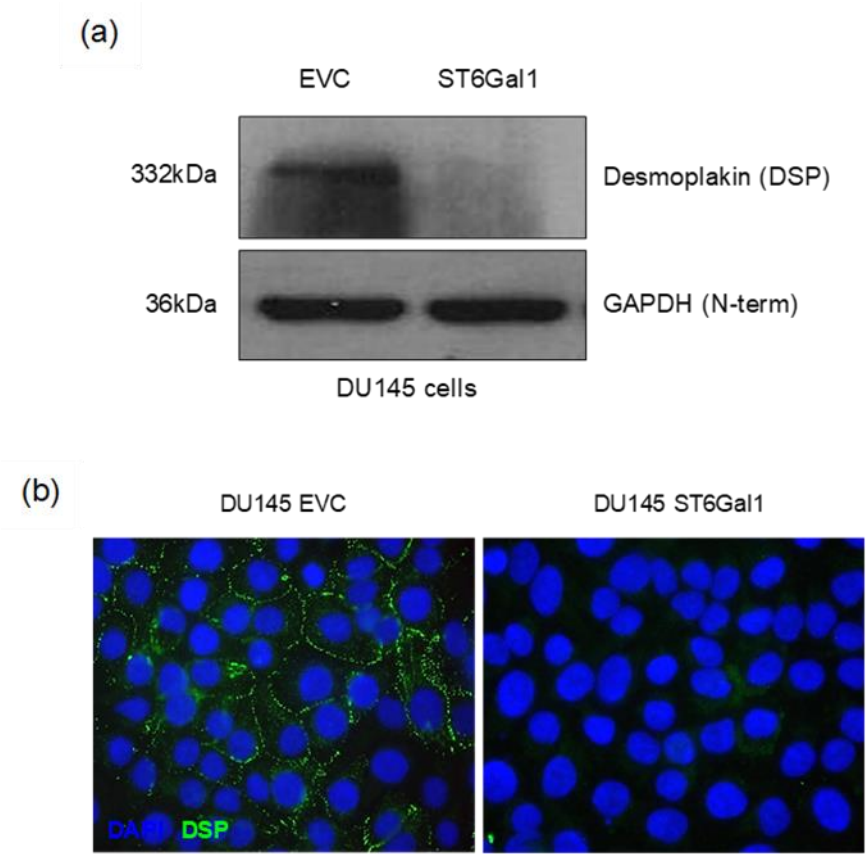

Figure 4.17 Desmoplakin protein expression in DU145 cells overexpressing ST6Gal1.

(a) Representative Western blots showing decreased expression of the desmoplakin protein in DU145 cells over-expressing ST6Gal1 compared to the empty vector control (EVC) cells. GAPDH (N-terminal) was used as a loading control.
(b) Decreased expression of the desmoplakin protein in DU145 cells over-expressing ST6Gal1 compared to the empty vector control (EVC) cells detected by immunofluorescence. Nuclei are stained with blue DAPI.

4.3.5 Effect of ST6Gal1 overexpression on the prostate cancer transcriptome

To evaluate the effect of increased ST6Gal1 on the PCa cell transcriptome, RNA-sequencing was performed on total RNA from a single sample of the ST6Gal1 over-expressing and empty vector DU145 cells. Figure 4.18 shows an MA plot of mean expression (log2 fold change) for all genes within the RNA sequencing data, genes with a log2fold change > 1 are coloured red. The plot clearly shows the over-expression of ST6Gal1 and the down-regulation of desmoplakin (labelled). Figure 4.19 shows a snapshot of the USCS Genome Browser with the RNA sequencing reads aligned to ST6Gal1, confirming over-expression in the cell line.

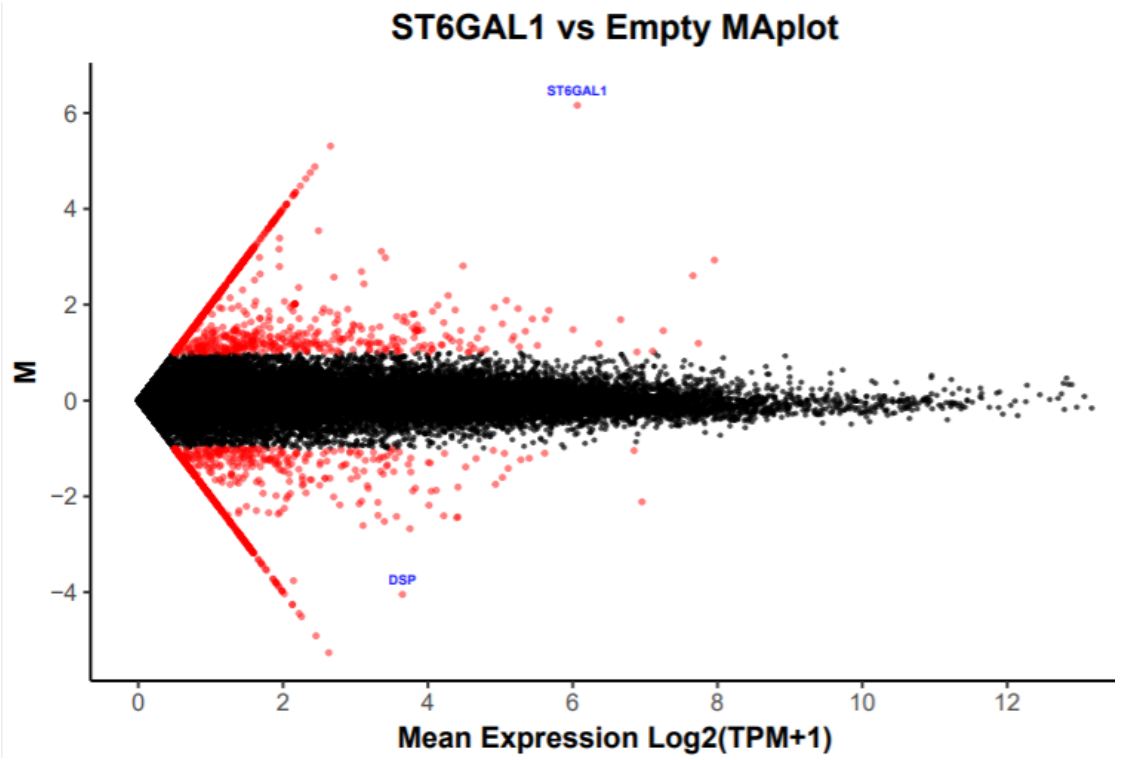

Figure 4.18 Expression MA plot of RNA sequencing data. An MA plot showing the mean expression (log2 fold change) for all genes within the RNA sequencing data (ST6Gal1 over-expressing vs empty vector DU145 cell line). Each gene is represented

with a dot, all genes with a log2fold change > 1 are coloured red. Dot representing ST6Gal1 and desmoplakin (DSP) are labelled.

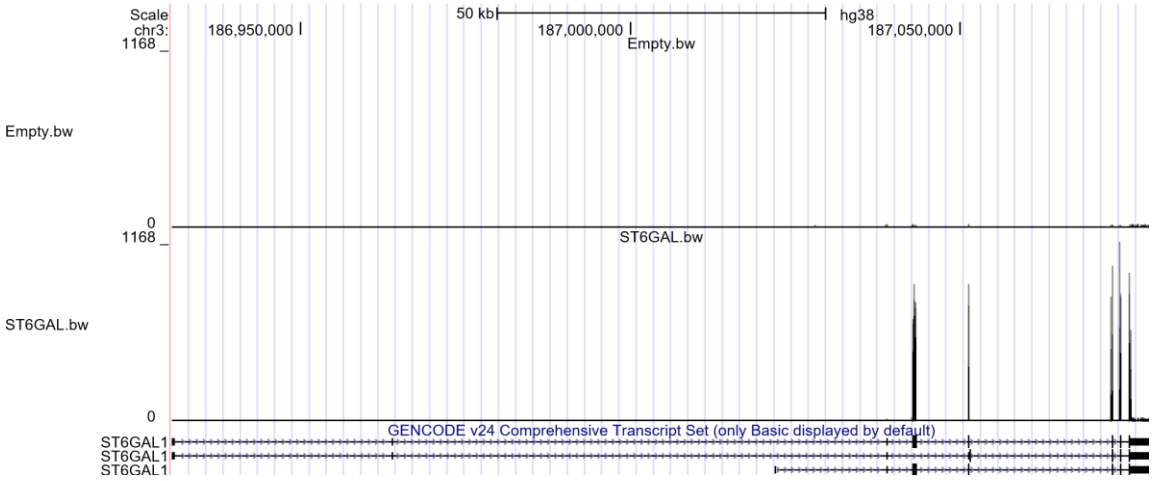

Figure 4.19 UCSC Genome Bowser snapshot of ST6Gal1 aligned RNA sequencing reads. UCSC snapshot showing RNA sequencing reads aligned to ST6Gal1 to confirm over-expression in the DU145 cell line in comparison to the empty vector control.

RNA sequencing profiles for 58,143 transcripts were obtained, out of which 90 were significant (p value <0.05). Of these, 74 genes showed >2 log_2fold change. Table 4.1 and Table 4.2 show the significant genes of which 39 were up-regulated and 35 were down-regulated in response to increased ST6Gal1.

Genes up-regulated in response to increased ST6Gal1 expression in DU145 cells				
RefSeq	**Gene symbol**	**Gene name**	**log2FoldChange**	**pvalue**
NM_001353	AKR1C1	Aldo-Keto Reductase Family 1, Member C1	2.58	0.009666981
NM_001547	IFIT2	Interferon Induced Protein With Tetratricopeptide Repeats 2	2.57	0.010015238
NM_001080512	BICC1	BicC Family RNA Binding Protein 1	2.52	0.0115535
NM_002977	SCN9A	Sodium Voltage-Gated Channel Alpha Subunit 9	2.51	0.011922949
NM_001512	GSTA4	Glutathione S-Transferase Alpha 4	2.49	0.012768256
NM_005502	ABCA1	ATP Binding Cassette Subfamily A Member 1	2.48	0.012783312
NM_001785	CDA	Cytidine Deaminase	2.48	0.013167699
NM_002167	ID3	Inhibitor Of DNA Binding 3, HLH Protein	2.48	0.013188004
NM_173653	SLC9A9	Solute Carrier Family 9 Member A9	2.46	0.01394595
NM_000127	EXT1	Exostosin Glycosyltransferase 1	2.45	0.01438023
NM_004334	BST1	Bone Marrow Stromal Cell Antigen 1	2.41	0.015759486
NM_021255	PELI2	Pellino E3 Ubiquitin Protein Ligase Family Member 2	2.41	0.015890456
NM_032827	ATOH8	Atonal BHLH Transcription Factor 8	2.40	0.016411824
NM_014322	OPN3	Opsin 3	2.39	0.016695099
NM_138420	AHNAK2	AHNAK Nucleoprotein 2	2.37	0.017950921
NM_001170820	IFITM10	Interferon Induced Transmembrane Protein 10	2.36	0.01827112
NM_015163	TRIM9	Tripartite Motif Containing 9	2.36	0.018495574
NM_020733	HEG1	Heart Development Protein With EGF Like Domains 1	2.34	0.019435972
NM_018094	GSPT2	G1 To S Phase Transition 2	2.33	0.019937334
NM_003658	BARX2	BARX Homeobox 2	2.32	0.020276372
NM_002775	HTRA1	HtrA Serine Peptidase 1	2.32	0.020455036
NR_034089	LOC100131564		2.31	0.021116672
NM_012081	ELL2	Elongation Factor For RNA Polymerase II 2	2.30	0.021586206
NM_212558	TMEM215	Transmembrane Protein 215	2.29	0.021818746
NM_015059	TLN2	Talin 2	2.29	0.02203411
NM_003713	PPAP2B	Phospholipid Phosphatase 3	2.28	0.02250555
NM_144717	IL20RB	Interleukin 20 Receptor Subunit Beta	2.27	0.023327958
NM_020704	STRIP2	Striatin Interacting Protein 2	2.26	0.023783739
NM_152486	SAMD11	Sterile Alpha Motif Domain Containing 11	2.26	0.023923235
NM_014705	DOCK4	Dedicator Of Cytokinesis 4	2.24	0.025383044
NM_145754	KIFC2	Kinesin Family Member C2	2.22	0.026252228
NM_001044	SLC6A3	Solute Carrier Family 6 Member 3	2.22	0.026275307
NM_001113547	LIMA1	LIM Domain And Actin Binding 1	2.22	0.026614099
NM_030641	APOL6	Apolipoprotein L6	2.17	0.030281343
NM_019593	GPCPD1	Glycerophosphocholine Phosphodiesterase 1	2.17	0.030290183
NM_024746	HHIPL2	HHIP Like 2	2.15	0.03153358
NM_001347	DGKQ	Diacylglycerol Kinase Theta	2.13	0.033316611
NM_181501	ITGA1	Integrin Subunit Alpha 1	2.11	0.034690466
NM_052924	RHPN1	Rhophilin, Rho GTPase Binding Protein 1	2.10	0.035789229

Table 4.1 Genes up-regulated in response to increased ST6Gal1 expression.
NCBI reference sequence, gene symbol, gene name, log2fold change and p value of the 39 genes up-regulated in response to increased ST6Gal1 expression in DU145 cells.

Genes down-regulated in response to increased ST6Gal1 expression in DU145 cells				
RefSeq	**Gene symbol**	**Gene name**	**log2FoldChange**	**pvalue**
NM_005960	MUC3A	Mucin 3A, Cell Surface Associated	-2.62	0.008882771
NM_001037160	CYS1	Cystin 1	-2.52	0.011745693
NM_006187	OAS3	2'-5'-Oligoadenylate Synthetase 3	-2.51	0.012035365
NM_006617	NES	Nestin	-2.50	0.012511812
NM_002334	LRP4	LDL Receptor Related Protein 4	-2.50	0.012569003
NM_053056	CCND1	Cyclin D1	-2.49	0.012848797
NM_003054	SLC18A2	Solute Carrier Family 18 Member A2	-2.46	0.013794193
NM_021020	LZTS1	Leucine Zipper, Putative Tumor Suppressor 1	-2.45	0.014267242
NM_004789	LHX2	LIM Homeobox 2	-2.41	0.015768056
NM_000435	NOTCH3	Notch 3	-2.39	0.016765884
NM_022725	FANCF	Fanconi Anemia Complementation Group F	-2.38	0.01741819
NM_015993	PLLP	Plasmolipin	-2.36	0.018515886
NM_001145176	SHISA7	Shisa Family Member 7	-2.35	0.018995548
NM_021954	GJA3	Gap Junction Protein Alpha 3	-2.32	0.02012836
NM_006547	IGF2BP3	Insulin Like Growth Factor 2 MRNA Binding Protein 3	-2.32	0.020460583
NM_019106	37865	Septin 3	-2.32	0.020572104
NM_173833	SCARA5	Scavenger Receptor Class A Member 5	-2.31	0.02087016
NM_032777	ADGRA2	Adhesion G Protein-Coupled Receptor A2	-2.31	0.021164784
NM_024690	MUC16	Mucin 16, Cell Surface Associated	-2.30	0.021243248
NM_021939	FKBP10	FK506 Binding Protein 10	-2.30	0.021714765
NM_031271	TEX15	Testis Expressed 15	-2.25	0.024318551
NM_004454	ETV5	ETS Variant 5	-2.24	0.024914537
NM_198573	ENHO	Energy Homeostasis Associated	-2.23	0.025671322
NM_014431	PALD1	Phosphatase Domain Containing, Paladin 1	-2.21	0.026764474
NM_005252	FOS	FBJ Murine Osteosarcoma Viral Oncogene Homolog	-2.21	0.026992541
NM_207361	FREM2	FRAS1 Related Extracellular Matrix Protein 2	-2.19	0.028251663
NM_020645	NRIP3	Nuclear Receptor Interacting Protein 3	-2.19	0.028484391
NM_006329	FBLN5	Fibulin 5	-2.18	0.028920068
NM_001004354	NRARP	NOTCH-Regulated Ankyrin Repeat Protein	-2.16	0.030922823
NM_006486	FBLN1	Fibulin 1	-2.16	0.031023029
NM_018365	MNS1	Meiosis Specific Nuclear Structural 1	-2.13	0.033268195
NM_175737	KLB	Klotho Beta	-2.11	0.034745426
NM_001453	FOXC1	Forkhead Box C1	-2.11	0.035002858
NM_022658	HOXC8	Homeobox C8	-2.11	0.035043307
NM_002442	MSI1	Musashi RNA Binding Protein	-2.07	0.038885024

Table 4.2 Genes down-regulated in response to increased ST6Gal1 expression. NCBI reference sequence, gene symbol, gene name, log2fold change and p value of the 35 genes down-regulated in response to increased ST6Gal1 expression in DU145 cells.

In order to validate the RNA sequencing results, expression changes for genes with the highest fold change were confirmed in triplicate in an independent sample set by real-time quantitative reverse transcription PCR (qRT-PCR) (Figure 4.20).

(a)

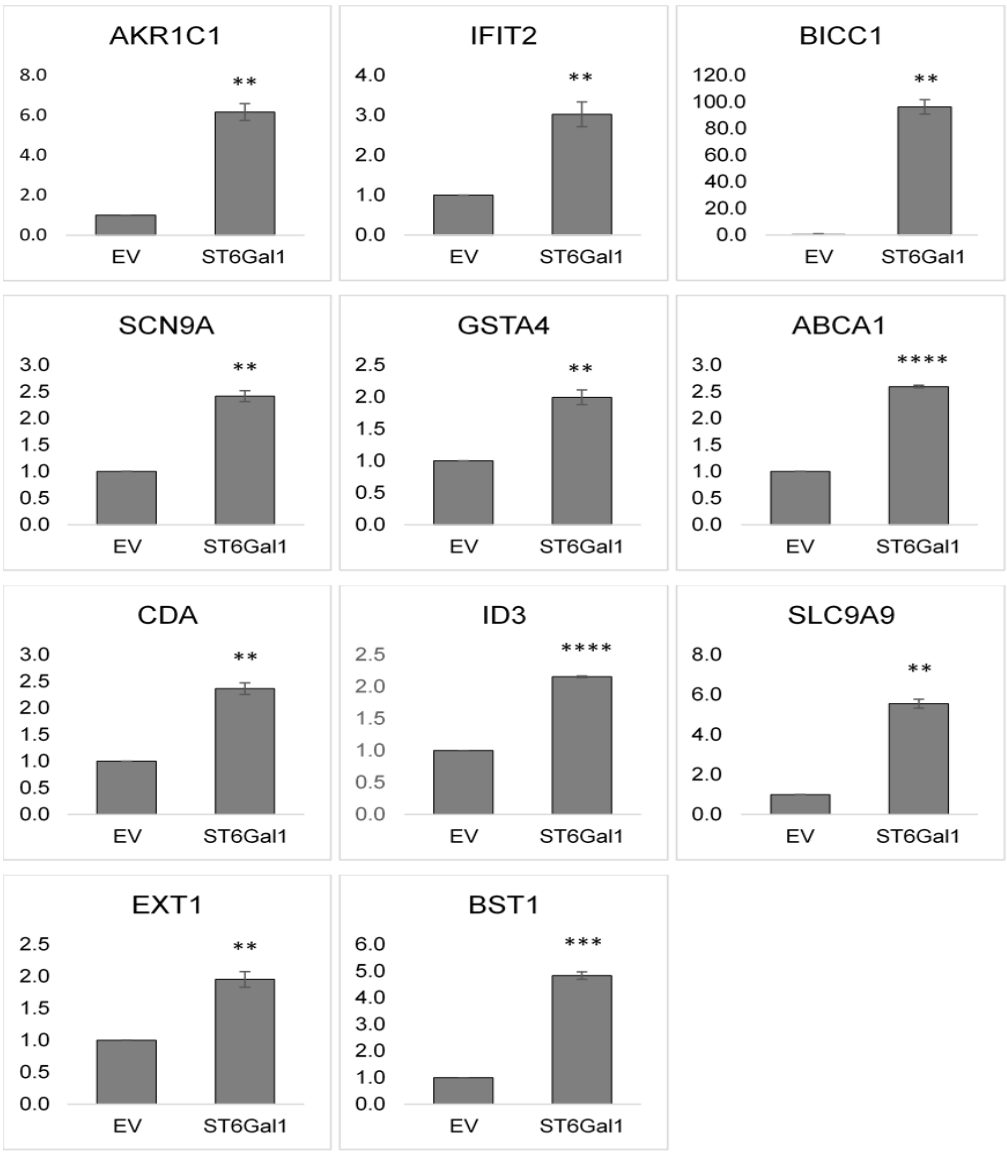

(b)

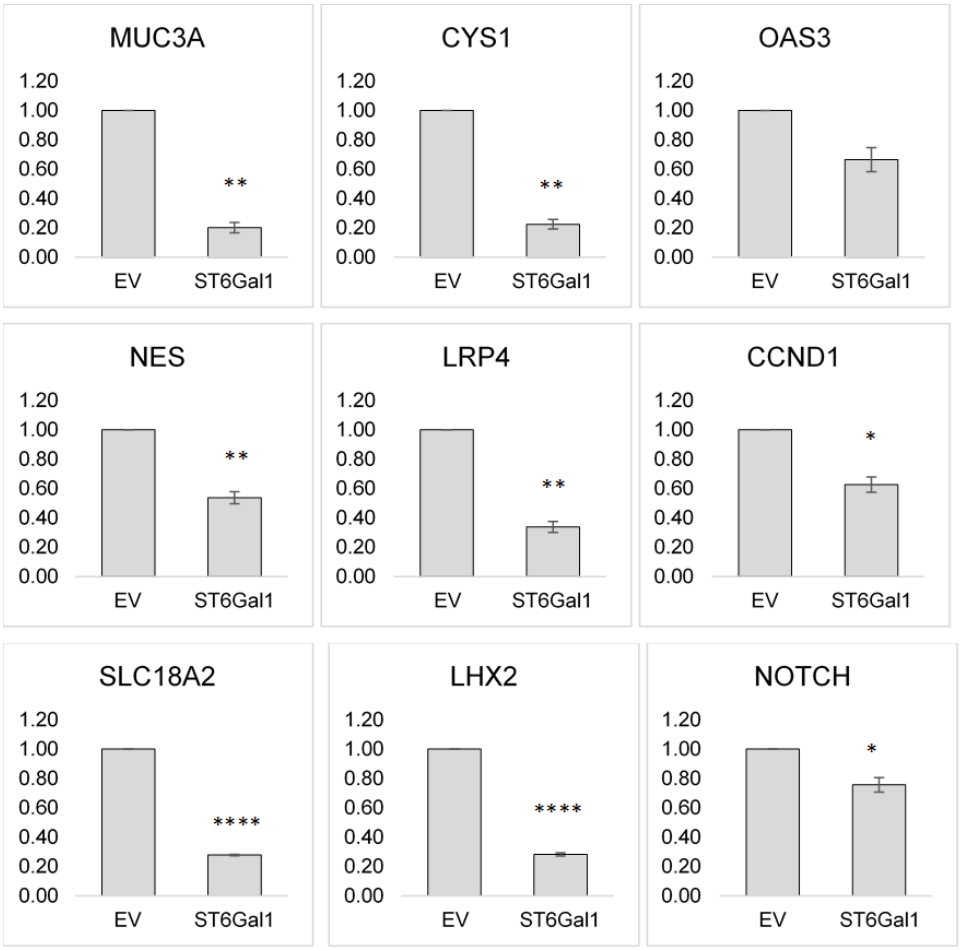

Figure 4.20 Differentially expressed genes in DU145 cell line in response to increased ST6Gal1 expression. Real-time quantitative reverse transcription PCR (qRT-PCR) analysis of 20 differentially expressed genes in response to increased ST6Gal1 expression in DU145 cells; (a) up-regulated genes, (b) down-regulated genes. Gene expression was calculated as the average (from 3 biological replicates) fold change (log2) relative quantification of DU145 cells over-expressing ST6Gal1 compared to empty vector DU145 cells (value set as 1). Samples were normalised using the average of three reference genes, GAPDH, β -tubulin and actin. Statistical significance was calculated using an independent two-sample t-test, where * $p < 0.05$, ** $p < 0.01$, *** $p < 0.0001$, **** $p < 0.00001$. All primer sequences are listed in Appendix B.

Gene Ontology (GO) enrichment analysis was carried out by Dr Katherine James (Newcastle University) with GOstat, a tool for identifying enriched GO terms in ranked gene lists (Beissbarth and Speed, 2004). GO analysis of the RNA sequencing gene lists identified 78 terms with significant gene enrichment ($p < 0.05$). There were 12 enriched GO terms within the up-regulated genes list, shown in Figure 4.21 and 66 enriched GO terms for the down-regulated genes, the top 20 of these are shown in Figure 4.22.

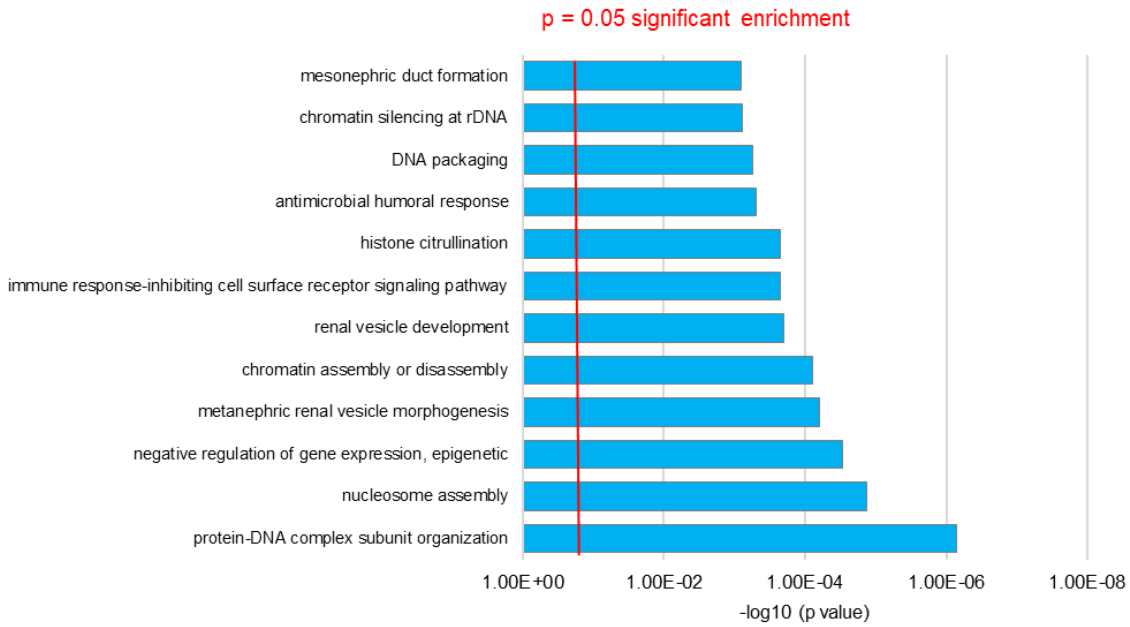

Figure 4.21 Gene ontology analysis of genes up-regulated in response to increased ST6Gal1 expression. Gene Ontology (GO) analysis of the genes up-regulated by ST6Gal1 identified 12 terms with significant gene enrichment ($p < 0.05$).

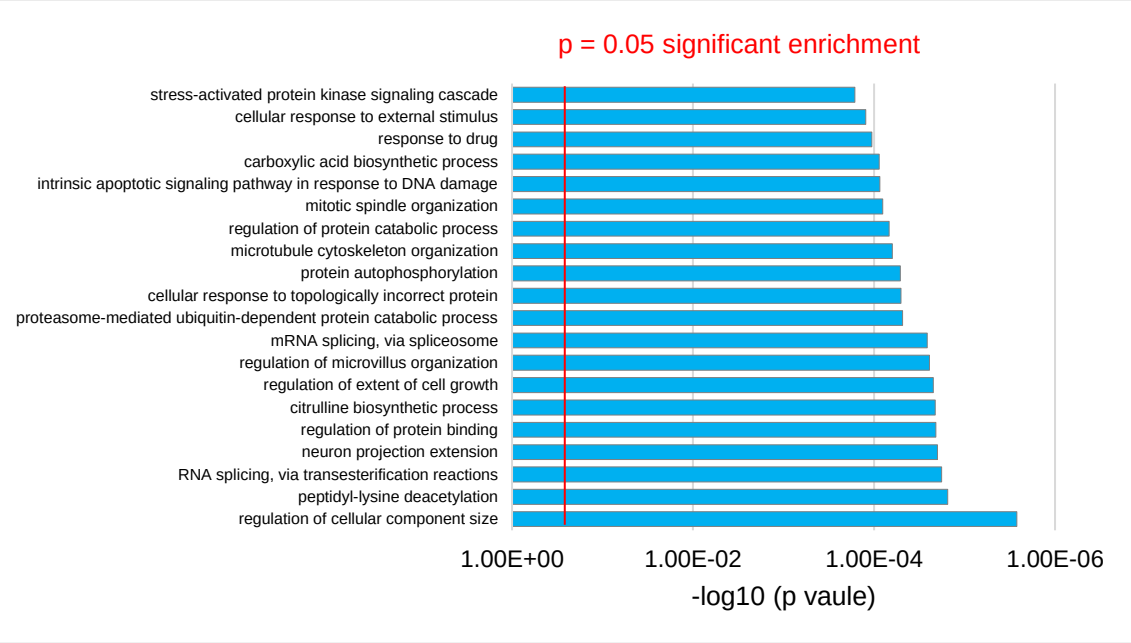

Figure 4.22 Gene ontology analysis of genes down-regulated in response to increased ST6Gal1 expression. Gene Ontology (GO) analysis of the genes down-regulated by ST6Gal1 identified 66 terms with significant gene enrichment ($p < 0.05$). The top 20 significantly enriched terms are shown in the graph.

The Kyoto Encyclopedia of Genes and Genomes (KEGG) (http://www.genome.jp/kegg/) database is used to link genomic information with higher order functional information (Kanehisa et al 2000). Analysis of our dataset using the KEGG metabolic pathway database identified 4 significant pathways from the up-regulated gene list and 68 pathways from the down-regulated gene list (Appendix C). There was one pathway significant in both gene lists, pathway 4380 - osteoclast differentiation.

4.3.6 Effect of ST6GAL1 knockdown on cellular properties

The effect of ST6Gal1 knockdown on the cellular properties of prostate cancer cells was investigated using a CW22-Rv1 cell line with silenced ST6Gal1 expression (section 4.4.3). The effect of ST6Gal1 knock-down on cell proliferation was investigated using the WST-1 proliferation assay kit. The results show that knockdown of ST6Gal1 in CW-22RV1 cells significantly decreased cell proliferation (Figure 4.23a) when compared to negative control cells.

The effect of ST6Gal1 knock-down on cell adhesion was investigated using a calcein-AM based cell adhesion assay. The results show that knockdown of ST6Gal1 in CW-22RV1 cells significantly decreased cell adhesion to fibronectin coated plates (Figure 4.23b) compared to negative control cells.

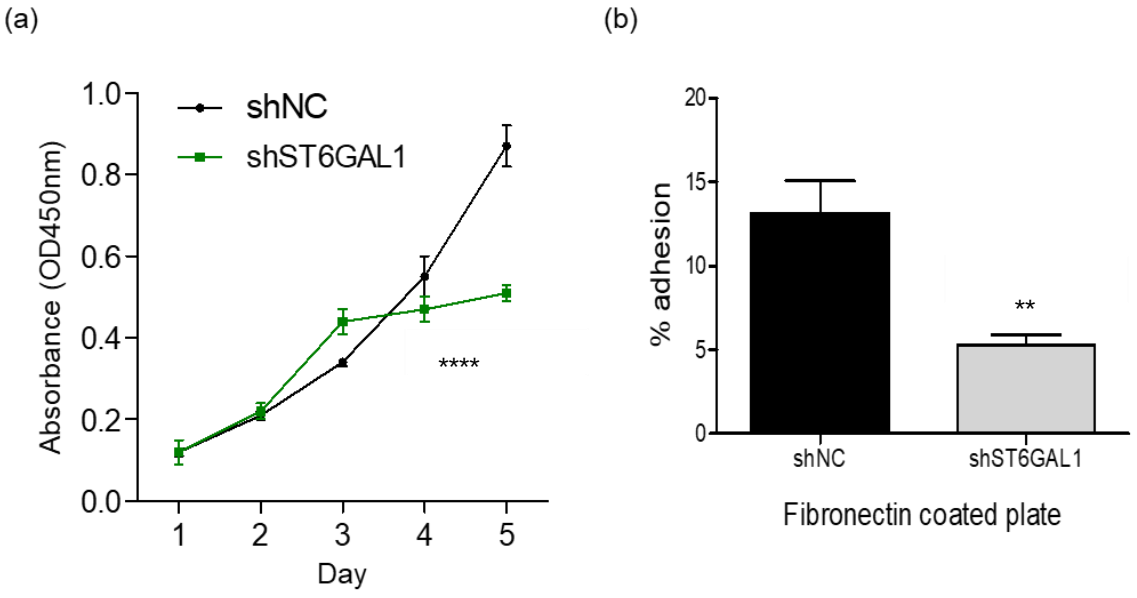

Figure 4.23 Knockdown of ST6Gal1 decreases cell proliferation and cell adhesion. The WST-1 cell proliferation assay and the calcein-AM based cell adhesion assay showed that ST6Gal1 knock-down significantly decreased cell proliferation and adhesion in CW-22Rv1 cells.

(a) WST-1 assay: ST6Gal1 knockdown CW22-Rv1 cells and negative control cells were grown in the presence of WST-1 reagent. Viable, actively dividing cells cleave the tetrazolium salt WST-1 to produce a formazan dye allowing spectrophotometric quantification. Cell proliferation was measured over a 5 day period.

(b) ST6Gal1 knockdown CW22-Rv1 cells and negative control cells were labelled with calcein-AM and allowed to adhere to fibronectin coated plates. The percentage adhesion was calculated by comparing a washed plate (representative of adherent cells) to an identical unwashed plate (representative of the total number of cells seeded).

Together with decreased proliferation and adhesion, ST6Gal1 knock-down also significantly decreased cell migration in CW-22Rv1 cells. A basic scratch assay showed that ST6Gal1 knock-down significantly decreased cell migration in CW-22Rv1 cells. Following 13 days incubation, the negative control cells had migrated into the scratched area of the plate (100% closure), whilst the ST6Gal1 knock-down cells had migrated into 50% of the scratched area (Figure 4.24a-b). The ST6Gal1 knock-down cells appeared to be growing on top of each other rather than migrating across the plate like the negative control cells. A major drawback of the scratch assay is that it relies on simply observing cells within the scratched zone and therefore cannot distinguish the effects of proliferation from migration. The assay was performed using RPMI-1640 full serum culture media, replacing this with serum free media or using a DNA synthesis inhibitor such as mitomycin C or hydroxyurea to inhibit proliferation would have allowed us to identify migrating cells.

The invasion properties of CW-22Rv1 cells with reduced ST6Gal1 expression was investigated using a Cultrex 96 well basement membrane extract (BME) cell invasion assay. Decreased ST6Gal1 expression significantly decreased the cell invasion potential of CW-22Rv1 cells ($p = 2.98E-06$).

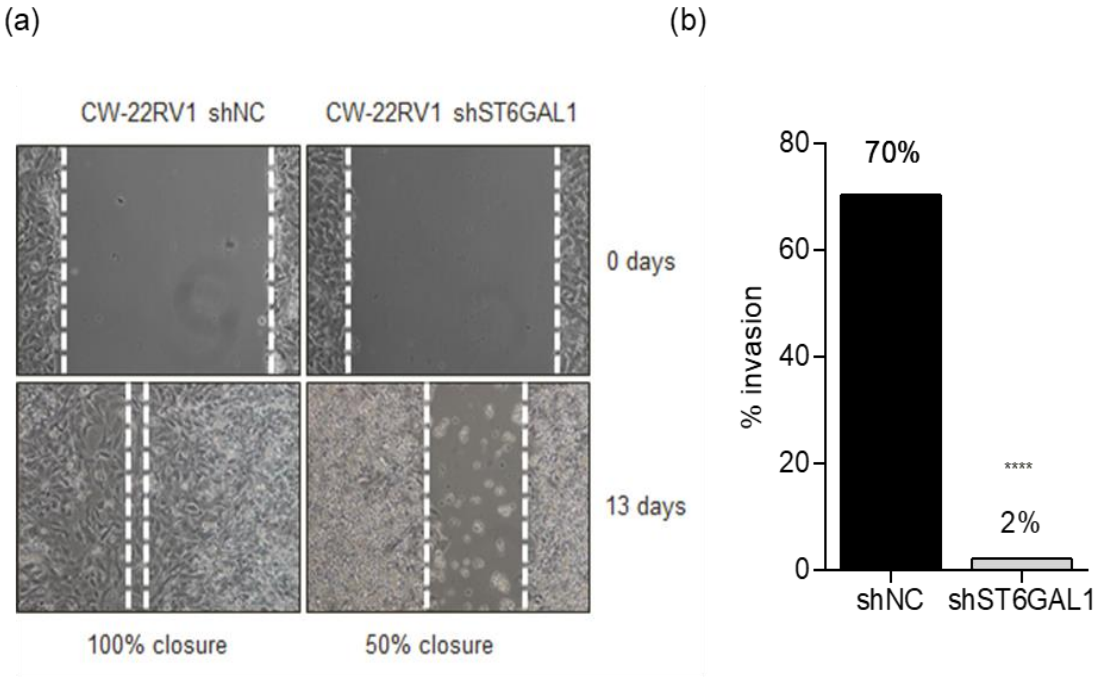

Figure 4.24 Knockdown of ST6Gal1 decreases cell migration and invasion.

(a) A scratch assay showed that ST6Gal1 knock-down significantly decreased cell migration in CW-22Rv1 cells. Cells were grown in culture for 13 days to observe the migration of cells into a scratched area of the plate. After 13 days incubation, the negative control cells had migrated into the scratched area of the plate (100% closure), whilst the ST6Gal1 knock-down cells had migrated into 50% of the scratched area

(b) The invasion properties of ST6Gal1 knock-down CW22-Rv1 cells was investigated using a Cultrex 96 well basement membrane extract (BME) cell invasion assay. Percentage invasion was calculated by comparing the fluorescence of the cells that had migrated through the BME to the bottom chamber with the fluorescence of the total input cells. Decreased ST6Gal1 expression significantly decreased the cell invasion potential of CW-22Rv1 cells ($p = 2.98E-06$).

To investigate the effect of reduced ST6Gal1 expression on prostate cancer cell motility and explore any reciprocal changes with the ST6Gal1 over-expression cell line, expression of the EMT gene marker panel was analysed in the CW-22Rv1 ST6Gal1 knock-down cells. In CW22-Rv1 cells, 4 EMT related genes showed significant changes in gene expression when ST6Gal1 expression was decreased (Figure 4.25). CDH2 (N-cadherin), FN1 (fibronectin), SNAI1 (snail) and SNAI2 (slug) were all down-regulated when ST6Gal1 was reduced. There was no significant effect on DSP (desmoplakin) expression when ST6Ga1 was reduced.

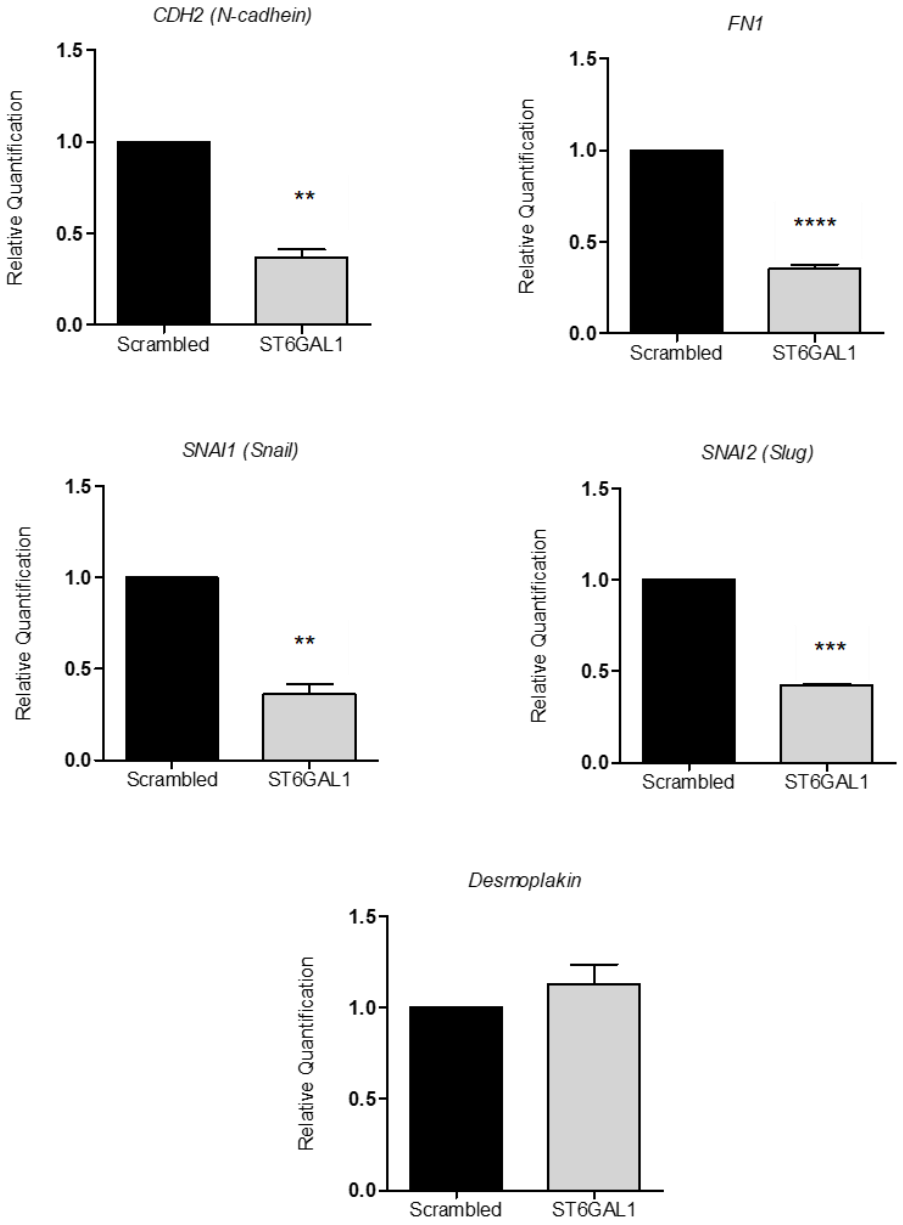

Figure 4.25 Effect of ST6Gal1 knock-down on the expression of genes involved in epithelial to mesenchymal transition (EMT). Real-time quantitative reverse transcription PCR (qRT-PCR) analysis of key genes involved in epithelial to mesenchymal transition (EMT) using mRNA from CW-22Rv1 cells with reduced ST6Gal1 expression. Gene expression was calculated as the average (from 3 biological replicates) fold change relative quantification of CW-22RV1 cells with knocked-down ST6Gal1

expression compared to negative control CW-22Rv1 cells (value set as 1). Samples were normalised using the average of three reference genes, GAPDH, β -tubulin and actin. Statistical significance was calculated using an independent two-sample t-test, where * $p < 0.05$, ** $p < 0.01$, *** $p < 0.0001$, **** $p < 0.00001$. All primer sequences are listed in Appendix B.

To help understand the role that ST6Gal1 may play in PCa progression and to identify genes whose expression is directly affected by ST6Gal1, RT-PCR was used to identify genes with reciprocal expression changes in the ST6Gal1 modified cell lines. Genes identified in the RNA sequencing dataset were analysed for reciprocal expression patterns between the DU145 ST6Gal1 over-expressing cells and the CW-22RV1 ST6Gal1 knock-down cells (Table 4.3). The genes identified with reciprocal expression patterns are more likely to be an effect by ST6Gal1.

Three independent sample sets of both ST6Gal1 modified cell lines were used to generate an average fold change (change in gene expression compared to the negative control cells). Of the 20 genes analysed, 13 showed reciprocal gene expression patterns in response to ST6Gal1 levels, i.e. increased expression in response to increased ST6Ga1 levels as well as decreased expression in response to decreased ST6Ga1 levels and vice versa. Aldo-keto reductase family 1 member C1 (*AKR1C1*), interferon induced protein with tetratricopeptide repeats 2 (*IFIT2*), bicC family RNA binding protein 1 (*BICC1*), glutathione s-transferase alpha 4 (*GSTA4*), ATP binding cassette subfamily A member 1 (*ABCA1*), cytidine deaminase (*CDA*), solute carrier family 9 member A9 (*SLC9A9*), exostosin glycosyltransferase 1 (*EXT1*) and bone marrow stromal cell antigen 1 (*BST1*) each have increased expression in response to increased ST6Gal1 levels and decreased expression in response to decreased ST6Gal1 levels. Reciprocally, cystin 1 (*CYS1*), 2'-5'-oligoadenylate synthetase 3 (*OAS3*), solute carrier family 18 member A2 (*SLC18A2*) and notch 3 (*NOTCH3*) have decreased expression in response to increased ST6Gal1 levels and increased expression in response to decreased ST6Gal1 levels.

A number of these gene are known to play important roles in cancer development & progression. AKR1C3 is involved in androgen biosynthesis and plays a role in the development of CRPC (Adeniji., *et al* 2013).

	DU145 ST6Gal1 over expressing cells				CW22 ST6Gal1 knock down cells			
Gene	**average fold change**	**SE**	**p value**		**average fold change**	**SE**	**p value**	
AKR1C1	6.159	0.85	3.65E-03	↑	0.763	0.15	1.81E-01	↓
IFIT2	3.023	0.31	0.00283	↑	0.336	0.02	5.21E-06	↓
BICC1	96.157	10.83	9.30E-04	↑	0.407	0.06	6.60E-04	↓
SCN9A	2.414	0.2	0.00229	↑	2.116	0.86	0.26386	↑
GSTA4	1.995	0.23	1.19E-02	↑	0.598	0.04	0.00069	↓
ABCA1	2.593	0.05	5.98E-06	↑	0.188	0.04	2.82E-05	↓
CDA	2.362	0.22	3.26E-03	↑	0.379	0.04	0.00012	↓
SLC9A9	5.547	0.46	5.80E-04	↑	0.932	0.13	0.62083	↓
EXT1	1.953	0.24	0.01734	↑	0.335	0.05	1.20E-04	↓
BST1	4.830	0.27	1.50E-04	↑	0.39	0.04	6.45E-05	↓
MUC3A	0.200	0.07	3.40E-04	↓	0.734	0.09	5.07E-02	↓
CYS1	0.223	0.07	0.00028	↓	1.068	0.39	8.73E-01	↑
OAS3	0.665	0.16	0.10608	↓	1.368	0.18	1.09E-01	↑
NES	0.537	0.08	4.73E-03	↓	0.253	0.03	1.63E-05	↓
LRP4	0.338	0.08	1.02E-03	↓	0.324	0.04	9.32E-05	↓
CCND1	0.626	0.11	2.29E-02	↓	0.811	0.12	0.1701	↓
SLC18A2	0.278	0.01	1.32E-07	↓	1.496	0.64	4.82E-01	↑
LZTS1	1.385	0.06	3.82E-03	↑	1.696	0.44	1.86E-01	↑
LHX2	0.282	0.02	4.17E-06	↓	0.433	0.04	0.00013	↓
NOTCH3	0.756	0.1	6.74E-02	↓	4.724	1.03	2.25E-02	↑

Table 4.3 Reciprocal gene expression changes in response to ST6Gal1 expression. Real-time quantitative reverse transcription PCR (qRT-PCR) analysis was carried out using mRNA from DU145 cells over-expressing ST6Gal1 and CW-22Rv1 cells with reduced ST6Gal1 expression. Red arrows indicate up-regulated genes and blue arrows indicate down-regulated genes. Genes in bold show reciprocal expression changes in response to ST6Gal1. Gene expression levels were calculated as an average (3 biological replicates from 3 sample sets with standard error (SE)) fold change compared to negative control cells in each case (value set as 1). Samples were

normalised using the average of three reference genes, GAPDH, β -tubulin and actin. Statistical significance was calculated using an independent two-sample t-test.

4.4 Discussion

Although aberrant glycosylation has previously been linked to PCa progression (Munkley *et al.*, 2016b), the role of ST6Gal1 a sialyltransferase which transfers sialic acid from CMP-sialic acid to galactose-containing substrates in PCa is unclear. While there are many studies which suggest an oncogenic role for ST6Gal1 (Zhu *et al.*, 2001; Lin *et al.*, 2002; Liu *et al.*, 2014b; Meng *et al.*, 2015; Hsieh *et al.*, 2017), there is also growing evidence that ST6Gal1 may also have tumour suppressor activity (Wild *et al.*, 2005; Park *et al.*, 2012; Antony *et al.*, 2014; Zhang *et al.*, 2017).

I have shown that expression of ST6Gal1 is up-regulated in PCa cells in response to androgen stimulation and that ST6Gal1 is likely to be a direct target of the androgen receptor. Meta-analysis of five publically available clinical gene expression datasets indicated that ST6Gal1 was up-regulated in PCa (Lapointe *et al.*, 2004; Varambally *et al.*, 2005; Tomlins *et al.*, 2007; Taylor *et al.*, 2010; Grasso *et al.*, 2012). The aim of this chapter was to identify ST6Gal1 expression patterns in clinical patient samples. I have found that ST6Gal1 expression was increased in 17 malignant tumour samples from transurethral resections of the prostate (TURP) compared with 32 non-malignant BPH tissue from our independent patient RNA cohort. A recent study supports this, that found ST6Gal1 expression was significantly upregulated in PCa tumour tissues compared with BPH and that elevated ST6Gal1 expression was correlated with higher Gleason scores (Wei *et al.*, 2016).

Contradictory to this, I also found that ST6Gal1 expression was down-regulated when compared with normal prostate tissue. Our matched tumour and adjacent normal tissue samples RNA dataset showed that 6 out of the 9 patients had a clear significant down-

regulation of ST6Gal1 in the tumour tissue compared to the adjacent normal tissue. Tumour tissue can consist of not only tumour cells but also stromal cells, immune cells and vascular cells. This sample heterogeneity can often influence the investigation of clinical tumour samples using genomic approaches, such as gene expression analysis. Normal cells within the sample, such as stromal and immune cells can have a different gene expression profile to that of the tumour cells, therefore it is important to accurately determine the tumour cellularity of the sample prior to any further analysis.

Analysis of our PCa tissue microarray (TMA) shows that ST6Gal1 protein expression was down-regulated in PCa patient tissue samples compared with BPH tissue samples. We also found no correlation with patient Gleason scores or links to metastasis, but lower levels of ST6Gal1 predicted poor overall survival in months.

Advanced metastatic PCa is the leading cause of death in PCa patients, but the underlying mechanisms are poorly understood. I used stable cells lines as an *in vitro* model to investigate the mechanistic role of ST6Gal1. DU145 cells are representative of the earlier androgen depletion independent prostate cancers and had the lowest levels of endogenous ST6Gal1 expression. DU145 cells with increased ST6Gal1 expression exhibited increased cell to matrix adhesion and reduced migratory potential. This correlates with the increased expression we observed in a number of key adherens junction genes such as *CTNNB1* (beta-catenin), *FN1* (fibronectin) and *CDH1* (E-cadherin).

High ST6Gal1 expression levels also increased the invasion potential in DU145 cells. Epithelial to mesenchymal transition (EMT) plays an important role in the invasiveness of cancer cells. We saw increased expression levels of a number of genes known to be up-regulated during the EMT process, including VIM (vimentin), SNAI1 (snail) and SNAI2 (slug) as well as a dramatic loss of DSP (desmoplakin).

Whilst the adhesion assay showed a significant increase in cell adhesion in response to ST6Gal1, analysis of the KEGG database highlighted a number of cellular adhesion pathways which were significantly down-regulated in response to increased ST6Gal1, these include pathway 4520 - adherens junction, 4530 – tight junctions, 4510 - focal adhesion and 4512 - extra-cellular matrix receptor interaction.

The osteoclast differentiation pathway was significant in both the up-regulated and down-regulated gene lists. Osteoclasts are specialised multinucleated cells derived from the monocyte/macrophage lineage which adhere to and degrade bone matrix (Boyle *et al.*, 2003). In advanced PCa, metastasis is often detectable in bone with tumours which are predominantly osteoblastic (Clarke *et al.*, 1993). The sialylation of immune complexes such as immunglobulin G (IgG) is known to control osteoclast differentiation, with reduced IgG sialyation enhancing osteoclastogenesis (Harre *et al.*, 2015).

To investigate the opposing effect of ST6Gal1, a ST6Gal1 knock-down cell line was created in the androgen sensitive CW-22Rv1 cells. The reduction of ST6Gal1 expression significantly decreased cell proliferation, cell to matrix adhesion, migration and invasion capability. This correlates with what has previously been observed in PC3 and DU145 knock-down cell lines. Wei *et al* reported that ST6Gal1 expression was upregulated in human PCa tissues compared to non-malignant prostate tissue and high expression positively correlated with Gleason scores. They also found that ST6Gal1 knockdown in PC3 and DU145 cells significantly inhibited the proliferation, growth, migration and invasion capability (Wei *et al.*, 2016). ST6Gal1 has previously been associated with the maintenance of the cell mesenchymal state in breast cancer cell lines (Lu *et al.*, 2014). In line with this we observed a significant decrease in *CDH2* (N-cadherin) expression, a mesenchymal cadherin associated with EMT (Whang et al 2015) as well as other EMT markers *FN1* (fibronectin), *SNAI1* (snail) and *SNAI2* (slug).

Using molecular cloning techniques in two different PCa cell lines I have shown that the role of ST6Gal1 is complex and depends on the cellular background. There is always the possibility that off-target effects can contribute to the observed experimental result when using this kind of genome editing techniques. When generating the stable cell lines, single clones were selected and grown up. Using an initial pool of siRNAs or selecting more clones and pooling them together may have helped to limit any off-target effects. Rescue experiments are a good way to show siRNA specificity. If by adding a shRNA rescue control, the knock down effects were regained you can be confident the effects are due to the target knockdown. Around 50% ST6Gal1 knock-down was achieved in the CW-22Rv1 cell line. At this level it is possible that sufficient function may still have been retained.

Experiments performed on cells grown in culture can be limiting as they lack the heterogeneity that exists in clinical tumours. They have been grown in a particular culture media with specific oxygen and serum concentrations, an environment not representative of how cells exist within an organism. By creating stable cells line with artificial expression levels (over-expression/knock-down) of a given protein, you are generating an environment which does not reflect the physiological conditions within the tumour cell. It can therefore be difficult to interpret any downstream functional effects. Three-dimensional (3D) organoid cultures in which cells are grouped together and arranged as in the prostate gland would help to overcome some of the limitations of basic monolayer cell cultures (Gao *et al.*, 2014).

In this chapter I have used cells lines and clinical patient samples to identify ST6Gal1 expression patterns in PCa. Stable ST6Gal1 prostate cancer cell lines have been used to investigate the effect of ST6Ga1l on the cellular functions of prostate cancer cells, whilst RNA sequencing has identified reciprocal transcriptional changes in prostate cancer in response to ST6Gal1. Our data suggests that although ST6Gal1 expression in prostate cancer is highly variable and most likely dependable on the other compensatory mechanism available within the tumour together with the collective expression of other

glyco-enzymes. I have shown that changes in ST6Gal1 expression can modify the expression of some key cancer associated genes such as AKR1C1 (Zeng *et al.*, 2017), ABCA1 (Lee *et al.*, 2013), SLC18A2 (Haldrup *et al.*, 2016) and NOTCH3 (Carvalho *et al.*, 2014). The next step for this study would be to carry out glycopeptide analysis (liquid chromatography–mass spectrometry/lectin arrays) to look at the effect on glycosylation of ST6Gal1 targets.

Chapter 5

Results

Androgen regulated relaxin mRNA isoforms

Chapter 5 Results

Androgen regulated Relaxin mRNA isoforms

5.1 Introduction

5.1.1 The relaxin peptide hormone family

Relaxins are peptide hormones that belong to the insulin-like super family. In humans, the family consists of seven cystine-rich peptides; relaxin 1, 2 and 3 (RLN1, RLN2 and RLN3) and the insulin-like peptides INSL3, INSL4, INSL5 and INSL6. The *RLN1* and *RLN2* genes share 90% DNA sequence similarity and have 82% predicted sequence identity at amino acid level. In females, RLN2 is predominantly known for its roles in reproduction and pregnancy (reviewed in (Bathgate *et al.*, 2013). In males, RLN2 is produced by the secretory epithelial cell of the prostate gland and secreted into the seminal fluid (Yki-Jarvinen *et al.*, 1983; Ivell *et al.*, 1989) where it is thought to play a role in prostate growth, development of the reproductive tract and sperm motility (Hsu *et al.*, 2002; Samuel *et al.*, 2003; Ferlin *et al.*, 2012). Although *RLN1* mRNA is expressed in the prostate its function remains unknown. *RLN3* has a low overall sequence identity to *RLN1* (26%) and *RLN2* (22%) and is more structurally like INSL5. *RLN3* expression is highest in the central nervous system (Smith *et al.*, 2011; Bathgate *et al.*, 2013) and is thought to play a role in arousal, feeding, anxiety and stress and drug addiction (Ryan *et al.*, 2013; Smith *et al.*, 2014; Hosken *et al.*, 2015; Zhang *et al.*, 2015a; Shirahase *et al.*, 2016).

RLN2 has been shown to promote cancer progression in multiple cancers including breast cancer (Binder *et al.*, 2004; Cao *et al.*, 2013), thyroid cancer (Hombach-Klonisch *et al.*, 2006; Radestock *et al.*, 2010; Bialek *et al.*, 2011), endometrial cancer (Kamat *et al.*, 2006), osteosarcoma (Ma *et al.*, 2013; Ren *et al.*, 2015) and prostate cancer (Silvertown *et al.*, 2006; Thompson *et al.*, 2006; Feng *et al.*, 2007; Silvertown *et al.*, 2007; Feng *et al.*, 2009; Trapnell *et al.*, 2010; Neschadim *et al.*, 2015). The role of relaxins in

PCa is well characterised, *RLN2* expression is elevated in PCa samples relative to BPH samples (Vinall *et al.*, 2011). *RLN2* expression is negatively regulated by androgens and increases during the progression of PCa to androgen independence by promoting tumour growth and vascularisation (Silvertown *et al.*, 2006; Thompson *et al.*, 2006). *RLN2* expression is also increased in neuroendocrine PCa (Figueiredo *et al.*, 2005). RNAi mediated RXFP1 knockdown and inhibition of RLN2/RXFP1 signalling impairs PCa tumour growth and invasion capabilities (Feng *et al.*, 2007; Silvertown *et al.*, 2007). A synthetic RLN2 antagonist (AT-001) has been shown to reduce the growth of human CRPC xenografts by up to 60% (Neschadim *et al.*, 2014). Combined inhibition of the PKA and NF-κB signalling pathways, which are activated by RLN2, reduced PCa tumour growth and induced apoptosis (Vinall *et al.*, 2011).

5.1.2 Relaxin fusion protein

The high sequence homology between *RLN1* and *RLN2* makes it difficult to accurately characterise their individual functions. In addition to this, an alternatively spliced larger variant of *RLN2* has been described in the prostate (Gunnersen et al 1996). More recently, a novel fusion transcript comprising sequences from the both *RLN1* and *RLN2* genes has been identified in normal and PCa tissue. Single molecule real time (SMRT) sequencing on LNCaP cells was performed using the PacBio platform which generates longer sequencing reads. This method detected a *RLN1/RLN2* novel transcript which was abundantly expressed in LNCaPs (Tevz *et al.*, 2016).

The fusion transcript contains incomplete sequences from both RLN1 and RLN2 as well as a novel exon in the intronic region between the genes. Analysis of the new fusion sequence predicated a protein isoform which contained all the intact functional domains of RLN2 (A and B chains and C-peptide) but was missing the signal sequence, which is essential for secretion. Expression of RLN1 is increased by androgens (Tevz *et al.*, 2016), whereas RLN2 is negatively regulated by androgens (Thompson *et al.*, 2006). As with RLN2, expression of the fusion transcript was also repressed by androgens (Tevz *et al.*, 2016).

5.2 Aims

This project has shown that the AR plays a key role in regulating gene expression in PCa cells. However, individual genes can produce multiple different mRNA isoforms, which can have quite different biological activities from each other. For example, alternative isoforms made by the same gene can make proteins which switch gene function between pro and anti-apoptotic isoforms, leading to cell death or survival, or from stable epithelial cells towards mesenchymal cells which move around the body (Rajan *et al.*, 2009; Sette *et al.*, 2013).

There is mounting evidence to suggest that gene transcription and pre-mRNA processing are co-ordinated events (Cramer *et al.*, 1997; Cramer *et al.*, 1999; Cramer *et al.*, 2001; Pagani *et al.*, 2003; Dowhan *et al.*, 2005). Androgens can control exon splicing through their control of regulators and coactivators (Dowhan *et al.*, 2005). The AR can recruit the RNA binding proteins Sam68 and p68 which have been shown to influence alternative splicing of a subset of genes (Clark *et al.*, 2008; Rajan *et al.*, 2008; Munkley *et al.*, 2017a). Androgens drive the production of a different mRNA isoform from the normally tumour suppressor TSC2 gene (Rajan *et al.*, 2011). This novel TSC2 isoform activates instead of repressing cell proliferation, and is expressed in clinical prostate cancer so provides a new route through which these cells might proliferate (Munkley *et al.*, 2014).

Together with the androgen regulated transcriptional changes (detailed in Chapter 3 of this thesis), the RNA sequencing data from LNCaP cells also identified 73 androgen regulated alternative mRNA isoforms. These included 56 alternative promoters, 4 alternative 3′ ends and 13 alternative spicing events (paper currently in preparation). This chapter will focus on the identified androgen regulated promoter switches for the RLN1 and RLN2 genes.

The aims of this chapter were to:

- Establish *RLN1* and *RLN2* isoform expression patterns in prostate cancer cells.
- Establish if RLN1 and RLN2 protein expression is androgen regulated.
- Investigate *RLN1* and *RLN2* isoform expression in clinical prostate cancer samples.

5.3 Results

5.3.1. Novel mRNA isoforms of RLN1 and RLN2 are androgen regulated

The RNA sequencing data identified androgen regulated promoter switches for the RLN1 and RLN2 genes. For RLN1, there was a decrease in expression from a promoter (promoter 2) driving a non-coding transcript in the presence of androgens, compared to the expression from an up-stream promoter (promoter 1) driving the expression of a coding mRNA isoform (Figure 5.1a). Therefore androgens were found to repress the expression of a non-coding RLN1 isoform in prostate cancer cells. A promoter switch for the adjacent RLN2 gene was also observed. Here there was an increase in expression from the up-stream promoter (promoter 1) in the presence of androgens (Figure 5.1b). Therefore androgens were found to induce the expression of the protein coding RLN2 isoform.

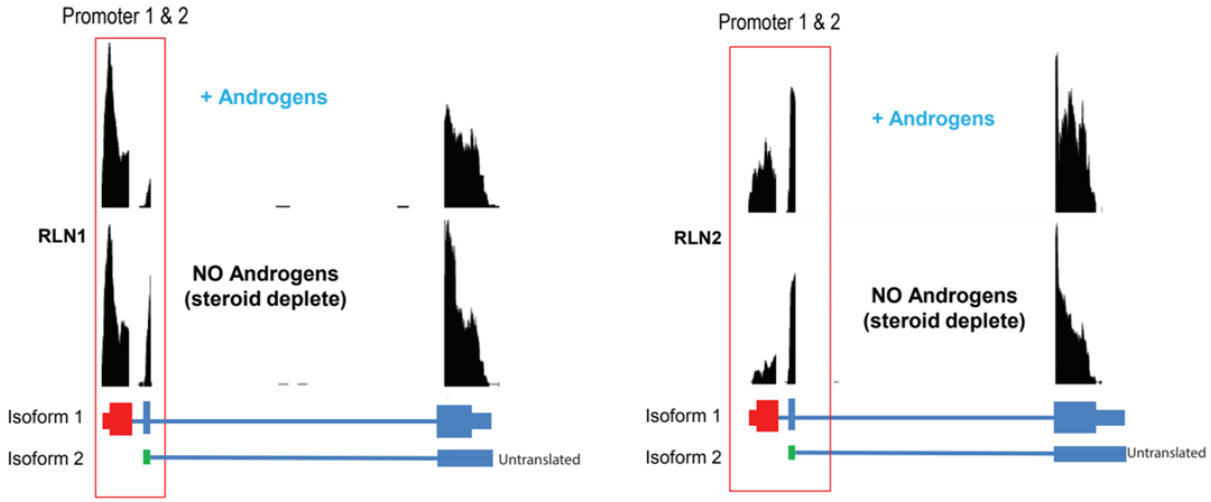

Figure 5.1 Androgen regulated alternative promoter switches for RLN1 and RLN2. RNAseq profiles for RLN1 and RLN2 from LNCaP cells grown in the presence of 10 nM synthetic androgen R1881 for 24 hours (+ androgens) and LNCaP cells grown in charcoal stripped steroid deplete media (steroid deplete). Alternative promoter switches and predicted protein isoforms are highlighted within the red boxes.

These isoform changes were confirmed in a further independent LNCaP sample set (Figure 5.2a-d).

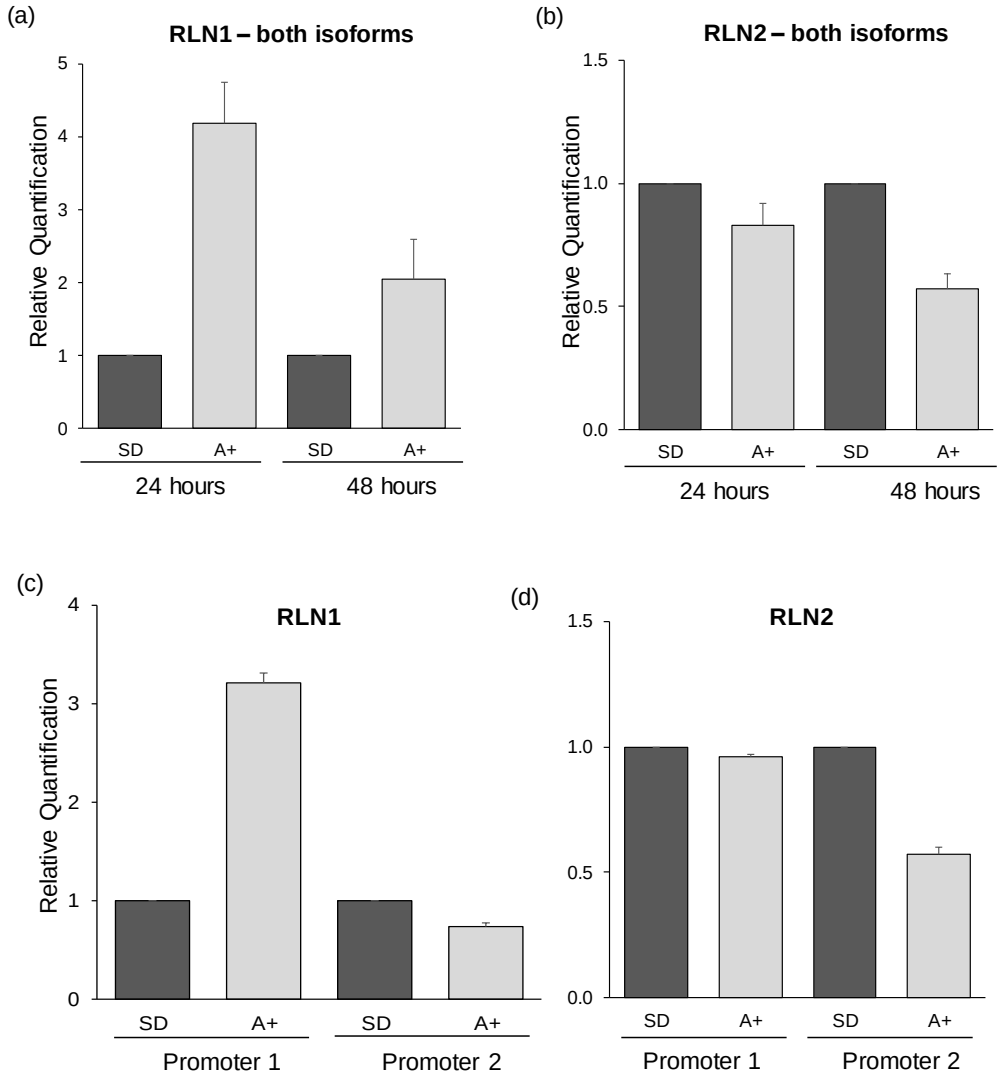

Figure 5.2 Expression of RLN1 and RLN2 in LNCaP cell line in response to androgens. Real-time quantitative reverse transcription PCR (qRT-PCR) analysis of:

(a) RLN1 (both isoforms) expression in LNCaP cells in response to 10 nM synthetic androgen (R1881) stimulation (24 hours and 48 hours). There was a significant

increase in RLN1 mRNA expression in response to androgens after 24 hours. This was detected using a primer set that amplifies both isoforms.

(b) RLN2 (both isoforms) expression in LNCaP cells in response to 10 nM synthetic androgen (R1881) stimulation (24 hours and 48 hours). There was a decrease in RLN2 mRNA expression in response to androgens after 48 hours. Detected using a primer set that amplifies both isoforms.

(c) RLN1 isoform expression in LNCaP cells in response to 10 nM synthetic androgen (R1881) stimulation (24 hours). There was an increase in expression of RLN1 promoter 1 expression in response to 24 hours androgen stimulation. There was no change is promoter 2 expression. This was detected using an isoform specific primer set (Figure 5.3).

(d) RLN2 isoform expression in LNCaP cells in response to 10 nM synthetic androgen (R1881) stimulation (24 hours). There was no change in expression of RLN2 promoter 1 expression and a decrease of RLN2 promoter 2 expression in response to 24 hours androgen stimulation. This was detected using an isoform specific primer set (Figure 5.3).

Gene expression was calculated as the average (3 biological replicates) fold change (log2) relative quantification of androgen treated LNCaP cells compared to steroid deplete cells (value set as 1). Samples were normalised using the average of three reference genes, GAPDH, β -tubulin and actin. All primer sequences are listed in Appendix B.

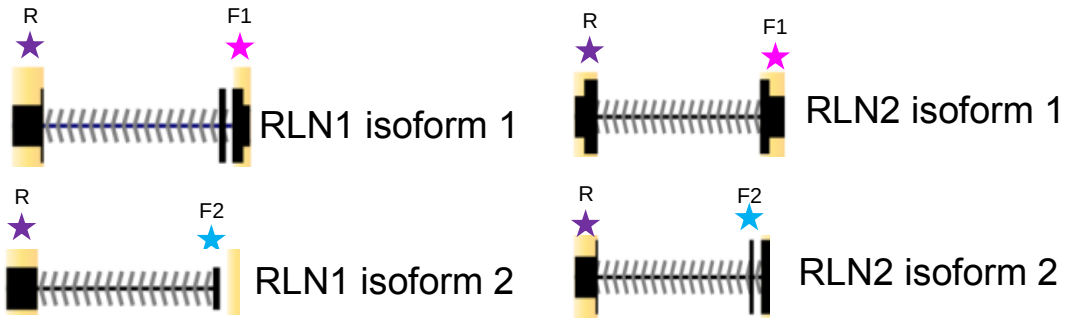

Figure 5.3 RLN1 and RLN2 transcript variants and qRT-PCR primers. RLN1 and RLN2 transcripts with isoform specific real-time quantitative reverse transcription PCR (qRT-PCR) primers. Pink star - forward primer location for isoform 1, blue star – forward primer location for isoform 2, purple star – common reverse primer location.

5.3.2 Generation of the RLN1 antibody

We next wanted to establish if RLN1 and RLN2 were androgen regulated at the protein level. A number of commercial available RLN1 antibodies were tested but none could be validated. Despite extensive optimisation, the antibodies tested did not produce a band at the predicted molecular weight nor did they recognise over-expressed protein.

To allow further investigation into the expression of RLN1 protein, a specific RLN1 antibody was raised. An antigenic peptide from amino acids 87-185 of the RLN1 protein sequence was chosen as an epitope that would identify expression of both isoforms. The sequence was checked for its similarity to other protein sequences in the databases by a BLAST protein search (http://www.ncbi.nlm.nih.gov/BLAST/). The cDNA encoding this peptide was amplified by PCR and subsequently cloned into pGEX-5X1 vector in frame with glutathione S-transferase (Figure 5.4) and the pET32a (+) vector in frame with histidine tags (Figure 5.5).

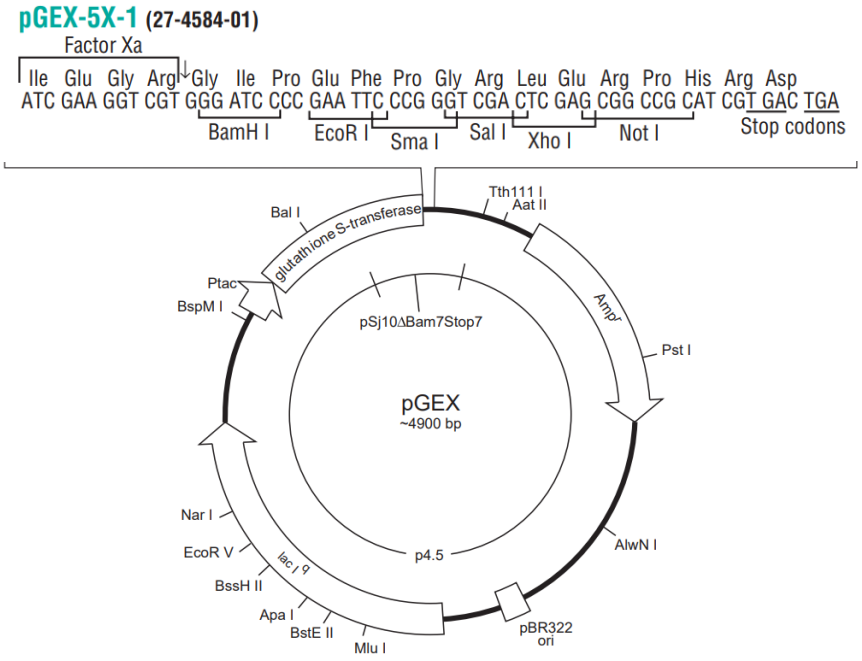

MfeI forward primer: AAAAAAAAC'AATTGATGTTGGAATTCATTGCTAATTTGCC

XhoI reverse primer: AAAAAAAACTCGAGTCAGCAATATTTAGCAAGAGACCTTTTGG

C'AATTGATGTTGGAATTCATTGCTAATTTGCCACCGGAGCTGAAGGCAGCCCTATCTGAGAGGC
AACCATCATTACCAGAGCTACAGCAGTATGTACCTGCATTAAAGGATTCCAATCTTAGCTTTGAAG
AATTTAAGAAACTTATTCGCAATAGGCAAAGTGAAGCCGCAGACAGCAATCCTTCAGAATTAAAAT
ACTTAGGCTTGGATACTCATTCTCAAAAAAAGAGACGACCCTACGTGGCACTGTTTGAGAAATGT
TGCCTAATTGGTTGTACCAAAAGGTCTCTTGCTAAATATTGCTGACTCGA'G

Figure 5.4 pGEX-5X-1 glutathione S-transferase fusion vector. Map of the pGEX-5X-1 vector showing the reading frames and main features. The GST fusion protein expression is under the control of the *tac* promoter, which is induced by the lactose analog isopropyl b-D thiogalactoside (IPTG). The vector also contains a *lac*Iq gene product, a repressor protein that binds to the operator region of the *tac* promoter, preventing expression until induction by IPTG. Primer sequences and restriction enzymes used to allow for directional cloning of the insert sequence into the vector are detailed in Appendix B.

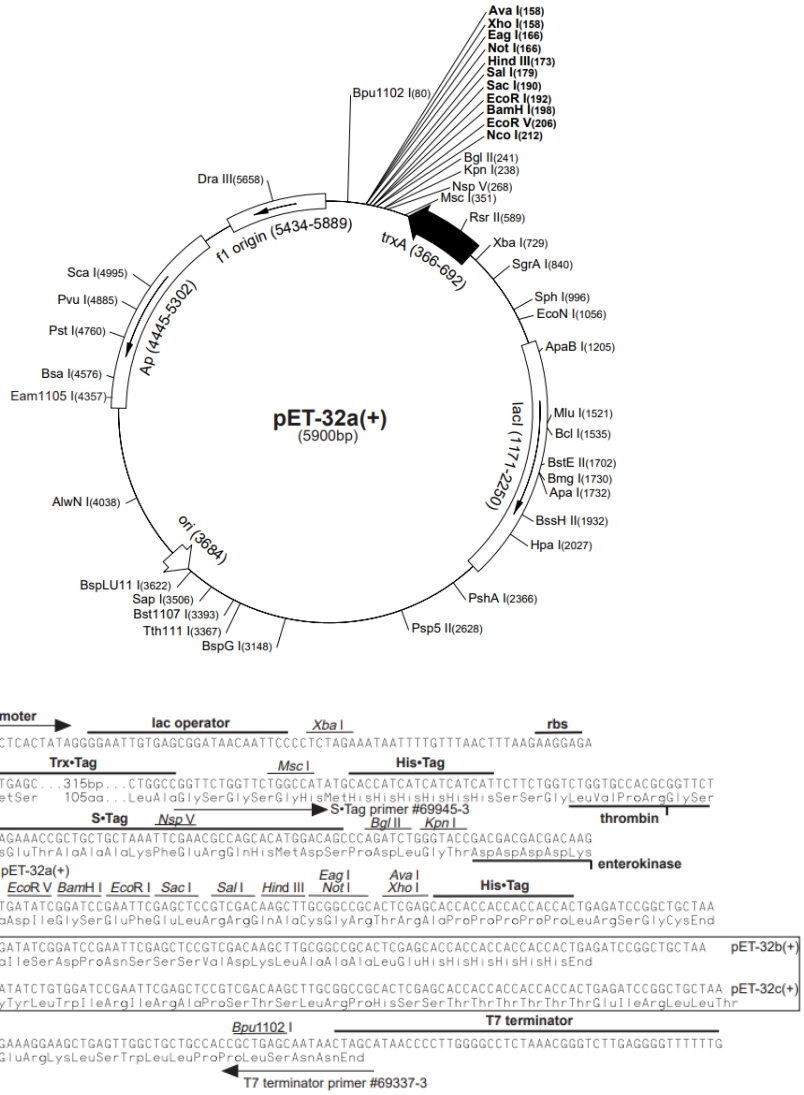

MfeI forward primer: AAAAAAAAC'AATTGATGTTGGAATTCATTGCTAATTTGCC

XhoI reverse primer: AAAAAAAACTCGAGTCAGCAATATTTAGCAAGAGACCTTTTGG

GAA TTG ATG TTG GAA TTC ATT GCT AAT TTG CCA CCG GAG CTG AAG GCA GCC CTA TCT GAG AGG CAA CCA TCA TTA CCA GAG CTA CAG CAG TAT GTA CCT GCA TTA AAG GAT TCC AAT CTT AGC TTT GAA GAA TTT AAG AAA CTT ATT CGC AAT AGG CAA AGT GAA GCC GCA GAC AGC AAT CCT TCA GAA TTA AAA TAC TTA GGC TTG GAT ACT CAT TCT CAA AAA AAG AGA CGA CCC TAC GTG GCA CTG TTT GAG AAA TGT TGC CTA ATT GGT TGT ACC AAA AGG TCT CTT GCT AAA TAT TGC TGA CTC GA

Figure 5.5 pET-32a(+) histidine tagged fusion vector. Map of the pET-32a(+) vector showing the reading frames and main features. The pET-32a(+) vector is designed for cloning and high-level expression of peptide sequences fused with

thioredoxin (Trx-Tag) histidine (His-Tag) and S-Tag proteins. Histidine fusion protein expression is under the control of the T7 promoter, which is induced by the lactose analog isopropyl b-D thiogalactoside (IPTG). The vector also contains a lacI repressor protein that binds to the operator region of the T7 promoter, preventing expression until induction by IPTG. Primer sequences and restriction enzymes used to allow for directional cloning of the insert sequence into the vector are detailed in Appendix B.

Plasmids encoding the fusion peptides were transformed into *E. coli* BL21 bacteria and expression was induced by addition of IPTG to the culture medium (Figure 5.6a). Three hours after induction the bacteria were harvested and cell lysates were prepared.

The GST-tagged fusion peptide was purified and used for immunization. To purify the peptide under non-denaturing conditions, the solubility of the peptides was tested by comparing whole bacterial cell lysate with supernatant from the sample after centrifugation and checking for the presence of the fusion-peptide (Figure 5.6b). Purification of the GST-fusion peptide was carried out using glutathione agarose (Figure 5.6c). The purified peptide was then resolved on a preparative SDS-PAGE gel. The gel was washed in 1X SDS-PAGE running buffer without SDS and the gel slice containing the peptide was excised and ground to a powder using liquid nitrogen and dry ice.

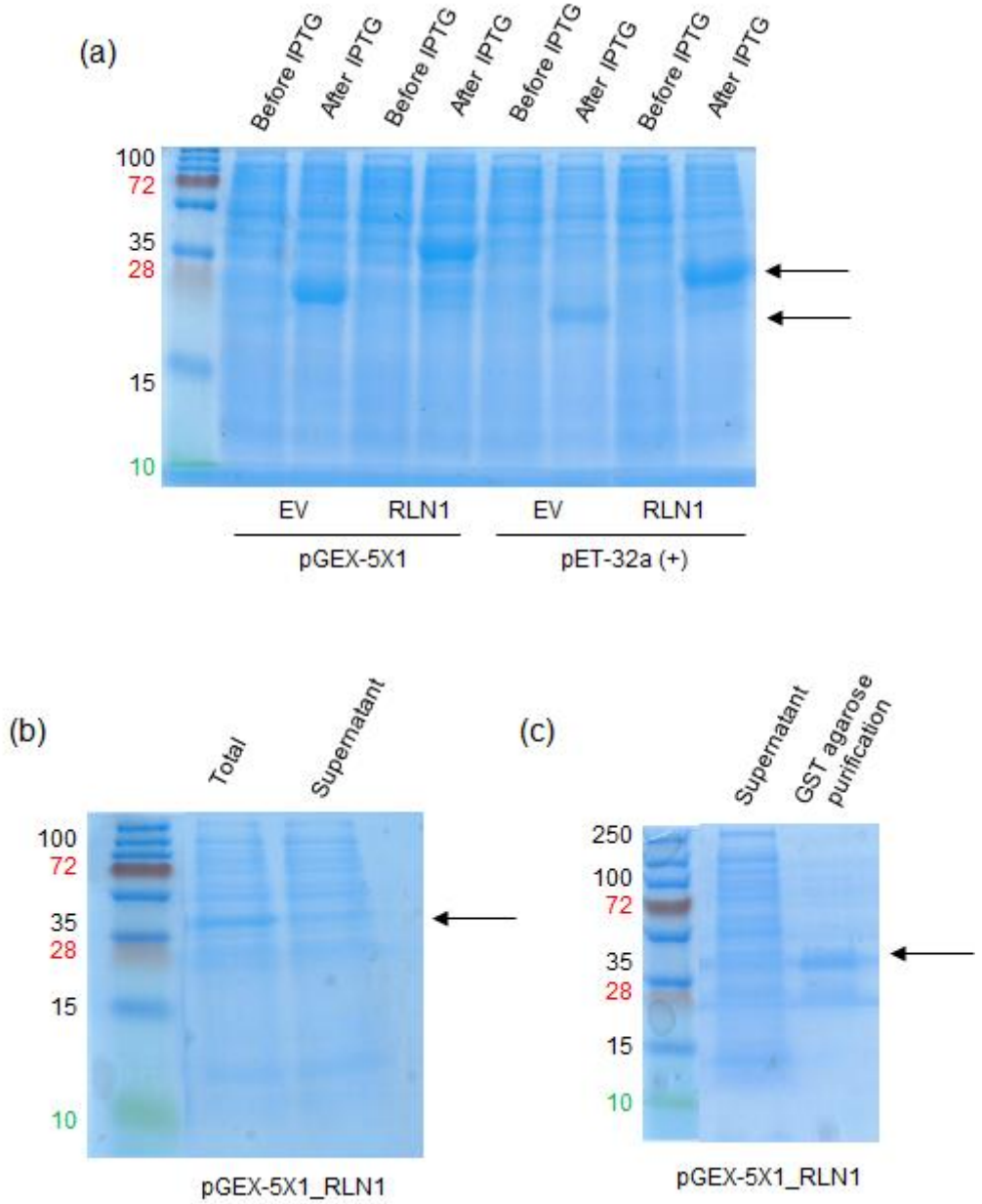

Figure 5.6 Preparation of the RLN1 antigenic peptide.

(a) Bacterial expression of the RLN1 GST (pGEX-5X1) and histidine (pET-32a (+) fusion peptides. Plasmids containing amino acids from the RLN1 protein were transformed into *E. coli* BL21 bacteria. Transformed bacteria was cultured and

expression from the plasmids was induced with IPTG. Samples were taken before and after induction (before IPTG) and after 3 hours (after IPTG) and resolved by SDS_PAGE. Gels were stained with Coomassie Brilliant Blue.

(b) Solubility of the GST_RLN1 fusion peptide. Following bacterial expression, the lysates were centrifuged and total lysate was compared to supernatant by SDS-PAGE.

(c) Purification of the GST_RLN1 fusion peptide. The bacterial lysate was purified using glutathione agarose.

Black arrows indicated the predicted size of the expressed proteins.

The GST fusion peptide was used for immunisation of a rabbit. The immunisation program was carried out by National Service Scotland, Pentlands Science Park, Midlothian. Serum from the immunised rabbit was collected and the RLN1 antibody was purified using the histidine tagged peptide.

The histidine-tagged peptide was purified using nickel affinity resin. The peptide was eluted with imidazole, which displaces histidine. This elution process was repeated to recover as much of the purified peptide as possible (Figure 5.7a). The eluted peptide was desalted using a P10 column and then coupled to a SulfoLink immobilising column. The collected flow through was analysed for protein content using a Bradford assay (Figure 5.7b).

IgG was isolated from the rabbit serum using caprylic acid. The IgG was dialysed against PBS overnight and affinity purified against the RLN1-histidine fusion coupled to the SulfoLink column. Both acidic and basic conditions were used for elution which were analysed for protein content using a Bradford assay (Figure 5.7c). The protein positive fraction (acidic conditions, elution 2) were dialysed against PBS overnight. For long term storage 10% glycerol and 0.05% sodium azide were added and the antibody.

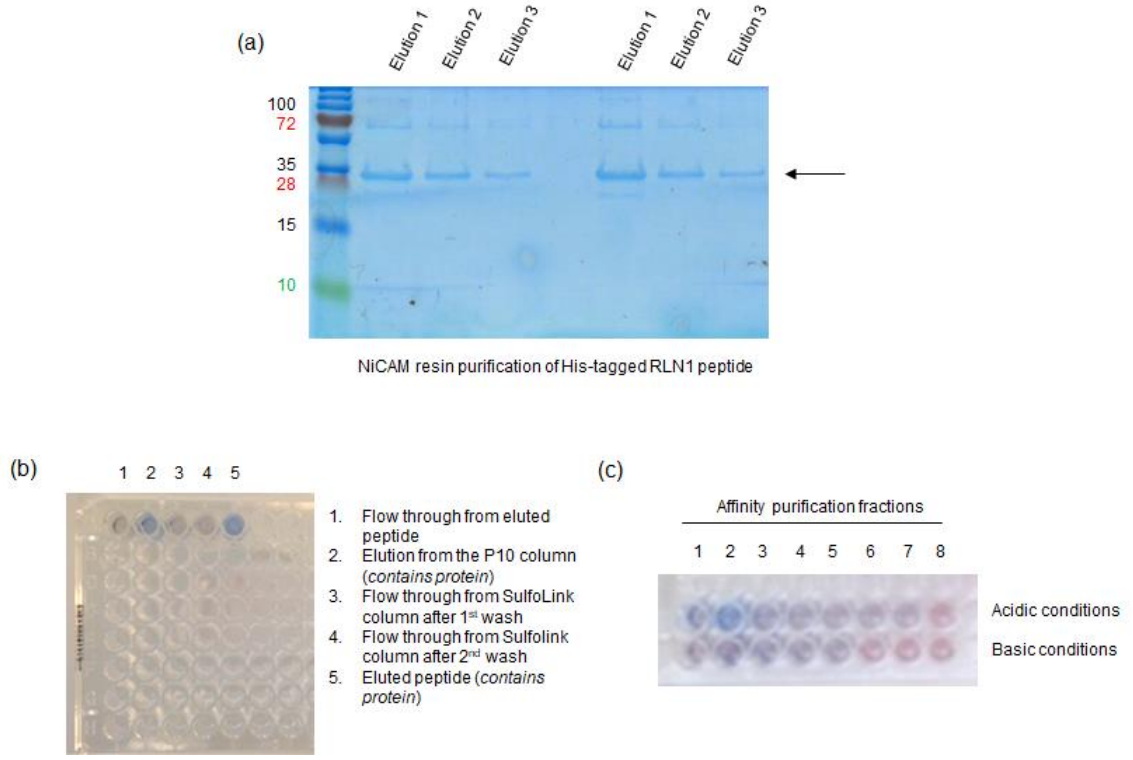

Figure 5.7 Affinity purification using RLN1-histidine fusion peptide

(a) Purification of the RLN1-histidine fusion peptide. Following bacterial expression the lysate was purified using nickel affinity resin. The bound peptide was eluted in 3 fractions which were analysed by SDS-PAGE.

(b) Bradford protein assay. The flow through from the P10 desalting and coupling to the SulfoLink column were analysed for protein. Protein was detected in the elution from the P10 column (well 2) and in the antibody elution from the SulfoLink column following affinity purification (well 5). No protein was detected in the initial flow though (well 1) or in the flow through from the wash stages (wells 3 and 4).

(c) Bradford protein assay analysis of antibody fraction following affinity purification under acidic and basic conditions. Positive fraction (containing protein) was fraction 2, acidic condition.

5.3.3 Characterisation of the RLN1 antibody

The purified RLN1 antibody was tested by Western blotting using protein prepared from Human Embryonic Kidney 293 (HEK-293) cells over-expressing the N-terminal 3xFlag tagged fusion RLN1 promoter 1 and promoter 2 proteins. The predicted sequences for RLN1 promoter 1 (RLN1_p1) and RLN1 promoter 2 (RLN1-p2) were cloned into the p3XFLAG-CMV-10 expression vector using restriction enzymes and transfected into HEK293 cells. The predicted molecular weight of the RLN1 protein (isoform 1) is 28kDa, whilst the RLN1 (isoform 2) sequence has a predicted molecular weight of 11kDa. This was calculated using a protein molecular weight calculator tool available at https://www.bioinformatics.org/sms/prot_mw.html.

Expression of the larger RLN1 protein isoform (that would be made using promoter 1) was detected at approximately 31kDa using a monoclonal anti-Flag M2 antibody. No band was detected for the RLN1 promoter 2 isoform_Flag fusion protein isoform (Figure 5.8a). The RLN1 antibody detected a protein band at approximately 28kDa as predicted for the RLN1 promoter 1_Flag fusion protein isoform. No smaller bands were detected for the promoter 2 isoform predicted fusion protein, despite mRNA expression (Figure 5.8b and c). These results suggest no short RLN1 protein isoform is made in HEK293 cells, despite over-expression. A number of different conditions for the SDS-PAGE gel transfer were tested to ensure smaller proteins would be detected.

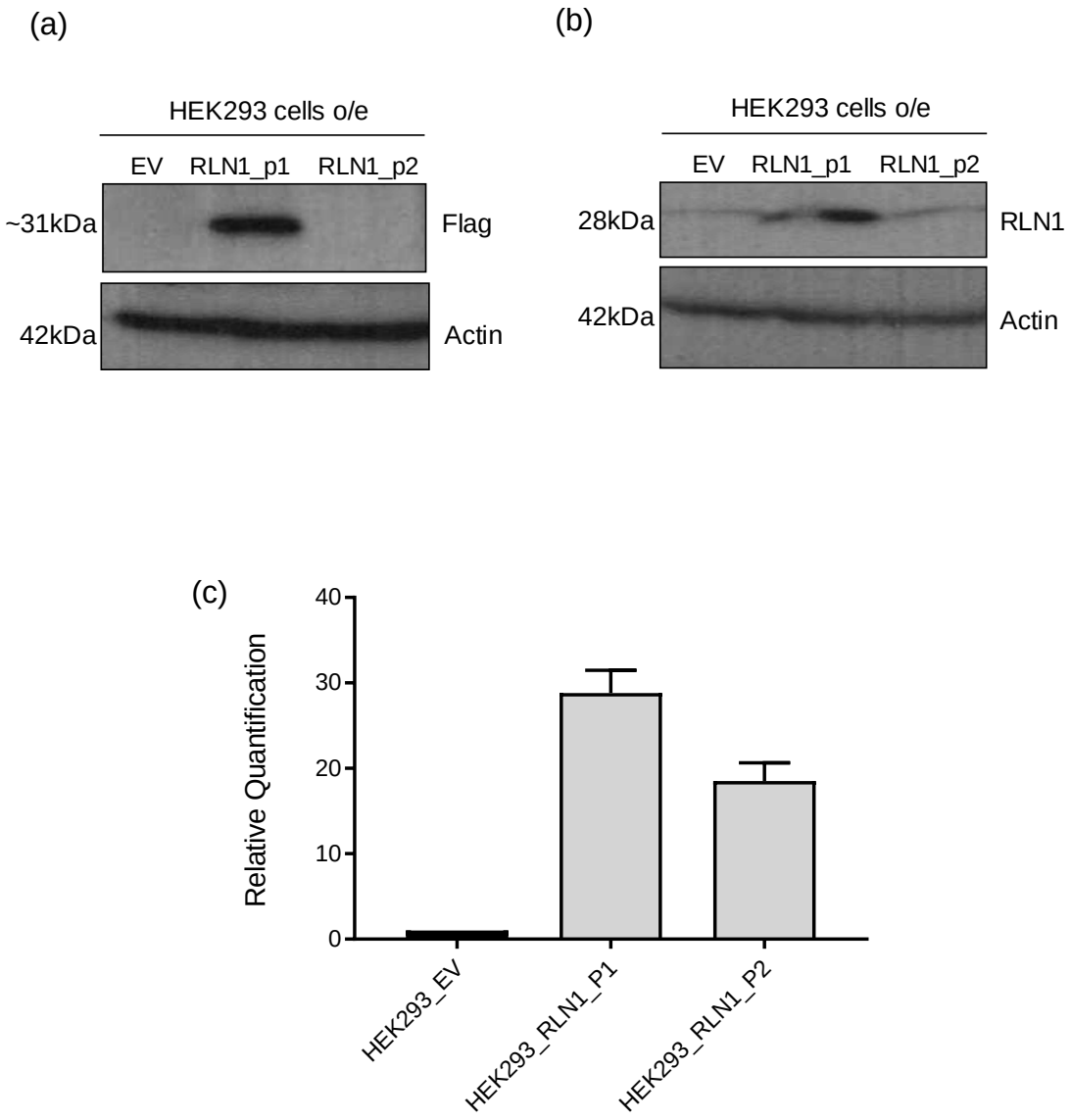

Figure 5.8 Validation of the RLN1 antibody. Detection of RLN1 protein (isoform 1) in human HEK-293 cells over-expressing N-Terminal 3XFlag tagged fusion proteins. No protein expression was detected for the non-coding isoform.

(a) Representative Western blot showing isoform 1 protein expression was detected using a monoclonal anti-Flag M2 antibody. Actin was used as a loading control.

(b) Representative Western blot showing RLN1 protein was detected using the RLN1 antibody. Actin was used as a loading control.
(c) Real-time quantitative reverse transcription PCR (qRT-PCR) confirmation of RLN1 isoform overexpression in HEK-293 cells. Expression was calculated as the average (from 3 biological replicates) fold change relative quantification compared to the empty vector control cells (EV) (value set as 1). Samples were normalised using the average of three reference genes, GAPDH, β -tubulin and actin.

5.3.4 Characterisation in prostate cancer cells

Although an increase in RLN1 promoter 1 mRNA expression was detected in LNCaP cells in response to androgen stimulation (Figure 5.2a), there was no corresponding increase in full length RLN1 protein expression at 24 hours or 48 hours. A slight increase was overserved after 72 hours. Expression of RLN2 protein was reduced following 24 hours androgen stimulation (Figure 5.2b). A smaller band was observed at ~15kDa, this is most likely non-specific. This could have been controlled for by using a RLN negative cell line, in which RLN1 is known to be absent such as Hela or MCF7 cells. If the band was a non-specific product it would still be visible in the negative cell lines.

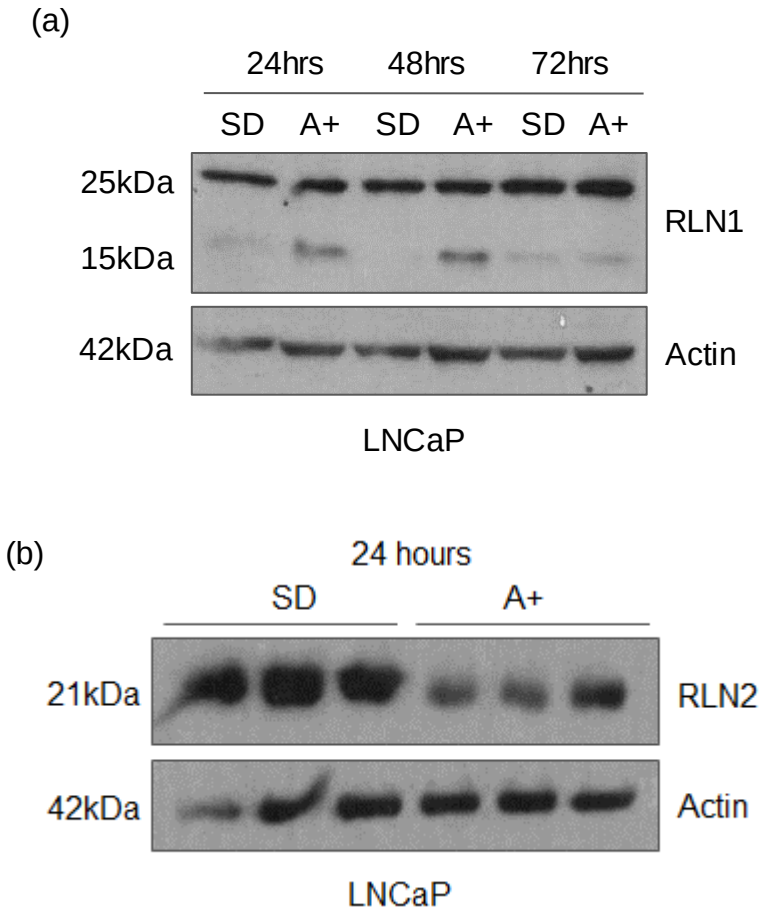

Figure 5.9 Androgen regulation of RLN1 and RLN2 protein expression

(a) Representative Western blot showing expression of RLN1 protein (25kDa) in LNCaP cells in response to 10 nM synthetic androgen (R1881) stimulation (24 hours, 48 hours and 72 hours). Actin was used as a loading control.

(b) Representative Western blot showing expression of RLN2 protein (21kDa) in three replicate samples of LNCaP cells in response to 10 nM synthetic androgen (R1881) stimulation (24 hours). Actin was used as a loading control.

5.3.5 Relaxin expression in clinical prostate cancer patient samples

Expression levels of RLN1 and RLN2 mRNA were analysed in prostate cancer patient RNA samples using qRT-PCR. The sample set contained RNA from carcinoma tissue and adjacent normal tissue from 9 patients. Clinical samples were provided with ethical approval through the Exeter NIHR Clinical Research Facility tissue bank (Ref: STB20). Written informed consent for the use of surgically obtained tissue was provided by all patients.

3 of the 9 patients showed an increase in RLN1 promoter 1 mRNA expression in prostate carcinoma tissue compared to adjacent normal tissue (patients 1, 4 and 9), whilst the remaining 6 patients showed a decrease (patients 2,3,5,6,7 and 8) (Figure 5.10a). 2 of the 9 patients showed an increase in RLN1 promoter 2 mRNA expression in prostate carcinoma tissue compared to adjacent normal tissue (patients 8 and 9) (Figure 5.10b). Patients 1 and 4 had an increase in promoter 1 transcripts compared to promoter 2 transcripts in the carcinoma tissue, whilst patients 8 and 9 had an increase in promoter 2 transcripts compared to promoter 1 transcripts in the carcinoma tissue. Patients 2,3,5,6 and 7 have lower levels of RLN1 (both isoforms) mRNA expression in prostate carcinoma tissue compared to adjacent normal tissue. For RLN2, 2 of the 9 patients showed an increase in promoter 1 mRNA expression in prostate carcinoma tissue compared to adjacent normal tissue (patients 4 and 9), whilst the remaining 7 patients showed a decrease (patients 1,2,3,5,6,7 and 8) (Figure 5.11a). 2 of the 9 patients showed an increase in RLN2 promoter 2 mRNA expression in prostate carcinoma tissue compared to adjacent normal tissue (patients 8 and 9) (Figure 5.11b). Patient 4 has an increase in promoter 1 transcripts compared to promoter 2 transcripts in the carcinoma tissue, whilst patients 8 and 9 had an increase in promoter 2 transcripts compared to promoter 1 transcripts in the carcinoma tissue. Patients 2,3,5,6 and 7 have lower levels of RLN2 (both isoforms) mRNA expression in prostate carcinoma tissue compared to adjacent normal tissue.

The difference in expression observed for each patient was highly variable. All samples have been normalised to the normal tissue expression levels, but this was not consistent between patients, cycle threshold (ct) values varied significantly.

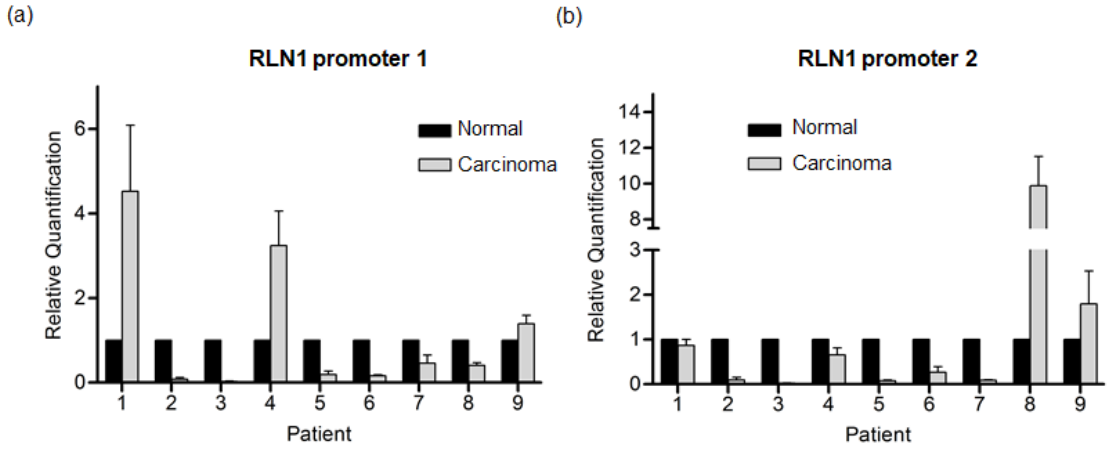

Figure 5.10 RLN1 mRNA expression levels in prostate cancer patient samples. Real-time quantitative reverse transcription PCR (qRT-PCR) analysis of RLN1 promoter 1 and promoter 2 mRNA expression in RNA from matched tumour tissue and adjacent normal tissue samples from 9 patients.

(a) 3 of the 9 patients showed an increase in RLN1 promoter 1 mRNA expression in prostate carcinoma tissue compared to adjacent normal tissue (patients 1, 4 and 9), whilst the remaining 6 patients showed a decrease (patients 2,3,5,6,7 and 8).

(b) 2 of the 9 patients showed an increase in RLN1 promoter 2 mRNA expression in prostate carcinoma tissue compared to adjacent normal tissue (patients 8 and 9).

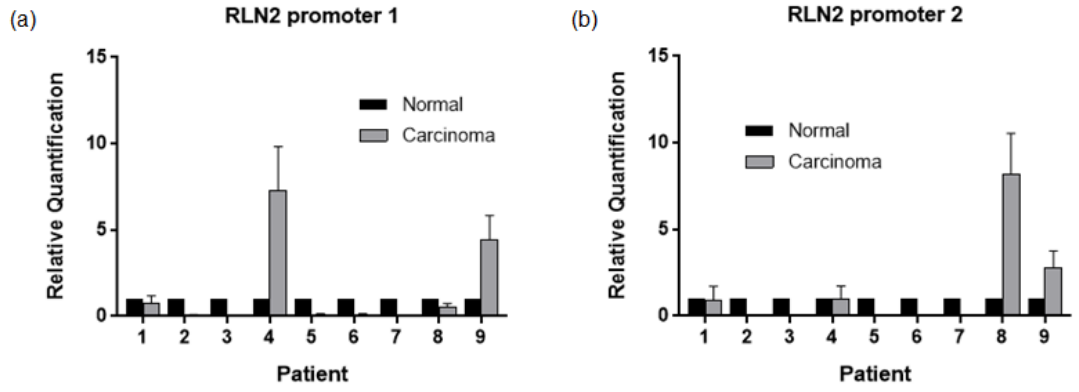

Figure 5.11 RLN2 mRNA expression levels in prostate cancer patient samples. Real-time quantitative reverse transcription PCR (qRT-PCR) analysis of RLN2 promoter 1 and promoter 2 mRNA expression in RNA from matched tumour tissue and adjacent normal tissue samples from 9 patients.

(a) 2 of the 9 patients showed an increase in RLN2 promoter 1 mRNA expression in prostate carcinoma tissue compared to adjacent normal tissue (patients 4 and 9), whilst the remaining 7 patients showed a decrease (patients 1,2,3,5,6,7 and 8).

(b) 2 of the 9 patients showed an increase in RLN2 promoter 2 mRNA expression in prostate carcinoma tissue compared to adjacent normal tissue (patients 8 and 9).

5.4 Discussion

As well as transcriptional changes, androgens can also drive the expression of alternative mRNA isoforms. An individual gene can produce multiple different mRNA isoforms, vastly expanding the range of proteins within the cell. These protein variants can have different functions and sub-cellular locations from each other (Stamm *et al.*, 2005). Transcriptome exon microarray experiments have previously identified androgen regulated cassette exons: an exon within the *ZNF121* gene was activated by androgens and an exon within the *NDUFV3* gene was repressed by androgens (Rajan 2011). The same study also identified an androgen regulated alternative *TSC2* mRNA isoform which encodes a protein promoting cell growth (Munkley et al. 2014). More recently RNA sequencing experiments have identified an androgen regulated ST6GalNac1 mRNA splice isoform encoding a shorter ST6GalNac1 protein which reduces cell adhesion, increases motility and promotes EMT in prostate cancer cells (Munkley *et al.*, 2015b).

The global RNA sequencing data from LNCaP cells reported here has identified 73 androgen regulated alternative mRNA isoforms, the majority of which are generated through alternative promoter selection. This thus significantly increases the number of known AR regulated mRNA isoforms and implies a much greater level of complexity whereby androgens are able to simultaneously regulate transcriptional and alternative mRNA isoform expression changes in prostate cancer (paper currently in preparation).

In this chapter I have particularly reported that the AR can induce expression of alternative mRNA isoforms of the *RLN1* and *RLN2* genes in prostate cancer cells. Androgen regulated promoter switches for the peptide hormones RLN1 and RLN2 were identified. Androgens were found to repress the expression of a non-coding RLN1 isoform, increasing the expression of the protein coding isoform. For RLN2, there was an increase in expression from the up-stream promoter (promoter 1) in the presence of androgens. In both cases, androgen stimulation resulted in an overall decrease in the non-coding isoform.

Expression levels of RLN1 are known to be up-regulated in LNCaP cells in response to androgens (Tevz *et al.*, 2016) and RLN1 is abundantly expressed in LNCaP cells, normal prostate tissue and prostate cancer tissue (Hansell *et al.*, 1991; Gunnersen *et al.*, 1996; Tevz *et al.*, 2016). This supports my findings that androgens increase the expression of RLN1 mRNA, although I was not able to confirm this change at the protein level. A shorter RLN1 isoform was detected by western blot in androgen stimulated LNCaP cells, however this is likely to be a non-specific artefact, further investigation is required. RLN2 expression is known to be negatively regulated by androgens and increases during the progression of prostate cancer to androgen independence by promoting tumour growth and vascularisation (Silvertown *et al.*, 2006; Thompson *et al.*, 2006). I also found that androgens decrease the expression of RLN2 mRNA and protein.

Comparison of matched prostate carcinoma and adjacent normal tissue samples in a 9 patient cohort identified significantly differentially expressed mRNA isoforms for RLN1 and RLN2. 2 patients showed an increase in RLN1 promoter 1 mRNA expression and a decrease in promoter 2 expression in the prostate carcinoma tissue. Another patient showed an increase in RLN1 promoter 2 mRNA expression and a decrease in promoter 1 expression in the prostate carcinoma tissue. The same pattern was observed for the RLN2 mRNA isoforms with one patient showing an increase in RLN2 promoter 1 mRNA expression and a decrease in promoter 2 expression and another patient showed an increase in RLN2 promoter 2 mRNA expression and a decrease in promoter 1 expression in the prostate carcinoma tissue. This is a small cohort of patients and as the results between patients are highly variable, a larger cohort would be needed to understand true expression patterns.

The novel fusion transcript which has recently been described contains incomplete sequences of both RLN1 and RLN2. This fusion transcript is expressed in LNCaP cells and normal prostate tissue and is down-regulated by androgens (Tevz *et al.*, 2016). When the RNA transcripts were aligned to the human genome, the RLN1-RLN2 fusion showed a significant overlap with the annotated RLN1 and RLN2 genes. Overlapping

transcripts included the 3' end of the first RLN1 exon and the 5' end of the second RLN1 exon, the 3' end of the first RLN2 exon and all of the second RLN2 exon. As with earlier studies, my primers were designed near the exon junction and would therefore not be able to discriminate between RLN1/RLN2 and RLN1-RLN2 fusion transcripts. The abundant expression of this fusion transcript in LNCaP cells may have skewed my results, although no fusion protein (larger protein band) was detected using the RLN1 or RLN2 specific antibodies and no reads were mapped between RLN1 and RLN2 in the analysis of our RNA sequencing.

Further investigation of these androgen regulated mRNA isoforms is necessary to establish which isoforms encode proteins that may be clinically relevant. The generation of a RLN1 antibody will allow further functional investigations into the expression patterns and localisation of this protein. Although the identification of this novel RLN1-RLN2 fusion will make it technically challenging to accurately characterise their independent expression.

Chapter 6

Concluding remarks and future direction

Chapter 6

Concluding remarks and future direction

Prostate cancer remains one of the leading causes of cancer-related death in men (Hassanipour-Azgomi *et al.*, 2016). Androgens and the AR are key players in the development and progression of the disease and have been the main target of therapeutic treatments for many years (Livermore *et al.*, 2016). Numerous genomic and transcriptomic studies have been carried out over the years, identifying AR binding sites and target genes (Massie *et al.*, 2007; Wang *et al.*, 2007; Wang *et al.*, 2009a; Massie *et al.*, 2011; Rajan *et al.*, 2011; Sharma *et al.*, 2013). The development of RNA sequencing technology has allowed for transcriptome interrogation on a much larger scale. Within the last decade, there have been a number of published clinical PCa transcriptome datasets, providing a comprehensive profile of advanced, metastatic, castrate resistant and neuroendocrine prostate cancer (Fenner, 2011; Rajan *et al.*, 2014; Robinson *et al.*, 2015; Beltran *et al.*, 2016; Kumar *et al.*, 2016; Mo *et al.*, 2017).

The aim of this project was to use current RNA sequencing technology to identify clinically relevant androgen regulated transcriptional changes. By correlating RNA sequencing data from androgens stimulated LNCaP cells with RNA sequencing from advanced prostate cancer patients before and after ADT (Rajan *et al.*, 2014), we identified over 600 potentially clinically relevant AR target genes. These genes had reciprocal expression signatures; androgen regulated in culture with reverse expression switches in the patients in response to clinical ADT. This dataset provides a comprehensive map of AR-regulated genes in clinical prostate cancer and has recently been published (Munkley *et al.*, 2016b). It offers a new window through which to understand the signalling pathways downstream of the AR and the role that these pathways play in both the development of prostate cancer and the response to ADT.

A meta-analysis approach was used to analyse the expression of these identified genes across multiple prostate cancer gene expression datasets. Gene Ontology (GO) analysis of the dataset identified a number of key AR regulated biological processes,

including glycosylation as a previously unidentified system-wide androgen-regulated process. Aberrant glycosylation, primarily caused by the altered expression or mis-localisation of glycoenzymes is a common feature of cancer cells (Pinho and Reis, 2015; Stowell *et al.*, 2015). Alterations in the expression of these glycoenzymes can lead to aberrant modifications which can alter many important biological processes such as cell-cell adhesion, migration, interactions with the cell matrix, immune surveillance, signalling and cellular metabolism (Munkley and Elliott, 2016). The enrichment of genes encoding glycosylation enzymes within our dataset suggests that these identified genes may play a role in modifying some of these processes in prostate cancer and could therefore contribute to disease progression.

Meta-analysis highlighted a sub-set of 10 glycosylation enzymes with significant gene expression changes: *EDEM3, GCNT1, SERP1, STT3A, ST6GALNAC1, ST6GAL1, GNPNAT1, UBE2J1*, *TUSC3 and UAP1. GCNT1, ST6GALNAC1, TUSC3* and *UAP1* have previously been linked to PCa. Increased expression of *GCNT1*, which is involved in the formation of branched O-linked glycans, has been shown to positively correlate with the aggressive potential of PCa (Hagisawa *et al.*, 2005; Chen *et al.*, 2014). Increased expression of *ST6GalNAc1* by androgens in prostate cancer cells can reduce prostate cancer cell adhesion (Munkley *et al.*, 2015b; Munkley *et al.*, 2016b). Knockdown of the novel tumour suppressor gene *TUSC3* in PCa cell lines alters the ER stress response and accelerates cell proliferation and invasion (Horak *et al.*, 2014). *UAP1* is highly overexpressed in prostate cancer and can protect cancer cells from ER stress by protecting against inhibitors (Itkonen *et al.*, 2014). SERP1 and UBE2J1 expression has been identified as androgen regulated but this is the first time androgen regulation of *EDEM3, STT3A*, and *ST6GAL1* has been described.

These enzymes are essential for prostate cancer cell survival, control key steps in glycan synthesis, and synthesise several cancer-associated glycans (Munkley *et al.*, 2016b). The identification of glycosylation as an androgen regulated process in prostate cancer could have important clinical implications both in patient diagnosis and therapeutic strategies. Glycans have been shown to play a role in all aspects of cancer progression

and are therefore attractive targets for therapeutic intervention (Munkley and Elliott, 2016). Inhibiting glycosylation, even in conditions where the AR is active, can decrease prostate cancer cell viability and invasion potential (Itkonen and Mills, 2013; Itkonen *et al.*, 2016). An increased understanding of how these individual glyco-enzmyes, and glycosylation as a whole, influences prostate cancer cell behaviour is required. This could assist in the development of new glyco-based specific biomarkers for use in the early detection and management of prostate cancer. Drugs targeting glycans have already been developed as therapies for other cancer types (Fuster and Esko, 2005; Rabu *et al.*, 2012; Vankemmelbeke *et al.*, 2016; Shimomura *et al.*, 2018). Further investigation into the role of these glycosylation enzymes could enable existing therapies to be utilised to treat prostate cancer.

Amongst the enzymes investigated further was ST6Gal1, a sialytransferase that catalyses the transfer of sialic acid from CMP-sialic acid to N-terminus of galactose-containing substrates. Increased sialylation is already known to be associated with cancer cell progression and metastasis, affecting cell adhesion, migration and invasion (Seales et al., 2005; Bull et al., 2013; Pinho and Reis, 2015) and up-regulation of ST6Gal1 has been described in several cancers (Dall'Olio *et al.*, 1989; Skacel *et al.*, 1991; Wang *et al.*, 2001; Lin *et al.*, 2002; Dall'Olio *et al.*, 2004; Poon *et al.*, 2005).

To investigate the biological significance of increased ST6Gal1 expression on prostate cancer cell aggressiveness, molecular cloning techniques were used to establish prostate cancer cell lines with ST6Gal1 over-expression and knock-down properties. Increased ST6Gal1 expression increased cell to matrix adhesion and reduced migratory potential in DU145 cells. This correlates with the increased expression observed in a number of key adherens junction genes such as *CTNNB1* (beta-catenin), *FN1* (fibronectin) and *CDH1* (E-cadherin). High ST6Gal1 expression levels also increased the invasion potential in DU145 cells. Epithelial to mesenchymal transition (EMT) plays an important role in the invasiveness of cancer cells (Yeung and Yang, 2017). Increased expression of a number of genes known to be up-regulated during the EMT process,

including vimentin, snail and slug as well as a dramatic loss of the desmosome junctional complex component desmoplakin were observed in the ST6Gal1 over-expressing DU145 cells. RNA sequencing of these cells has identified ST6Gal1 regulated expression changes in a number of key cancer associated genes such as AKR1C1 (Zeng *et al.*, 2017), ABCA1 (Lee *et al.*, 2013), SLC18A2 (Haldrup *et al.*, 2016) and NOTCH3 (Carvalho *et al.*, 2014)

The reduction of ST6Gal1 expression significantly decreased cell proliferation, cell to matrix adhesion, migration and invasion capability in CW-22Rv1 cells. This correlates with what has previously been observed in other prostate cancer cell lines (Wei *et al.*, 2016). ST6Gal1 has previously been associated with the maintenance of the cell mesenchymal state in breast cancer cell lines (Lu *et al.*, 2014). In line with this we observed a significant decrease in *CDH2* (N-cadherin) expression, a mesenchymal cadherin associated with EMT (Whang et al 2015) as well as other EMT markers *FN1* (fibronectin), *SNAI1* (snail) and *SNAI2* (slug).

The role of ST6Gal1 in clinical prostate cancer is less clear. ST6Gal1 expression was shown to be increased in our RNA sequencing dataset and the subsequent meta-analysis. This was confirmed in our independent patient RNA cohort of 17 malignant tumour samples from transurethral resections of the prostate (TURP) and 32 non-malignant BPH tissue from our independent patient RNA cohort. A recent study also supports this, that found ST6Gal1 expression was significantly upregulated in prostate cancer tumour tissues compared with BPH, and that elevated ST6Gal1 expression was correlated with higher Gleason scores (Wei *et al.*, 2016). Contradictory to this, we found that ST6Gal1 expression was down-regulated when compared with normal prostate tissue. Our matched tumour and adjacent normal tissue samples RNA dataset showed that 6 out of the 9 patients had a clear significant down-regulation of ST6Gal1 in the tumour tissue compared to the adjacent normal tissue. In addition, analysis of our prostate cancer tissue microarray shows that ST6Gal1 protein expression was down-regulated in the prostate cancer patient tissue samples compared with the BPH tissue

samples. Targeting ST6Gal1 therapeutically has shown potential, however globally targeting sialylation could have detrimental side effects for the patient. A targeted or pro-drug approach would allow selective inhibition of sialylation in prostate cancer cells. The fluorinated sialic acid analogue P-3Fax-Neu5Ac selectively blocks sialylation in B16F10 cells (Bull et al., 2013) and has shown potential for anticancer therapy. P-3Fax-Neu5Ac treatment blocks tumour cell adhesion to extra cellular matrix and migration in vitro and tumour engraftment in vivo (Bull et al., 2013).

The findings of this project indicate that establishing the role of individual glyco-enzymes in prostate cancer is difficult. The role of ST6Gal1 in prostate cancer is complex and more than likely dependable on the other compensatory mechanisms available within the tumour, together with the collective expression of other glyco-enzymes. General two-dimensional (2D) monolayer cell cultures fail to represent the complex behaviour of native tissue and lack the heterogeneity that exists within tumours. They are grown in a particular media supplemented with nutrients to support their growth, an environment not representative of how cells exist within an organism. The lack of cell-cell and tissue-matrix interactions can alter gene and protein expression levels. Cells grown on flat, ridged plastic surfaces are often stressed, which can trigger abnormally high cell proliferation rates, impacting on results (Breslin and O'Driscoll, 2013).

Over the past decade, there has been a surge in the development of platforms that enable the growth of three-dimensional (3D) spheroid cultures. These cultures can provide a more realistic environment, better replicating the natural morphology and physiology found *in vivo* (Edmondson *et al.*, 2014). Recent platforms include hydrogels (Drury and Mooney, 2003), porous scaffolds (Fischbach *et al.*, 2007), hanging drops (Aijian and Garrell, 2015) and microwell-mesh (Mosaad *et al.*, 2018). Further functional experiments using 3D spheroid cultures could be useful to fully understand the role each of these individual enzymes plays in prostate cancer. Together with the androgen regulated transcriptional changes, the RNA sequencing data also identified 73 androgen regulated alternative mRNA isoforms. These included 56 alternative promoters, 4

alternative 3′ ends and 13 alternative spicing events. 64 of these events are novel to this project and 26 involve previously unannotated isoforms. This significantly increases the number of known AR regulated mRNA isoforms and implies a much greater level of complexity whereby androgens are able to simultaneously regulate transcriptional and alternative mRNA isoform expression changes in prostate cancer. Never the less, further investigation is necessary to establish which isoforms encode proteins that may be clinically relevant. It will also be important to define the role of specific AR co-regulators in AR mediated isoform selection.

Androgen regulated promoter switches for the peptide hormones RLN1 and RLN2 were identified. Alternative promoter use can generate mRNA isoforms with distinct functional activities from the same gene, which can sometimes having opposing functions (Munkley *et al.*, 2017a). Androgens were found to repress the expression of a non-coding RLN1 isoform, increasing the expression of the protein coding isoform. For RLN2, there was an increase in expression from the up-stream promoter in the presence of androgens. In both cases, androgen stimulation resulted in an overall decrease in the non-coding isoform. However, the recent discovery of a novel RLN1-RLN2 fusion transcript has made it difficult to accurately characterise their independent expression.

In conclusion, this project has identified a new panel of androgen regulated genes and novel mRNA isoforms. Analysis of this panel has demonstrated important androgen control over glycosylation modifications that has important implications for prostate cancer biology, and also suggests further targets for future analysis.

Bibliography

Ablin, R.J., Soanes, W.A., Bronson, P. and Witebsky, E. (1970) 'Precipitating antigens of the normal human prostate', *J Reprod Fertil*, 22(3), pp. 573-4.

Aijian, A.P. and Garrell, R.L. (2015) 'Digital microfluidics for automated hanging drop cell spheroid culture', *J Lab Autom*, 20(3), pp. 283-95.

Alinezhad, S., Vaananen, R.M., Mattsson, J., Li, Y., Tallgren, T., Tong Ochoa, N., Bjartell, A., Akerfelt, M., Taimen, P., Bostrom, P.J., Pettersson, K. and Nees, M. (2016) 'Validation of Novel Biomarkers for Prostate Cancer Progression by the Combination of Bioinformatics, Clinical and Functional Studies', *PLoS One*, 11(5), p. e0155901.

Amado, M., Carneiro, F., Seixas, M., Clausen, H. and Sobrinho-Simoes, M. (1998) 'Dimeric sialyl-Le(x) expression in gastric carcinoma correlates with venous invasion and poor outcome', *Gastroenterology*, 114(3), pp. 462-70.

Amano, M., Galvan, M., He, J. and Baum, L.G. (2003) 'The ST6Gal I sialyltransferase selectively modifies N-glycans on CD45 to negatively regulate galectin-1-induced CD45 clustering, phosphatase modulation, and T cell death', *J Biol Chem*, 278(9), pp. 7469-75.

Antonarakis, E.S. (2015) 'Predicting treatment response in castration-resistant prostate cancer: could androgen receptor variant-7 hold the key?', *Expert Rev Anticancer Ther*, 15(2), pp. 143-5.

Antonarakis, E.S., Lu, C., Luber, B., Wang, H., Chen, Y., Nakazawa, M., Nadal, R., Paller, C.J., Denmeade, S.R., Carducci, M.A., Eisenberger, M.A. and Luo, J. (2015) 'Androgen Receptor Splice Variant 7 and Efficacy of Taxane Chemotherapy in Patients With Metastatic Castration-Resistant Prostate Cancer', *JAMA Oncol*, 1(5), pp. 582-91.

Antonarakis, E.S., Lu, C., Wang, H., Luber, B., Nakazawa, M., Roeser, J.C., Chen, Y., Mohammad, T.A., Fedor, H.L., Lotan, T.L., Zheng, Q., De Marzo, A.M., Isaacs, J.T., Isaacs, W.B., Nadal, R., Paller, C.J., Denmeade, S.R., Carducci, M.A., Eisenberger, M.A. and Luo, J. (2014) 'AR-V7 and resistance to enzalutamide and abiraterone in prostate cancer', *N Engl J Med*, 371(11), pp. 1028-38.

Antony, P., Rose, M., Heidenreich, A., Knuchel, R., Gaisa, N.T. and Dahl, E. (2014) 'Epigenetic inactivation of ST6GAL1 in human bladder cancer', *BMC Cancer*, 14, p. 901.

Arroyo, J.I., Hoffmann, F.G. and Opazo, J.C. (2014) 'Evolution of the relaxin/insulin-like gene family in anthropoid primates', *Genome Biol Evol*, 6(3), pp. 491-9.

Baldus, S.E., Zirbes, T.K., Monig, S.P., Engel, S., Monaca, E., Rafiqpoor, K., Hanisch, F.G., Hanski, C., Thiele, J., Pichlmaier, H. and Dienes, H.P. (1998) 'Histopathological subtypes and prognosis of gastric cancer are correlated with the expression of mucin-associated sialylated antigens: Sialosyl-Lewis(a), Sialosyl-Lewis(x) and sialosyl-Tn', *Tumour Biol*, 19(6), pp. 445-53.

Barfeld, S.J., East, P., Zuber, V. and Mills, I.G. (2014) 'Meta-analysis of prostate cancer gene expression data identifies a novel discriminatory signature enriched for glycosylating enzymes', *BMC Med Genomics*, 7, p. 513.

Bathgate, R.A., Halls, M.L., van der Westhuizen, E.T., Callander, G.E., Kocan, M. and Summers, R.J. (2013) 'Relaxin family peptides and their receptors', *Physiol Rev*, 93(1), pp. 405-80.

Bathgate, R.A., Samuel, C.S., Burazin, T.C., Layfield, S., Claasz, A.A., Reytomas, I.G., Dawson, N.F., Zhao, C., Bond, C., Summers, R.J., Parry, L.J., Wade, J.D. and Tregear, G.W. (2002) 'Human relaxin gene 3 (H3) and the equivalent mouse relaxin (M3) gene. Novel members of the relaxin peptide family', *J Biol Chem*, 277(2), pp. 1148-57.

Beissbarth, T. and Speed, T.P. (2004) 'GOstat: find statistically overrepresented Gene Ontologies within a group of genes', *Bioinformatics*, 20(9), pp. 1464-5.

Beltran, H., Prandi, D., Mosquera, J.M., Benelli, M., Puca, L., Cyrta, J., Marotz, C., Giannopoulou, E., Chakravarthi, B.V., Varambally, S., Tomlins, S.A., Nanus, D.M., Tagawa, S.T., Van Allen, E.M., Elemento, O., Sboner, A., Garraway, L.A., Rubin, M.A. and Demichelis, F. (2016) 'Divergent clonal evolution of castration-resistant neuroendocrine prostate cancer', *Nat Med*, 22(3), pp. 298-305.

Beltran, H., Rickman, D.S., Park, K., Chae, S.S., Sboner, A., MacDonald, T.Y., Wang, Y., Sheikh, K.L., Terry, S., Tagawa, S.T., Dhir, R., Nelson, J.B., de la Taille, A., Allory, Y., Gerstein, M.B., Perner, S., Pienta, K.J., Chinnaiyan, A.M., Collins, C.C., Gleave, M.E., Demichelis, F., Nanus, D.M. and Rubin, M.A. (2011) 'Molecular characterization of neuroendocrine prostate cancer and identification of new drug targets', *Cancer Discov*, 1(6), pp. 487-95.

Beltran, H., Tomlins, S., Aparicio, A., Arora, V., Rickman, D., Ayala, G., Huang, J., True, L., Gleave, M.E., Soule, H., Logothetis, C. and Rubin, M.A. (2014) 'Aggressive variants of castration-resistant prostate cancer', *Clin Cancer Res*, 20(11), pp. 2846-50.

Berry, S.J., Coffey, D.S., Walsh, P.C. and Ewing, L.L. (1984) 'The development of human benign prostatic hyperplasia with age', *J Urol*, 132(3), pp. 474-9.

Bhanushali, P.B., Badgujar, S.B., Tripathi, M.M., Gupta, S., Murthy, V., Krishnasastry, M.V. and Puri, C.P. (2016) 'Development of glycan specific lectin based immunoassay for detection of prostate specific antigen', *Int J Biol Macromol*, 86, pp. 468-80.

Bialek, J., Kunanuvat, U., Hombach-Klonisch, S., Spens, A., Stetefeld, J., Sunley, K., Lippert, D., Wilkins, J.A., Hoang-Vu, C. and Klonisch, T. (2011) 'Relaxin enhances the collagenolytic activity and in vitro invasiveness by upregulating matrix metalloproteinases in human thyroid carcinoma cells', *Mol Cancer Res*, 9(6), pp. 673-87.

Binder, C., Simon, A., Binder, L., Hagemann, T., Schulz, M., Emons, G., Trumper, L. and Einspanier, A. (2004) 'Elevated concentrations of serum relaxin are associated with metastatic disease in breast cancer patients', *Breast Cancer Res Treat*, 87(2), pp. 157-66.

Boccalini, G., Sassoli, C., Formigli, L., Bani, D. and Nistri, S. (2015) 'Relaxin protects cardiac muscle cells from hypoxia/reoxygenation injury: involvement of the Notch-1 pathway', *FASEB J*, 29(1), pp. 239-49.

Bonilla, C., Lewis, S.J., Martin, R.M., Donovan, J.L., Hamdy, F.C., Neal, D.E., Eeles, R., Easton, D., Kote-Jarai, Z., Al Olama, A.A., Benlloch, S., Muir, K., Giles, G.G., Wiklund, F., Gronberg, H., Haiman, C.A., Schleutker, J., Nordestgaard, B.G., Travis, R.C., Pashayan, N., Khaw, K.T., Stanford, J.L., Blot, W.J., Thibodeau, S., Maier, C., Kibel, A.S., Cybulski, C., Cannon-Albright, L., Brenner, H., Park, J., Kaneva, R., Batra, J., Teixeira, M.R., Pandha, H., Lathrop, M. and Davey Smith, G. (2016) 'Pubertal development and prostate cancer risk: Mendelian randomization study in a population-based cohort', *BMC Med*, 14, p. 66.

Bonkhoff, H., Stein, U. and Remberger, K. (1995) 'Endocrine-paracrine cell types in the prostate and prostatic adenocarcinoma are postmitotic cells', *Hum Pathol*, 26(2), pp. 167-70.

Bottcher, R., Dulla, K., van Strijp, D., Dits, N., Verhoef, E.I., Baillie, G.S., van Leenders, G.J., Houslay, M.D., Jenster, G. and Hoffmann, R. (2016) 'Human PDE4D isoform composition is deregulated in primary prostate cancer and indicative for disease progression and development of distant metastases', *Oncotarget*, 7(43), pp. 70669-70684.

Bottcher, R., Henderson, D.J., Dulla, K., van Strijp, D., Waanders, L.F., Tevz, G., Lehman, M.L., Merkle, D., van Leenders, G.J., Baillie, G.S., Jenster, G., Houslay, M.D. and Hoffmann, R. (2015) 'Human phosphodiesterase 4D7 (PDE4D7) expression is increased in TMPRSS2-ERG-positive primary prostate cancer and independently adds to a reduced risk of post-surgical disease progression', *Br J Cancer*, 113(10), pp. 1502-11.

Boyle, W.J., Simonet, W.S. and Lacey, D.L. (2003) 'Osteoclast differentiation and activation', *Nature*, 423(6937), pp. 337-42.

Breslin, S. and O'Driscoll, L. (2013) 'Three-dimensional cell culture: the missing link in drug discovery', *Drug Discov Today*, 18(5-6), pp. 240-9.

Briganti, A., Capitanio, U., Suardi, N., Gallina, A., Salonia, A., Bianchi, M., Tutolo, M., Di Girolamo, V., Guazzoni, G., Rigatti, P. and Montorsi, F. (2009) 'Benign Prostatic Hyperplasia and Its Aetiologies', *European Urology Supplements*, 8(13), pp. 865-871.

Brockhausen, I. (2006) 'Mucin-type O-glycans in human colon and breast cancer: glycodynamics and functions', *EMBO Rep*, 7(6), pp. 599-604.

Bull, C., Boltje, T.J., Wassink, M., de Graaf, A.M., van Delft, F.L., den Brok, M.H. and Adema, G.J. (2013) 'Targeting aberrant sialylation in cancer cells using a fluorinated sialic acid analog impairs adhesion, migration, and in vivo tumor growth', *Mol Cancer Ther*, 12(10), pp. 1935-46.

Bullock, N., Potts, J., Simpkin, A.J., Koupparis, A., Harper, S.J., Oxley, J. and Oltean, S. (2016) 'Serine-arginine protein kinase 1 (SRPK1), a determinant of angiogenesis, is upregulated in prostate cancer and correlates with disease stage and invasion', *J Clin Pathol*, 69(2), pp. 171-5.

Busa, R., Paronetto, M.P., Farini, D., Pierantozzi, E., Botti, F., Angelini, D.F., Attisani, F., Vespasiani, G. and Sette, C. (2007) 'The RNA-binding protein Sam68 contributes to proliferation and survival of human prostate cancer cells', *Oncogene*, 26(30), pp. 4372-82.

Cancer Research UK (2013) *Prostate cancer statistics*. Available at: http://www.cancerresearchuk.org/health-professional/cancer-statistics/statistics-by-cancer-type/prostate-cancer.

Cano, L.Q., Lavery, D.N. and Bevan, C.L. (2013) 'Mini-review: Foldosome regulation of androgen receptor action in prostate cancer', *Mol Cell Endocrinol*, 369(1-2), pp. 52-62.

Cao, W.H., Liu, H.M., Liu, X., Li, J.G., Liang, J., Liu, M. and Niu, Z.H. (2013) 'Relaxin enhances in-vitro invasiveness of breast cancer cell lines by upregulation of S100A4/MMPs signaling', *Eur Rev Med Pharmacol Sci*, 17(5), pp. 609-17.

Carvalho-Cruz, P., Alisson-Silva, F., Todeschini, A.R. and Dias, W.B. (2017) 'Cellular glycosylation senses metabolic changes and modulates cell plasticity during epithelial to mesenchymal transition', *Dev Dyn*.

Carvalho, F.L., Simons, B.W., Eberhart, C.G. and Berman, D.M. (2014) 'Notch signaling in prostate cancer: a moving target', *Prostate*, 74(9), pp. 933-45.

Carver, B.S., Chapinski, C., Wongvipat, J., Hieronymus, H., Chen, Y., Chandarlapaty, S., Arora, V.K., Le, C., Koutcher, J., Scher, H., Scardino, P.T., Rosen, N. and Sawyers, C.L. (2011) 'Reciprocal feedback regulation of PI3K and androgen receptor signaling in PTEN-deficient prostate cancer', *Cancer Cell*, 19(5), pp. 575-86.

Cerami, E., Gao, J., Dogrusoz, U., Gross, B.E., Sumer, S.O., Aksoy, B.A., Jacobsen, A., Byrne, C.J., Heuer, M.L., Larsson, E., Antipin, Y., Reva, B., Goldberg, A.P., Sander, C. and Schultz, N. (2012) 'The cBio cancer genomics portal: an open platform for exploring multidimensional cancer genomics data', *Cancer Discov*, 2(5), pp. 401-4.

Chakravarty, D., Sboner, A., Nair, S.S., Giannopoulou, E., Li, R., Hennig, S., Mosquera, J.M., Pauwels, J., Park, K., Kossai, M., MacDonald, T.Y., Fontugne, J., Erho, N., Vergara, I.A., Ghadessi, M., Davicioni, E., Jenkins, R.B., Palanisamy, N., Chen, Z., Nakagawa, S., Hirose, T., Bander, N.H., Beltran, H., Fox, A.H., Elemento, O. and Rubin, M.A. (2014) 'The oestrogen receptor alpha-regulated lncRNA NEAT1 is a critical modulator of prostate cancer', *Nat Commun*, 5, p. 5383.

Chang, R.T., Kirby, R. and Challacombe, B.J. (2012) 'Is there a link between BPH and prostate cancer?', *Practitioner*, 256(1750), pp. 13-6, 2.

Chen, C. and Colley, K.J. (2000) 'Minimal structural and glycosylation requirements for ST6Gal I activity and trafficking', *Glycobiology*, 10(5), pp. 531-83.

Chen, T., Wang, L.H. and Farrar, W.L. (2000) 'Interleukin 6 activates androgen receptor-mediated gene expression through a signal transducer and activator of transcription 3-dependent pathway in LNCaP prostate cancer cells', *Cancer Res*, 60(8), pp. 2132-5.

Chen, X., Wang, L., Zhao, Y., Yuan, S., Wu, Q., Zhu, X., Niang, B., Wang, S. and Zhang, J. (2016) 'ST6Gal-I modulates docetaxel sensitivity in human hepatocarcinoma cells via the p38 MAPK/caspase pathway', *Oncotarget*, 7(32), pp. 51955-51964.

Chen, Z., Gulzar, Z.G., St Hill, C.A., Walcheck, B. and Brooks, J.D. (2014) 'Increased expression of GCNT1 is associated with altered O-glycosylation of PSA, PAP, and MUC1 in human prostate cancers', *Prostate*, 74(10), pp. 1059-67.

Chow, L.T., Gelinas, R.E., Broker, T.R. and Roberts, R.J. (1977) 'An amazing sequence arrangement at the 5' ends of adenovirus 2 messenger RNA', *Cell*, 12(1), pp. 1-8.

Christiansen, M.N., Chik, J., Lee, L., Anugraham, M., Abrahams, J.L. and Packer, N.H. (2014) 'Cell surface protein glycosylation in cancer', *Proteomics*, 14(4-5), pp. 525-46.

Chung, S., Tamura, K., Furihata, M., Uemura, M., Daigo, Y., Nasu, Y., Miki, T., Shuin, T., Fujioka, T., Nakamura, Y. and Nakagawa, H. (2009) 'Overexpression of the potential kinase serine/ threonine/tyrosine kinase 1 (STYK 1) in castration-resistant prostate cancer', *Cancer Sci*, 100(11), pp. 2109-14.

Clamp, M., Fry, B., Kamal, M., Xie, X., Cuff, J., Lin, M.F., Kellis, M., Lindblad-Toh, K. and Lander, E.S. (2007) 'Distinguishing protein-coding and noncoding genes in the human genome', *Proc Natl Acad Sci U S A*, 104(49), pp. 19428-33.

Clark, E.L., Coulson, A., Dalgliesh, C., Rajan, P., Nicol, S.M., Fleming, S., Heer, R., Gaughan, L., Leung, H.Y., Elliott, D.J., Fuller-Pace, F.V. and Robson, C.N. (2008) 'The RNA helicase p68 is a novel androgen receptor coactivator involved in splicing and is overexpressed in prostate cancer', *Cancer Res*, 68(19), pp. 7938-46.

Clarke, N.W., McClure, J. and George, N.J. (1993) 'Osteoblast function and osteomalacia in metastatic prostate cancer', *Eur Urol*, 24(2), pp. 286-90.

Cleutjens, K.B., van Eekelen, C.C., van der Korput, H.A., Brinkmann, A.O. and Trapman, J. (1996) 'Two androgen response regions cooperate in steroid hormone regulated activity of the prostate-specific antigen promoter', *J Biol Chem*, 271(11), pp. 6379-88.

Collins, A.T., Berry, P.A., Hyde, C., Stower, M.J. and Maitland, N.J. (2005) 'Prospective identification of tumorigenic prostate cancer stem cells', *Cancer Res*, 65(23), pp. 10946-51.

Conn, P.M. and Crowley, W.F., Jr. (1994) 'Gonadotropin-releasing hormone and its analogs', *Annu Rev Med*, 45, pp. 391-405.

Cramer, P., Caceres, J.F., Cazalla, D., Kadener, S., Muro, A.F., Baralle, F.E. and Kornblihtt, A.R. (1999) 'Coupling of transcription with alternative splicing: RNA pol II promoters modulate SF2/ASF and 9G8 effects on an exonic splicing enhancer', *Mol Cell*, 4(2), pp. 251-8.

Cramer, P., Pesce, C.G., Baralle, F.E. and Kornblihtt, A.R. (1997) 'Functional association between promoter structure and transcript alternative splicing', *Proc Natl Acad Sci U S A*, 94(21), pp. 11456-60.

Cramer, P., Srebrow, A., Kadener, S., Werbajh, S., de la Mata, M., Melen, G., Nogues, G. and Kornblihtt, A.R. (2001) 'Coordination between transcription and pre-mRNA processing', *FEBS Lett*, 498(2-3), pp. 179-82.

Crawford, R.J., Hudson, P., Shine, J., Niall, H.D., Eddy, R.L. and Shows, T.B. (1984) 'Two human relaxin genes are on chromosome 9', *EMBO J*, 3(10), pp. 2341-5.

Crona, D.J. and Whang, Y.E. (2017) 'Androgen Receptor-Dependent and -Independent Mechanisms Involved in Prostate Cancer Therapy Resistance', *Cancers (Basel)*, 9(6).

Culig, Z., Bartsch, G. and Hobisch, A. (2002) 'Interleukin-6 regulates androgen receptor activity and prostate cancer cell growth', *Mol Cell Endocrinol*, 197(1-2), pp. 231-8.

Cultrex BME Cell Invasion Assay, 96 well (R&D Systems). Available at: https://www.rndsystems.com/products/cultrex-bme-cell-invasion-assay-96-well_3455-096-k (Accessed: 11th April 2018).

Dall'Olio, F. (2000) 'The sialyl-alpha2,6-lactosaminyl-structure: biosynthesis and functional role', *Glycoconj J*, 17(10), pp. 669-76.

Dall'Olio, F. and Chiricolo, M. (2001) 'Sialyltransferases in cancer', *Glycoconj J*, 18(11-12), pp. 841-50.

Dall'Olio, F., Chiricolo, M., Ceccarelli, C., Minni, F., Marrano, D. and Santini, D. (2000) 'Beta-galactoside alpha2,6 sialyltransferase in human colon cancer: contribution of multiple transcripts to regulation of enzyme activity and reactivity with Sambucus nigra agglutinin', *Int J Cancer*, 88(1), pp. 58-65.

Dall'Olio, F., Chiricolo, M., D'Errico, A., Gruppioni, E., Altimari, A., Fiorentino, M. and Grigioni, W.F. (2004) 'Expression of beta-galactoside alpha2,6 sialyltransferase and of alpha2,6-sialylated glycoconjugates in normal human liver, hepatocarcinoma, and cirrhosis', *Glycobiology*, 14(1), pp. 39-49.

Dall'Olio, F., Malagolini, N., di Stefano, G., Minni, F., Marrano, D. and Serafini-Cessi, F. (1989) 'Increased CMP-NeuAc:Gal beta 1,4GlcNAc-R alpha 2,6 sialyltransferase activity in human colorectal cancer tissues', *Int J Cancer*, 44(3), pp. 434-9.

de Bono, J.S., Logothetis, C.J., Molina, A., Fizazi, K., North, S., Chu, L., Chi, K.N., Jones, R.J., Goodman, O.B., Jr., Saad, F., Staffurth, J.N., Mainwaring, P., Harland, S., Flaig, T.W., Hutson, T.E., Cheng, T., Patterson, H., Hainsworth, J.D., Ryan, C.J., Sternberg,

C.N., Ellard, S.L., Flechon, A., Saleh, M., Scholz, M., Efstathiou, E., Zivi, A., Bianchini, D., Loriot, Y., Chieffo, N., Kheoh, T., Haqq, C.M. and Scher, H.I. (2011) 'Abiraterone and increased survival in metastatic prostate cancer', *N Engl J Med*, 364(21), pp. 1995-2005.

De Mol, E., Fenwick, R.B., Phang, C.T., Buzon, V., Szulc, E., de la Fuente, A., Escobedo, A., Garcia, J., Bertoncini, C.W., Estebanez-Perpina, E., McEwan, I.J., Riera, A. and Salvatella, X. (2016) 'EPI-001, A Compound Active against Castration-Resistant Prostate Cancer, Targets Transactivation Unit 5 of the Androgen Receptor', *ACS Chem Biol*, 11(9), pp. 2499-505.

Diao, Y., Wu, D., Dai, Z., Kang, H., Wang, Z. and Wang, X. (2015) 'Prognostic value of transformer 2beta expression in prostate cancer', *Int J Clin Exp Pathol*, 8(6), pp. 6967-73.

Dowhan, D.H., Hong, E.P., Auboeuf, D., Dennis, A.P., Wilson, M.M., Berget, S.M. and O'Malley, B.W. (2005) 'Steroid hormone receptor coactivation and alternative RNA splicing by U2AF65-related proteins CAPERalpha and CAPERbeta', *Mol Cell*, 17(3), pp. 429-39.

Drabik, A., Bodzon-Kulakowska, A., Suder, P., Silberring, J., Kulig, J. and Sierzega, M. (2017) 'Glycosylation changes in serum proteins identify patients with pancreatic cancer', *J Proteome Res*.

Drury, J.L. and Mooney, D.J. (2003) 'Hydrogels for tissue engineering: scaffold design variables and applications', *Biomaterials*, 24(24), pp. 4337-51.

Dutertre, M., Gratadou, L., Dardenne, E., Germann, S., Samaan, S., Lidereau, R., Driouch, K., de la Grange, P. and Auboeuf, D. (2010) 'Estrogen regulation and physiopathologic significance of alternative promoters in breast cancer', *Cancer Res*, 70(9), pp. 3760-70.

Dwek, M.V., Jenks, A. and Leathem, A.J. (2010) 'A sensitive assay to measure biomarker glycosylation demonstrates increased fucosylation of prostate specific antigen (PSA) in patients with prostate cancer compared with benign prostatic hyperplasia', *Clin Chim Acta*, 411(23-24), pp. 1935-9.

Edmondson, R., Broglie, J.J., Adcock, A.F. and Yang, L. (2014) 'Three-dimensional cell culture systems and their applications in drug discovery and cell-based biosensors', *Assay Drug Dev Technol*, 12(4), pp. 207-18.

Edwards, A., Hammond, H.A., Jin, L., Caskey, C.T. and Chakraborty, R. (1992) 'Genetic variation at five trimeric and tetrameric tandem repeat loci in four human population groups', *Genomics*, 12(2), pp. 241-53.

Edwards, J., Krishna, N.S., Witton, C.J. and Bartlett, J.M. (2003) 'Gene amplifications associated with the development of hormone-resistant prostate cancer', *Clin Cancer Res*, 9(14), pp. 5271-81.

Erho, N., Buerki, C., Triche, T.J., Davicioni, E. and Vergara, I.A. (2012) 'Transcriptome-wide detection of differentially expressed coding and non-coding transcripts and their clinical significance in prostate cancer', *J Oncol*, 2012, p. 541353.

Erzurumlu, Y. and Ballar, P. (2017) 'Androgen Mediated Regulation of Endoplasmic Reticulum-Associated Degradation and its Effects on Prostate Cancer', *Sci Rep*, 7, p. 40719.

Fabris, L., Ceder, Y., Chinnaiyan, A.M., Jenster, G.W., Sorensen, K.D., Tomlins, S., Visakorpi, T. and Calin, G.A. (2016) 'The Potential of MicroRNAs as Prostate Cancer Biomarkers', *Eur Urol*, 70(2), pp. 312-22.

Feng, S., Agoulnik, I.U., Bogatcheva, N.V., Kamat, A.A., Kwabi-Addo, B., Li, R., Ayala, G., Ittmann, M.M. and Agoulnik, A.I. (2007) 'Relaxin promotes prostate cancer progression', *Clin Cancer Res*, 13(6), pp. 1695-702.

Feng, S., Agoulnik, I.U., Li, Z., Han, H.D., Lopez-Berestein, G., Sood, A., Ittmann, M.M. and Agoulnik, A.I. (2009) 'Relaxin/RXFP1 signaling in prostate cancer progression', *Ann N Y Acad Sci*, 1160, pp. 379-80.

Fenner, A. (2011) 'Prostate cancer: next-generation RNA sequencing identifies gene signature of neuroendocrine differentiation in prostate tumors', *Nat Rev Urol*, 9(1), p. 8.

Fenteany, F.H. and Colley, K.J. (2005) 'Multiple signals are required for alpha2,6-sialyltransferase (ST6Gal I) oligomerization and Golgi localization', *J Biol Chem*, 280(7), pp. 5423-9.

Ferlay, J., Soerjomataram, I., Dikshit, R., Eser, S., Mathers, C., Rebelo, M., Parkin, D.M., Forman, D. and Bray, F. (2015) 'Cancer incidence and mortality worldwide: sources, methods and major patterns in GLOBOCAN 2012', *Int J Cancer*, 136(5), pp. E359-86.

Ferlin, A., Menegazzo, M., Gianesello, L., Selice, R. and Foresta, C. (2012) 'Effect of relaxin on human sperm functions', *J Androl*, 33(3), pp. 474-82.

Figueiredo, K.A., Palmer, J.B., Mui, A.L., Nelson, C.C. and Cox, M.E. (2005) 'Demonstration of upregulated H2 relaxin mRNA expression during neuroendocrine differentiation of LNCaP prostate cancer cells and production of biologically active mammalian recombinant 6 histidine-tagged H2 relaxin', *Ann N Y Acad Sci*, 1041, pp. 320-7.

Fischbach, C., Chen, R., Matsumoto, T., Schmelzle, T., Brugge, J.S., Polverini, P.J. and Mooney, D.J. (2007) 'Engineering tumors with 3D scaffolds', *Nat Methods*, 4(10), pp. 855-60.

Fujita, K., Hayashi, T., Matsuzaki, K., Nakata, W., Masuda, M., Kawashima, A., Ujike, T., Nagahara, A., Tsuchiya, M., Kobayashi, Y., Nojima, S., Uemura, M., Morii, E., Miyoshi, E. and Nonomura, N. (2016) 'Decreased fucosylated PSA as a urinary marker for high Gleason score prostate cancer', *Oncotarget*, 7(35), pp. 56643-56649.

Fukushima, K., Hara-Kuge, S., Seko, A., Ikehara, Y. and Yamashita, K. (1998) 'Elevation of alpha2-->6 sialyltransferase and alpha1-->2 fucosyltransferase activities in human choriocarcinoma', *Cancer Res*, 58(19), pp. 4301-6.

Fuster, M.M. and Esko, J.D. (2005) 'The sweet and sour of cancer: glycans as novel therapeutic targets', *Nat Rev Cancer*, 5(7), pp. 526-42.

Fuzio, P., Ditonno, P., Rutigliano, M., Battaglia, M., Bettocchi, C., Loverre, A., Grandaliano, G. and Perlino, E. (2012) 'Regulation of TGF-beta1 expression by androgen deprivation therapy of prostate cancer', *Cancer Lett*, 318(2), pp. 135-44.

Gaddipati, J.P., McLeod, D.G., Heidenberg, H.B., Sesterhenn, I.A., Finger, M.J., Moul, J.W. and Srivastava, S. (1994) 'Frequent detection of codon 877 mutation in the androgen receptor gene in advanced prostate cancers', *Cancer Res*, 54(11), pp. 2861-4.

Gao, D., Vela, I., Sboner, A., Iaquinta, P.J., Karthaus, W.R., Gopalan, A., Dowling, C., Wanjala, J.N., Undvall, E.A., Arora, V.K., Wongvipat, J., Kossai, M., Ramazanoglu, S., Barboza, L.P., Di, W., Cao, Z., Zhang, Q.F., Sirota, I., Ran, L., MacDonald, T.Y., Beltran, H., Mosquera, J.M., Touijer, K.A., Scardino, P.T., Laudone, V.P., Curtis, K.R., Rathkopf, D.E., Morris, M.J., Danila, D.C., Slovin, S.F., Solomon, S.B., Eastham, J.A., Chi, P., Carver, B., Rubin, M.A., Scher, H.I., Clevers, H., Sawyers, C.L. and Chen, Y. (2014) 'Organoid cultures derived from patients with advanced prostate cancer', *Cell*, 159(1), pp. 176-187.

Garibay-Tupas, J.L., Bao, S., Kim, M.T., Tashima, L.S. and Bryant-Greenwood, G.D. (2000) 'Isolation and analysis of the 3'-untranslated regions of the human relaxin H1 and H2 genes', *J Mol Endocrinol*, 24(2), pp. 241-52.

Gelmann, E.P. (2002) 'Molecular biology of the androgen receptor', *J Clin Oncol*, 20(13), pp. 3001-15.

George, D.J. (2013) 'Recent advances in the management of castration-resistant prostate cancer', *Clin Adv Hematol Oncol*, 11(3), pp. 181-3.

Gilgunn, S., Conroy, P.J., Saldova, R., Rudd, P.M. and O'Kennedy, R.J. (2013) 'Aberrant PSA glycosylation--a sweet predictor of prostate cancer', *Nat Rev Urol*, 10(2), pp. 99-107.

Gleason, D.F. and Mellinger, G.T. (1974) 'Prediction of prognosis for prostatic adenocarcinoma by combined histological grading and clinical staging', *J Urol*, 111(1), pp. 58-64.

Goldstein, A., Valda Toro, P., Lee, J., Silberstein, J.L., Nakazawa, M., Waters, I., Cravero, K., Chu, D., Cochran, R.L., Kim, M., Shinn, D., Torquato, S., Hughes, R.M., Pallavajjala, A., Carducci, M.A., Paller, C.J., Denmeade, S.R., Kressel, B., Trock, B.J., Eisenberger, M.A., Antonarakis, E.S., Park, B.H. and Hurley, P.J. (2017) 'Detection fidelity of AR mutations in plasma derived cell-free DNA', *Oncotarget*.

Gottlieb, B., Beitel, L.K., Nadarajah, A., Paliouras, M. and Trifiro, M. (2012) 'The androgen receptor gene mutations database: 2012 update', *Hum Mutat*, 33(5), pp. 887-94.

Graham, F.L., Smiley, J., Russell, W.C. and Nairn, R. (1977) 'Characteristics of a human cell line transformed by DNA from human adenovirus type 5', *J Gen Virol*, 36(1), pp. 59-74.

Grasso, C.S., Wu, Y.M., Robinson, D.R., Cao, X., Dhanasekaran, S.M., Khan, A.P., Quist, M.J., Jing, X., Lonigro, R.J., Brenner, J.C., Asangani, I.A., Ateeq, B., Chun, S.Y., Siddiqui, J., Sam, L., Anstett, M., Mehra, R., Prensner, J.R., Palanisamy, N., Ryslik, G.A., Vandin, F., Raphael, B.J., Kunju, L.P., Rhodes, D.R., Pienta, K.J., Chinnaiyan, A.M. and Tomlins, S.A. (2012) 'The mutational landscape of lethal castration-resistant prostate cancer', *Nature*, 487(7406), pp. 239-43.

Gunnersen, J.M., Fu, P., Roche, P.J. and Tregear, G.W. (1996) 'Expression of human relaxin genes: characterization of a novel alternatively-spliced human relaxin mRNA species', *Mol Cell Endocrinol*, 118(1-2), pp. 85-94.

Guo, C., Yeh, S., Niu, Y., Li, G., Zheng, J., Li, L. and Chang, C. (2017) 'Targeting androgen receptor versus targeting androgens to suppress castration resistant prostate cancer', *Cancer Lett*.

Guzvic, M., Braun, B., Ganzer, R., Burger, M., Nerlich, M., Winkler, S., Werner-Klein, M., Czyz, Z.T., Polzer, B. and Klein, C.A. (2014) 'Combined genome and transcriptome analysis of single disseminated cancer cells from bone marrow of prostate cancer patients reveals unexpected transcriptomes', *Cancer Res*, 74(24), pp. 7383-94.

Haab, B.B., Porter, A., Yue, T., Li, L., Scheiman, J., Anderson, M.A., Barnes, D., Schmidt, C.M., Feng, Z. and Simeone, D.M. (2010) 'Glycosylation variants of mucins and CEACAMs as candidate biomarkers for the diagnosis of pancreatic cystic neoplasms', *Ann Surg*, 251(5), pp. 937-45.

Hagberg Thulin, M., Nilsson, M.E., Thulin, P., Ceraline, J., Ohlsson, C., Damber, J.E. and Welen, K. (2016) 'Osteoblasts promote castration-resistant prostate cancer by altering intratumoral steroidogenesis', *Mol Cell Endocrinol*, 422, pp. 182-91.

Hagisawa, S., Ohyama, C., Takahashi, T., Endoh, M., Moriya, T., Nakayama, J., Arai, Y. and Fukuda, M. (2005) 'Expression of core 2 beta1,6-N-acetylglucosaminyltransferase facilitates prostate cancer progression', *Glycobiology*, 15(10), pp. 1016-24.

Hakomori, S. (2002) 'Glycosylation defining cancer malignancy: new wine in an old bottle', *Proc Natl Acad Sci U S A*, 99(16), pp. 10231-3.

Haldrup, C., Lynnerup, A.S., Storebjerg, T.M., Vang, S., Wild, P., Visakorpi, T., Arsov, C., Schulz, W.A., Lindberg, J., Gronberg, H., Egevad, L., Borre, M., Orntoft, T.F., Hoyer, S. and Sorensen, K.D. (2016) 'Large-scale evaluation of SLC18A2 in prostate cancer reveals diagnostic and prognostic biomarker potential at three molecular levels', *Mol Oncol*, 10(6), pp. 825-37.

Haley, J., Hudson, P., Scanlon, D., John, M., Cronk, M., Shine, J., Tregear, G. and Niall, H. (1982) 'Porcine relaxin: molecular cloning and cDNA structure', *DNA*, 1(2), pp. 155-62.

Halkidou, K., Gnanapragasam, V.J., Mehta, P.B., Logan, I.R., Brady, M.E., Cook, S., Leung, H.Y., Neal, D.E. and Robson, C.N. (2003) 'Expression of Tip60, an androgen receptor coactivator, and its role in prostate cancer development', *Oncogene*, 22(16), pp. 2466-77.

Halls, M.L., Bathgate, R.A. and Summers, R.J. (2006) 'Relaxin family peptide receptors RXFP1 and RXFP2 modulate cAMP signaling by distinct mechanisms', *Mol Pharmacol*, 70(1), pp. 214-26.

Halls, M.L., Bathgate, R.A. and Summers, R.J. (2007) 'Comparison of signaling pathways activated by the relaxin family peptide receptors, RXFP1 and RXFP2, using reporter genes', *J Pharmacol Exp Ther*, 320(1), pp. 281-90.

Halls, M.L., Hewitson, T.D., Moore, X.L., Du, X.J., Bathgate, R.A. and Summers, R.J. (2009) 'Relaxin activates multiple cAMP signaling pathway profiles in different target cells', *Ann N Y Acad Sci*, 1160, pp. 108-11.

Haltiwanger, R.S. (2002) 'Regulation of signal transduction pathways in development by glycosylation', *Curr Opin Struct Biol*, 12(5), pp. 593-8.

Hamid, A.R., Pfeiffer, M.J., Verhaegh, G.W., Schaafsma, E., Brandt, A., Sweep, F.C., Sedelaar, J.P. and Schalken, J.A. (2012) 'Aldo-keto reductase family 1 member C3 (AKR1C3) is a biomarker and therapeutic target for castration-resistant prostate cancer', *Mol Med*, 18, pp. 1449-55.

Hanahan, D. and Weinberg, R.A. (2011) 'Hallmarks of cancer: the next generation', *Cell*, 144(5), pp. 646-74.

Hansell, D.J., Bryant-Greenwood, G.D. and Greenwood, F.C. (1991) 'Expression of the human relaxin H1 gene in the decidua, trophoblast, and prostate', *J Clin Endocrinol Metab*, 72(4), pp. 899-904.

Harre, U., Lang, S.C., Pfeifle, R., Rombouts, Y., Fruhbeisser, S., Amara, K., Bang, H., Lux, A., Koeleman, C.A., Baum, W., Dietel, K., Grohn, F., Malmstrom, V., Klareskog, L., Kronke, G., Kocijan, R., Nimmerjahn, F., Toes, R.E., Herrmann, M., Scherer, H.U. and Schett, G. (2015) 'Glycosylation of immunoglobulin G determines osteoclast differentiation and bone loss', *Nat Commun*, 6, p. 6651.

Harris, W.P., Mostaghel, E.A., Nelson, P.S. and Montgomery, B. (2009) 'Androgen deprivation therapy: progress in understanding mechanisms of resistance and optimizing androgen depletion', *Nat Clin Pract Urol*, 6(2), pp. 76-85.

Harrison, P.M., Kumar, A., Lang, N., Snyder, M. and Gerstein, M. (2002) 'A question of size: the eukaryotic proteome and the problems in defining it', *Nucleic Acids Res*, 30(5), pp. 1083-90.

Harrison, S., Lennon, R., Holly, J., Higgins, J.P., Gardner, M., Perks, C., Gaunt, T., Tan, V., Borwick, C., Emmet, P., Jeffreys, M., Northstone, K., Rinaldi, S., Thomas, S., Turner, S.D., Pease, A., Vilenchick, V., Martin, R.M. and Lewis, S.J. (2017) 'Does milk intake promote prostate cancer initiation or progression via effects on insulin-like growth factors (IGFs)? A systematic review and meta-analysis', *Cancer Causes Control*.

Hassanipour-Azgomi, S., Mohammadian-Hafshejani, A., Ghoncheh, M., Towhidi, F., Jamehshorani, S. and Salehiniya, H. (2016) 'Incidence and mortality of prostate cancer and their relationship with the Human Development Index worldwide', *Prostate Int*, 4(3), pp. 118-24.

Hauselmann, I. and Borsig, L. (2014) 'Altered tumor-cell glycosylation promotes metastasis', *Front Oncol*, 4, p. 28.

He, B., Kemppainen, J.A., Voegel, J.J., Gronemeyer, H. and Wilson, E.M. (1999) 'Activation function 2 in the human androgen receptor ligand binding domain mediates interdomain communication with the NH(2)-terminal domain', *J Biol Chem*, 274(52), pp. 37219-25.

Hedlund, M., Ng, E., Varki, A. and Varki, N.M. (2008) 'alpha 2-6-Linked sialic acids on N-glycans modulate carcinoma differentiation in vivo', *Cancer Res*, 68(2), pp. 388-94.

Heidegger, I., Klocker, H., Pichler, R., Horninger, W. and Bektic, J. (2015) 'PSA Isoforms' Velocities for Early Diagnosis of Prostate Cancer', *Anticancer Res*, 35(6), pp. 3567-70.

Heinrich, P.C., Behrmann, I., Haan, S., Hermanns, H.M., Muller-Newen, G. and Schaper, F. (2003) 'Principles of interleukin (IL)-6-type cytokine signalling and its regulation', *Biochem J*, 374(Pt 1), pp. 1-20.

Henning, J.D., Karamchandani, J.M., Bonachea, L.A., Bunker, C.H., Patrick, A.L. and Jenkins, F.J. (2017) 'Elevated Serum PSA is Associated With Human Herpesvirus 8 Infection and Increased Circulating Cytokine Levels in Men From Tobago', *Prostate*, 77(6), pp. 617-624.

Hirano, D., Okada, Y., Minei, S., Takimoto, Y. and Nemoto, N. (2004) 'Neuroendocrine differentiation in hormone refractory prostate cancer following androgen deprivation therapy', *Eur Urol*, 45(5), pp. 586-92; discussion 592.

Hirao, K., Natsuka, Y., Tamura, T., Wada, I., Morito, D., Natsuka, S., Romero, P., Sleno, B., Tremblay, L.O., Herscovics, A., Nagata, K. and Hosokawa, N. (2006) 'EDEM3, a soluble EDEM homolog, enhances glycoprotein endoplasmic reticulum-associated degradation and mannose trimming', *J Biol Chem*, 281(14), pp. 9650-8.

Ho, L.L., Kench, J.G., Handelsman, D.J., Scheffer, G.L., Stricker, P.D., Grygiel, J.G., Sutherland, R.L., Henshall, S.M., Allen, J.D. and Horvath, L.G. (2008) 'Androgen regulation of multidrug resistance-associated protein 4 (MRP4/ABCC4) in prostate cancer', *Prostate*, 68(13), pp. 1421-9.

Hobisch, A., Rogatsch, H., Hittmair, A., Fuchs, D., Bartsch, G., Jr., Klocker, H., Bartsch, G. and Culig, Z. (2000) 'Immunohistochemical localization of interleukin-6 and its receptor in benign, premalignant and malignant prostate tissue', *J Pathol*, 191(3), pp. 239-44.

Holzbeierlein, J., Lal, P., LaTulippe, E., Smith, A., Satagopan, J., Zhang, L., Ryan, C., Smith, S., Scher, H., Scardino, P., Reuter, V. and Gerald, W.L. (2004) 'Gene expression analysis of human prostate carcinoma during hormonal therapy identifies androgen-responsive genes and mechanisms of therapy resistance', *Am J Pathol*, 164(1), pp. 217-27.

Hombach-Klonisch, S., Bialek, J., Trojanowicz, B., Weber, E., Holzhausen, H.J., Silvertown, J.D., Summerlee, A.J., Dralle, H., Hoang-Vu, C. and Klonisch, T. (2006) 'Relaxin enhances the oncogenic potential of human thyroid carcinoma cells', *Am J Pathol*, 169(2), pp. 617-32.

Horak, P., Tomasich, E., Vanhara, P., Kratochvilova, K., Anees, M., Marhold, M., Lemberger, C.E., Gerschpacher, M., Horvat, R., Sibilia, M., Pils, D. and Krainer, M. (2014) 'TUSC3 loss alters the ER stress response and accelerates prostate cancer growth in vivo', *Sci Rep*, 4, p. 3739.

Hornberg, E., Ylitalo, E.B., Crnalic, S., Antti, H., Stattin, P., Widmark, A., Bergh, A. and Wikstrom, P. (2011) 'Expression of androgen receptor splice variants in prostate cancer bone metastases is associated with castration-resistance and short survival', *PLoS One*, 6(4), p. e19059.

Horoszewicz, J.S., Leong, S.S., Kawinski, E., Karr, J.P., Rosenthal, H., Chu, T.M., Mirand, E.A. and Murphy, G.P. (1983) 'LNCaP model of human prostatic carcinoma', *Cancer Res*, 43(4), pp. 1809-18.

Hosken, I.T., Sutton, S.W., Smith, C.M. and Gundlach, A.L. (2015) 'Relaxin-3 receptor (Rxfp3) gene knockout mice display reduced running wheel activity: implications for role of relaxin-3/RXFP3 signalling in sustained arousal', *Behav Brain Res*, 278, pp. 167-75.

Hsiao, C.J., Tzai, T.S., Chen, C.H. and Yang, W.H. (2016) 'Analysis of Urinary Prostate-Specific Antigen Glycoforms in Samples of Prostate Cancer and Benign Prostate Hyperplasia', *Dis Markers*, 2016, p. 8915809.

Hsieh, C.C., Shyr, Y.M., Liao, W.Y., Chen, T.H., Wang, S.E., Lu, P.C., Lin, P.Y., Chen, Y.B., Mao, W.Y., Han, H.Y., Hsiao, M., Yang, W.B., Li, W.S., Sher, Y.P. and Shen, C.N. (2017) 'Elevation of beta-galactoside alpha2,6-sialyltransferase 1 in a fructoseresponsive manner promotes pancreatic cancer metastasis', *Oncotarget*, 8(5), pp. 7691-7709.

Hsu, S.Y., Nakabayashi, K., Nishi, S., Kumagai, J., Kudo, M., Sherwood, O.D. and Hsueh, A.J. (2002) 'Activation of orphan receptors by the hormone relaxin', *Science*, 295(5555), pp. 671-4.

Hu, R., Dunn, T.A., Wei, S., Isharwal, S., Veltri, R.W., Humphreys, E., Han, M., Partin, A.W., Vessella, R.L., Isaacs, W.B., Bova, G.S. and Luo, J. (2009) 'Ligand-independent androgen receptor variants derived from splicing of cryptic exons signify hormone-refractory prostate cancer', *Cancer Res*, 69(1), pp. 16-22.

Hu, R., Lu, C., Mostaghel, E.A., Yegnasubramanian, S., Gurel, M., Tannahill, C., Edwards, J., Isaacs, W.B., Nelson, P.S., Bluemn, E., Plymate, S.R. and Luo, J. (2012) 'Distinct transcriptional programs mediated by the ligand-dependent full-length androgen receptor and its splice variants in castration-resistant prostate cancer', *Cancer Res*, 72(14), pp. 3457-62.

Hudson, P., Haley, J., Cronk, M., Shine, J. and Niall, H. (1981) 'Molecular cloning and characterization of cDNA sequences coding for rat relaxin', *Nature*, 291(5811), pp. 127-31.

Hudson, T.J., Anderson, W., Artez, A., Barker, A.D., Bell, C., Bernabe, R.R., Bhan, M.K., Calvo, F., Eerola, I., Gerhard, D.S., Guttmacher, A., Guyer, M., Hemsley, F.M., Jennings, J.L., Kerr, D., Klatt, P., Kolar, P., Kusada, J., Lane, D.P., Laplace, F., Youyong, L., Nettekoven, G., Ozenberger, B., Peterson, J., Rao, T.S., Remacle, J., Schafer, A.J., Shibata, T., Stratton, M.R., Vockley, J.G., Watanabe, K., Yang, H., Yuen, M.M., Knoppers, B.M., Bobrow, M., Cambon-Thomsen, A., Dressler, L.G., Dyke, S.O., Joly, Y., Kato, K., Kennedy, K.L., Nicolas, P., Parker, M.J., Rial-Sebbag, E., Romeo-Casabona, C.M., Shaw, K.M., Wallace, S., Wiesner, G.L., Zeps, N., Lichter, P., Biankin, A.V., Chabannon, C., Chin, L., Clement, B., de Alava, E., Degos, F., Ferguson, M.L., Geary, P., Hayes, D.N., Johns, A.L., Kasprzyk, A., Nakagawa, H., Penny, R., Piris, M.A., Sarin, R., Scarpa, A., van de Vijver, M., Futreal, P.A., Aburatani, H., Bayes, M., Botwell, D.D., Campbell, P.J., Estivill, X., Grimmond, S.M., Gut, I., Hirst, M., Lopez-Otin, C., Majumder, P., Marra, M., McPherson, J.D., Ning, Z., Puente, X.S., Ruan, Y., Stunnenberg, H.G., Swerdlow, H., Velculescu, V.E., Wilson, R.K., Xue, H.H., Yang, L., Spellman, P.T., Bader, G.D., Boutros, P.C., Flicek, P., Getz, G., Guigo, R., Guo, G., Haussler, D., Heath, S., Hubbard, T.J., Jiang, T., et al. (2010) 'International network of cancer genome projects', *Nature*, 464(7291), pp. 993-8.

Huggins, C. and Hodges, C.V. (1972) 'Studies on prostatic cancer. I. The effect of castration, of estrogen and androgen injection on serum phosphatases in metastatic carcinoma of the prostate', *CA Cancer J Clin*, 22(4), pp. 232-40.

Huggins, C. and Hodges, C.V. (2002) 'Studies on prostatic cancer: I. The effect of castration, of estrogen and of androgen injection on serum phosphatases in metastatic carcinoma of the prostate. 1941', *J Urol*, 168(1), pp. 9-12.

Isaacs, J.T. (1994) 'Etiology of benign prostatic hyperplasia', *Eur Urol*, 25 Suppl 1, pp. 6-9.

Ishikawa, T., Yoneyama, T., Tobisawa, Y., Hatakeyama, S., Kurosawa, T., Nakamura, K., Narita, S., Mitsuzuka, K., Duivenvoorden, W., Pinthus, J.H., Hashimoto, Y., Koie, T., Habuchi, T., Arai, Y. and Ohyama, C. (2017) 'An Automated Micro-Total Immunoassay System for Measuring Cancer-Associated alpha2,3-linked Sialyl N-Glycan-Carrying

Prostate-Specific Antigen May Improve the Accuracy of Prostate Cancer Diagnosis', *Int J Mol Sci*, 18(2).

Itkonen, H.M., Engedal, N., Babaie, E., Luhr, M., Guldvik, I.J., Minner, S., Hohloch, J., Tsourlakis, M.C., Schlomm, T. and Mills, I.G. (2014) 'UAP1 is overexpressed in prostate cancer and is protective against inhibitors of N-linked glycosylation', *Oncogene*.

Itkonen, H.M., Engedal, N., Babaie, E., Luhr, M., Guldvik, I.J., Minner, S., Hohloch, J., Tsourlakis, M.C., Schlomm, T. and Mills, I.G. (2015) 'UAP1 is overexpressed in prostate cancer and is protective against inhibitors of N-linked glycosylation', *Oncogene*, 34(28), pp. 3744-50.

Itkonen, H.M., Gorad, S.S., Duveau, D.Y., Martin, S.E., Barkovskaya, A., Bathen, T.F., Moestue, S.A. and Mills, I.G. (2016) 'Inhibition of O-GlcNAc transferase activity reprograms prostate cancer cell metabolism', *Oncotarget*, 7(11), pp. 12464-76.

Itkonen, H.M. and Mills, I.G. (2013) 'N-linked glycosylation supports cross-talk between receptor tyrosine kinases and androgen receptor', *PLoS One*, 8(5), p. e65016.

Ivell, R., Hunt, N., Khan-Dawood, F. and Dawood, M.Y. (1989) 'Expression of the human relaxin gene in the corpus luteum of the menstrual cycle and in the prostate', *Mol Cell Endocrinol*, 66(2), pp. 251-5.

Ivell, R., Kotula-Balak, M., Glynn, D., Heng, K. and Anand-Ivell, R. (2011) 'Relaxin family peptides in the male reproductive system--a critical appraisal', *Mol Hum Reprod*, 17(2), pp. 71-84.

Jariwala, U., Prescott, J., Jia, L., Barski, A., Pregizer, S., Cogan, J.P., Arasheben, A., Tilley, W.D., Scher, H.I., Gerald, W.L., Buchanan, G., Coetzee, G.A. and Frenkel, B. (2007) 'Identification of novel androgen receptor target genes in prostate cancer', *Mol Cancer*, 6, p. 39.

Jensen, O.N. (2004) 'Modification-specific proteomics: characterization of post-translational modifications by mass spectrometry', *Curr Opin Chem Biol*, 8(1), pp. 33-41.

Jiang, F. and Wang, Z. (2004) 'Identification and characterization of PLZF as a prostatic androgen-responsive gene', *Prostate*, 59(4), pp. 426-35.

Joshi, N., Bissada, N.F., Bodner, D., Maclennan, G.T., Narendran, S., Jurevic, R. and Skillicorn, R. (2010) 'Association between periodontal disease and prostate-specific antigen levels in chronic prostatitis patients', *J Periodontol*, 81(6), pp. 864-9.

Kaighn, M.E., Narayan, K.S., Ohnuki, Y., Lechner, J.F. and Jones, L.W. (1979) 'Establishment and characterization of a human prostatic carcinoma cell line (PC-3)', *Invest Urol*, 17(1), pp. 16-23.

Kamat, A.A., Feng, S., Agoulnik, I.U., Kheradmand, F., Bogatcheva, N.V., Coffey, D., Sood, A.K. and Agoulnik, A.I. (2006) 'The role of relaxin in endometrial cancer', *Cancer Biol Ther*, 5(1), pp. 71-7.

Kang, X., Wang, N., Pei, C., Sun, L., Sun, R., Chen, J. and Liu, Y. (2012) 'Glycan-related gene expression signatures in human metastatic hepatocellular carcinoma cells', *Exp Ther Med*, 3(3), pp. 415-422.

Karantanos, T., Corn, P.G. and Thompson, T.C. (2013) 'Prostate cancer progression after androgen deprivation therapy: mechanisms of castrate resistance and novel therapeutic approaches', *Oncogene*, 32(49), pp. 5501-11.

Karin, M. (2006) 'Nuclear factor-kappaB in cancer development and progression', *Nature*, 441(7092), pp. 431-6.

Kaushal, A., Myers, S.A., Dong, Y., Lai, J., Tan, O.L., Bui, L.T., Hunt, M.L., Digby, M.R., Samaratunga, H., Gardiner, R.A., Clements, J.A. and Hooper, J.D. (2008) 'A novel transcript from the KLKP1 gene is androgen regulated, down-regulated during prostate cancer progression and encodes the first non-serine protease identified from the human kallikrein gene locus', *Prostate*, 68(4), pp. 381-99.

Kaushik, A.K., Shojaie, A., Panzitt, K., Sonavane, R., Venghatakrishnan, H., Manikkam, M., Zaslavsky, A., Putluri, V., Vasu, V.T., Zhang, Y., Khan, A.S., Lloyd, S., Szafran, A.T., Dasgupta, S., Bader, D.A., Stossi, F., Li, H., Samanta, S., Cao, X., Tsouko, E., Huang, S., Frigo, D.E., Chan, L., Edwards, D.P., Kaipparettu, B.A., Mitsiades, N., Weigel, N.L., Mancini, M., McGuire, S.E., Mehra, R., Ittmann, M.M., Chinnaiyan, A.M., Putluri, N., Palapattu, G.S., Michailidis, G. and Sreekumar, A. (2016) 'Inhibition of the hexosamine biosynthetic pathway promotes castration-resistant prostate cancer', *Nat Commun*, 7, p. 11612.

Keren, H., Lev-Maor, G. and Ast, G. (2010) 'Alternative splicing and evolution: diversification, exon definition and function', *Nat Rev Genet*, 11(5), pp. 345-55.

Kim, J. and Coetzee, G.A. (2004) 'Prostate specific antigen gene regulation by androgen receptor', *J Cell Biochem*, 93(2), pp. 233-41.

Kim, J.H., Lee, S.H., Choi, S., Kim, U., Yeo, I.S., Kim, S.H., Oh, M.J., Moon, H., Lee, J., Jeong, S., Choi, M.G., Lee, J.H., Sohn, T.S., Bae, J.M., Kim, S., Min, Y.W., Lee, H., Rhee, P.L., Kim, J.J., Lee, S.J., Kim, S.T., Park, S.H., Park, J.O., Park, Y.S., Lim, H.Y., Kang, W.K. and An, H.J. (2016) 'Direct analysis of aberrant glycosylation on haptoglobin in patients with gastric cancer', *Oncotarget*.

Kishimoto, T. (1989) 'The biology of interleukin-6', *Blood*, 74(1), pp. 1-10.

Klijn, C., Durinck, S., Stawiski, E.W., Haverty, P.M., Jiang, Z., Liu, H., Degenhardt, J., Mayba, O., Gnad, F., Liu, J., Pau, G., Reeder, J., Cao, Y., Mukhyala, K., Selvaraj, S.K., Yu, M., Zynda, G.J., Brauer, M.J., Wu, T.D., Gentleman, R.C., Manning, G., Yauch, R.L., Bourgon, R., Stokoe, D., Modrusan, Z., Neve, R.M., de Sauvage, F.J., Settleman, J., Seshagiri, S. and Zhang, Z. (2015) 'A comprehensive transcriptional portrait of human cancer cell lines', *Nat Biotechnol*, 33(3), pp. 306-12.

Kluetz, P.G., Pierce, W., Maher, V.E., Zhang, H., Tang, S., Song, P., Liu, Q., Haber, M.T., Leutzinger, E.E., Al-Hakim, A., Chen, W., Palmby, T., Alebachew, E., Sridhara, R.,

Ibrahim, A., Justice, R. and Pazdur, R. (2014) 'Radium Ra 223 dichloride injection: U.S. Food and Drug Administration drug approval summary', *Clin Cancer Res*, 20(1), pp. 9-14.

Klugo, R.C., Farah, R.N. and Cerny, J.C. (1981) 'Bilateral orchiectomy for carcinoma of prostate. Response of serum testosterone and clinical response to subsequent estrogen therapy', *Urology*, 17(1), pp. 49-50.

Knuuttila, M., Yatkin, E., Kallio, J., Savolainen, S., Laajala, T.D., Aittokallio, T., Oksala, R., Hakkinen, M., Keski-Rahkonen, P., Auriola, S., Poutanen, M. and Makela, S. (2014) 'Castration induces up-regulation of intratumoral androgen biosynthesis and androgen receptor expression in an orthotopic VCaP human prostate cancer xenograft model', *Am J Pathol*, 184(8), pp. 2163-73.

Kojima, Y., Yoneyama, T., Hatakeyama, S., Mikami, J., Sato, T., Mori, K., Hashimoto, Y., Koie, T., Ohyama, C., Fukuda, M. and Tobisawa, Y. (2015) 'Detection of Core2 beta-1,6-N-Acetylglucosaminyltransferase in Post-Digital Rectal Examination Urine Is a Reliable Indicator for Extracapsular Extension of Prostate Cancer', *PLoS One*, 10(9), p. e0138520.

Korenchuk, S., Lehr, J.E., L, M.C., Lee, Y.G., Whitney, S., Vessella, R., Lin, D.L. and Pienta, K.J. (2001) 'VCaP, a cell-based model system of human prostate cancer', *In Vivo*, 15(2), pp. 163-8.

Kozlowski, J.M., Fidler, I.J., Campbell, D., Xu, Z.L., Kaighn, M.E. and Hart, I.R. (1984) 'Metastatic behavior of human tumor cell lines grown in the nude mouse', *Cancer Res*, 44(8), pp. 3522-9.

Krijnen, J.L., Janssen, P.J., Ruizeveld de Winter, J.A., van Krimpen, H., Schroder, F.H. and van der Kwast, T.H. (1993) 'Do neuroendocrine cells in human prostate cancer express androgen receptor?', *Histochemistry*, 100(5), pp. 393-8.

Krishn, S.R., Kaur, S., Smith, L.M., Johansson, S.L., Jain, M., Patel, A., Gautam, S.K., Hollingsworth, M.A., Mandel, U., Clausen, H., Lo, W.C., Fan, W.T., Manne, U. and Batra, S.K. (2016) 'Mucins and associated glycan signatures in colon adenoma-carcinoma sequence: Prospective pathological implication(s) for early diagnosis of colon cancer', *Cancer Lett*, 374(2), pp. 304-14.

Kuhn, B., Benz, J., Greif, M., Engel, A.M., Sobek, H. and Rudolph, M.G. (2013) 'The structure of human alpha-2,6-sialyltransferase reveals the binding mode of complex glycans', *Acta Crystallogr D Biol Crystallogr*, 69(Pt 9), pp. 1826-38.

Kumar, A., Coleman, I., Morrissey, C., Zhang, X., True, L.D., Gulati, R., Etzioni, R., Bolouri, H., Montgomery, B., White, T., Lucas, J.M., Brown, L.G., Dumpit, R.F., DeSarkar, N., Higano, C., Yu, E.Y., Coleman, R., Schultz, N., Fang, M., Lange, P.H., Shendure, J., Vessella, R.L. and Nelson, P.S. (2016) 'Substantial interindividual and limited intraindividual genomic diversity among tumors from men with metastatic prostate cancer', *Nat Med*, 22(4), pp. 369-78.

Kumar, R. and McEwan, I.J. (2012) 'Allosteric modulators of steroid hormone receptors: structural dynamics and gene regulation', *Endocr Rev*, 33(2), pp. 271-99.

Kwegyir-Afful, A.K., Ramalingam, S., Purushottamachar, P., Ramamurthy, V.P. and Njar, V.C. (2015) 'Galeterone and VNPT55 induce proteasomal degradation of AR/AR-V7, induce significant apoptosis via cytochrome c release and suppress growth of castration resistant prostate cancer xenografts in vivo', *Oncotarget*, 6(29), pp. 27440-60.

Labrie, C., Lessard, J., Ben Aicha, S., Savard, M.P., Pelletier, M., Fournier, A., Lavergne, E. and Calvo, E. (2008) 'Androgen-regulated transcription factor AIbZIP in prostate cancer', *J Steroid Biochem Mol Biol*, 108(3-5), pp. 237-44.

Labrie, F., Belanger, A., Dupont, A., Luu-The, V., Simard, J. and Labrie, C. (1993) 'Science behind total androgen blockade: from gene to combination therapy', *Clin Invest Med*, 16(6), pp. 475-92.

Labrie, F., Dupont, A., Belanger, A., St-Arnaud, R., Giguere, M., Lacourciere, Y., Emond, J. and Monfette, G. (1986) 'Treatment of prostate cancer with gonadotropin-releasing hormone agonists', *Endocr Rev*, 7(1), pp. 67-74.

Ladomery, M. (2013) 'Aberrant alternative splicing is another hallmark of cancer', *Int J Cell Biol*, 2013, p. 463786.

Lallous, N., Volik, S.V., Awrey, S., Leblanc, E., Tse, R., Murillo, J., Singh, K., Azad, A.A., Wyatt, A.W., LeBihan, S., Chi, K.N., Gleave, M.E., Rennie, P.S., Collins, C.C. and Cherkasov, A. (2016) 'Functional analysis of androgen receptor mutations that confer anti-androgen resistance identified in circulating cell-free DNA from prostate cancer patients', *Genome Biol*, 17, p. 10.

Lander, E.S. (2011) 'Initial impact of the sequencing of the human genome', *Nature*, 470(7333), pp. 187-97.

Lapointe, J., Li, C., Higgins, J.P., van de Rijn, M., Bair, E., Montgomery, K., Ferrari, M., Egevad, L., Rayford, W., Bergerheim, U., Ekman, P., DeMarzo, A.M., Tibshirani, R., Botstein, D., Brown, P.O., Brooks, J.D. and Pollack, J.R. (2004) 'Gene expression profiling identifies clinically relevant subtypes of prostate cancer', *Proc Natl Acad Sci U S A*, 101(3), pp. 811-6.

Lee, B.H., Taylor, M.G., Robinet, P., Smith, J.D., Schweitzer, J., Sehayek, E., Falzarano, S.M., Magi-Galluzzi, C., Klein, E.A. and Ting, A.H. (2013) 'Dysregulation of cholesterol homeostasis in human prostate cancer through loss of ABCA1', *Cancer Res*, 73(3), pp. 1211-8.

Li, J., Ren, S., Piao, H.L., Wang, F., Yin, P., Xu, C., Lu, X., Ye, G., Shao, Y., Yan, M., Zhao, X., Sun, Y. and Xu, G. (2016a) 'Integration of lipidomics and transcriptomics unravels aberrant lipid metabolism and defines cholesteryl oleate as potential biomarker of prostate cancer', *Sci Rep*, 6, p. 20984.

Li, Q., Zhang, C.S. and Zhang, Y. (2016b) 'Molecular aspects of prostate cancer with neuroendocrine differentiation', *Chin J Cancer Res*, 28(1), pp. 122-9.

Li, Q.K., Chen, L., Ao, M.H., Chiu, J.H., Zhang, Z., Zhang, H. and Chan, D.W. (2015) 'Serum fucosylated prostate-specific antigen (PSA) improves the differentiation of aggressive from non-aggressive prostate cancers', *Theranostics*, 5(3), pp. 267-76.

Li, Y., Donmez, N., Sahinalp, C., Xie, N., Wang, Y., Xue, H., Mo, F., Beltran, H., Gleave, M., Collins, C. and Dong, X. (2017) 'SRRM4 Drives Neuroendocrine Transdifferentiation of Prostate Adenocarcinoma Under Androgen Receptor Pathway Inhibition', *Eur Urol*, 71(1), pp. 68-78.

Lin, S., Kemmner, W., Grigull, S. and Schlag, P.M. (2002) 'Cell surface alpha 2,6 sialylation affects adhesion of breast carcinoma cells', *Exp Cell Res*, 276(1), pp. 101-10.

Liu, C., Armstrong, C., Zhu, Y., Lou, W. and Gao, A.C. (2016) 'Niclosamide enhances abiraterone treatment via inhibition of androgen receptor variants in castration resistant prostate cancer', *Oncotarget*, 7(22), pp. 32210-20.

Liu, C., Chen, J., Sutton, S., Roland, B., Kuei, C., Farmer, N., Sillard, R. and Lovenberg, T.W. (2003a) 'Identification of relaxin-3/INSL7 as a ligand for GPCR142', *J Biol Chem*, 278(50), pp. 50765-70.

Liu, C., Eriste, E., Sutton, S., Chen, J., Roland, B., Kuei, C., Farmer, N., Jornvall, H., Sillard, R. and Lovenberg, T.W. (2003b) 'Identification of relaxin-3/INSL7 as an endogenous ligand for the orphan G-protein-coupled receptor GPCR135', *J Biol Chem*, 278(50), pp. 50754-64.

Liu, C., Lou, W., Zhu, Y., Nadiminty, N., Schwartz, C.T., Evans, C.P. and Gao, A.C. (2014a) 'Niclosamide inhibits androgen receptor variants expression and overcomes enzalutamide resistance in castration-resistant prostate cancer', *Clin Cancer Res*, 20(12), pp. 3198-210.

Liu, H.O., Wu, Q., Liu, W.S., Liu, Y.D., Fu, Q., Zhang, W.J., Xu, L. and Xu, J.J. (2014b) 'ST6Gal-I predicts postoperative clinical outcome for patients with localized clear-cell renal cell carcinoma', *Asian Pac J Cancer Prev*, 15(23), pp. 10217-23.

Liu, W., Xie, C.C., Zhu, Y., Li, T., Sun, J., Cheng, Y., Ewing, C.M., Dalrymple, S., Turner, A.R., Isaacs, J.T., Chang, B.L., Zheng, S.L., Isaacs, W.B. and Xu, J. (2008) 'Homozygous deletions and recurrent amplifications implicate new genes involved in prostate cancer', *Neoplasia*, 10(8), pp. 897-907.

Liu, Z., Swindall, A.F., Kesterson, R.A., Schoeb, T.R., Bullard, D.C. and Bellis, S.L. (2011) 'ST6Gal-I regulates macrophage apoptosis via alpha2-6 sialylation of the TNFR1 death receptor', *J Biol Chem*, 286(45), pp. 39654-62.

Livermore, K.E., Munkley, J. and Elliott, D.J. (2016) 'Androgen receptor and prostate cancer', *AIMS Molecular Science*, 3(2), pp. 280-299.

Llop, E., Ferrer-Batalle, M., Barrabes, S., Guerrero, P.E., Ramirez, M., Saldova, R., Rudd, P.M., Aleixandre, R.N., Comet, J., de Llorens, R. and Peracaula, R. (2016) 'Improvement of Prostate Cancer Diagnosis by Detecting PSA Glycosylation-Specific Changes', *Theranostics*, 6(8), pp. 1190-204.

Lohr, J.G., Adalsteinsson, V.A., Cibulskis, K., Choudhury, A.D., Rosenberg, M., Cruz-Gordillo, P., Francis, J.M., Zhang, C.Z., Shalek, A.K., Satija, R., Trombetta, J.J., Lu, D., Tallapragada, N., Tahirova, N., Kim, S., Blumenstiel, B., Sougnez, C., Lowe, A., Wong, B., Auclair, D., Van Allen, E.M., Nakabayashi, M., Lis, R.T., Lee, G.S., Li, T., Chabot, M.S., Ly, A., Taplin, M.E., Clancy, T.E., Loda, M., Regev, A., Meyerson, M., Hahn, W.C., Kantoff, P.W., Golub, T.R., Getz, G., Boehm, J.S. and Love, J.C. (2014) 'Whole-exome sequencing of circulating tumor cells provides a window into metastatic prostate cancer', *Nat Biotechnol*, 32(5), pp. 479-84.

Lu, C. and Luo, J. (2013) 'Decoding the androgen receptor splice variants', *Transl Androl Urol*, 2(3), pp. 178-186.

Lu, J. and Gu, J. (2015) 'Significance of beta-Galactoside alpha2,6 Sialyltranferase 1 in Cancers', *Molecules*, 20(5), pp. 7509-27.

Lu, J., Isaji, T., Im, S., Fukuda, T., Hashii, N., Takakura, D., Kawasaki, N. and Gu, J. (2014) 'beta-Galactoside alpha2,6-sialyltranferase 1 promotes transforming growth factor-beta-mediated epithelial-mesenchymal transition', *J Biol Chem*, 289(50), pp. 34627-41.

Lu, Q., Xu, L., Li, C., Yuan, Y., Huang, S. and Chen, H. (2016) 'miR-214 inhibits invasion and migration via downregulating GALNT7 in esophageal squamous cell cancer', *Tumour Biol*, 37(11), pp. 14605-14614.

Lubahn, D.B., Joseph, D.R., Sullivan, P.M., Willard, H.F., French, F.S. and Wilson, E.M. (1988) 'Cloning of human androgen receptor complementary DNA and localization to the X chromosome', *Science*, 240(4850), pp. 327-30.

Luu, H.N., Lin, H.Y., Sorensen, K.D., Ogunwobi, O.O., Kumar, N., Chornokur, G., Phelan, C., Jones, D., Kidd, L., Batra, J., Yamoah, K., Berglund, A., Rounbehler, R.J., Yang, M., Lee, S.H., Kang, N., Kim, S.J., Park, J.Y. and Di Pietro, G. (2017) 'miRNAs associated with prostate cancer risk and progression', *BMC Urol*, 17(1), p. 18.

Lynch, H.T., Kosoko-Lasaki, O., Leslie, S.W., Rendell, M., Shaw, T., Snyder, C., D'Amico, A.V., Buxbaum, S., Isaacs, W.B., Loeb, S., Moul, J.W. and Powell, I. (2016) 'Screening for familial and hereditary prostate cancer', *Int J Cancer*, 138(11), pp. 2579-91.

Ma, H., Cheng, L., Hao, K., Li, Y., Song, X., Zhou, H. and Jia, L. (2014) 'Reversal effect of ST6GAL 1 on multidrug resistance in human leukemia by regulating the PI3K/Akt pathway and the expression of P-gp and MRP1', *PLoS One*, 9(1), p. e85113.

Ma, J.F., Von Kalle, M., Plautz, Q., F, M.X., Singh, L. and Wang, L. (2013) 'Relaxin promotes in vitro tumour growth, invasion and angiogenesis of human Saos-2

osteosarcoma cells by AKT/VEGF pathway', *Eur Rev Med Pharmacol Sci*, 17(10), pp. 1345-50.

Ma, Q., Wu, X., Wu, J., Liang, Z. and Liu, T. (2017) 'SERP1 is a novel marker of poor prognosis in pancreatic ductal adenocarcinoma patients via anti-apoptosis and regulating SRPRB/NF-kappaB axis', *Int J Oncol*, 51(4), pp. 1104-1114.

Maitland, N.J., Frame, F.M., Polson, E.S., Lewis, J.L. and Collins, A.T. (2011) 'Prostate cancer stem cells: do they have a basal or luminal phenotype?', *Horm Cancer*, 2(1), pp. 47-61.

Malinowska, K., Neuwirt, H., Cavarretta, I.T., Bektic, J., Steiner, H., Dietrich, H., Moser, P.L., Fuchs, D., Hobisch, A. and Culig, Z. (2009) 'Interleukin-6 stimulation of growth of prostate cancer in vitro and in vivo through activation of the androgen receptor', *Endocr Relat Cancer*, 16(1), pp. 155-69.

Marriott, D., Gillece-Castro, B. and Gorman, C.M. (1992) 'Prohormone convertase-1 will process prorelaxin, a member of the insulin family of hormones', *Mol Endocrinol*, 6(9), pp. 1441-50.

Massie, C.E., Adryan, B., Barbosa-Morais, N.L., Lynch, A.G., Tran, M.G., Neal, D.E. and Mills, I.G. (2007) 'New androgen receptor genomic targets show an interaction with the ETS1 transcription factor', *EMBO Rep*, 8(9), pp. 871-8.

Massie, C.E., Lynch, A., Ramos-Montoya, A., Boren, J., Stark, R., Fazli, L., Warren, A., Scott, H., Madhu, B., Sharma, N., Bon, H., Zecchini, V., Smith, D.M., Denicola, G.M., Mathews, N., Osborne, M., Hadfield, J., Macarthur, S., Adryan, B., Lyons, S.K., Brindle, K.M., Griffiths, J., Gleave, M.E., Rennie, P.S., Neal, D.E. and Mills, I.G. (2011) 'The androgen receptor fuels prostate cancer by regulating central metabolism and biosynthesis', *EMBO J*, 30(13), pp. 2719-33.

Matlin, A.J., Clark, F. and Smith, C.W. (2005) 'Understanding alternative splicing: towards a cellular code', *Nat Rev Mol Cell Biol*, 6(5), pp. 386-98.

McKiernan, J., Donovan, M.J., O'Neill, V., Bentink, S., Noerholm, M., Belzer, S., Skog, J., Kattan, M.W., Partin, A., Andriole, G., Brown, G., Wei, J.T., Thompson, I.M., Jr. and Carroll, P. (2016) 'A Novel Urine Exosome Gene Expression Assay to Predict High-grade Prostate Cancer at Initial Biopsy', *JAMA Oncol*, 2(7), pp. 882-9.

McNeal, J.E. (1978) 'Origin and evolution of benign prostatic enlargement', *Invest Urol*, 15(4), pp. 340-5.

McNeal, J.E. (1981) 'The zonal anatomy of the prostate', *Prostate*, 2(1), pp. 35-49.

Mcneal, J.E. (1988) 'Normal Histology of the Prostate', *American Journal of Surgical Pathology*, 12(8), pp. 619-633.

Mellinger, G.T., Gleason, D. and Bailar, J., 3rd (1967) 'The histology and prognosis of prostatic cancer', *J Urol*, 97(2), pp. 331-7.

Meng, Q., Ren, C., Wang, L., Zhao, Y. and Wang, S. (2015) 'Knockdown of ST6Gal-I inhibits the growth and invasion of osteosarcoma MG-63 cells', *Biomed Pharmacother*, 72, pp. 172-8.

Miles, D.W., Happerfield, L.C., Smith, P., Gillibrand, R., Bobrow, L.G., Gregory, W.M. and Rubens, R.D. (1994) 'Expression of sialyl-Tn predicts the effect of adjuvant chemotherapy in node-positive breast cancer', *Br J Cancer*, 70(6), pp. 1272-5.

Mirosevich, J., Bentel, J.M., Zeps, N., Redmond, S.L., D'Antuono, M.F. and Dawkins, H.J. (1999) 'Androgen receptor expression of proliferating basal and luminal cells in adult murine ventral prostate', *J Endocrinol*, 162(3), pp. 341-50.

Miyamoto, D.T., Ting, D.T., Toner, M., Maheswaran, S. and Haber, D.A. (2016) 'Single-Cell Analysis of Circulating Tumor Cells as a Window into Tumor Heterogeneity', *Cold Spring Harb Symp Quant Biol*, 81, pp. 269-274.

Mo, F., Lin, D., Takhar, M., Ramnarine, V.R., Dong, X., Bell, R.H., Volik, S.V., Wang, K., Xue, H., Wang, Y., Haegert, A., Anderson, S., Brahmbhatt, S., Erho, N., Wang, X., Gout, P.W., Morris, J., Karnes, R.J., Den, R.B., Klein, E.A., Schaeffer, E.M., Ross, A., Ren, S., Sahinalp, S.C., Li, Y., Xu, X., Wang, J., Wang, J., Gleave, M.E., Davicioni, E., Sun, Y., Wang, Y. and Collins, C.C. (2017) 'Stromal Gene Expression is Predictive for Metastatic Primary Prostate Cancer', *Eur Urol*.

Mohler, J.L., Gregory, C.W., Ford, O.H., 3rd, Kim, D., Weaver, C.M., Petrusz, P., Wilson, E.M. and French, F.S. (2004) 'The androgen axis in recurrent prostate cancer', *Clin Cancer Res*, 10(2), pp. 440-8.

Mohorko, E., Owen, R.L., Malojcic, G., Brozzo, M.S., Aebi, M. and Glockshuber, R. (2014) 'Structural basis of substrate specificity of human oligosaccharyl transferase subunit N33/Tusc3 and its role in regulating protein N-glycosylation', *Structure*, 22(4), pp. 590-601.

Mondal, S., Chandra, S. and Mandal, C. (2010) 'Elevated mRNA level of hST6Gal I and hST3Gal V positively correlates with the high risk of pediatric acute leukemia', *Leuk Res*, 34(4), pp. 463-70.

Montgomery, R.B., Mostaghel, E.A., Vessella, R., Hess, D.L., Kalhorn, T.F., Higano, C.S., True, L.D. and Nelson, P.S. (2008) 'Maintenance of intratumoral androgens in metastatic prostate cancer: a mechanism for castration-resistant tumor growth', *Cancer Res*, 68(11), pp. 4447-54.

Mosaad, E.O., Chambers, K.F., Futrega, K., Clements, J.A. and Doran, M.R. (2018) 'The Microwell-mesh: A high-throughput 3D prostate cancer spheroid and drug-testing platform', *Sci Rep*, 8(1), p. 253.

Mostaghel, E.A., Solomon, K.R., Pelton, K., Freeman, M.R. and Montgomery, R.B. (2012) 'Impact of circulating cholesterol levels on growth and intratumoral androgen concentration of prostate tumors', *PLoS One*, 7(1), p. e30062.

Motamedinia, P., Scott, A.N., Bate, K.L., Sadeghi, N., Salazar, G., Shapiro, E., Ahn, J., Lipsky, M., Lin, J., Hruby, G.W., Badani, K.K., Petrylak, D.P., Benson, M.C., Donovan, M.J., Comper, W.D., McKiernan, J.M. and Russo, L.M. (2016) 'Urine Exosomes for Non-Invasive Assessment of Gene Expression and Mutations of Prostate Cancer', *PLoS One*, 11(5), p. e0154507.

Munkley, J. (2017) 'Glycosylation is a global target for androgen control in prostate cancer cells', *Endocr Relat Cancer*, 24(3), pp. R49-R64.

Munkley, J. and Elliott, D.J. (2016) 'Hallmarks of glycosylation in cancer', *Oncotarget*.

Munkley, J., Livermore, K., Rajan, P. and Elliott, D.J. (2017a) 'RNA splicing and splicing regulator changes in prostate cancer pathology', *Hum Genet*.

Munkley, J., Livermore, K.E., McClurg, U.L., Kalna, G., Knight, B., McCullagh, P., McGrath, J., Crundwell, M., Leung, H.Y., Robson, C.N., Harries, L.W., Rajan, P. and Elliott, D.J. (2015a) 'The PI3K regulatory subunit gene PIK3R1 is under direct control of androgens and repressed in prostate cancer cells', *Oncoscience*, 2(9), pp. 755-64.

Munkley, J., McClurg, U.L., Livermore, K.E., Ehrmann, I., Knight, B., McCullagh, P., McGrath, J., Crundwell, M., Harries, L.W., Leung, H.Y., Mills, I.G., Robson, C.N., Rajan, P. and Elliott, D.J. (2017b) 'The cancer-associated cell migration protein TSPAN1 is under control of androgens and its upregulation increases prostate cancer cell migration', *Sci Rep*, 7(1), p. 5249.

Munkley, J., Mills, I.G. and Elliott, D.J. (2016a) 'The role of glycans in the development and progression of prostate cancer', *Nat Rev Urol*.

Munkley, J., Oltean, S., Vodak, D., Wilson, B.T., Livermore, K.E., Zhou, Y., Star, E., Floros, V.I., Johannessen, B., Knight, B., McCullagh, P., McGrath, J., Crundwell, M., Skotheim, R.I., Robson, C.N., Leung, H.Y., Harries, L.W., Rajan, P., Mills, I.G. and Elliott, D.J. (2015b) 'The androgen receptor controls expression of the cancer-associated sTn antigen and cell adhesion through induction of ST6GalNAc1 in prostate cancer', *Oncotarget*, 6(33), pp. 34358-74.

Munkley, J., Rajan, P., Lafferty, N.P., Dalgliesh, C., Jackson, R.M., Robson, C.N., Leung, H.Y. and Elliott, D.J. (2014) 'A novel androgen-regulated isoform of the TSC2 tumour suppressor gene increases cell proliferation', *Oncotarget*, 5(1), pp. 131-9.

Munkley, J., Vodak, D., Livermore, K., James, K., Wilson, B., Knight, B., McCullagh, P., McGrath, J., Crundwell, M., Harries, L., Leung, H., Robson, C., Mills, I., Rajan, P. and Elliott, D. (2016b) 'Glycosylation is an androgen-regulated process essential for prostate cancer cell viability', *EBioMedicine*, p. In press.

Nadiminty, N., Lou, W., Sun, M., Chen, J., Yue, J., Kung, H.J., Evans, C.P., Zhou, Q. and Gao, A.C. (2010) 'Aberrant activation of the androgen receptor by NF-kappaB2/p52 in prostate cancer cells', *Cancer Res*, 70(8), pp. 3309-19.

Nadler, R.B., Humphrey, P.A., Smith, D.S., Catalona, W.J. and Ratliff, T.L. (1995) 'Effect of inflammation and benign prostatic hyperplasia on elevated serum prostate specific antigen levels', *J Urol*, 154(2 Pt 1), pp. 407-13.

Narita, T., Funahashi, H., Satoh, Y., Watanabe, T., Sakamoto, J. and Takagi, H. (1993) 'Association of expression of blood group-related carbohydrate antigens with prognosis in breast cancer', *Cancer*, 71(10), pp. 3044-53.

Neelamegham, S. and Mahal, L.K. (2016) 'Multi-level regulation of cellular glycosylation: from genes to transcript to enzyme to structure', *Curr Opin Struct Biol*, 40, pp. 145-152.

Neschadim, A., Pritzker, L.B., Pritzker, K.P., Branch, D.R., Summerlee, A.J., Trachtenberg, J. and Silvertown, J.D. (2014) 'Relaxin receptor antagonist AT-001 synergizes with docetaxel in androgen-independent prostate xenografts', *Endocr Relat Cancer*, 21(3), pp. 459-71.

Neschadim, A., Summerlee, A.J. and Silvertown, J.D. (2015) 'Targeting the relaxin hormonal pathway in prostate cancer', *Int J Cancer*, 137(10), pp. 2287-95.

Nguyen, B.T., Yang, L., Sanborn, B.M. and Dessauer, C.W. (2003) 'Phosphoinositide 3-kinase activity is required for biphasic stimulation of cyclic adenosine 3',5'-monophosphate by relaxin', *Mol Endocrinol*, 17(6), pp. 1075-84.

Nie, G.H., Luo, L., Duan, H.F., Li, X.Q., Yin, M.J., Li, Z. and Zhang, W. (2016) 'GALNT7, a target of miR-494, participates in the oncogenesis of nasopharyngeal carcinoma', *Tumour Biol*, 37(4), pp. 4559-67.

Nilsson, I., Kelleher, D.J., Miao, Y., Shao, Y., Kreibich, G., Gilmore, R., von Heijne, G. and Johnson, A.E. (2003) 'Photocross-linking of nascent chains to the STT3 subunit of the oligosaccharyltransferase complex', *J Cell Biol*, 161(4), pp. 715-25.

Nowell, P.C. (1976) 'The clonal evolution of tumor cell populations', *Science*, 194(4260), pp. 23-8.

Okamoto, M., Lee, C. and Oyasu, R. (1997) 'Autocrine effect of androgen on proliferation of an androgen responsive prostatic carcinoma cell line, LNCAP: role of interleukin-6', *Endocrinology*, 138(11), pp. 5071-4.

Olayioye, M.A., Neve, R.M., Lane, H.A. and Hynes, N.E. (2000) 'The ErbB signaling network: receptor heterodimerization in development and cancer', *EMBO J*, 19(13), pp. 3159-67.

Olivari, S. and Molinari, M. (2007) 'Glycoprotein folding and the role of EDEM1, EDEM2 and EDEM3 in degradation of folding-defective glycoproteins', *FEBS Lett*, 581(19), pp. 3658-64.

Oltean, S. and Bates, D.O. (2014) 'Hallmarks of alternative splicing in cancer', *Oncogene*, 33(46), pp. 5311-8.

Olzmann, J.A., Kopito, R.R. and Christianson, J.C. (2013) 'The mammalian endoplasmic reticulum-associated degradation system', *Cold Spring Harb Perspect Biol*, 5(9).

Onstenk, W., Sieuwerts, A.M., Kraan, J., Van, M., Nieuweboer, A.J., Mathijssen, R.H., Hamberg, P., Meulenbeld, H.J., De Laere, B., Dirix, L.Y., van Soest, R.J., Lolkema, M.P., Martens, J.W., van Weerden, W.M., Jenster, G.W., Foekens, J.A., de Wit, R. and Sleijfer, S. (2015) 'Efficacy of Cabazitaxel in Castration-resistant Prostate Cancer Is Independent of the Presence of AR-V7 in Circulating Tumor Cells', *Eur Urol*, 68(6), pp. 939-45.

Orsted, D.D. and Bojesen, S.E. (2013) 'The link between benign prostatic hyperplasia and prostate cancer', *Nat Rev Urol*, 10(1), pp. 49-54.

Osuga, T., Takimoto, R., Ono, M., Hirakawa, M., Yoshida, M., Okagawa, Y., Uemura, N., Arihara, Y., Sato, Y., Tamura, F., Sato, T., Iyama, S., Miyanishi, K., Takada, K., Hayashi, T., Kobune, M. and Kato, J. (2016) 'Relationship Between Increased Fucosylation and Metastatic Potential in Colorectal Cancer', *J Natl Cancer Inst*, 108(9).

Ozcan, S., Barkauskas, D.A., Renee Ruhaak, L., Torres, J., Cooke, C.L., An, H.J., Hua, S., Williams, C.C., Dimapasoc, L.M., Han Kim, J., Camorlinga-Ponce, M., Rocke, D., Lebrilla, C.B. and Solnick, J.V. (2014) 'Serum glycan signatures of gastric cancer', *Cancer Prev Res (Phila)*, 7(2), pp. 226-35.

Ozsolak, F. and Milos, P.M. (2011) 'RNA sequencing: advances, challenges and opportunities', *Nat Rev Genet*, 12(2), pp. 87-98.

Pagani, F., Stuani, C., Zuccato, E., Kornblihtt, A.R. and Baralle, F.E. (2003) 'Promoter architecture modulates CFTR exon 9 skipping', *J Biol Chem*, 278(3), pp. 1511-7.

Pajares, M.J., Ezponda, T., Catena, R., Calvo, A., Pio, R. and Montuenga, L.M. (2007) 'Alternative splicing: an emerging topic in molecular and clinical oncology', *Lancet Oncol*, 8(4), pp. 349-57.

Pan, Q., Shai, O., Lee, L.J., Frey, B.J. and Blencowe, B.J. (2008) 'Deep surveying of alternative splicing complexity in the human transcriptome by high-throughput sequencing', *Nat Genet*, 40(12), pp. 1413-5.

Papsidero, L.D., Wang, M.C., Valenzuela, L.A., Murphy, G.P. and Chu, T.M. (1980) 'A prostate antigen in sera of prostatic cancer patients', *Cancer Res*, 40(7), pp. 2428-32.

Park, J.J., Yi, J.Y., Jin, Y.B., Lee, Y.J., Lee, J.S., Lee, Y.S., Ko, Y.G. and Lee, M. (2012) 'Sialylation of epidermal growth factor receptor regulates receptor activity and chemosensitivity to gefitinib in colon cancer cells', *Biochem Pharmacol*, 83(7), pp. 849-57.

Pearce, O.M. and Laubli, H. (2016) 'Sialic acids in cancer biology and immunity', *Glycobiology*, 26(2), pp. 111-28.

Pinho, S.S. and Reis, C.A. (2015) 'Glycosylation in cancer: mechanisms and clinical implications', *Nat Rev Cancer*, 15(9), pp. 540-55.

Poon, T.C., Chiu, C.H., Lai, P.B., Mok, T.S., Zee, B., Chan, A.T., Sung, J.J. and Johnson, P.J. (2005) 'Correlation and prognostic significance of beta-galactoside alpha-2,6-sialyltransferase and serum monosialylated alpha-fetoprotein in hepatocellular carcinoma', *World J Gastroenterol*, 11(42), pp. 6701-6.

Qi, H., Fillion, C., Labrie, Y., Grenier, J., Fournier, A., Berger, L., El-Alfy, M. and Labrie, C. (2002) 'AIbZIP, a novel bZIP gene located on chromosome 1q21.3 that is highly expressed in prostate tumors and of which the expression is up-regulated by androgens in LNCaP human prostate cancer cells', *Cancer Res*, 62(3), pp. 721-33.

Qiu, Y., Robinson, D., Pretlow, T.G. and Kung, H.J. (1998) 'Etk/Bmx, a tyrosine kinase with a pleckstrin-homology domain, is an effector of phosphatidylinositol 3'-kinase and is involved in interleukin 6-induced neuroendocrine differentiation of prostate cancer cells', *Proc Natl Acad Sci U S A*, 95(7), pp. 3644-9.

Qu, F., Xie, W., Nakabayashi, M., Zhang, H., Jeong, S.H., Wang, X., Komura, K., Sweeney, C.J., Sartor, O., Lee, G.M. and Kantoff, P.W. (2017) 'Association of AR-V7 and Prostate-Specific Antigen RNA Levels in Blood with Efficacy of Abiraterone Acetate and Enzalutamide Treatment in Men with Prostate Cancer', *Clin Cancer Res*, 23(3), pp. 726-734.

Rabu, C., McIntosh, R., Jurasova, Z. and Durrant, L. (2012) 'Glycans as targets for therapeutic antitumor antibodies', *Future Oncol*, 8(8), pp. 943-60.

Racioppi, L. (2013) 'CaMKK2: a novel target for shaping the androgen-regulated tumor ecosystem', *Trends Mol Med*, 19(2), pp. 83-8.

Radestock, Y., Willing, C., Kehlen, A., Hoang-Vu, C. and Hombach-Klonisch, S. (2010) 'Relaxin enhances S100A4 and promotes growth of human thyroid carcinoma cell xenografts', *Mol Cancer Res*, 8(4), pp. 494-506.

Radhakrishnan, P., Dabelsteen, S., Madsen, F.B., Francavilla, C., Kopp, K.L., Steentoft, C., Vakhrushev, S.Y., Olsen, J.V., Hansen, L., Bennett, E.P., Woetmann, A., Yin, G., Chen, L., Song, H., Bak, M., Hlady, R.A., Peters, S.L., Opavsky, R., Thode, C., Qvortrup, K., Schjoldager, K.T., Clausen, H., Hollingsworth, M.A. and Wandall, H.H. (2014) 'Immature truncated O-glycophenotype of cancer directly induces oncogenic features', *Proc Natl Acad Sci U S A*, 111(39), pp. E4066-75.

Radmayr, C., Lunacek, A., Schwentner, C., Oswald, J., Klocker, H. and Bartsch, G. (2008) '5-alpha-reductase and the development of the human prostate', *Indian J Urol*, 24(3), pp. 309-12.

Radtke, J.P., Takhar, M., Bonekamp, D., Kesch, C., Erho, N., du Plessis, M., Buerki, C., Ong, K., Davicioni, E., Hohenfellner, M. and Hadaschik, B.A. (2017) 'Transcriptome Wide Analysis of Magnetic Resonance Imaging-targeted Biopsy and Matching Surgical Specimens from High-risk Prostate Cancer Patients Treated with Radical Prostatectomy: The Target Must Be Hit', *Eur Urol Focus*.

Rajan, P., Dalgliesh, C., Carling, P.J., Buist, T., Zhang, C., Grellscheid, S.N., Armstrong, K., Stockley, J., Simillion, C., Gaughan, L., Kalna, G., Zhang, M.Q., Robson, C.N., Leung, H.Y. and Elliott, D.J. (2011) 'Identification of novel androgen-regulated pathways and mRNA isoforms through genome-wide exon-specific profiling of the LNCaP transcriptome', *PLoS One*, 6(12), p. e29088.

Rajan, P., Elliott, D.J., Robson, C.N. and Leung, H.Y. (2009) 'Alternative splicing and biological heterogeneity in prostate cancer', *Nat Rev Urol*, 6(8), pp. 454-60.

Rajan, P., Frew, J.A., Wilson, J.M., Azzabi, A.S., McMenemin, R.M., Stockley, J., Soomro, N.A., Durkan, G., Pedley, I.D. and Leung, H.Y. (2015) 'Feasibility study of a randomized controlled trial comparing docetaxel chemotherapy and androgen deprivation therapy with sequential prostatic biopsies from patients with advanced non-castration-resistant prostate cancer', *Urol Oncol*, 33(8), pp. 337 e1-6.

Rajan, P., Gaughan, L., Dalgliesh, C., El-Sherif, A., Robson, C.N., Leung, H.Y. and Elliott, D.J. (2008) 'The RNA-binding and adaptor protein Sam68 modulates signal-dependent splicing and transcriptional activity of the androgen receptor', *J Pathol*, 215(1), pp. 67-77.

Rajan, P., Sudbery, I.M., Villasevil, M.E., Mui, E., Fleming, J., Davis, M., Ahmad, I., Edwards, J., Sansom, O.J., Sims, D., Ponting, C.P., Heger, A., McMenemin, R.M., Pedley, I.D. and Leung, H.Y. (2014) 'Next-generation sequencing of advanced prostate cancer treated with androgen-deprivation therapy', *Eur Urol*, 66(1), pp. 32-9.

Ramasamy, A., Mondry, A., Holmes, C.C. and Altman, D.G. (2008) 'Key issues in conducting a meta-analysis of gene expression microarray datasets', *PLoS Med*, 5(9), p. e184.

Ren, X.F., Zhao, H., Gong, X.C., Wang, L.N. and Ma, J.F. (2015) 'RLN2 regulates in vitro invasion and viability of osteosarcoma MG-63 cells via S100A4/MMP-9 signal', *Eur Rev Med Pharmacol Sci*, 19(6), pp. 1030-6.

Rhodes, D.R., Yu, J., Shanker, K., Deshpande, N., Varambally, R., Ghosh, D., Barrette, T., Pandey, A. and Chinnaiyan, A.M. (2004) 'ONCOMINE: a cancer microarray database and integrated data-mining platform', *Neoplasia*, 6(1), pp. 1-6.

Rider, J.R., Wilson, K.M., Sinnott, J.A., Kelly, R.S., Mucci, L.A. and Giovannucci, E.L. (2016) 'Ejaculation Frequency and Risk of Prostate Cancer: Updated Results with an Additional Decade of Follow-up', *Eur Urol*, 70(6), pp. 974-982.

Rigas, A.C., Robson, C.N. and Curtin, N.J. (2007) 'Therapeutic potential of CDK inhibitor NU2058 in androgen-independent prostate cancer', *Oncogene*, 26(55), pp. 7611-9.

Ritch, C.R. and Cookson, M.S. (2016) 'Advances in the management of castration resistant prostate cancer', *BMJ*, 355, p. i4405.

Roberts, A.B., Anzano, M.A., Wakefield, L.M., Roche, N.S., Stern, D.F. and Sporn, M.B. (1985) 'Type beta transforming growth factor: a bifunctional regulator of cellular growth', *Proc Natl Acad Sci U S A*, 82(1), pp. 119-23.

Robinson, D., Van Allen, E.M., Wu, Y.M., Schultz, N., Lonigro, R.J., Mosquera, J.M., Montgomery, B., Taplin, M.E., Pritchard, C.C., Attard, G., Beltran, H., Abida, W., Bradley, R.K., Vinson, J., Cao, X., Vats, P., Kunju, L.P., Hussain, M., Feng, F.Y., Tomlins, S.A., Cooney, K.A., Smith, D.C., Brennan, C., Siddiqui, J., Mehra, R., Chen, Y., Rathkopf, D.E., Morris, M.J., Solomon, S.B., Durack, J.C., Reuter, V.E., Gopalan, A., Gao, J., Loda, M., Lis, R.T., Bowden, M., Balk, S.P., Gaviola, G., Sougnez, C., Gupta, M., Yu, E.Y., Mostaghel, E.A., Cheng, H.H., Mulcahy, H., True, L.D., Plymate, S.R., Dvinge, H., Ferraldeschi, R., Flohr, P., Miranda, S., Zafeiriou, Z., Tunariu, N., Mateo, J., Perez-Lopez, R., Demichelis, F., Robinson, B.D., Schiffman, M., Nanus, D.M., Tagawa, S.T., Sigaras, A., Eng, K.W., Elemento, O., Sboner, A., Heath, E.I., Scher, H.I., Pienta, K.J., Kantoff, P., de Bono, J.S., Rubin, M.A., Nelson, P.S., Garraway, L.A., Sawyers, C.L. and Chinnaiyan, A.M. (2015) 'Integrative clinical genomics of advanced prostate cancer', *Cell*, 161(5), pp. 1215-28.

Romero Otero, J., Garcia Gomez, B., Campos Juanatey, F. and Touijer, K.A. (2014) 'Prostate cancer biomarkers: an update', *Urol Oncol*, 32(3), pp. 252-60.

Rudd, P.M., Elliott, T., Cresswell, P., Wilson, I.A. and Dwek, R.A. (2001) 'Glycosylation and the immune system', *Science*, 291(5512), pp. 2370-6.

Ruhaak, L.R., Stroble, C., Dai, J., Barnett, M., Taguchi, A., Goodman, G.E., Miyamoto, S., Gandara, D., Feng, Z., Lebrilla, C.B. and Hanash, S. (2016) 'Serum Glycans as Risk Markers for Non-Small Cell Lung Cancer', *Cancer Prev Res (Phila)*, 9(4), pp. 317-23.

Ryan, P.J., Kastman, H.E., Krstew, E.V., Rosengren, K.J., Hossain, M.A., Churilov, L., Wade, J.D., Gundlach, A.L. and Lawrence, A.J. (2013) 'Relaxin-3/RXFP3 system regulates alcohol-seeking', *Proc Natl Acad Sci U S A*, 110(51), pp. 20789-94.

Saartok, T., Dahlberg, E. and Gustafsson, J.A. (1984) 'Relative binding affinity of anabolic-androgenic steroids: comparison of the binding to the androgen receptors in skeletal muscle and in prostate, as well as to sex hormone-binding globulin', *Endocrinology*, 114(6), pp. 2100-6.

Sagnak, L., Topaloglu, H., Ozok, U. and Ersoy, H. (2011) 'Prognostic significance of neuroendocrine differentiation in prostate adenocarcinoma', *Clin Genitourin Cancer*, 9(2), pp. 73-80.

Saldova, R., Fan, Y., Fitzpatrick, J.M., Watson, R.W. and Rudd, P.M. (2011) 'Core fucosylation and alpha2-3 sialylation in serum N-glycome is significantly increased in prostate cancer comparing to benign prostate hyperplasia', *Glycobiology*, 21(2), pp. 195-205.

Samuel, C.S., Tian, H., Zhao, L. and Amento, E.P. (2003) 'Relaxin is a key mediator of prostate growth and male reproductive tract development', *Lab Invest*, 83(7), pp. 1055-67.

Sarrats, A., Saldova, R., Comet, J., O'Donoghue, N., de Llorens, R., Rudd, P.M. and Peracaula, R. (2010) 'Glycan characterization of PSA 2-DE subforms from serum and seminal plasma', *OMICS*, 14(4), pp. 465-74.

Sato, T., Yoneyama, T., Tobisawa, Y., Hatakeyama, S., Yamamoto, H., Kojima, Y., Mikami, J., Mori, K., Hashimoto, Y., Koie, T. and Ohyama, C. (2016) 'Core 2 (beta-1, 6-N-acetylglucosaminyltransferase-1 expression in prostate biopsy specimen is an indicator of prostate cancer aggressiveness', *Biochemical and Biophysical Research Communications*, 470(1), pp. 150-156.

Scholz, M., Yep, S., Chancey, M., Kelly, C., Chau, K., Turner, J., Lam, R. and Drake, C.G. (2017) 'Phase I clinical trial of sipuleucel-T combined with escalating doses of ipilimumab in progressive metastatic castrate-resistant prostate cancer', *Immunotargets Ther*, 6, pp. 11-16.

Schultz, M.J., Swindall, A.F. and Bellis, S.L. (2012) 'Regulation of the metastatic cell phenotype by sialylated glycans', *Cancer Metastasis Rev*, 31(3-4), pp. 501-18.

Schultz, M.J., Swindall, A.F., Wright, J.W., Sztul, E.S., Landen, C.N. and Bellis, S.L. (2013) 'ST6Gal-I sialyltransferase confers cisplatin resistance in ovarian tumor cells', *J Ovarian Res*, 6(1), p. 25.

Seales, E.C., Jurado, G.A., Brunson, B.A., Wakefield, J.K., Frost, A.R. and Bellis, S.L. (2005) 'Hypersialylation of beta1 integrins, observed in colon adenocarcinoma, may contribute to cancer progression by up-regulating cell motility', *Cancer Res*, 65(11), pp. 4645-52.

Sette, C., Ladomery, M. and Ghigna, C. (2013) 'Alternative splicing: role in cancer development and progression', *Int J Cell Biol*, 2013, p. 421606.

Shaikh, F.M., Seales, E.C., Clem, W.C., Hennessy, K.M., Zhuo, Y. and Bellis, S.L. (2008) 'Tumor cell migration and invasion are regulated by expression of variant integrin glycoforms', *Exp Cell Res*, 314(16), pp. 2941-50.

Shappell, S.B. (2008) 'Clinical utility of prostate carcinoma molecular diagnostic tests', *Rev Urol*, 10(1), pp. 44-69.

Sharma, N.L., Massie, C.E., Ramos-Montoya, A., Zecchini, V., Scott, H.E., Lamb, A.D., MacArthur, S., Stark, R., Warren, A.Y., Mills, I.G. and Neal, D.E. (2013) 'The androgen receptor induces a distinct transcriptional program in castration-resistant prostate cancer in man', *Cancer Cell*, 23(1), pp. 35-47.

Sheng, X., Arnoldussen, Y.J., Storm, M., Tesikova, M., Nenseth, H.Z., Zhao, S., Fazli, L., Rennie, P., Risberg, B., Waehre, H., Danielsen, H., Mills, I.G., Jin, Y., Hotamisligil, G. and Saatcioglu, F. (2015) 'Divergent androgen regulation of unfolded protein response pathways drives prostate cancer', *EMBO Mol Med*, 7(6), pp. 788-801.

Shental-Bechor, D. and Levy, Y. (2009) 'Folding of glycoproteins: toward understanding the biophysics of the glycosylation code', *Curr Opin Struct Biol*, 19(5), pp. 524-33.

Shimomura, O., Oda, T., Tateno, H., Ozawa, Y., Kimura, S., Sakashita, S., Noguchi, M., Hirabayashi, J., Asashima, M. and Ohkohchi, N. (2018) 'A Novel Therapeutic Strategy for Pancreatic Cancer: Targeting Cell Surface Glycan Using rBC2LC-N Lectin-Drug Conjugate (LDC)', *Mol Cancer Ther*, 17(1), pp. 183-195.

Shirahase, T., Aoki, M., Watanabe, R., Watanabe, Y. and Tanaka, M. (2016) 'Increased alcohol consumption in relaxin-3 deficient male mice', *Neurosci Lett*, 612, pp. 155-60.

Shui, I.M., Kolb, S., Hanson, C., Sutcliffe, S., Rider, J.R. and Stanford, J.L. (2016) 'Trichomonas vaginalis infection and risk of advanced prostate cancer', *Prostate*, 76(7), pp. 620-3.

Signoretti, S., Montironi, R., Manola, J., Altimari, A., Tam, C., Bubley, G., Balk, S., Thomas, G., Kaplan, I., Hlatky, L., Hahnfeldt, P., Kantoff, P. and Loda, M. (2000) 'Her-2-neu expression and progression toward androgen independence in human prostate cancer', *J Natl Cancer Inst*, 92(23), pp. 1918-25.

Silvertown, J.D., Neschadim, A., Liu, H.N., Shannon, P., Walia, J.S., Kao, J.C., Robertson, J., Summerlee, A.J. and Medin, J.A. (2010) 'Relaxin-3 and receptors in the human and rhesus brain and reproductive tissues', *Regul Pept*, 159(1-3), pp. 44-53.

Silvertown, J.D., Ng, J., Sato, T., Summerlee, A.J. and Medin, J.A. (2006) 'H2 relaxin overexpression increases in vivo prostate xenograft tumor growth and angiogenesis', *Int J Cancer*, 118(1), pp. 62-73.

Silvertown, J.D., Symes, J.C., Neschadim, A., Nonaka, T., Kao, J.C., Summerlee, A.J. and Medin, J.A. (2007) 'Analog of H2 relaxin exhibits antagonistic properties and impairs prostate tumor growth', *FASEB J*, 21(3), pp. 754-65.

Skacel, P.O., Edwards, A.J., Harrison, C.T. and Watkins, W.M. (1991) 'Enzymic control of the expression of the X determinant (CD15) in human myeloid cells during maturation: the regulatory role of 6-sialytransferase', *Blood*, 78(6), pp. 1452-60.

Slamon, D.J., Godolphin, W., Jones, L.A., Holt, J.A., Wong, S.G., Keith, D.E., Levin, W.J., Stuart, S.G., Udove, J., Ullrich, A. and et al. (1989) 'Studies of the HER-2/neu proto-oncogene in human breast and ovarian cancer', *Science*, 244(4905), pp. 707-12.

Smith, C.M., Chua, B.E., Zhang, C., Walker, A.W., Haidar, M., Hawkes, D., Shabanpoor, F., Hossain, M.A., Wade, J.D., Rosengren, K.J. and Gundlach, A.L. (2014) 'Central injection of relaxin-3 receptor (RXFP3) antagonist peptides reduces motivated food seeking and consumption in C57BL/6J mice', *Behav Brain Res*, 268, pp. 117-26.

Smith, C.M., Ryan, P.J., Hosken, I.T., Ma, S. and Gundlach, A.L. (2011) 'Relaxin-3 systems in the brain--the first 10 years', *J Chem Neuroanat*, 42(4), pp. 262-75.

Spiotto, M.T. and Chung, T.D. (2000) 'STAT3 mediates IL-6-induced neuroendocrine differentiation in prostate cancer cells', *Prostate*, 42(3), pp. 186-95.

Srinivasan, S., Patil, A.H., Verma, M., Bingham, J.L. and Srivatsan, R. (2012) 'Genome-wide Profiling of RNA splicing in prostate tumor from RNA-seq data using virtual microarrays', *J Clin Bioinforma*, 2(1), p. 21.

Stamm, S., Ben-Ari, S., Rafalska, I., Tang, Y., Zhang, Z., Toiber, D., Thanaraj, T.A. and Soreq, H. (2005) 'Function of alternative splicing', *Gene*, 344, pp. 1-20.

Stanbrough, M., Bubley, G.J., Ross, K., Golub, T.R., Rubin, M.A., Penning, T.M., Febbo, P.G. and Balk, S.P. (2006) 'Increased expression of genes converting adrenal androgens to testosterone in androgen-independent prostate cancer', *Cancer Res*, 66(5), pp. 2815-25.

Steinkamp, M.P., O'Mahony, O.A., Brogley, M., Rehman, H., Lapensee, E.W., Dhanasekaran, S., Hofer, M.D., Kuefer, R., Chinnaiyan, A., Rubin, M.A., Pienta, K.J. and Robins, D.M. (2009) 'Treatment-dependent androgen receptor mutations in prostate cancer exploit multiple mechanisms to evade therapy', *Cancer Res*, 69(10), pp. 4434-42.

Steketee, K., Timmerman, L., Ziel-van der Made, A.C., Doesburg, P., Brinkmann, A.O. and Trapman, J. (2002) 'Broadened ligand responsiveness of androgen receptor mutants obtained by random amino acid substitution of H874 and mutation hot spot T877 in prostate cancer', *Int J Cancer*, 100(3), pp. 309-17.

Steketee, K., Ziel-van der Made, A.C., van der Korput, H.A., Houtsmuller, A.B. and Trapman, J. (2004) 'A bioinformatics-based functional analysis shows that the specifically androgen-regulated gene SARG contains an active direct repeat androgen response element in the first intron', *J Mol Endocrinol*, 33(2), pp. 477-91.

Stockley, J., Markert, E., Zhou, Y., Robson, C.N., Elliott, D.J., Lindberg, J., Leung, H.Y. and Rajan, P. (2015) 'The RNA-binding protein Sam68 regulates expression and transcription function of the androgen receptor splice variant AR-V7', *Sci Rep*, 5, p. 13426.

Stone, K.R., Mickey, D.D., Wunderli, H., Mickey, G.H. and Paulson, D.F. (1978) 'Isolation of a human prostate carcinoma cell line (DU 145)', *Int J Cancer*, 21(3), pp. 274-81.

Storm, M., Sheng, X., Arnoldussen, Y.J. and Saatcioglu, F. (2016) 'Prostate cancer and the unfolded protein response', *Oncotarget*, 7(33), pp. 54051-54066.

Stowell, S.R., Ju, T. and Cummings, R.D. (2015) 'Protein glycosylation in cancer', *Annu Rev Pathol*, 10, pp. 473-510.

Suburu, J. and Chen, Y.Q. (2012) 'Lipids and prostate cancer', *Prostaglandins Other Lipid Mediat*, 98(1-2), pp. 1-10.

Suh, J., Payvandi, F., Edelstein, L.C., Amenta, P.S., Zong, W.X., Gelinas, C. and Rabson, A.B. (2002) 'Mechanisms of constitutive NF-kappaB activation in human prostate cancer cells', *Prostate*, 52(3), pp. 183-200.

Sun, M., Yang, L., Feldman, R.I., Sun, X.M., Bhalla, K.N., Jove, R., Nicosia, S.V. and Cheng, J.Q. (2003) 'Activation of phosphatidylinositol 3-kinase/Akt pathway by androgen through interaction of p85alpha, androgen receptor, and Src', *J Biol Chem*, 278(44), pp. 42992-3000.

Sun, S., Sprenger, C.C., Vessella, R.L., Haugk, K., Soriano, K., Mostaghel, E.A., Page, S.T., Coleman, I.M., Nguyen, H.M., Sun, H., Nelson, P.S. and Plymate, S.R. (2010) 'Castration resistance in human prostate cancer is conferred by a frequently occurring androgen receptor splice variant', *J Clin Invest*, 120(8), pp. 2715-30.

Suominen, M.I., Fagerlund, K.M., Rissanen, J.P., Konkol, Y.M., Morko, J.P., Peng, Z., Alhoniemi, E.J., Laine, S.K., Corey, E., Mumberg, D., Ziegelbauer, K., Kakonen, S.M., Halleen, J., Vessella, R.L. and Scholz, A. (2017) 'Radium-223 inhibits osseous prostate cancer growth by dual targeting of cancer cells and bone microenvironment in mouse models', *Clin Cancer Res*.

Suzuki, O., Abe, M. and Hashimoto, Y. (2015) 'Sialylation by beta-galactoside alpha-2,6-sialyltransferase and N-glycans regulate cell adhesion and invasion in human anaplastic large cell lymphoma', *Int J Oncol*, 46(3), pp. 973-80.

Swindall, A.F. and Bellis, S.L. (2011) 'Sialylation of the Fas death receptor by ST6Gal-I provides protection against Fas-mediated apoptosis in colon carcinoma cells', *J Biol Chem*, 286(26), pp. 22982-90.

Swinnen, J.V., Vanderhoydonc, F., Elgamal, A.A., Eelen, M., Vercaeren, I., Joniau, S., Van Poppel, H., Baert, L., Goossens, K., Heyns, W. and Verhoeven, G. (2000) 'Selective activation of the fatty acid synthesis pathway in human prostate cancer', *Int J Cancer*, 88(2), pp. 176-9.

Tao, W., Pennica, D., Xu, L., Kalejta, R.F. and Levine, A.J. (2001) 'Wrch-1, a novel member of the Rho gene family that is regulated by Wnt-1', *Genes Dev*, 15(14), pp. 1796-807.

Taylor, A.E., Martin, R.M., Geybels, M.S., Stanford, J.L., Shui, I., Eeles, R., Easton, D., Kote-Jarai, Z., Amin Al Olama, A., Benlloch, S., Muir, K., Giles, G.G., Wiklund, F., Gronberg, H., Haiman, C.A., Schleutker, J., Nordestgaard, B.G., Travis, R.C., Neal, D., Pashayan, N., Khaw, K.T., Blot, W., Thibodeau, S., Maier, C., Kibel, A.S., Cybulski, C., Cannon-Albright, L., Brenner, H., Park, J., Kaneva, R., Batra, J., Teixeira, M.R., Pandha, H., Donovan, J. and Munafo, M.R. (2017) 'Investigating the possible causal role of coffee consumption with prostate cancer risk and progression using Mendelian randomization analysis', *Int J Cancer*, 140(2), pp. 322-328.

Taylor, B.S., Schultz, N., Hieronymus, H., Gopalan, A., Xiao, Y., Carver, B.S., Arora, V.K., Kaushik, P., Cerami, E., Reva, B., Antipin, Y., Mitsiades, N., Landers, T., Dolgalev, I., Major, J.E., Wilson, M., Socci, N.D., Lash, A.E., Heguy, A., Eastham, J.A., Scher, H.I., Reuter, V.E., Scardino, P.T., Sander, C., Sawyers, C.L. and Gerald, W.L. (2010) 'Integrative genomic profiling of human prostate cancer', *Cancer Cell*, 18(1), pp. 11-22.

Tepper, C.G., Boucher, D.L., Ryan, P.E., Ma, A.H., Xia, L., Lee, L.F., Pretlow, T.G. and Kung, H.J. (2002) 'Characterization of a novel androgen receptor mutation in a relapsed CWR22 prostate cancer xenograft and cell line', *Cancer Res*, 62(22), pp. 6606-14.

Terry, S. and Beltran, H. (2014) 'The many faces of neuroendocrine differentiation in prostate cancer progression', *Front Oncol*, 4, p. 60.

Tevz, G., McGrath, S., Demeter, R., Magrini, V., Jeet, V., Rockstroh, A., McPherson, S., Lai, J., Bartonicek, N., An, J., Batra, J., Dinger, M.E., Lehman, M.L., Williams, E.D. and Nelson, C.C. (2016) 'Identification of a novel fusion transcript between human relaxin-1 (RLN1) and human relaxin-2 (RLN2) in prostate cancer', *Mol Cell Endocrinol*, 420, pp. 159-68.

Thiery, J.P. and Sleeman, J.P. (2006) 'Complex networks orchestrate epithelial-mesenchymal transitions', *Nat Rev Mol Cell Biol*, 7(2), pp. 131-42.

Thompson, V.C., Morris, T.G., Cochrane, D.R., Cavanagh, J., Wafa, L.A., Hamilton, T., Wang, S., Fazli, L., Gleave, M.E. and Nelson, C.C. (2006) 'Relaxin becomes upregulated during prostate cancer progression to androgen independence and is negatively regulated by androgens', *Prostate*, 66(16), pp. 1698-709.

Tomlins, S.A., Mehra, R., Rhodes, D.R., Cao, X., Wang, L., Dhanasekaran, S.M., Kalyana-Sundaram, S., Wei, J.T., Rubin, M.A., Pienta, K.J., Shah, R.B. and Chinnaiyan, A.M. (2007) 'Integrative molecular concept modeling of prostate cancer progression', *Nat Genet*, 39(1), pp. 41-51.

Tran, C., Ouk, S., Clegg, N.J., Chen, Y., Watson, P.A., Arora, V., Wongvipat, J., Smith-Jones, P.M., Yoo, D., Kwon, A., Wasielewska, T., Welsbie, D., Chen, C.D., Higano, C.S., Beer, T.M., Hung, D.T., Scher, H.I., Jung, M.E. and Sawyers, C.L. (2009) 'Development of a second-generation antiandrogen for treatment of advanced prostate cancer', *Science*, 324(5928), pp. 787-90.

Trapnell, C., Williams, B.A., Pertea, G., Mortazavi, A., Kwan, G., van Baren, M.J., Salzberg, S.L., Wold, B.J. and Pachter, L. (2010) 'Transcript assembly and quantification by RNA-Seq reveals unannotated transcripts and isoform switching during cell differentiation', *Nat Biotechnol*, 28(5), pp. 511-5.

Traving, C. and Schauer, R. (1998) 'Structure, function and metabolism of sialic acids', *Cell Mol Life Sci*, 54(12), pp. 1330-49.

Travis, R.C., Appleby, P.N., Martin, R.M., Holly, J.M., Albanes, D., Black, A., Bueno-de-Mesquita, H.B., Chan, J.M., Chen, C., Chirlaque, M.D., Cook, M.B., Deschasaux, M., Donovan, J.L., Ferrucci, L., Galan, P., Giles, G.G., Giovannucci, E.L., Gunter, M.J., Habel, L.A., Hamdy, F.C., Helzlsouer, K.J., Hercberg, S., Hoover, R.N., Janssen, J.A., Kaaks, R., Kubo, T., Le Marchand, L., Metter, E.J., Mikami, K., Morris, J.K., Neal, D.E., Neuhouser, M.L., Ozasa, K., Palli, D., Platz, E.A., Pollak, M.N., Price, A.J., Roobol, M.J., Schaefer, C., Schenk, J.M., Severi, G., Stampfer, M.J., Stattin, P., Tamakoshi, A., Tangen, C.M., Touvier, M., Wald, N.J., Weiss, N.S., Ziegler, R.G., Key, T.J. and Allen, N.E. (2016) 'A Meta-analysis of Individual Participant Data Reveals an Association

between Circulating Levels of IGF-I and Prostate Cancer Risk', *Cancer Res*, 76(8), pp. 2288-300.

Tucci, M., Bertaglia, V., Vignani, F., Buttigliero, C., Fiori, C., Porpiglia, F., Scagliotti, G.V. and Di Maio, M. (2016) 'Addition of Docetaxel to Androgen Deprivation Therapy for Patients with Hormone-sensitive Metastatic Prostate Cancer: A Systematic Review and Meta-analysis', *Eur Urol*, 69(4), pp. 563-73.

Twillie, D.A., Eisenberger, M.A., Carducci, M.A., Hseih, W.S., Kim, W.Y. and Simons, J.W. (1995) 'Interleukin-6: a candidate mediator of human prostate cancer morbidity', *Urology*, 45(3), pp. 542-9.

van Soest, R.J., Nieuweboer, A.J., de Morree, E.S., Chitu, D., Bergman, A.M., Goey, S.H., Bos, M.M., van der Meer, N., Hamberg, P., de Wit, R. and Mathijssen, R.H. (2015) 'The influence of prior novel androgen receptor targeted therapy on the efficacy of cabazitaxel in men with metastatic castration-resistant prostate cancer', *Eur J Cancer*, 51(17), pp. 2562-9.

Vankemmelbeke, M., Chua, J.X. and Durrant, L.G. (2016) 'Cancer cell associated glycans as targets for immunotherapy', *Oncoimmunology*, 5(1), p. e1061177.

Varambally, S., Yu, J., Laxman, B., Rhodes, D.R., Mehra, R., Tomlins, S.A., Shah, R.B., Chandran, U., Monzon, F.A., Becich, M.J., Wei, J.T., Pienta, K.J., Ghosh, D., Rubin, M.A. and Chinnaiyan, A.M. (2005) 'Integrative genomic and proteomic analysis of prostate cancer reveals signatures of metastatic progression', *Cancer Cell*, 8(5), pp. 393-406.

Vasaitis, T., Belosay, A., Schayowitz, A., Khandelwal, A., Chopra, P., Gediya, L.K., Guo, Z., Fang, H.B., Njar, V.C. and Brodie, A.M. (2008) 'Androgen receptor inactivation contributes to antitumor efficacy of 17{alpha}-hydroxylase/17,20-lyase inhibitor 3beta-hydroxy-17-(1H-benzimidazole-1-yl)androsta-5,16-diene in prostate cancer', *Mol Cancer Ther*, 7(8), pp. 2348-57.

Venables, J.P. (2004) 'Aberrant and alternative splicing in cancer', *Cancer Res*, 64(21), pp. 7647-54.

Verrijdt, G., Haelens, A. and Claessens, F. (2003) 'Selective DNA recognition by the androgen receptor as a mechanism for hormone-specific regulation of gene expression', *Mol Genet Metab*, 78(3), pp. 175-85.

Vinall, R.L., Mahaffey, C.M., Davis, R.R., Luo, Z., Gandour-Edwards, R., Ghosh, P.M., Tepper, C.G. and de Vere White, R.W. (2011) 'Dual blockade of PKA and NF-kappaB inhibits H2 relaxin-mediated castrate-resistant growth of prostate cancer sublines and induces apoptosis', *Horm Cancer*, 2(4), pp. 224-38.

Visvader, J.E. and Lindeman, G.J. (2012) 'Cancer stem cells: current status and evolving complexities', *Cell Stem Cell*, 10(6), pp. 717-28.

Wallen, M.J., Linja, M., Kaartinen, K., Schleutker, J. and Visakorpi, T. (1999) 'Androgen receptor gene mutations in hormone-refractory prostate cancer', *J Pathol*, 189(4), pp. 559-63.

Wang, L., Lin, Y., Meng, H., Liu, C., Xue, J., Zhang, Q., Li, C., Zhang, P., Cui, F., Chen, W. and Jiang, A. (2016a) 'Long non-coding RNA LOC283070 mediates the transition of LNCaP cells into androgen-independent cells possibly via CAMK1D', *Am J Transl Res*, 8(12), pp. 5219-5234.

Wang, L., Liu, Y., Wu, L. and Sun, X.L. (2016b) 'Sialyltransferase inhibition and recent advances', *Biochim Biophys Acta*, 1864(1), pp. 143-53.

Wang, L., Zhang, M., Tan, K., Guo, Y., Tong, H., Fan, X., Fang, K. and Li, R. (2014a) 'Preparation of nanobubbles carrying androgen receptor siRNA and their inhibitory effects on androgen-independent prostate cancer when combined with ultrasonic irradiation', *PLoS One*, 9(5), p. e96586.

Wang, P.H., Li, Y.F., Juang, C.M., Lee, Y.R., Chao, H.T., Tsai, Y.C. and Yuan, C.C. (2001) 'Altered mRNA expression of sialyltransferase in squamous cell carcinomas of the cervix', *Gynecol Oncol*, 83(1), pp. 121-7.

Wang, Q., Li, W., Zhang, Y., Yuan, X., Xu, K., Yu, J., Chen, Z., Beroukhim, R., Wang, H., Lupien, M., Wu, T., Regan, M.M., Meyer, C.A., Carroll, J.S., Manrai, A.K., Janne, O.A., Balk, S.P., Mehra, R., Han, B., Chinnaiyan, A.M., Rubin, M.A., True, L., Fiorentino, M., Fiore, C., Loda, M., Kantoff, P.W., Liu, X.S. and Brown, M. (2009a) 'Androgen receptor regulates a distinct transcription program in androgen-independent prostate cancer', *Cell*, 138(2), pp. 245-56.

Wang, Q.B., Li, W., Liu, X.S., Carroll, J.S., Janne, O.A., Keeton, E.K., Chinnaiyan, A.M., Pienta, K.J. and Brown, M. (2007) 'A hierarchical network of transcription factors governs androgen receptor-dependent prostate cancer growth', *Molecular Cell*, 27(3), pp. 380-392.

Wang, R., Lin, W., Lin, C., Li, L., Sun, Y. and Chang, C. (2016c) 'ASC-J9((R)) suppresses castration resistant prostate cancer progression via degrading the enzalutamide-induced androgen receptor mutant AR-F876L', *Cancer Lett*, 379(1), pp. 154-60.

Wang, X., Chen, J., Li, Q.K., Peskoe, S.B., Zhang, B., Choi, C., Platz, E.A. and Zhang, H. (2014b) 'Overexpression of alpha (1,6) fucosyltransferase associated with aggressive prostate cancer', *Glycobiology*, 24(10), pp. 935-44.

Wang, Z., Gerstein, M. and Snyder, M. (2009b) 'RNA-Seq: a revolutionary tool for transcriptomics', *Nat Rev Genet*, 10(1), pp. 57-63.

Wei, A., Fan, B., Zhao, Y., Zhang, H., Wang, L., Yu, X., Yuan, Q., Yang, D. and Wang, S. (2016) 'ST6Gal-I overexpression facilitates prostate cancer progression via the PI3K/Akt/GSK-3beta/beta-catenin signaling pathway', *Oncotarget*, 7(40), pp. 65374-65388.

Weijers, C.A., Franssen, M.C. and Visser, G.M. (2008) 'Glycosyltransferase-catalyzed synthesis of bioactive oligosaccharides', *Biotechnol Adv*, 26(5), pp. 436-56.

Weinstein, J.N., Collisson, E.A., Mills, G.B., Shaw, K.R., Ozenberger, B.A., Ellrott, K., Shmulevich, I., Sander, C. and Stuart, J.M. (2013) 'The Cancer Genome Atlas Pan-Cancer analysis project', *Nat Genet*, 45(10), pp. 1113-20.

Welti, J., Rodrigues, D.N., Sharp, A., Sun, S., Lorente, D., Riisnaes, R., Figueiredo, I., Zafeiriou, Z., Rescigno, P., de Bono, J.S. and Plymate, S.R. (2016) 'Analytical Validation and Clinical Qualification of a New Immunohistochemical Assay for Androgen Receptor Splice Variant-7 Protein Expression in Metastatic Castration-resistant Prostate Cancer', *Eur Urol*, 70(4), pp. 599-608.

Wen, S., Niu, Y., Lee, S.O. and Chang, C. (2014) 'Androgen receptor (AR) positive vs negative roles in prostate cancer cell deaths including apoptosis, anoikis, entosis, necrosis and autophagic cell death', *Cancer Treat Rev*, 40(1), pp. 31-40.

Wen, Y., Hu, M.C., Makino, K., Spohn, B., Bartholomeusz, G., Yan, D.H. and Hung, M.C. (2000) 'HER-2/neu promotes androgen-independent survival and growth of prostate cancer cells through the Akt pathway', *Cancer Res*, 60(24), pp. 6841-5.

WHO International Programme on Chemical Safety Biomarkers in Risk Assessment: Validity and Validation. (2001). Available at: http://www.inchem.org/documents/ehc/ehc/ehc222.htm. (Accessed: 15/03/2017).

Wild, P.J., Herr, A., Wissmann, C., Stoehr, R., Rosenthal, A., Zaak, D., Simon, R., Knuechel, R., Pilarsky, C. and Hartmann, A. (2005) 'Gene expression profiling of progressive papillary noninvasive carcinomas of the urinary bladder', *Clin Cancer Res*, 11(12), pp. 4415-29.

Wilkinson, T.N., Speed, T.P., Tregear, G.W. and Bathgate, R.A. (2005) 'Evolution of the relaxin-like peptide family', *BMC Evol Biol*, 5, p. 14.

Wu, C. and Huang, J. (2007) 'Phosphatidylinositol 3-kinase-AKT-mammalian target of rapamycin pathway is essential for neuroendocrine differentiation of prostate cancer', *J Biol Chem*, 282(6), pp. 3571-83.

Wu, V.J., Pang, D., Tang, W.W., Zhang, X., Li, L. and You, Z. (2017) 'Obesity, age, ethnicity, and clinical features of prostate cancer patients', *Am J Clin Exp Urol*, 5(1), pp. 1-9.

Wu, X., Daniels, G., Lee, P. and Monaco, M.E. (2014) 'Lipid metabolism in prostate cancer', *Am J Clin Exp Urol*, 2(2), pp. 111-20.

Xiao, Y., Han, J., Wang, Q., Mao, Y., Wei, M., Jia, W. and Wei, L. (2017) 'A Novel Interacting Protein SERP1 Regulates the N-Linked Glycosylation and Function of GLP-1 Receptor in the Liver', *J Cell Biochem*, 118(11), pp. 3616-3626.

Xu, J., Lamouille, S. and Derynck, R. (2009) 'TGF-beta-induced epithelial to mesenchymal transition', *Cell Res*, 19(2), pp. 156-72.

Yamaguchi, A., Hori, O., Stern, D.M., Hartmann, E., Ogawa, S. and Tohyama, M. (1999) 'Stress-associated endoplasmic reticulum protein 1 (SERP1)/Ribosome-associated membrane protein 4 (RAMP4) stabilizes membrane proteins during stress and facilitates subsequent glycosylation', *J Cell Biol*, 147(6), pp. 1195-204.

Yamamoto, Y., Lin, P.J., Beraldi, E., Zhang, F., Kawai, Y., Leong, J., Katsumi, H., Fazli, L., Fraser, R., Cullis, P.R. and Gleave, M. (2015) 'siRNA Lipid Nanoparticle Potently Silences Clusterin and Delays Progression When Combined with Androgen Receptor Cotargeting in Enzalutamide-Resistant Prostate Cancer', *Clin Cancer Res*, 21(21), pp. 4845-55.

Yan, Q. and Lennarz, W.J. (2002) 'Studies on the function of oligosaccharyl transferase subunits: a glycosylatable photoprobe binds to the luminal domain of Ost1p', *Proc Natl Acad Sci U S A*, 99(25), pp. 15994-9.

Yang, F., Chen, Y., Shen, T., Guo, D., Dakhova, O., Ittmann, M.M., Creighton, C.J., Zhang, Y., Dang, T.D. and Rowley, D.R. (2014) 'Stromal TGF-beta signaling induces AR activation in prostate cancer', *Oncotarget*, 5(21), pp. 10854-69.

Yang, F., Tuxhorn, J.A., Ressler, S.J., McAlhany, S.J., Dang, T.D. and Rowley, D.R. (2005) 'Stromal expression of connective tissue growth factor promotes angiogenesis and prostate cancer tumorigenesis', *Cancer Res*, 65(19), pp. 8887-95.

Yeung, K.T. and Yang, J. (2017) 'Epithelial-mesenchymal transition in tumor metastasis', *Mol Oncol*, 11(1), pp. 28-39.

Yki-Jarvinen, H., Wahlstrom, T. and Seppala, M. (1983) 'Immunohistochemical demonstration of relaxin in the genital tract of men', *J Reprod Fertil*, 69(2), pp. 693-5.

Young, M.D., Wakefield, M.J., Smyth, G.K. and Oshlack, A. (2010) 'Gene ontology analysis for RNA-seq: accounting for selection bias', *Genome Biol*, 11(2), p. R14.

Yu, S., Xia, S., Yang, D., Wang, K., Yeh, S., Gao, Z. and Chang, C. (2013) 'Androgen receptor in human prostate cancer-associated fibroblasts promotes prostate cancer epithelial cell growth and invasion', *Med Oncol*, 30(3), p. 674.

Zeng, C.M., Chang, L.L., Ying, M.D., Cao, J., He, Q.J., Zhu, H. and Yang, B. (2017) 'Aldo-Keto Reductase AKR1C1-AKR1C4: Functions, Regulation, and Intervention for Anti-cancer Therapy', *Front Pharmacol*, 8, p. 119.

Zhang, C., Chua, B.E., Yang, A., Shabanpoor, F., Hossain, M.A., Wade, J.D., Rosengren, K.J., Smith, C.M. and Gundlach, A.L. (2015a) 'Central relaxin-3 receptor (RXFP3) activation reduces elevated, but not basal, anxiety-like behaviour in C57BL/6J mice', *Behav Brain Res*, 292, pp. 125-32.

Zhang, L., Altuwaijri, S., Deng, F., Chen, L., Lal, P., Bhanot, U.K., Korets, R., Wenske, S., Lilja, H.G., Chang, C., Scher, H.I. and Gerald, W.L. (2009) 'NF-kappaB regulates androgen receptor expression and prostate cancer growth', *Am J Pathol*, 175(2), pp. 489-99.

Zhang, Q., Liu, S.H., Erikson, M., Lewis, M. and Unemori, E. (2002) 'Relaxin activates the MAP kinase pathway in human endometrial stromal cells', *J Cell Biochem*, 85(3), pp. 536-44.

Zhang, S., Lu, J., Xu, Z., Zou, X., Sun, X., Xu, Y., Shan, A., Lu, J., Yan, X., Cui, Y., Yan, W., Du, Y., Gu, J., Zheng, M., Feng, B. and Zhang, Y. (2017) 'Differential expression of ST6GAL1 in the tumor progression of colorectal cancer', *Biochem Biophys Res Commun*, 486(4), pp. 1090-1096.

Zhang, X., Coleman, I.M., Brown, L.G., True, L.D., Kollath, L., Lucas, J.M., Lam, H.M., Dumpit, R., Corey, E., Chery, L., Lakely, B., Higano, C.S., Montgomery, B., Roudier, M., Lange, P.H., Nelson, P.S., Vessella, R.L. and Morrissey, C. (2015b) 'SRRM4 Expression and the Loss of REST Activity May Promote the Emergence of the Neuroendocrine Phenotype in Castration-Resistant Prostate Cancer', *Clin Cancer Res*, 21(20), pp. 4698-708.

Zhang, X., Morrissey, C., Sun, S., Ketchandji, M., Nelson, P.S., True, L.D., Vakar-Lopez, F., Vessella, R.L. and Plymate, S.R. (2011) 'Androgen receptor variants occur frequently in castration resistant prostate cancer metastases', *PLoS One*, 6(11), p. e27970.

Zhang, X., Pan, C., Zhou, L., Cai, Z., Zhao, S. and Yu, D. (2016) 'Knockdown of ST6Gal-I increases cisplatin sensitivity in cervical cancer cells', *BMC Cancer*, 16(1), p. 949.

Zhu, Y., Srivatana, U., Ullah, A., Gagneja, H., Berenson, C.S. and Lance, P. (2001) 'Suppression of a sialyltransferase by antisense DNA reduces invasiveness of human colon cancer cells in vitro', *Biochim Biophys Acta*, 1536(2-3), pp. 148-60.

Appendix A

Genes up-regulated in response to androgen treatment in LNCaP cells, but down-regulated in 7 PCa patient samples post ADT.

Gene	Information
AACS	Fatty acid synthesis
ABAT	GABA catabolism
ABCC4	May be an organic anion pump relevant to cellular detoxification
ABHD11	Protein containing an alpha/beta hydrolase fold domain. Lung cancer
ABHD2	Migration. Enzyme alpha/beta hydrolase fold
ACAA1	Acetyl-CoA acyltransferase 1. Beta-oxidation system of the peroxisomes
ACACA	Acetyl-CoA carboxylase. Long chain fatty acid biogenesis
ACAD8	Acyl-CoA dehydrogenase family member 8 mitochondrial enzyme
ACLY	Enzyme responsible for the synthesis of cytosolic acetyl-CoA
ACP2	Lysosomal acid phosphatase
ACSL1	Activation of long-chain fatty acids
ACSL3	Acyl-CoA synthetases (ACSL) activates long-chain fatty acids
ACSM1	Fatty acid:CoA ligase activity. Acyl-CoA Synthetase2
ACSM3	Fatty acid:CoA ligase activity
ADAM9	Probable zinc protease. May mediate cell-cell or cell-matrix interactions
ADI1	Aci-reductone dioxygenase. mRNA processing
ADIPOR1	Fatty acid catabolism and glucose levels
ADM2	Calcitonin-related hormones. Homeostasis. CRLR/RAMP receptor
ADRB1	Activation of adenylate cyclase
ADRBK1	Key regulator of LPAR1 signaling
AFF3	Putative transcription activator
AGR2	Proto-oncogene that may play a role in cell migration, cell differentiation and cell growth
AGTRAP	Negative regulator of type-1 angiotensin II
AK4	Adenylate Kinase 4. Protein is localised to the mitochondrial matrix.
AKR1A1	Catalyzes the NADPH-dependent reduction
ALDH1A3	Aldehyde dehydrogenase
ALDH4A1	Mitochondrial matrix NAD-dependent dehydrogenase
ALG2	Glycosyltransferase
ALG5	N-linked glycosylation
ALOX15	Metabolism of fatty acid hydroperoxidases
AMACR	Alpha-methylacyl-CoA racemase
AMD1	Intermediate enzyme in polyamine biosynthesis. Proliferation
ANO7	Prostate specific may play a role in cell-cellinteractions
AP1B1	Role in protein sorting in the late-Golgi/trans-Golgi network (TGN) and/or endosomes
AP2S1	Protein transport. Vescicles. Component of the adaptor protein complex 2 (AP-2)
APLN	Endogenous ligand for the G protein coupled receptor APJ
ARF4	GTP-binding protein. Protein trafficking vesicle budding and uncoating within the golgi
ARFGAP3	GTPase-activating protein (GAP) for ADP ribosylation factor
ARFIP2	Involved in membrane ruffling
ARHGEF26	Rho-guanine nucleotide exchange factor
ARSD	Sulfatase localized to the lysosome

ASRGL1	L-asparaginase and beta-aspartyl peptidase
ATG101	Autophagy
ATP10A	P-type cation transport ATPases
ATP11B	P-type ATPases. Transport of ions across membranes
ATP6V0B	V-ATPase dependent organelle acidification
ATP6V1G1	Component of vacuolar ATPase (V-ATPase)
ATXN1	Chromatin-binding factor that repress Notch signaling
AZGP1	Lipd degradation. May bind polyunsaturated fatty acids
AZGP1P1	Pseudogene, and is affiliated with the lncRNA class
B3GAT1	Glucuronyltransferase
B4GALT1	One of seven beta-1,4-galactosyltransferase (beta4GalT) genes
BAIAP2	CDC42-mediated reorganization of the actin cytoskeleton and for RAC1-mediated membrane ruffling
BDH1	Homotetrameric lipid-requiring enzyme of the mitochondrial membrane
BEND4	BEN domain containing 4
BHLHA15	Plays a role in controlling the transcriptional activity of MYOD1. Gene expression. mitochondrial calcium ion transport
BLOC1S5	Component of biogenesis of lysosome-related organelles complex 1
BMPR1B	Bone morphogenetic protein (BMP) receptor family of transmembrane serine/threonine kinases. TGF-beta
BNIP3	Mitochondrial protein. Pro-apoptotic factor
BZW1	Enhances histone H4 gene transcription
C14orf1	Probable ergosterol biosynthetic protein
C19orf10	Not characterised
C19orf48	Not characterised
C1orf116	Putative androgen-specific receptor
C1orf210	May be involved in membrane trafficking between endosomes and plasma membrane
C1orf85	GLMP glycosylated lysosomal membrane protein
C1QTNF3	C1q And tumor necrosis factor related protein 3
C9orf152	Not characterised
C9orf91	Transmembrane protein
CALR	Calcium-binding chaperone. Lectin that interacts with glycoproteins in ER
CAMK1	Calcium/calmodulin-dependent protein kinase I
CAMKK2	Calcium/calmodulin-dependent protein kinase
CANT1	Calcium-dependent nucleotidase
CCDC167	Transmembrane and coiled-coil domain-containing protein
CD320	Uptake of transcobalamin bound cobalamin (vitamin B12
CDYL2	Linked to prostate cancer. Methylated histone residue binding
CECR6	Cat Eye Syndrome chromosome region, candidate 61
CENPN	Mitosis
CHCHD1	mitochondrial protein
CHP1	Calcium-binding protein involved in different processes such as regulation of vesicular trafficking
CHPF	3-Beta-glucuronosyltransferase
CHRNA2	Nicotinic acetylcholine receptors. Opening of an ion-conducting channel across the plasma membrane
CKAP4	Anchoring of ER to microtubules. Golgi. Cytoskelton
CLDN3	Role in tight junctions. Calcium dependent adhesion
CLDN8	Plays a major role in tight junction-specific obliteration of the intercellular space
CLGN	Calmegin is a testis-specific endoplasmic reticulum chaperone protein. Spermatogenesis

CLPP	Mitochondrial protein
CLPTM1L	Enhances cisplatin-mediated apoptosis when overexpressed. Breast cancer
CLTC	Clathrin is the major protein of the polyhedral coat of coated pits and vesicles
CMC2	Mitochondrial protein
CNDP2	Non-specific dipeptidase. Tumor suppressor in hepatocellular carcinoma
CNTNAP2	Saltatory conduction of nerve impulses in myelinated nerve fibres
COA3	Mitochondrial protein
COPB1	p53, AKT activation and promotion of cell survival
COPB2	Reversibly associates with Golgi non-clathrin-coated vesicles. Mediate biosynthetic protein transport from the ER
COPE	Subunit of coatomer protein complex. Golgi. Vesicles
COPG1	Reversibly associates with Golgi non-clathrin-coated vesicles. Mediate biosynthetic protein transport from the ER
CORO1B	Cell motility
CORO2A	Member of the WD repeat protein family. Cell cycle?
COX7A2	Nuclear-coded polypeptide chains of cytochrome c oxidase, the terminal oxidase in mitochondrial electron transport
COX7B	Cytochrome c oxidase (COX), the terminal component of the mitochondrial respiratory chain
COX8A	Mitochondrial protein
CPT1A	Mitochondrial protein
CREB3L4	Transcriptional activator
CRELD2	May regulate transport of alpha4-beta2 neuronal acetylcholine receptor
CRISP3	Cysteine-rich secretory protein 3
CRLS1	Cardiolipin Synthase
CSGALNACT1	Chondroitin sulfate N-acetylgalactosaminyltransferase
CTBS	Lysosomal glycosidase
CYB561	Transmembrane electron transfer carrier and *ferric-chelate reductase activity*
CYP51A1	ER protein. member of the cytochrome P450 superfamily of enzymes. Synthesis of cholesterol, sterods and other lipds
DAP	Mediator of programmed cell death induced by interferon gamma
DBI	Binds medium- and long-chain acyl-CoA esters. GABA receptor
DCAF6	Transcriptional activity of NR3C1 and AR
DCXR	Uronate cycle of glucose metabolism
DDAH1	Role in nitric oxide generation
DEGS1	Migration, membrane fatty acids
DGKD	Diacylglycerol kinases
DHCR24	Oxidoreductase
DHCR7	Production of cholesterol
DLX1	Regulator of signals from multiple TGFB superfamily members
DNAJB11	Soluble glycoprotein of the ER lumen required for the proper folding and assembly of proteins
DNAJC10	ER disulfide reductase. Protein folding and degradation. ER quality control
DNAJC3	Unfolded protein response (UPR) during ER stress. May inhibit EIF2AK3/PERK activity
DSC2	Glycoprotein. Adhesion
DUS1L	Catalyzes the synthesis of dihydrouridine in D-loop of most tRNAs
EAF2	Testosterone-regulated apoptosis inducer. Transcriptional transactivator
EBP	Integral membrane protein of the endoplasmic reticulum
ECI1	Mitochondrial protein
EDEM3	Glycoenzyme

EEF1E1	Eukaryotic translation elongation factor 1 epsilon 1
EGF	Receptor tyrosine kinase of the ErbB family. Involved in gene expression and cell proliferation
EIF4G1	Translation
ELK4	Transcription
ELL2	RNA Polymerase II Elongation Factor ELL22. Increase the catalytic rate of RNA polymerase II transcription
ELOVL1	Fatty acid metabolism
ELOVL2	Catalyzes the synthesis of polyunsaturated very long chain fatty
ELOVL5	Role in elongation of long-chain polyunsaturated fatty acids
ELOVL7	Enzyme that catalyzes the synthesis of saturated and polyunsaturated very long chain fatty acids
ELP6	Transcriptional elongation
EMC7	ER membrane comples protein
ENDOD1	May act as a DNase and a RNase
ENTPD2	E-NTPDases are a family of ecto-nucleosidases that hydrolyze 5'-triphosphates
ENTPD6	Might support glycosylation reactions in the Golgi apparatus
EPHX2	Binds to specific epoxides and converts them to the corresponding dihydrodiols
ERBB3	Over expressed in prostate cancer. EGFR family
ERGIC1	Possible role in transport between endoplasmic reticulum and Golgi
ERLEC1	Probable lectin that binds selectively to improperly folded lumenal proteins
ERP44	ER protein. role in the control of oxidative protein folding in the endoplasmic reticulum
ESRP2	mRNA splicing factor. EMT isoforms. CD44. catenin
F2RL1	Coagulation factor II (thrombin) receptor-like 1. Inflammatory responses
F5	Hemostasis
FAAH	Fatty acid metabolism
FADS1	Fatty acid desaturase
FADS2	Fatty acid desaturase
FAM111B	Cancer-associated nucleoprotein
FAM174B	Membrane protein
FAM189A2	Family with sequence similarity 189, member A21
FAR2P1	Fatty Acyl CoA reductase 2 pseudogene
FAR2P2	lncRNA. Fatty Acyl CoA reductase 2 pseudogene 21
FASN	Fatty acid synthetase
FDFT1	First specific enzyme in cholesterol biosynthesis
FECH	Mitochondrial protein
FGFR3	Tyrosine-protein kinase. Cell-surface receptor for fibroblast growth factors. Cell proliferation and apoptosis
FGFRL1	Fibroblast growth factor receptor
FICD	Adenylyltransferase
FKBP2	Protein folding and trafficking
FKBP5	Protein folding and trafficking. Intracellular trafficking of heterooligomeric forms of steroid hormone receptors
FLJ20021	Not characterised
FURIN	Protease process protein and peptide precursors trafficking
FUT1	Galactoside 2-L-fucosyltransferase enzyme
FXYD3	FXYD-domain containing regulators of Na+/K+ ATPases
FZD5	Receptor for Wnt proteins
FZD8	Receptor for Wnt proteins
G3BP2	mRNA transport? GTPase-activating protein

GABRB3	GABA. Ligand-gated ionic channel family
GABRG3	Gamma-aminobutyric acid (GABA) receptor
GALNT7	Glycopeptide transferase involved in O-linked oligosaccharide biosynthesis
GCAT	Glycine C-acetyltransferase
GCNT1	Glycosyltransferase
GCNT2	Branching enzyme that converts linear into branched poly-N-acetyllactosaminoglycans
GGT1	Type I gamma-glutamyltransferase. Metabolism
GLB1L2	Galactosidase, beta 1-like 2
GLUD1	Mitochondrial protein
GMDS	Catalyzes the conversion of GDP-D-mannose to GDP-4-dehydro-6-deoxy-D-mannose
GNB2	Guanine nucleotide-binding proteins (G proteins). Transmembrane signalling
GNPNAT1	Metabolism. Glucosamine-phosphate N-acetyltransferase
GOLM1	Golgi membrane protein 1
GOLPH3	Role in golgi membrane trafficking and could indirectly give its flattened shape to the Golgi apparatus
GOT2	Mitochondrial protein. Long chain fatty acids
GPT2	Amino acid metabolism and gluconeogenesis
GREB1	May play a role in estrogen-stimulated cell proliferation
GRHL2	May function as a transcription factor
GRIN3A	Subunit of the N-methyl-D-aspartate (NMDA) receptors
GSKIP	Wnt signaling pathway. Retinoic acid
GSTZ1	Metabolism. Glutathione S-transferase
GTF3C6	Involved in RNA polymerase III-mediated transcription. General transcription factor
GUCY1A3	Guanylate cyclases conversion of GTP to 3',5'-cyclic GMP and pyrophosphate
H1F0	Histones H1 are necessary for the condensation of nucleosome chains into higher-order structures
H2AFJ	Core component of nucleosome
HEBP2	Can promote mitochondrial permeability transition and facilitate necrotic cell death under stress conditions
HERPUD1	ER quality control
HGD	Enzyme homogentisate 1,2 dioxygenase. This enzyme is involved in the catabolism amino acids
HID1	Downregulated in cancer
HINT1	Hydrolyze substrates such as AMP-morpholidate. Transcription. P53
HIPK2	Serine/threonine-protein kinase. Transcription regulation, p53 mediated cellular apoptosis. Cell cycle
HIST1H1C	Histone cluster 1, H1c. Gene expression
HIST1H2BJ	Histone cluster 1, H2bj. Core component of nucleosome. Gene expression
HIST1H2BK	Histone cluster 1, H2bk. Core component of nucleosome. Gene expression
HIST2H2BE	Transcription regulation
HM13	Catalyzes intramembrane proteolysis of some signal peptides
HMG20B	Mitosis
HMGCR	Transmembrane glycoprotein that is the rate-limiting enzyme in cholesterol biosynthesis
HMGCS1	This enzyme condenses acetyl-CoA with acetoacetyl-CoA to form HMG-CoA
HMGCS2	Mitochondrial enzyme
HMGXB3	HMG box domain containing 3. Transcription factor?
HN1L	Hematological and neurological expressed 1-like protein2
HOMER2	Postsynaptic density scaffolding protein. Calcium. PIK3
HPN	Prostate cancer. Cell growth. Transmembrane serine protease
HSD17B4	Bifunctional enzyme acting on the peroxisomal beta-oxidation pathway for fatty acids

HSP90B1	Processing transport of secreted proteins. Tumour formation
HSPA5	Involved in the folding and assembly of proteins in the ER
HYOU1	Protein folding and secretion in the ER. Invasiveness
ICA1	May play a role in neurotransmitter secretion. Membrane bound in golgi
IDE	Peptide signaling
IDH1	Isocitrate dehydrogenases catalyze the oxidative decarboxylation of isocitrate to 2-oxoglutarate
IDH2	Metabolism and energy production
IDI1	Cholesterol
IER3IP1	Apoptosis. Golgi. ER. Protein transport
IMPDH1	Cell growth. de novo synthesis of guanine nucleotides
INSIG1	Oxysterols regulate cholesterol homeostasis. Insulin induced. ER membrane protein
IQGAP2	IQGAP family. Cytoskeleton, cell adhesion
JAM3	Adhesion, migration
KCNN2	Forms a voltage-independent potassium channel activated by intracellular calcium
KCTD1	May repress the transcriptional activity of AP-2 family members
KDELR2	Luminal ER protein retention system required for normal vesicular traffic through the Golgi
KDM4B	Histone demethylase
KIAA1244	Not characterised
KIF22	Mitosis
KIF5C	Mediates dendritic trafficking of mRNAs. Organnelle transport
KLK15	Protease whose physiological substrate is not yet known
KLK4	Kallikrein 4
KLKP1	lncRNA. Kallikrein pseudogene
KRT18	Filament reorganization
KRT8	Intermediate filament
LCP1	Processing of triglyceride rich proteins
LDLR	Binds LDL, and transports it into cells by endocytosis. Cholesterol
LEAP2	Liver expressed antimicrobial peptide 2
LIFR	Signal-transducing molecule. benign epithelial tumor of the salivary gland. Proliferation
LIFR-AS1	LIFR antisense RNA 1
LINC00035	lncRNA
LINC00920	lncRNA
LMAN2	Type I transmembrane lectin. shuttles between ER, Golgi and plasma membrane. Binds O-glycans
LOC100294145	ncRNA
LOC101927482	antisense RNA lncRNA?
LOC440910	lncRNA
LOC81691	Putative RNA exonuclease
LPAR2	Lysophosphatidic acid (LPA) receptor and contributes to Ca2+ mobilization
LPAR3	Calcium-mobilizing lysophosphatidic
LRFN4	Leucine rich repeat and fibronectin type III domain containing 41
LRIG1	Acts as a feedback negative regulator of signaling by receptor tyrosine kinases
LRRC59	Required for nuclear import of FGF1
LRRC75B	Leucine Rich Repeat Containing 75B1
LSR	Clearance of triglyceride-rich lipoprotein from blood. Fatty acids
LSS	Catalyzes the first step in the biosynthesis of cholesterol, steroid hormones, and vitamin D
LYPLA2	Lysophospholipase acts on membrane
MAF	DNA-binding, leucine zipper-containing transcription factor

MAGED1	Involved in the apoptotic response after nerve growth factor (NGF) binding in neuronal cells. P53. Tumour specific antigen
MAGED2	Melanoma antigen family D, 2
MANF	Golgi. susceptibility to ER stress-induced death. Cell proliferation. GABA
MAOA	Mitochondrial enzymes
MAP7	Polarization and differentiation of epithelial cells during polorisation of epithelial cells
MARVELD3	As a component of tight junctions, plays a role in paracellular ion conductivity
MBOAT2	Membrane bound O-acyltransferase domain containing 2
MCCC2	Carboxyltransferase subunit of the 3-methylcrotonyl-CoA carboxylase. leucine and isovaleric acid catabolism
MESP1	Transcription factor. Mesoderm. Notch signalling
MFSD3	Major facilitator superfamily domain-containing protein
MGST3	Inflammation
MICAL2	Monooxygenase
MIEN1	Migration and invasion enhancer
MIF	Glycosylation-inhibiting factor 3 macrophage migration inhibitory factor2
MIR141	Metastatic prostate cancer
MLEC	N-glycosylation
MLPH	Melanophilin. Rab effector protein involved in melanosome transport
MMAB	Conversion of vitamin B(12) into AdoCbl
MPC2	Mitochondrial protein
MRPL36	Component of the large subunit of the mitochondrial ribosome
MRPL41	Component of the mitochondrial ribosome large subunit. Apoptosis. Cell cycle p53
MRPS18A	Mitochondrial ribosomal proteins
MRPS23	Mitochondrial protein
MRPS28	Mitochondrial ribosomal protein S28
MSMO1	Sterol-C4-mehtyl oxidase-like protein. ER localised. Cholesterol biosynthesis
MT1F	Metallothioneins have a high content of cysteine residues that bind various heavy metals
MT1X	Metallothionein
MTCH2	Mitochondrial protein
MTFP1	Mitochondia division
MTMR2	Phosphoinositide lipid phosphatase
MVD	Cholesterol biosynthesis
MYBPC1	Thick filament-associated protein
NAA35	N(alpha)-acetyltransferase. Acetylation of N-terminal methionine residues
NAAA	Degrades bioactive fatty acid amides to their corresponding acids
NAMPT	Nicotinic acid phosphoribosyltransferase. Metabolism, stress, ageing
NANS	Biosynthetic pathways of sialic acids
NCAPD3	Mitosis
NDRG1	Stress-responsive protein involved in hormone responses, cell growth, and differentiation. P53
NDUFA2	Accessory subunit of the mitochondrial membrane respiratory chain NADH dehydrogenase
NDUFB10	Mitochondrial protein
NDUFS6	Mitochondrial protein
NDUFV2	Mitochondrial protein
NEAT1	lncRNA
NEDD4L	E3 ubiquitin-protein ligase. Inhibits TGF-beta signaling
NEU1	Catalyzes the removal of sialic acid (N-acetylneuraminic acid) moities from glycoproteins and glycoprotein

NKX3-1	Transcription factor. Role in prostate development. Tumour suppressor in PC3 cells
NOP10	Ribosome biogenesis and telomere maintenance
NPDC1	May be involved in transcriptional regulation. Suppresses oncogenic transformation in neural and non-neural cells
NUDT9	Nudix hydrolase family. ADP-ribosepyrophosphatase
ODC1	Polyamine biosynthesis
OR7E47P	lncRNA. Olfactory receptor
ORC5	DNA replication
OSTC	Oligosaccharyltransferase complex subunit
P4HB	Disulfide bonds
PACSIN2	Intracellular vesicle-mediated transport. Endocytosis of cell surface receptors
PAK1IP1	Negatively regulates the PAK1 kinase
PANK3	Pantothenate kinase is a key regulatory enzyme in he biosynthesis of coenzyme A
PAOX	Oxidation of N(1)-acetylspermine to spermidine
PAQR4	Progestin And AdipoQ Receptor Family Member 42
PART1	Prostate androgen-regulated transcript 1. Antisense RNA
PASK	Serine/threonine-protein kinase involved in energy homeostasis and protein translation
PC	Mitochondrial protein
PCCA	Mitochondrial protein
PCDH1	Cadherin superfamily. Cell-cell interaction processes and in cell adhesion
PCTP	Catalyzes the transfer of phosphatidylcholine between membranes. Binds a single lipid molecule
PDE9A	Catalyzes the hydrolysis of cAMP and cGMP to their corresponding monophosphates
PDIA4	ER protein
PDIA5	Protein disulfide isomerase family A, member 5
PDIA6	Chaperone that inhibits aggregation of misfolded proteins. ER resident
PDLIM5	PDZ and LIM domains protein 2
PEBP4	Promote cellular resistance to TNF-induced apoptosis by inhibiting activation of ERK1/2 pathway
PEMT	Phosphatidylcholine (PC) is the most abundant mammalian phospholipid
PEX10	Biogenesis of peroxisomes
PGM3	Interconverts GlcNAc-6-P and GlcNAc-1-P
PHPT1	Catalyzes the reversible dephosphorylation of histidine residues in proteins
PIGH	Phosphatidylinositol glycan anchor biosynthesis
PITPNA	Phospholipase C signaling. PIK3
PLA1A	Phospholipase that hydrolyzes fatty acids
PLA2G12A	Secreted phospholipase A2 (sPLA2) enzymes liberate arachidonic acid from phospholipids
PLA2G4F	Hydrolyze phospholipids into fatty acids
PLEKHB2	Involved in retrograde transport of recycling endosomes
PMEPA1	Down-regulation of AR. Enhances ubiquitination and proteasome-mediated degradation of AR
POLR2L	Subunit of RNA polymerase II
PPAP2A	Membrane glycoprotein function in synthesis of glycerolipids and in phospholipase D-mediated signal transduction
PPAPDC2	Phosphatidic Acid Phosphatase. Immunity. Lipid
PPIB	PPIases accelerate the folding of proteins. ER. Secretion
PPP1CA	Serine/threonine phosphatase. 100s targets. Cell cycle
PPP1R7	Regulatory subunit of protein phosphatase 1. Mitosis
PPP2R2D	Mitosis

PRDX4	Peroxidase. Probably involved in redox regulation of the cell
PREB	Probable role in the regulation of pituitary gene transcription
PRSS8	Trypsinogen, serine protease, seminal fluid
PSMA2	Processing of class I MHC peptides. Proteosome subunit
PSMD8	Ptoteosome. Antigen processing
PTPLB	Protein tyrosine phosphatase like. Long chin fatty acid synthesis
PTPRJ	deP PIK3R1
PTPRN2	Protein tyrosine phosphatase. Nervous system development
PVR	Transmembrane glycoprotein. Mediates NK cell adhesion and triggers NK cell effector functions
PVRL2	Membrane glycoprotein. Cell adhesion
PVRL3	Adhesion molecules at adherens junctions
PXDN	Extracellular matrix-associated peroxidase
PYCR1	Proline biosynthesis. Oxidative stress
RAB11A	GTPase. Intracellular membrane trafficking
RAB1B	Transport between ER and golgi
RAB27A	Cytotoxic granule exocytosis
RAB3B	Protein transport, vesicle trafficing
RAB3D	Protein transport. Exocytosis
RAB3IP	Guanine nucleotide exchange factor
RABEP2	Membrane trafficking. Endosome fusion
RAC3	GTPase which belongs to the RAS superfamily. Cell growth and spreading
RAP1GAP	GTPase-activating-protein
REPS2	Regulates the endocytosis of growth factor receptors. Influence on the Ral signaling pathway
RER1	Golgi
RFPL2	Ret finger protein-like 21
RHBDD2	Rhomboid domain containing 2
RHOU	Wnt signalling, adhesion, migration
RHPN2	Rho pathway. Limit stress fiber formation. Increase turnover F actin
RNF41	Acts as E3 ubiquitin-protein ligase and regulates the degradation of target proteins
RPN1	Essential subunit of the N-oligosaccharyl transferase (OST) complex
RPN2	Essential subunit of the N-oligosaccharyl transferase (OST) complex
RWDD2A	RWD domain containing 2A
SAPCD2	Tumor specificity and mitosis phase-dependent expression protein 2
SAR1B	Involved in transport from the endoplasmic reticulum to the Golgi apparatus
SAT1	Acetyltransferase family catalyzes the acetylation of spermidine and spermine
SCAND1	May regulate the function of the transcription factor myeloid zinc finger 1B. SCAN domain
SCD	Fatty acid biosynthesis
SDK1	Cell adhesion protein that guides axonal terminals to specific synapses in developing neurons
SEC11C	Component of the microsomal signal peptidase complex
SEC14L2	Cholesterol biosynthetic pathway
SEC23B	Vesicle trafficking. Golgi to ER
SEC61A1	Plays a crucial role in the insertion of secretory and membrane polypeptides into the ER
SEC61B	The Sec61 complex is the central component of the protein translocation apparatus of the ER
SERINC2	Lung cancer
SERINC5	Enhances the incorporation of serine into phosphatidylserine and sphingolipids

SERP1	Interacts with target proteins during translocation to the ER lumen. Protects unfolded target proteinsduring ER stress
SETD7	Histone methyltransferase. Transcriptional activation of insulin
SFXN2	Potential iron transporter
SFXN5	Transports citrate. Potential iron transporter
SH3BP4	Endocytosis. mTOR signalling
SHC2	Signaling adapter that couples activated growth factor receptors to signaling pathway in neurons
SHROOM2	May be involved in endothelial cell morphology changes during cell spreading
SIL1	Required for protein translocation and folding in the endoplasmic reticulum (ER).
SIM2	Transcription factor that may be a master gene of CNS development in cooperation with Arnt
SLC15A2	Solute Carrier Family 15 (H+/Peptide Transporter
SLC1A5	Sodium-dependent neutral amino acid transporter
SLC22A23	Transport organic ions across cell membranes
SLC22A3	Mediates potential-dependent transport of a variety of organic cations
SLC25A16	Mitochondrial protein
SLC25A20	Mitochondrial protein
SLC25A33	Mitochondrial protein
SLC26A2	Sulfate transporter. Transmembrane glycoprotein
SLC27A4	Member of a family of fatty acid transport proteins, which are involved in translocation of long chain fatty acids
SLC35B1	Probable sugar transporter
SLC35E1	Putative transporter
SLC35F2	Putative solute transporter. Lung cancer
SLC39A1	Zinc uptake
SLC39A10	May act as a zinc-influx transporter
SLC39A6	May act as a zinc-influx transporter
SLC39A7	Transports zinc from the Golgi and endoplasmic reticulum to the cytoplasm. Activation of tyrosine kinases
SLC43A1	Prostate cancer associated. Transport of large neutral amino acids
SLC45A3	Prostate cancer associated
SLC50A1	Sugar transport across membranes
SLC52A2	Riboflavin transporter
SLC5A4	Sodium-dependent glucose transporter
SLC9A3R1	Scaffold protein . Wnt signalling
SLC9A3R2	Scaffold protein connects plasma membrane proteins with members of the ezrin/moesin/radixin family
SMCO4	Single-pass membrane protein
SMDT1	Essential regulatory subunit of the mitochondrial calcium uniporter complex
SMPD1	Sphingomyelin phosphodiesterase 1, acid lysosomal
SMS	Catalyzes the production of spermine from spermidine and decarboxylated S-adenosylmethionine (dcSAM)
SNAP91	Adaptins are components of the adapter complexes which link clathrin to receptors in coated vesicles
SND1	Functions as a bridging factor between STAT6 and the basal transcription factor
SNN	Plays a role in the toxic effects of organotins
SNX25	Sorting nexin. May be involved in several stages of intracellular trafficking
SOAT1	Catalyzes the formation of fatty acid-cholesterol esters
SOCS2	Cytokine signal transduction
SOCS2-AS1	JAK/STAT pathway. cytokine signaling (SOCS) family

SORD	Converts sorbitol to fructose. Sperm motility
SPDEF	ETS family of transcription factors. androgen-independent transactivator of PSA promoter. Prostate cancer
SPOCK1	May play a role in cell-cell and cell-matrix interactions
SPON2	Cell adhesion protein that promotes adhesion and outgrowth of hippocampal embryonic neurons
SPTBN2	Glutamate signaling
SQLE	Catalyzes the first oxygenation step in sterol biosynthesis
SREBF2	Transcriptional activator required for lipid homeostasis
SRM	Spermidine synthase
SRPR	Targeting and translocation across ER
SRPRB	Correct targeting of the nascent secretory proteins to the ER
SSR3	TRAP proteins regulates retention or ER resident proteins
SSR4	Translocating protein across the ER
ST14	Protease. Degrades extracellular matrix.
ST6GAL1	Siayltransferase. Generation cell surface carbohydrates
ST6GALNAC1	Metastasis, syltransferase, sialyl-Tn
STARD10	Phospholipid transfer protein
STARD3NL	Endosomal protein. Binds cholesterol
STEAP4	Metalloreductase. Metabolic homeostasis
STK39	Serine/threonine kinase, cellular stress response pathway, p38 MAPK
STPG1	Sperm-tail PG-rich repeat containing 1, apoptosis
STRA13	DNA damage repair. Mitosis
STT3A	N-glycosylation
STXBP2	Intracellular vesicle trafficking and vesicle fusion with membranes
STYK1	Tyrosine protein-kinase. Tumour cell invasion, metastasis, PIK3 signalling
SUOX	Mitochondrial protein
SURF4	Maintenance of the architecture of the endoplasmic reticulum-Golgi intermediate compartment and the golgi
SYAP1	Synapse associated protein 1
SYNGR2	Synaptogyrin family. may play a role in regulating membrane traffic
SYT7	Prostate cancer associated. Ca(2+)-dependent exocytosis of secretory vesicles
SYTL1	Vesicle trafficking
TALDO1	Transaldolase: metabolites in pentose-phosphate pathway
TARP	Regulates the trafficking and gating properties of AMPA-selective glutamate receptors
TARS	Aminoacyl-tRNA synthetases catalyze the aminoacylation of tRNA by their cognate amino acid
TBC1D16	May act as a GTPase-activating protein for Rab family protein
TBC1D30	Rab GTPase activator activity
TECPR1	Tethering factor involved in autophagy
TIGD6	Tigger transposable element derived 6
TIMM10B	Mitochondrial protein
TIMM13	Mitochondrial protein
TIMM23	Mitochondrial protein
TM9SF1	Transmembrane protein. Autophagy
TMED10	Vesicular protein trafficking
TMED2	Vesicular protein trafficking. Maintainance golgi
TMED3	Vesicular protein trafficking. Golgi
TMED9	Vesicular protein trafficking. Organization of intracellular membranes
TMEFF2	Up-regulates cancer cell proliferation, probably by promoting ERK1/2 phosphorylation

TMEM125	Breast colorectal cancer
TMEM134	Transmembrane protein
TMEM141	Transmembrane protein
TMEM251	Transmembrane protein
TMEM258	Transmembrane Protein 258
TMEM33	Transmembrane protein 33
TMEM79	Epidermal integrity
TMEM79	Transmembrane protein
TMEM87B	Transmembrane protein
TMEM8A	Cell surface adhesion
TMPRSS2	Transmembrane protease, serine 2
TMSB15A	Plays an important role in the organization of the cytoskeleton
TP53TG1	TP53 target. lncRNA
TPD52	Tumor protein D52
TRAPPC5	May play a role in vesicular transport from endoplasmic reticulum to Golgi
TRIM36	E3 ubiquitin-protein ligase. mediates ubiquitination and proteasomal degradation of proteins. Cell cycle
TRPM2	calcium-permeable cation channel regulated by free intracellular ADP ribose
TRPM4	Calcium-activated non selective (CAN) cation channel that mediates membrane depolarization
TRPM8	Transient receptor potential (TRP) superfamily of ion channels
TSPAN1	Signal transduction, cell growth, motility
TSPAN13	Transmembrane 4 superfamily
TSPO	Manifestation of peripheral-type benzodiazepine recognition sites. Mitochondria. Cholesterol
TSTA3	NADP(H)-binding protein
TTC39A	Not characterised
TUBA1C	Microtubules
TUBB4B	Tubulin, beta 4B class IVb
TUSC3	Magnesium transporter. May be involved in N-glycosylation
TWIST1	Basic helix-loop-helix (bHLH) transcription factors have been implicated in cell lineage determination
TXNDC11	May act as a redox regulator involved in DUOX proteins folding
TXNDC16	Thioredoxin domain-containing protein
TXNDC5	Protects hypoxic cells from apoptosis
UAP1	UDP-N-acteylglucosamine pyrophosphorylase 1
UBE2J1	Catalyzes the covalent attachment of ubiquitin to other proteins. Degradation of misfolded protein from ER
UGGT1	UDP-glucose:glycoprotein glucosyltransferase. ER quality control
UQCC2	Nucleoid protein localized to the mitochondria inner membrane
UQCR10	Mitochondrial respiratory chain
UQCRQ	Mitochondrial respiratory chain
VCP	Golgi stacks during mitosis and for their reassembly after mitosis. Vesicle transport
VEGFA	Growth factor. Cell growth. Migration
VIMP	Degradation process of misfolded ER luminal proteins
VPS26B	Component of the retromer complex
VSTM2L	V-set and transmembrane domain containing 2 like
WDR37	Cell cycle
WSB2	Ubiquitination and proteasomal degradation of target proteins

WWC1	Regulator of the Hippo/SWH signaling pathway. Tumour suppression. Apoptosis. Activation of ERK1/1
XBP1	Acts during ER stress by activating unfolded protein response (UPR) target genes
YIF1A	Possible role in transport between endoplasmic reticulum and Golgi
YIPF1	RNA bindingand ribonuclease activity
YKT6	Functions in endoplasmic reticulum to Golgi transport; as part of a SNAREn complex
ZBTB16	Cell cycle. Transcription factor
ZCCHC6	Uridylyltransferase that mediates the terminal uridylation of some specific RNAs
ZDHHC23	Palmitoyltransferase that mediates palmitoylation of KCNMA1
ZDHHC8P1	Zinc Finger, DHHC-type containing 8 pseudogene
ZDHHC9	Zinc finger DHHC domain-containing protein family. Palmitoyltransferase
ZG16B	Zymogen granule protein
ZNF350	Transcriptional repressor
ZNF613	May be involved in transcriptional regulation
ZNF697	Transcriptional regulatuion

Genes down-regulated in response to androgen treatment in LNCaP cells, but up-regulated in 7 PCa patient samples post ADT.

Gene	Information
ABLIM1	May act as scaffold protein
ACACB	Provision of malonyl-CoA or in the regulation of fatty acid oxidation
ADAM22	Probable ligand for integrin in the brain. Cell adhesion. Inhibits cell proliferation
AJUBA	Repression of gene transcription, mitosis, cell-cell adhesion, cell differentiation, proliferation and migration
ANTXR1	Plays a role in cell attachment and migration. Mediates adhesion of cells to type 1 collagen and gelatin
ARHGEF17	Acts as guanine nucleotide exchange factor (GEF) for RhoA GTPases
ARHGEF25	Guanine nucleotide exchange factor for Rho family of small GTPases
ASPH	Probable role in mitotic spindle regulation and coordination of mitotic processes
ASS1	Arginine biosynthetic pathway
ATP11C	Phospholipid-Transporting ATPase
ATP2B4	Hydrolysis of ATP coupled with the transport of calcium out of the cell
BARX2	Transcription factor. Adhesion
BCHE	Cholinesterases inactivate the neurotransmitter acetylcholine
BTG2	Anti-proliferative protein. G1/S cell cycle
C14orf132	Not characterised
C16orf45	Not characterised
C9orf106	Not characterised
C9orf47	Not characterised
CAMK1D	Calcium/calmodulin-dependent protein kinase
CDK18	Protein serine/threonine kinase
CELSR2	Flamingo subfamily, part of the cadherin superfamily, contact mediated communication?
CERK	Converts ceramide to ceramide 1-phosphate (C1P), a sphingolipid metabolite
CLU	Extracellular chaperone that prevents aggregation of nonnative proteins
COL16A1	Alpha chain of type XVI collagen, cell attachment and inducing integrin-mediated cellular reactions
DDB2	Required for DNA repair
DDC	Catalyzes the decarboxylation
DIO3	Catalyzes the inactivation of thyroid hormone
DPYSL2	Neuronal development and polarity. Migration
EFNB3	Cell surface transmembrane ligand for Eph receptors. Migration, adhesion
ELF3	ERBB2 signaling pathway. Epithelial-specific transcriptional activator
ENO2	lncRNA?. Neuroprotector, cell survival
EPB41L2	Erythrocyte membrane protein band 4.1 like-protein 22
EPHA2	Receptor tyrosine kinase. Migration. ERK1/2
FAM172A	Not characterised
FAM182B	lncRNA

FAM86B1	Not characterised
FAM86B2	Noy
FRMD6	lncRNA?
FZD7	Receptor for Wnt proteins
GALK1	Major enzyme for galactose metabolism
GBP2	Guanine-binding protein (GBP) family
GLIS2	Transcriptional repressor or as a transcriptional activator. Wnt signalling
GPC3	Cell surface proteoglycan that bears heparan sulfate. Suppresses growth in mesoderm tissues
GPM6B	Membrane glycoprotein. Membrane trafficing. Cell cell communication
GPR126	Orphan receptor
HLF	bZIP transcription factors
HOXB3	Sequence-specific transcription factor
HOXB5	Sequence-specific transcription factor
HOXB6	Sequence-specific transcription factor
HSPB8	Displays temperature-dependent chaperone activity. Carcinogenesis
ID1	Cell growth. Senescence. inhibit the DNA binding and transcriptional activation ability of basic HLH proteins
ID3	Inhibits the DNA binding of any HLH protein
ITGA2	Integrin alpha-2/beta-1. Adhesion
ITGB4	Integrin alpha-6/beta-4 is a receptor for laminin. regulation of keratinocyte polarity and motility
KANK2	transcription regulation by sequestering nuclear receptor coactivators
LINC00161	lncRNA. Prostitis
LOC100130417	lncRNA uncharacterised
LOC101926935	ncRNA
LOC145837	Not characterised
LOC283070	lncRNA
LPCAT2	Acyltransferase and acetyltransferase
LRP1	Endocytosis and in phagocytosis of apoptotic. Lipid homeostasis
LYPD6B	Cancer/Testis Antigen 1161
MAP1B	Facilitates tyrosination of alpha-tubulin
MAP7D3	Not characterised
MATN2	Involved in matrix assembly
MECOM	Transcriptional regulator and oncoprotein
MGAT5	Glycosyltransferase. regulation of the biosynthesis of glycoprotein oligosaccharides
MID1	Deprotection of protein phosphatase PP2A. formation of multiprotein structures acting as anchor points to microtubules
MIR4697HG	lncRNA
MXRA8	Matrix-Remodelling Associated
NFASC	Cell adhesion
NOTCH1	Functions as a receptor for membrane-bound ligands Jagged1, Jagged2 and Delta1 to regulate cell-fate
NOVA1	May regulate RNA splicing or metabolism in developing neurons. Found in sera of breast cancer patients

NRM	Nuclear envelope membrane protein
NUAK1	Serine/threonine-protein kinase. ATM p53. Cell adhesion
OSR2	Odd-skipped related transciption factor 2
PBX1	PBX homeobox family of transcriptional factors.
PFKFB3	Synthesis and degradation of fructose 2,6-bisphosphate
PKIG	Competitive inhibitor of cAMP-dependent protein kinase activity
PLCD3	Phospholipases are a group of enzymes that hydrolyze phospholipids into fatty acids
PLK2	Tumor suppressor serine/threonine-protein kinase, centriole duplication. G1/S transition
PRNP	Glycosylphosphatidylinositol-anchored glycoprotein
PTPN14	Protein tyrosine phosphatase. Adhesion an migration
RAPGEFL1	Probable guanine nucleotide exchange factor (GEF)
RASSF5	Tumor suppressor, and is inactivated in variety of cancers
RCAN2	Inhibits calcineurin-dependent transcriptional responses
ROBO1	Receptor for SLIT1 and SLIT2 which are thought to act as molecular guidance cue in cellular migration
S1PR3	Receptor for the lysosphingolipid sphingosine 1-phosphate (S1P)
SCD5	Fatty acid delta-9-desaturase that introduces a double bond in fatty acyl-coenzyme A
SELENBP1	Selenium-binding protein. Golgi transport
SERPINB5	Tumor suppressor. It blocks the growth, invasion, and metastatic properties of mammary tumors
SLC16A2	Very active and specific thyroid hormone transporter
SLITRK3	Suppresses neurite outgrowth
SMARCD3	SWI/SNF family of proteins. Chromatin remodelling. Wnt signalling. EMT
SORBS1	Required for insulin-stimulated glucose transport. Focal adhesions
SPRY1	Antagonist of fibroblast growth factor (FGF) pathways
STXBP1	Regulation of synaptic vesicle docking
TIMP2	Natural inhibitors of the matrix metalloproteinases. Degrades ECM. Suppress proliferation
TRIM29	Transcriptional regulatory factor involved in carcinogenesis
TSLP	Cytokine
TSPAN7	Cell surface glycoprotein. May be involved in cell proliferation and cell motility
TYRP1	Melanosomal enzyme
UNC5B	Mediates apoptosis by activating DAPK1
USP27X	Ubiquitin-Specific-Processing Protease
VRK1	Serine/threonine kinase involved in Golgi disassembly during the cell cycle
VWA2	Structural protein. Willebrand factor A-like domain protein superfamily
WNT10A	WNT gene family
ZAK	S/G2 cell cycle. pCHEK2. protein kinase. Regulates the JNK and p38 pathways
ZC3H6	Zinc finger CCCH-type containing 6
ZFP36L1	Probable regulatory protein involved in regulating the response to growth factors
ZFP36L2	mRNA-binding protein. Binds AU rich elements for degradation

Appendix B

Complete list of real-time quantitative PCR (RT-qPCR) primer sequences used in this thesis:

Primer	Sequence
ABCA1 F	CGAGACTAACCAGGCAATCC
ABCA1 F	GAACACAATACCAGCCCAGAA
ACTIN F	CATCGAGCACGGCATCGTCA
ACTIN R	TAGCACAGCCTGGATAGCAAC
ALG2 F	ATCGTGGCAGGTGGTTATGA
ALG2 R	GCTGTGGAGGAGGGAGATTT
ALG5 F	TGGGACTCACCTACCAAACA
ALG5 R	GCTTCATCCATCATCACAGG
ARF4 F	TGGCAAGACAACCATCATTCTGT
ARF4 R	ACCACCAACATCCCATACTG
B2-MICROGLOBULIN (HLA-G) F	TGTCCTTGCAGCTGTAGTCA
B2-MICROGLOBULIN (HLA-G) R	GCAGCTGTTTCACATTGCAG
B3GNT2 F	CAAGGGCGATGACGATGTTT
B3GNT2 R	CTGCATAGGGTGGGTAGAGG
B4GALT1 F	TGTTGGGAGCTATTGAGCCA
B4GALT1 R	CTCAACCCTGGGATTAGGCA
B-CATENIN (CTNNB1) F	CTTACACCCACCATCCCACT
B-CATENIN (CTNNB1) R	TGCACGAACAAGCAACTGAA
BICC1 F	TCCTCGGACTTGAAAGCAGT
BICC1 R	CAAGGCCTGCTGAAGCTAAG
BST1 F	CCCATCCTGACTGTGCCTTA
BST1 R	TGATAAGACCCGCCCTTTGT
B-TUBULIN F	CTTCGGCCAGATCTTCAGAC
B-TUBULIN R	AGAGAGTGGGTCAGCTGGAA
C1orf116 F	ACTGGACACGGAGGCTGAC
C1orf116 R	CCTTGCTGAGTGATGGTCTC
CALR F	CGAATCCAAACACAAGTCAGA
CALR R	GCCGACAGAGCATAAAAGC
CCND1 F	ACAGATCATCCGCAAACACG
CCND1 R	ATCACTCTGGAGAGGAAGCG
CDA F	ACAAGGATTTCAGGGCAAT
CDA R	AAAGGAGGAGGGCAGCAG
CDNS F	CGTATCACCTCCCCTAACGA
CDNS R	CTTCTGGCACTGGAAATGGA
CHPF F	CCTGTGCGTGACCCTGTG
CHPF R	CGGGATGGTGCTGGAATAC
CORO1B F	GCCTCCACCACCACTGCT
CORO1B R	GTCGGCCTGCTCCTTGAC
CREB3L4 F	AGGCACAACATCTCCTTGGT

CREB3L4 R	CCGTGAGGCTGGTAATCCT
CSGALNACT1 F	ACTTTGGATTTGGGATGACG
CSGALNACT1 R	GGTTGCTGTGGAGATACTTGC
CTBS F	GGTCTTTGTGTTTGATGTTGGA
CTBS R	ACTCTGGCTCCTTTTGAATGA
CYS1 F	TGCCTGATACTGGCTTTCCA
CYS1 R	ACCAGGAACATTCCAAGGCT
DCAF6 F	CACATCCGTTTGACCCAAT
DCAF6 R	GAGGCTGGAACTGTAATGGTG
DSP F	GACTGGAGCGACAAGAACAC
DSP R	TGTCTGAAGCTGGATGCTGA
E-CADHERIN (CDH1) F	ACGCATTGCCACATACACTC
E-CADHERIN (CDH1) R	AGAGGTTCCTGGAAGAGCAC
EDEM1 F	CTCCAGCTCCAACTGCAATC
EDEM1 R	TTTGGCATGGTCTGGGTTTG
EDEM2 F	AGAGGCTGAAGGAAGAGCAG
EDEM2 R	ATTTCGACCTGCTCCGTTTG
EDEM3 R	TGGAACAGAGGGGCAGTATC
EDME3 F	CAGAAAAGGCACGCAACAT
ERLEC1 F	GTGACAAGTGGGGATGAGGA
ERLEC1 R	CTGCCGAATGTGTTTTCCAT
ESRP2 F	CCTGAACTACACAGCCTACTACCC
ESRP2 R	TCCTGACTGGGACAACACTG
EXT1 F	TGCCAACTCCAGCATCTACA
EXT1 R	GGGTGAAATCGAAGCAGGAC
FIBRONECTIN (FN1) F	GGTACAGGGTGACCTACTCG
FIBRONECTIN (FN1) R	GGGCTGGCTCTCCATATCAT
FUT1 F	GCCACGAAAAGCGGACTG
FUT1 R	ATGGAGGAAGAAGATTACAGAGAGG
FUT8 F	TTGGAACGGGAAGCTCATCT
FUT8 R	CCCAGCACACAAAGTAGTCG
FZD5 F	GGCAACCAGAACCTGAACTC
FZD5 R	CGTGTAGAGCAGCGTGAAGA
FZD7 F	GGTAGACGGGGACCTGCT
FZD7 R	GATACGGAAGAGGGACACGA
FZD8 F	GGCTTCGTGTCCCTCTTCC
FZD8 R	CGGTTGTGCTGCTCGTAGA
GALNT10 F	TACCGCAAAGACAAGACCCT
GALNT10 R	GGTGTGTTCAAACAGCCACT
GALNT12 F	AGCCTGGTCAACTCTCCTTC
GALNT12 R	CAGTCCCGAAAGCTCATTGG
GALNT14 F	ATCGAGCACATAGCATCCCA
GALNT14 R	TTGACGACGATTTCCTTGCC
GALNT3 F	TGATCACTGCTCGGTTGCTA
GALNT3 R	TTCTGGCCAACAGAGGTTCT
GALNT7 F	TCACCTCACACTACCCTTTGC

GALNT7 R	CTGATTCCCTCCCATCCTGT
GAPDH F	AACAGCGACACCCATCCTC
GAPDH R	CATACCAGGAAATGAGCTTGACAA
GCNT1 F	AACCTGGAAACGGAGAGGAT
GCNT1 R	TGACCACGAAGTAGGCACTG
GCNT2 F	AGTGCTGCCTCCTGACCAC
GCNT2 R	CCGTGCCAAAGTAAATCACC
GLB1L2 F	TTTTGACCACCTGATGTCCA
GLB1L2 R	GTCCTCCAGTGCCTTCTTGA
GLIS2 F	ATGTCAAGCCCGAGAAGGAT
GLIS2 R	GTGTGCGGATGTGGATGA
GNPNAT1 F	GTGCTAAGAGAGGAAGAGTAGAAGATG
GNPNAT1 R	TTTTGTGGTAGACATTCAAGGGTA
GSKIP F	CAGGGCTCAAGGTGGTAGG
GSKIP R	TCCAAATGCTTCTCGGTAGG
GSTA4 F	ATTGACGGGATGAAGTTGGT
GSTA4 R	TGATAAGCAGTTCCAGCAGA
ID3 F	AAATCCTACAGCGCGTCATC
ID3 R	AAGCTCCTTTTGTCGTTGGA
IFIT2 F	AAGCCTCATCCCTTCAGCAT
IFIT2 R	AACCCTGTCCAGTGGTATGG
JUP F	GCACACAGCAGCCCTACAC
JUP R	GATGTTCTCCACCGACGAGT
KLKP1 F	TACCATTTCGGCAACTTCCA
KLKP1 R	CAGCACAGTCAACACAGTAATCA
LHX2 F	CACTTCGGCATGAAGGACAG
LHX2 R	TAGGGAAGACCCAGAGGGTT
LINC00161 F	AGGCTTAGGAAGAAGAGAACTGT
LINC00161 R	GTCCATCTGAATGCCCACAC
LINC00920 F	AACTCTGCCTTTGGCTTTTG
LINC00920 R	TCACTCTTCCCTATGCTTTGC
LMAN2 F	TTCAAAGTCCACGGCACAG
LMAN2 R	ATCATTGGGGTAGGTGTCCA
LOC100130417 F	GAGTGAGGGTGGAGGGATG
LOC100130417 F	CAGCAGACATTGCCCAGT
LOC100130417 R	TCAGAACAAGCGGTGTGG
LOC100130417 R	CAGGACACCGCCTTGGAT
LOC101926935 F	GTGTGCGTGTGTGTGTGTGT
LOC101926935 R	AACCGCCAGAAAAATGACTG
LOC283070 F	CACTCACCTGGCACCTGTT
LOC283070 R	GCTGACTCCTTCCCACTGAC
LOC440910 F	GGCAGCACCAGTTGAAAGC
LOC440910 R	CATCTCCTGACCCCGTGAT
LRP4 F	ATGGAACAGGACAGGAGGTG
LRP4 R	CTGCCATCTGTGTTGGCTAC
MALAT1 F	CTGGGAGCAGAAAACAGCAG

MALAT1 R	GGAAGGGGTCAGGAGAAAGT
MAN1A1 F	AGCAGAGTTTCTTCCTGGCA
MAN1A1 R	ACAGTGAAGGGAATGGAGCA
MAN1C1 R	TATGCAAACCTCCGGTCCTT
MAN1C1 F	CAGCAGATGTGTCGGACAAG
MAN2A2 F	GGCCCTTTCTTCTCAGAGGT
MAN2A2 R	CCCTGGCAGATTGTAAAGCC
MANBA F	TTCTTTGCTCCACTGTTGCC
MANBA R	GTTCAGTCACACGAGAGCAC
MGAT2 F	AGTTGCGGGTTGTCATAACG
MGAT2 R	CCTCTGCGCTCTCATCCTTA
MIEN1 F	GCTGTGAAGGAGCAGTATCC
MIEN1 R	GGGAAAGCCCCCATTCTC
MIR4697HG F	GGCTTGGTTGACAGTTTTGG
MIR4697HG R	GGGGAGTGTTCTCAGCAGTT
MLEC F	GAGGAGACCTTTGGCTACGA
MLEC R	TACCTTTTGCTGGGACTGTG
MUC3A F	CTGGGACCCAAACATCTCCT
MUC3A R	GCTCAAGGCTGTTGATGGAG
MVD F	CGCCCATCTCTTACCTCAAT
MVD R	ACACAGCAGCCACAAATCCA
NANS F	TGGATGAGATGGGAGTTGAA
NANS R	GCAGAAGTTGGGGTTGAGG
N-CADHERIN (CDH2) F	AATCGTGTCTCAGGCTCCAA
N-CADHERIN (CDH2) R	TGGGATTGCCTTCCATGTCT
NEAT1 F	ACCCCTTCTTCCTCCCTTTA
NEAT1 R	GCCTCTCTTCTTCCACCATT
NES F	AAGTCTGCGGGACAAGAGAA
NES R	TCCACAGACTCCAGTGGTTC
NEU1 F	GCAAGGATGATGGTGTTTCC
NEU1 R	GTGGCTCCCGCTGTTTCT
NOTCH F	TCAAGCGTCTTGTGCTATGC
NOTCH R	GTATTGGCACGGCTGAACAT
OAS3 F	CAGTTCTGGCACCAAACCAA
OAS3 R	GCTTCACCAGCAGAATCAGG
PGM3 F	GCTGGTGATGCTATTTCTGACA
PGM3 R	CTCGGGGTGTAACTGCTTGT
PKP1 F	TGGGCAAGAGCAAGAAAGAT
PKP1 R	GACCGCACCACATCAGAGTT
PKP2 F	GCAGCACACCCGAAAGAT
PKP2 R	TGGAAACCAAATCAGGGAGA
PKP3 F	CCCGAGACCTGCTGTATTTT
PKP3 R	AAGTCCTCCTTCCGATAGCC
PKP4 F	AACCCAGCCACCTTGGAA
PKP4 R	CACGGAAGAAACAACTCTATCG
PNN F	AGAAGAGAATCACGCCAGGA

PNN R	ACCCATCAACAAGCCAAATA
PPL F	ACA GACAGCCTCGCCAAATA
PPL R	TCCTCCCATTCTCCAAGTCG
PPP1CA F	AGTGTGGACGAGACCCTCAT
PPP1CA R	GGGCTATTTCTTGGCTTTGG
PREB F	CTCCAACTTCTTGCCCCTTC
PREB R	CCACATCCGTCACCACAA
PVRL2 F	GGCTATGACTGGAGCACGAC
PVRL2 R	GCAGACGAAGGTGGTATTGAA
RAP1GAP F	GCGGCTTCTTTGAGTCTTTC
RAP1GAP R	GTGTTGGGCTTCTTGTTGCT
RHOU F	GCTCTGCTTCAGTGTCGTGA
RHOU R	TAGGATGATGGGGGCTTTG
RLN1 P1 F	CCTGTTCTTGTTCCACCTGC
RLN1 P2 F	TCTCACTGGGAATCTCACCG
RLN1 R	AGCCTCGGTAATGATGGTTGC
RLN2 P1 F	CGGACTCATGGATGGAGCAA
RLN2 P2 F	TCTCACTGGGAATCTCACCG
RLN2 R	GTAGCTGTGGTAATGCTGGC
RLN2 R	CAGCCACATTCCAGAGGATT
RPN1 F	GCCCTGTGATTGTTGCCTAC
RPN1 R	CCTTGGTGATGGAGAAGTCC
RPN2 F	CCGAGCCAGACAACAAGAAC
SAR1B F	GGCATTGTATTTCTGGTGGA
SAR1B R	CTCGCAACCTCTCTTCACTG
SCN9A F	AGGACCTCAGAGCTTTGTCC
SCN9A R	AAGTCACTGCTTGGCTTTGG
SERP1 F	CAACGAGAAGCACAGCAAGA
SERP1 R	GCAGAACCACAGACAACAAAA
SLC18A2 F	CGGGAGTGTGCTCTATGAGT
SLC18A2 R	GCAGCAATGAGGATGTACGG
SLC9A3R1 F	GAAGGAGAACAGTCGTGAAGC
SLC9A3R1 R	GGTCGGAGGAGGAGGTAGAC
SLC9A9 F	TCGGCTCTTCAGAATGTGGT
SLC9A9 R	GTAAGCAGCCTGGAAATCGG
SLUG (SNAI2) F	TGTCATACCACAACCAGAGA
SLUG (SNAI2) R	CTTGGAGGAGGTGTCAGAT
SMARCD3 F	GGAGGTGGAGGAGCCATTA
SMARCD3 R	ATAGCCTTTGGGGTCTCTGG
SNAIL (SNAI1) F	CCTCCCTGTCAGATGAGGAC
SNAIL (SNAI1) R	CTTTCGAGCCTGGAGATCCT
ST6GAL1 F	ACCATTCGCCTGATGAACTC
ST6GAL1 R	CTGGGGCTTGAGGATGTAAA
ST6GALNAC1 F	AGGCACAGACCCCAGGAAG
ST6GALNAC1 R	TGAAGCCATAAGCACTCACC
ST8SIA4 F	CAGAGGTTACTGGCTGACCA

ST8SIA4 R	GGGCCAGAATCCATACAGGT
STT3A F	GGAGGGAGCACAGATACAGG
STT3A R	GGAGGACGCTTGGCTTCT
STYK1 F	TATGGTGTTGGAGGATGTGG
STYK1 R	GACCTGCTTTCCGATGTGAT
TMEM8A F	ACAACAGCACAGCCCAGAC
TMEM8A R	GCCTCCACCAGGAAGAATC
TSPAN1 F	GAAAGGGCTCAAGTGCTGTG
TSPAN1 R	TCATTCGCTGTGTTGGTGAC
TUSC3 F	TTCACTGCTCTTCAGCCTCA
TUSC3 R	CCCCTCATCATAGTCCACCA
TWIST1 F	ATTCTCAAGAGGTCGTGCCA
TWIST1 R	TTTGCAGGCCAGTTTGATCC
UAP1 F	TGGTCTTTATCGGGCACTTG
UAP1 R	CCACCTTTGCTCCACAGTCT
UBE2J1 F	AGCCATCATTGGGTTTATGC
UBE2J1 R	CAGAGCCACATCCTTCACAA
UGGT1 F	GGTGGTTATCGTCCTCAACAA
UGGT1 R	CTCGTTCCATCACTCAGCAA
VCP F	AGAAGTCCCGTGTGGCCATC
VCP R	TCCAGAGAAGCCATTAGTCATTT
VIMENTIN (VIM) F	CCCTCACCTGTGAAGTGGAT
VIMENTIN (VIM) R	TGACGAGCCATTTCCTCCTT
ZEB1 F	TCAGGGAAGCCTGGGTTTAG
ZEB1 R	CCCTGTTAGGCAGTGAGGAA
ZO1 F	TTCACGCAGTTACGAGCAAG
ZO1 R	TTGGTGTTTGAAGGCAGAGC

Complete list of cloning primer sequences used in this thesis:

Primer	Sequence
ST6GAL1_p3XFLAG CMV10 _NotI_F	AATTAAGCGGCCGCTATGATTCACACCAACCTGAAG
ST6GAL1_p3XFLAG CMV10 _BamHI_R	AAAAAAGGATCCTTAGCAGTGAATGGTCCGGAAGC
RLN1_pGEX-5X-1_MfeI_F	AAAAAAAACAATTGATGTTGGAATTCATTGCTAATTTGCC
RLN1_pGEX-5X-1_XhoI_R	AAAAAAAACTCGAGTCAGCAATATTTAGCAAGAGACCTTTTGG
RLN1_pET32a(+)_MfeI_F	AAAAAAAACAATTGATGTTGGAATTCATTGCTAATTTGCC
RLN1_pET32a(+)_XhoI_R	AAAAAAAACTCGAGGCAATATTTAGCAAGAGACCTTTTGGTAC
RLN1_P1_p3XFLAG CMV10_HindIII_F	TTAATTAAGCCTTATGCCTCGCCTGTTCTTGTTCCACCTGC
RLN1_P1_p3XFLAG CMV10_BamHI_R	AAAAAAGGATCCTCAGCAATATTTAGCAAGAGACCTTTTGG
RLN1_P2_p3XFALG CMV10_HindIII_F	TTAATTAAGCTTATGTTGGAATTCATTGCTAATTTGCCACC
RLN1_P2_p3XFALG CMV10_BamHI_R	AAAAAAGGATCCTCAGCAATATTTAGCAAGAGACCTTTTGGTAC
RLN2_P1_p3XFLAG CMV10_HindIII_F	TTAATTAAGCTTATGCCTCGCCTGTTTTTTTTCCACCTGCTAGG
RLN2_P1_p3XFLAG CMV10_XbaI_R	AAAAAATCTAGATTATGGTTTCTGTATCTTTGTTGATGAAGG
RLN2_P2_p3XFALG CMV10_HindIII_F	TTAATTAAGCTTATGATGTCAGAATTTGTTGCTAATTTGCC
RLN2_P2_p3XFALG CMV10_XbaI_R	AAAAAATCTAGATCAGCAAAATCTAGCAAGAGATCTTTTGG

siRNA and shRNA details:

ST6GAL1_siRNA1 NO03032.12.1 (IDT)

ST6GAL1_siRNA2 NO03032.12.2 (IDT)

ST6GAL1_shRNA TRCN0000035432n (Sigma)

Sequence:

CCGGCGTGTGCTACTACTACCAGAACTCGAGTTCTGGTAGTAGTAGCACACGTTT

TTG

Appendix C

Significant KEGG pathways from the up-regulated gene list:

pathway	p-value	numDE	numTotal	pathway name
5322	0.018926505	20	136	systemic lupus erythematosus
4380	**0.035574276**	**11**	**128**	**osteoclast differentiation**
4973	0.035574276	5	44	carbohydrate digestion and absorption
4070	0.035574276	6	78	phosphatidylinositol signaling system

Significant KEGG pathways from the down-regulated gene list:

pathway	p-value	numDE	numTotal	pathway name
5200	8.358E-09	67	326	pathways in cancer
4141	2.08503E-07	39	165	protein processing in endoplasmic reticulum
4120	8.46749E-05	30	135	ubiquitin mediated proteolysis
4144	0.000117322	39	201	endocytosis
4520	0.000285038	20	73	adherens junction
4360	0.000356825	29	129	axon guidance
4010	0.000356825	45	268	MAPK signaling pathway
3013	0.000482503	28	151	RNA transport
4810	0.000482503	38	212	regulation of actin cytoskeleton
4110	0.000546431	25	124	cell cycle
4670	0.000738838	24	116	leukocyte transendothelial migration
5412	0.000807649	19	74	arrhythmogenic right ventricular cardiomyopathy (ARVC)
4114	0.000845215	23	112	oocyte meiosis
4972	0.001007929	21	101	pancreatic secretion
240	0.001183873	19	99	pyrimidine metabolism
5100	0.001183873	17	70	bacterial invasion of epithelial cells
5222	0.001605772	20	85	small cell lung cancer
330	0.00194809	13	54	arginine and proline metabolism
480	0.002050735	11	50	glutathione metabolism
4530	0.00235686	25	132	tight junction
4145	0.00235686	25	152	phagosome
5131	0.002600853	14	61	shigellosis

4142	0.002600982	22	121	lysosome
4510	0.002615751	35	200	focal adhesion
4380	**0.003596872**	**23**	**128**	**osteoclast differentiation**
4976	0.004106219	16	71	bile secreation
4020	0.004106219	30	177	calcium signaling pathway
5016	0.005004073	24	177	Huntington's disease
4514	0.005216532	23	133	cell adhesion molecules (CAMs)
620	0.005554414	10	40	pyruvate metabolism
4640	0.005923295	16	88	hematopoietic cell lineage
5130	0.005939458	12	55	pathogenic Escherichia coli infection
4270	0.005939458	21	116	vascular smooth muscle contraction
5010	0.005939458	22	161	Alzheimer's disease
1040	0.00620268	7	21	biosynthesis of unsaturated fatty acids
4914	0.007164869	17	86	progesterone-mediated oocyte maturation
5146	0.007360401	20	106	amoebiasis
4970	0.007780873	17	89	salivary secretion
5145	0.009113855	22	132	toxoplasmosis
3410	0.013162439	8	33	base excision repair
280	0.013590623	10	44	valine, leucine and isoleucine degradation
230	0.013828582	24	162	purine metabolism
4912	0.014143484	18	101	GnRH signaling pathway
3040	0.014578268	19	127	spliceosome
4971	0.014951751	15	74	gastric acid secretion
5210	0.016946687	13	62	colorectal cancer
4974	0.016946687	15	81	protein digestion and absorption
190	0.017301769	14	119	oxidative phosphorylation
3020	0.017301769	7	29	RNA polymerase
4916	0.018786685	18	101	melanogenesis
860	0.019738671	9	43	porphyrin and chlorophyll metabolism
5142	0.0201889	17	104	Chagas disease (American trypanosomiasis)
4621	0.022022787	11	58	NOD-like receptor signaling pathway
3440	0.024077094	7	28	homologous recombination
5414	0.027986965	16	90	dilated cardiomyopathy (DCM)
340	0.028443867	7	29	histidine metabolism
3430	0.028443867	6	23	mismatch repair
650	0.030477911	7	30	butanoate metabolism

4210	0.032899447	15	87	Apoptosis
4666	0.034253961	16	94	Fc gamma R-mediated phagocytosis
4722	0.034253961	20	127	neurotrophin signaling pathway
561	0.036842165	10	50	glycerolipid metabolism
3008	0.037089202	12	74	ribosome biogenesis in eukaryotes
4512	0.039789176	16	85	ECM-receptor interaction
5110	0.041060998	10	54	vibrio cholerae infection
982	0.041060998	11	73	drug metabolism - cytochrome P450
5215	0.04421863	15	89	prostate cancer
290	0.044298387	4	11	valine, leucine and isoleucine biosynthesis

Appendix D

Pre-absorption assay to validate the ST6Gal1 antibody. Protein from LNCaP cells treated with 10 nM synthetic androgen R1881 (A+) for 48 hours was separated using SDS-PAGE. The ST6Gal1 antibody was pre-incubated with various concentrations of a specific blocking peptide (0ug/ml – 10ug/ml). 1ug/ml blocking peptide reduced the intensity of the protein band compared to no blocking peptide, whilst higher concentrations completely blocks antibody binding. GAPDH (N-terminal) was used as a loading control.

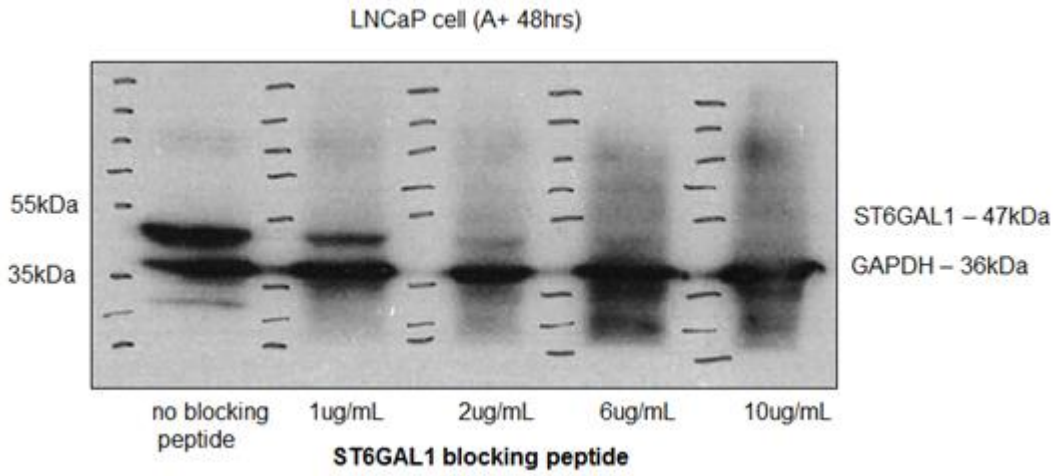

Appendix E

List of publications associated with this thesis:

Munkley, J., **Livermore, K.E.**, McClurg, U.L., Kalna, G., Knight, B., McCullagh, P., McGrath, J., Crundwell, M., Leung, H.Y., Robson, C.N., Harries, L.W., Rajan, P. and Elliott, D.J. (2015) 'The PI3K regulatory subunit gene PIK3R1 is under direct control of androgens and repressed in prostate cancer cells', Oncoscience, 2(9), pp. 755-64.

Munkley, J., Oltean, S., Vodak, D., Wilson, B.T., **Livermore, K.E.**, Zhou, Y., Star, E., Floros, V.I., Johannessen, B., Knight, B., McCullagh, P., McGrath, J., Crundwell, M., Skotheim, R.I., Robson, C.N., Leung, H.Y., Harries, L.W., Rajan, P., Mills, I.G. and Elliott, D.J. (2015) 'The androgen receptor controls expression of the cancer-associated sTn antigen and cell adhesion through induction of ST6GalNAc1 in prostate cancer', Oncotarget, 6(33), pp. 34358-74.

Munkley, J, Vodak, D, **Livermore, KE**, James, K, Wilson, BT, Knight, B, McCullagh, P, McGrath, J, Crundwell, M, Harries, LW, Leung, HY, Robson, CN, Mills, IG, Rajan, P, and Elliott, DJ. Glycosylation is an androgen regulated process essential for prostate cancer cell viability. EBioMedicine 8 (2016), pp. 103-116.

Livermore, K.E., Munkley, J. and Elliott, D.J. (2016) 'Androgen receptor and prostate cancer', AIMS Molecular Science, 3(2), pp. 280-299.

Munkley, J., **Livermore, KE**, Rajan, P. and Elliott, D.J. (2017) 'RNA splicing and splicing regulator changes in prostate cancer pathology', Hum Genet, 136(9), pp. 1143-1154.

Munkley, J., McClurg, U.L., **Livermore, K.E.**, Ehrmann, I., Knight, B., McCullagh, P., McGrath, J., Crundwell, M., Harries, L.W., Leung, H.Y., Mills, I.G., Robson, C.N., Rajan, P. and Elliott, D.J. (2017) 'The cancer-associated cell migration protein TSPAN1 is under control of androgens and its upregulation increases prostate cancer cell migration', Sci Rep, 7(1), pp. 5249.

Publications in preparation:

Munkley, J, Maia, T, Ibarluzea, N, **Livermore, KE**, Vodak, D, Ehrmann, I, Xu, J, James, K, Mills, IG, Rajan, P, Barbosa-Morais, NL, Elliott, DJ. 'Androgen-dependent alternative mRNA isoform expression in prostate cancer cells'